

Lattice towers and masts —

**Part 2: Guide to the background and use
of Part 1 “Code of practice for loading”**

UDC 624.97.074.5

Committees responsible for this British Standard

The preparation of this British Standard was entrusted by the Civil Engineering and Building Structures Standards Committee (CSB/-) to Technical Committee CSB/40, upon which the following bodies were represented:

British Broadcasting Corporation
 British Steel Industry
 British Telecommunications plc
 Constructional Steel Research and Development Organisation
 Department of Energy (Electricity Division)
 Department of the Environment (Building Research Establishment)
 Department of the Environment (Property Services Agency)
 Electricity Supply Industry in England and Wales
 Home Office
 Independent Broadcasting Authority
 Institution of Civil Engineers
 Institution of Structural Engineers
 Joint Radio Committee of the Nationalized Power Industries
 Ministry of Defence
 National Maritime Institute
 North of Scotland Hydro-electric Board
 Transmission and Distribution Association (BEAMA Ltd.)

This British Standard, having been prepared under the direction of the Civil Engineering and Building Structures Standards Committee, was published under the authority of the Board of BSI and comes into effect on 28 November 1986

© BSI 09-1999

The following BSI references relate to the work on this standard:
 Committee reference CSB/40
 Draft for comment 78/13078 DC

ISBN 0 580 14624 3

Amendments issued since publication

Amd. No.	Date of issue	Comments

Contents

	Page
Committees responsible	Inside front cover
Foreword	v
<hr/>	
1 Scope	1
2 Definitions	1
3 Symbols	1
4 Worked examples	1
5 Background to the use of Part 1	1
<hr/>	
Appendix A Worked example 1	5
A.1 Site and tower details	6
A.2 Performance requirements	6
A.3 Meteorological parameters	8
A.4 Wind resistance	11
A.5 Structural response to wind	14
A.6 Strength assessment	17
A.7 Alternative sites	23
Appendix B Worked example 2	25
B.1 Site and tower details	26
B.2 Performance requirements	26
B.3 Meteorological parameters	28
B.4 Wind resistance	30
B.5 Structural response to wind	39
B.6 Safety assessment	42
Appendix C Background to the use of Part 1	42
C.1 General	42
C.2 Performance requirements	43
C.3 Meteorological parameters	59
C.4 Wind resistance	111
C.5 Structural response to wind	138
C.6 Requirements for wind tunnel testing	167
<hr/>	
Figure A.1 — Worked example 1. 30 m broadcasting tower with shroud (general arrangement)	6
Figure B.1 — Worked example 2. 135 m broadcasting tower (showing typical panels)	26
Figure C.2.1 — Relationship between relative initial costs and probability of failure	46
Figure C.2.2 — Relationship between relative total costs and probability of failure for class A structure (design life of 50 years)	46
Figure C.2.3 — Example of the use Figure 2.1 of Part 1	51
Figure C.2.4 — Variation in risk of failure by modifying relative locations of loading and strength distribution	54
Figure C.2.5 — Dynamic response factor, K_m	57
Figure C.2.6 — Dynamic sensitivity check parameter	58
Figure C.3.1 — Terrain description chart	66
Figure C.3.2 — Comparison of gust ratios	68
Figure C.3.3 — Relationship between power law index, α , terrain roughness parameter, z_o , and terrain factor, K_R , for gust winds	69

	Page
Figure C.3.4 — Values of gradient wind speed reduction factor, K_g	71
Figure C.3.5 — Comparison between power law and log law profiles derived from theory of Deaves and Harris allowing for wind speed and terrain effect on formulae	73
Figure C.3.6 — Variation of power law index of mean wind speed with terrain roughness	74
Figure C.3.7 — Comparison of wind and pressure profiles at low levels	76
Figure C.3.8 — Notation for wind flow over hills	77
Figure C.3.9 — Wind speed over hills: comparison with field observation for Sutton Coldfield site	78
Figure C.3.10 — Wind speed over hills: comparison with results of wind tunnel tests, $H_h = 0.125 z_g$	79
Figure C.3.11 — Wind speed over hills: comparison with results of wind tunnel tests, $H_h = 0.083 z_g$	80
Figure C.3.12 — Wind over hills: comparison with results obtained at Durriss	81
Figure C.3.13 — Topography of surrounding region at Durriss	82
Figure C.3.14 — Wind over hills: comparison with records from Durriss mast	83
Figure C.3.15 — Comparison of wind speed over hills: terrain category II, $\alpha = 0.14$, height above hill $z - h_e = 50$ m	84
Figure C.3.16 — Comparison of wind speed over hills: terrain category II, $\alpha = 0.14$, height above hill $z - h_e = 200$ m	85
Figure C.3.17 — Comparison of wind speed over hills: terrain category V, $\alpha = 0.23$, height above hill $z - h_e = 50$ m	86
Figure C.3.18 — Comparison of wind speed over hills: terrain category V, $\alpha = 0.23$, height above hill $z - h_e = 200$ m	87
Figure C.3.19 — Datum levels for definition of hill height	88
Figure C.3.20 — Analysis of wind speed distributions	90
Figure C.3.21 — Frequency distribution for extreme mean hourly wind speeds	91
Figure C.3.22 — Conditions conducive to icing severity	93
Figure C.3.23 — Predicted severity of icing for the UK	94
Figure C.3.24 — Variation of thickness of ice with altitude	95
Figure C.3.25 — Frequency of icing in Germany	96
Figure C.3.26 — Intensity of icing in Germany	97
Figure C.3.27 — Variation of intensity of icing with cable diameter	99
Figure C.3.28 — Typical theoretical densities of accreted ice based on the work of Macklin and Page	100
Figure C.3.29 — Frequency distribution of the unit weight of ice deposits in Europe	101
Figure C.3.30 — Ice thickness distribution in Czechoslovakia	102

	Page
Figure C.3.31 — Development of atmospheric boundary layer (ABL) from change in terrain roughness	105
Figure C.3.32 — Boundary layer development due to change of terrain	106
Figure C.3.33 — Intermediate changes in terrain	108
Figure C.4.1 — Comparison of drag coefficients for square and triangular lattice towers composed of flat-sided members	113
Figure C.4.2 — Drag coefficients for square and equilateral triangular towers composed of circular-section members	114
Figure C.4.3 — Variation of basic drag coefficient with solidity ratio for a square lattice tower composed of flat-sided members	115
Figure C.4.4 — Variation of basic drag coefficient with solidity ratio for a triangular lattice tower composed of flat-sided members	116
Figure C.4.5 — Variation of basic drag coefficient with solidity ratio for a square lattice tower composed of circular-section members (in subcritical flow)	117
Figure C.4.6 — Variation of basic drag coefficient with solidity ratio for a triangular lattice tower composed of circular-section members (in subcritical flow)	118
Figure C.4.7 — Comparison of drag coefficients for triangular towers with test results (circular-section members)	119
Figure C.4.8 — Comparison of monograph with Part 1 for square towers with circular-section members	121
Figure C.4.9 — Variation of drag coefficient with wind direction for a square lattice tower composed of flat-sided members	122
Figure C.4.10 — Variation of drag coefficient with wind direction for a square lattice tower composed of circular-section members	123
Figure C.4.11 — Variation of K_θ ($\theta = 45^\circ$) with solidity ratio for a square lattice tower	124
Figure C.4.12 — Variation of K_θ with wind direction for a triangular tower composed of circular-section members	125
Figure C.4.13 — Variation of K_θ with wind direction for a triangular lattice tower composed of flat-sided members	126
Figure C.4.14 — Comparison of drag coefficients for triangular towers with test results (flat-sided members)	127
Figure C.4.15 — Drag coefficients for square lattice towers	129
Figure C.4.16 — Drag coefficients for triangular lattice towers	130
Figure C.4.17 — Normal drag coefficients for single frames composed of flat-sided members	131
Figure C.4.18 — Comparison of predicted and measured drag coefficients for square and triangular towers with various ancillaries	132
Figure C.4.19 — Wind loading on inclined cable	133
Figure C.4.20 — Tests on model communication tower: general arrangement of the tower model	134
Figure C.4.21 — Tests on model communication tower: configuration D (smooth uniform regime)	136

	Page
Figure C.4.22 — Tests on model communication tower: configuration H (smooth uniform regime)	137
Figure C.5.1 — Bracing member forces	140
Figure C.5.2 — Resistance of tower and ancillaries for use with appropriate gust factors	144
Figure C.5.3 — Forces in members	147
Figure C.5.4 — Aerodynamic lift coefficients for circular cylinders	149
Figure C.5.5 — Peak factor, g	151
Figure C.5.6 — Excitation by background turbulence	156
Figure C.5.7 — Size reduction factor	157
<hr/>	
Table 4.1 — References to Part 1 covered by the worked examples	2
Table A.3.1 — Mean wind speed, \bar{V}_z	9
Table A.3.2 — Ice thickness and weight for typical members	11
Table A.4.1 — Typical projected areas of tower panels	13
Table A.4.2 — Resistance of typical tower panels	13
Table A.5.1 — Mean wind loads on typical panels	15
Table A.5.2 — Gust response factors	16
Table A.7.1 — Comparison of wind profiles	23
Table C.2.1 — Analysis of test data for CEGB D type towers	48
Table C.2.2 — Alternative presentation of Figure 2.1 of Part 1	52
Table C.2.3 — Ratio τ_T to t_{av}	56
Table C.2.4 — Parameter variability (60 m; square; sharp-edged)	56
Table C.2.5 — Typical values of dynamic parameters	56
Table C.2.6 — Examples of comparison of static and dynamic stress predictions	56
Table C.3.1 — Mean return period, \bar{T} , of annual climatic maxima in other codes of practice	61
Table C.3.2 — Time averaging interval for basic wind speed	62
Table C.3.3 — Comparisons of power law index, α , gust factor, G , and terrain factor, K_R	65
Table C.3.4 — Comparison of $\bar{V}_{z/\gamma_d} V_B$ for (a) log law (b) power law	72
Table C.3.5 — Intensity of turbulence, I_w	103
Table C.3.6 — Simplified expressions for $\sigma(V)/V_B$, independent of height	104
Table C.4.1 — Comparison between Part 1 and experimental results	135
Table C.5.1 — Simplified derivation of $g \times f$	158
Table C.5.2 — Examples of actual towers using simplified derivation of $g \times f$	158
<hr/>	
Publications referred to	Inside back cover

Foreword

This Part of BS 8100 has been prepared under the direction of the Civil Engineering and Building Structures Standards Committee. BS 8100 is a standard combining a code of practice and a guide covering the loading and design of lattice towers of metallic construction.

It comprises the following Parts:

- *Part 1: Code of practice for loading;*
- *Part 2: Guide to the background and use of Part 1 “Code of practice for loading”.*

DD 133 covers the strength assessment of members.

This Part of BS 8100 does not apply to other metallic structures. Other British Standards exist for some of those structures.

It has been assumed in the drafting of this British Standard that the execution of its provisions will be entrusted to appropriately qualified and experienced people.

A British Standard does not purport to include all the necessary provisions of a contract. Users of British Standards are responsible for their correct application.

Compliance with a British Standard does not of itself confer immunity from legal obligations.

Summary of pages

This document comprises a front cover, an inside front cover, pages i to vi, pages 1 to 170, an inside back cover and a back cover.

This standard has been updated (see copyright date) and may have had amendments incorporated. This will be indicated in the amendment table on the inside front cover.

1 Scope

This Part of BS 8100 contains both guidance on the interpretation of and background to the use of BS 8100-1, which is the code of practice covering the loading of lattice towers and masts.

NOTE 1 Where references are made in the text to “Part 1” they refer to BS 8100-1:1986.

Two worked examples are provided to assist designers with the application of Part 1.

NOTE 2 The titles of the publications referred to in this standard are listed on the inside back cover.

2 Definitions

For the purposes of this Part of BS 8100, the definitions given in Part 1 apply.

3 Symbols

The main symbols and subscripts used in this Part of BS 8100 are as given in Part 1. However, due to the nature of this Part of BS 8100, it has not been possible to adopt a unique set of symbols and hence all additional symbols are defined as they appear in the text.

4 Worked examples

Two worked examples are given in Appendix A and Appendix B as guidance to Part 1. They both relate to typical broadcasting towers, but the method of calculation is equally applicable to other types of tower. The examples show how the appropriate clauses of Part 1 may be used in practice, with some guidance on interpretation and simplification, where appropriate. Such guidance may only relate to the examples chosen and should not be taken as being applicable in all situations. Only sufficient calculations have been provided to show the method of calculation required.

Although worked example 1 (see Appendix A) is a smaller tower than worked example 2 (see Appendix B) with fewer aerials and attachments, the two examples should not be considered as simple and complex, respectively. In order to cover as many as possible of the recommendations of Part 1, considerations of interpretation of wind data, hill sites, vortex shedding, serviceability and fatigue have been covered in worked example 1, since they are not relevant to the particular example chosen for worked example 2, which concentrates more thoroughly on the full (general) method of assessment of wind resistance given in 4.3 and 4.4 of Part 1 and the consequent loading considerations of 5.3 of Part 1.

The examples are referenced throughout to the relevant clauses of Part 1 (and this Part of BS 8100) in typical calculation format. As a further aid to the user of Part 1, Table 4.1 is provided listing the references in Appendix A and Appendix B in which calculations (or notes) relating to the clauses of Part 1 can be found.

The numbering of Appendix A and Appendix B is generally aligned with the numbering of Part 1 so that equivalently numbered subclauses cover the same subject matter in order to aid cross-referencing.

5 Background to the use of Part 1

The background to the use of Part 1 is given in Appendix C.

In Appendix C, reference is made to source material and where new procedures have been developed, particularly those concerning safety provisions and gust response of structures, the theoretical background is summarized. Comparison is made between the results of application of the various clauses of Part 1, existing codes and experimental evidence.

The numbering of Appendix C has been aligned with the numbering of Part 1 so that equivalently numbered subclauses cover the same subject matter in order to aid cross-referencing. Additional subclauses have been included in Appendix C covering different areas of the subject matter to those in Part 1, or where additional background information is considered to be useful.

NOTE The numbers in square brackets used throughout Appendix C refer to the bibliographic references given in C.1.3, C.2.8, C.3.8, C.4.10 and C.5.12.

Table 4.1 — References to Part 1 covered by the worked examples

Reference to Part 1			Reference in worked example	
Clause	Figure	Table	Example 1	Example 2
Section 1. General				
1.1	Scope			
1.2	Definitions			
1.3	Symbols			
1.3.1	Main symbols			
1.3.2	Subscripts			
Section 2. Performance requirements				
2.1	Safety and service life		A.2.1	B.2.1
2.1.1	General			
2.1.2	Service life		A.2.1	B.2.1
2.2	Classification of required reliability		A.2.2	B.2.2
2.2.1	General		A.2.2	
2.2.2	Environmental conditions		A.2.2	B.2.2
2.2.3	Economic consequences of usage		A.2.2	B.2.2
2.3	Classification of quality		A.2.3	B.2.3
2.3.1	General			
2.3.2	Class A towers		A.2.3	B.2.3
2.3.3	Class B towers			
2.3.4	Class C towers			
2.4	Safety factors		A.2.2	B.2.4
2.4.1	Wind speed and ice thickness factors	Figure 2.1	A.2.2	B.2.4
2.4.2	Dead load and partial factors	Figure 2.1	A.2.4	B.2.4
2.5	Safety assessment	Figure 2.1	A.6.1	B.2.4, B.6
2.6	Serviceability		A.6.3	
Section 3. Meteorological parameters				
3.1	Wind speed data		A.3.1	B.3.1
3.1.1	General		A.7.2	
3.1.2	Basic wind speed	Figure 3.1	A.3.1, A.7.2	B.3.1
3.1.3	Wind direction factor	Figure 3.2	A.3.1, A.7.2	B.3.1
3.1.4	Terrain roughness factor	Figure 3.3	A.3.1, A.7.2	B.3.1
3.1.5	Site reference wind speed		A.3.1, A.6.3, A.7.2	B.3.1
3.2	Variation of wind speed with height		A.3.2	B.3.2
3.2.1	Sites on level terrain	Figure 3.3	A.3.2, A.7.2	B.3.1, B.3.2, B.5.1
3.2.2	Sites on hills	Figure 3.4, Figure 3.5	A.6.5, A.7.1	
3.3	Serviceability		A.3.3, A.6.2, A.6.3	B.3.3
3.3.1	Distribution of wind speeds			
3.3.2	Downwind deflections	Figure 3.6	A.6.3	B.5.3
3.3.3	Crosswind deflection (vortex shedding)	Figure 3.7, Figure 3.8	A.6.3, A.6.4	

Table 4.1 — References to Part 1 covered by the worked examples

Reference to Part 1			Reference in worked example	
Clause	Figure	Table	Example 1	Example 2
3.4 Fatigue life assessment			A.3.4	B.3.4
3.4.1 In-line vibrations			A.6.4	
3.4.2 Crosswind vibrations			A.6.2, A.6.4	
3.5 Ice loading			A.3.5	B.3.5
3.5.1 General			A.3.5	B.3.5
3.5.2 Basic ice thickness	Figure 3.9		A.3.5	B.3.5
3.5.3 Reference ice thickness			A.3.5	B.3.5
3.5.4 Ice weight			A.3.5	B.3.5
Section 4. Wind resistance				
4.1 General			A.4.1	B.4.1
4.1.1 Method of derivation	Figure 4.1		A.4.1	B.4.1
4.1.2 Symmetrical towers without ancillaries			A.4.1	B.4.2, B.4.3, B.4.4
4.1.3 Symmetrical towers with limited ancillaries			A.4.1	B.4.3, B.4.4
4.1.4 Other cases				B.4.4
4.2 Method for symmetrical towers without ancillaries			A.4.1, A.4.3	B.4.2, B.4.5
4.2.1 Calculation of total wind resistance	Figure 4.2		A.4.1, A.4.3	B.4.2, B.4.3
4.2.2 Overall drag coefficients	Figure 4.3		A.4.3	B.4.2
4.3 Method for symmetrical towers with limited ancillaries				B.4.5
4.3.1 Constraints for simplified method				B.4.3
4.3.2 Calculation of total wind resistance				B.4.3, B.5.1
4.4 General method for towers containing ancillaries or unsymmetrical towers				B.4.5
4.4.1 Calculation of total wind resistance	Figure 4.4			B.4.4
4.4.2 Drag (pressure) coefficients for single frames	Figure 4.5			B.4.4
4.5 Linear ancillaries		Table 4.1, Table 4.2	A.4.2	B.4.3, B.4.4
4.6 Discrete ancillaries				B.4.4
4.7 Cables				
4.8 Icing			A.3.5	
Section 5. Structural response to wind				
5.1 Procedure			A.5.1	B.5.1
5.1.1 General			A.5.1	B.5.1
5.1.2 Equivalent static method			A.5.1	B.5.1
5.1.3 Spectral analytical method				
5.1.4 Deflections			A.6.3	B.5.3
5.1.5 Vortex-excited vibrations			A.6.2	

Table 4.1 — References to Part 1 covered by the worked examples

Reference to Part 1			Reference in worked example	
Clause	Figure	Table	Example 1	Example 2
5.2 Wind loading for symmetrical towers				
5.2.1 General			A.5.1	B.5.1
5.2.2 Basic gust response factor	Figure 5.1, Figure 5.2 Figure 5.3		A.5.1	B.5.1
5.2.3 Loading for calculating bending moments			A.5.1	B.5.1
5.2.4 Loading for calculating shear forces	Figure 5.4		A.5.1	B.5.1
5.2.5 Loading for calculating deflections			A.6.3	B.5.3
5.2.6 Calculation of wind forces in tower members			A.5.2	
5.3 Wind loading for towers with complex attachments				B.5.1
5.3.1 General				B.4.6, B.5.1
5.3.2 Loading on ancillary items				B.5.1
5.3.3 Loading on cables	Figure 5.5 to Figure 5.7			
5.3.4 Calculation of wind forces in tower members				B.5.2
5.3.5 Loading for calculating deflections				B.5.3
5.4 Spectral analytical method				
5.5 Crosswind response due to vortex excitation			A.6.2	B.3.3, B.3.4
5.5.1 Critical wind speed			A.6.2	
5.5.2 Excitation	Figure 5.8		A.6.2, A.6.3	
Appendix A Measurement and interpretation of wind data	Figure A.1		A.7.2	
Appendix B Terrain parameters			A.7.2	
Appendix C Gradient wind speeds	Figure C.1, Figure C.2		A.7.2	
Appendix D Hill parameters in undulating terrain	Figure D.1		A.7.1	
Appendix E Parameters for spectral analytical methods		Table E.1, Table E.2		
Appendix F Method of assessment for classification of quality		Table F.1, Table F.2	A.2.3	B.2.3
Appendix G Equations used for the production of curves used in the figures				

Appendix A Worked example 1

Reference in Part 1	Worked example 1
	<p>A.1 Site and tower details</p> <p>A.1.1 General The structure is a 30 m high triangular unmanned broadcasting tower with cylindrical aerial shroud on top. Location is East Riding, Yorkshire at 170 m above mean sea level (AMSL), situated in very open flat moorland with very few obstructions (hedges, fences, trees, etc.).</p> <p>A.1.2 Form of structure From preliminary considerations and previous experience, member sizes as shown in Figure A.1 have been adopted.</p>
<p>2.1</p> <p>2.1.2</p> <p>2.2, 2.4</p> <p>2.2.1</p> <p>2.2.2</p> <p>2.2.3</p> <p>Figure 2.1</p> <p>(C.2.5 of this part of BS 8100) 2.2.3.3</p>	<p>A.2 Performance requirements</p> <p>A.2.1 Service life The intended service life of the structure is 30 years.</p> <p>A.2.2 Performance requirements and safety factors No specific cost criteria have been provided, and hence safety factors are selected from:</p> <ul style="list-style-type: none"> a) environment, i.e. potential hazards; b) usage of the tower. <p>For a) the environmental category is “unmanned in open countryside”. For b) the usage is “broadcasting”. From Figure 2.1 of Part 1, it can be seen that b) governs and the governing γ_v is taken as 1.15, i.e. appropriate to the right-hand limit of the governing performance requirement, which in this case has been assumed to have been specified by the client.</p> <p>The corresponding γ_{DL}, and γ_m are then:</p> <p style="margin-left: 40px;">$\gamma_{DL} = 1.01$ for dead load effects increasing wind effects;</p> <p style="margin-left: 80px;">or</p> <p style="margin-left: 40px;">0.90 for dead load effects decreasing wind effects;</p> <p style="margin-left: 40px;">$\gamma_m = 1.10$ for quality class A (see note to A.2.3).</p> <p>NOTE 1 If possible, due account should be made of any known future change to the environment. If, for example, a main road was to be situated adjacent to the tower, the governing performance requirement would then be a) environment: “adjacent to main road” giving increased safety factors thus:</p> <p style="margin-left: 40px;">$\gamma_v = 1.20$;</p> <p style="margin-left: 40px;">$\gamma_{DL} = 1.05$.</p> <p>However, provided no such criteria need be considered, the required safety factors are:</p> <p style="margin-left: 40px;">$\gamma_v = 1.15$;</p> <p style="margin-left: 40px;">$\gamma_{DL} = 1.01$ or 0.90, according to load effect;</p> <p style="margin-left: 40px;">$\gamma_m = 1.10$ for quality class A</p> <p>These values can be confirmed by inspection of Table C.2.2.</p> <p>NOTE In this example the usage criteria have been used, and the right-hand limit from “broadcasting” adopted. The left-hand limit, i.e. $\gamma_v = 1.07$, would be used if no value had been specified by the client.</p>

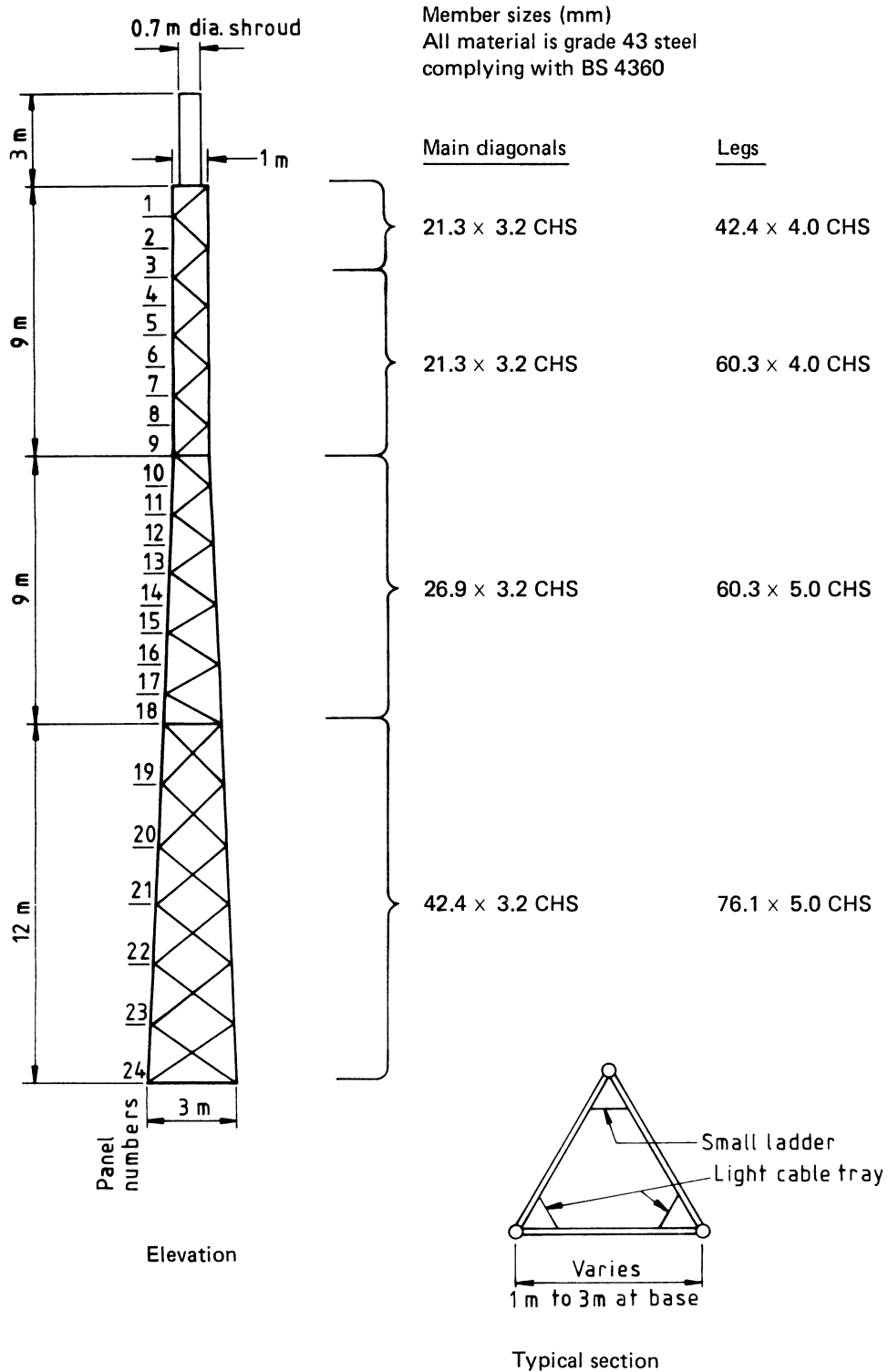


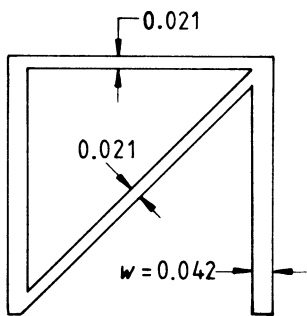
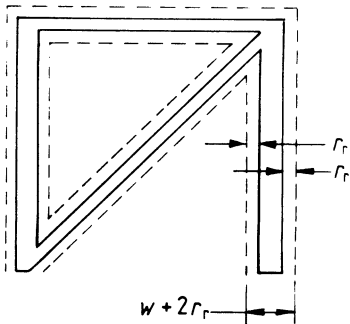
Figure A.1 — Worked example 1. 30 m broadcasting tower with shroud (general arrangement)

Reference in Part 1	Worked example 1																		
<p>2.2.3.2</p> <p>2.4</p>	<p>The consequential cost ratio appropriate to selected criteria can then be evaluated in accordance with 2.2.3.2 of Part 1. Hence for the selected right-hand limit of the “broadcasting” category;</p> <p>$\log_{10}(gi_s)$ is in the range 1.75 to 1.98</p> <p>For $i_s = 30$ years, this gives g in the range 1.9 to 3.2, which is the ratio of the consequential cost of replacement to the initial cost, and can be reported back to the client, who may require a higher allowance.</p> <p>Alternatively, if a γ_v of 1.20 was chosen in accordance with note 1 for the “adjacent to main road” category this gives:</p> <p>$\log_{10}(gi_s)$ in the range 1.9 to 2.2</p> <p>Again for $i_s = 30$ years, this gives g in the range 2.6 to 5.3</p> <p>Hence it can be seen that a full assessment of all possible performance requirements is required before finalizing the appropriate safety factors.</p>																		
<p>2.3</p> <p>2.3.2 Appendix F Table F.1</p> <p>Table F.2</p>	<p>A.2.3 Design, fabrication and erection standards and tower classification</p> <p>The structural design will be in accordance with Part 1 and DD 133, the design and detailing will be independently appraised, the materials, quality control and workmanship will be in accordance with the appropriate British Standard, and the tower will be subject to inspection after fabrication. Routine inspections will be conducted every 2 years after erection. On this basis, the tower may be considered to be a class A tower, as it complies with all the recommendations of 2.3.2 of Part 1.</p> <p>NOTE Alternatively, Appendix F of Part 1 could be used for the assessment of quality classification. This gives the following rating from Table F.1 of Part 1:</p> <table border="0" data-bbox="523 1104 826 1279"> <tr> <td>Item 1:</td> <td>(b)</td> <td>Rating 1</td> </tr> <tr> <td>Item 2:</td> <td>(b)</td> <td>Rating 1</td> </tr> <tr> <td>Item 3:</td> <td>(a)</td> <td>Rating 1</td> </tr> <tr> <td>Item 4:</td> <td>(a)</td> <td>Rating 2</td> </tr> <tr> <td>Item 5:</td> <td>(a)</td> <td>Rating 2</td> </tr> <tr> <td colspan="2"></td> <td style="border-top: 1px solid black;">Total 7</td> </tr> </table> <p>From Table F.2 of Part 1, the quality category is therefore class A.</p> <p>It should be noted that if there was no independent design check <i>or</i> there was no regular inspection and maintenance procedure, the rating would drop to 6 (or 5) and the quality category would become class B, in which case γ_v and γ_{DL} would be unchanged, but γ_m would become 1.20)</p>	Item 1:	(b)	Rating 1	Item 2:	(b)	Rating 1	Item 3:	(a)	Rating 1	Item 4:	(a)	Rating 2	Item 5:	(a)	Rating 2			Total 7
Item 1:	(b)	Rating 1																	
Item 2:	(b)	Rating 1																	
Item 3:	(a)	Rating 1																	
Item 4:	(a)	Rating 2																	
Item 5:	(a)	Rating 2																	
		Total 7																	
<p>2.4.2.2</p>	<p>A.2.4 Dead loads</p> <p>Dead loads resulting from the self weight of the tower, including the weight of the ladder, cable trays and aerial structure, are calculated in accordance with 2.4.2.2 of Part 1, with appropriate allowances for connections, etc.</p>																		
<p>3.1</p> <p>3.1.2 Figure 3.1</p> <p>3.1.3</p>	<p>A.3 Meteorological parameters</p> <p>A.3.1 General</p> <p>a) <i>Basic wind speed.</i> The map wind speed for the site is given as 24 m/s at 10 m AMSL in Figure 3.1 of part 1. Allowance has to be made for the altitude, giving the basic wind speed;</p> $\bar{V}_B = 1.17 \times 24 = 28.1 \text{ m/s}$ <p>b) <i>wind direction factor.</i> Since the tower is on sensibly level ground and uniform terrain [see c)] and is symmetric with regard to wind resistance, no advantage can be gained from the use of Figure 3.2 of part 1. Consequently, the wind direction factor, K_d, has been taken as 1.0 for ice-free conditions, and 0.85 for the combination of wind with ice.</p>																		

Reference in Part 1	Worked example 1										
<p>3.1.4 Figure 3.3 or Table 3.1</p> <p>(C.3.1.4 of this part of BS 8100)</p>	<p>c) <i>Terrain roughness parameters.</i> The site is an open moorland with very few isolated obstructions. Consequently, from Table 3.1 of Part 1 it may be deemed to be in category II from which the appropriate parameters for the site are as follows:</p> $\begin{aligned} K_R &= 1.10; \\ \alpha &= 0.14; \\ h_e &= 0. \end{aligned}$ <p>NOTE These values are confirmed by inspection of Figure C.3.1</p>										
<p>3.1.5</p>	<p>d) <i>Site reference wind speed, \bar{V}_r.</i> The site reference wind speed is given by:</p> $\begin{aligned} \bar{V}_r &= \gamma_v K_d K_R \bar{V}_B \\ &= 1.15 \times 1.0 \times 1.1 \times 28.1 \\ &= \underline{35.5 \text{ m/s}} \end{aligned}$ <p>Also the characteristic wind speed is given by:</p> $\begin{aligned} \bar{V}_k &= K_R \bar{V}_B \\ &= 1.10 \times 28.1 \\ &= \underline{30.9 \text{ m/s}} \end{aligned}$ <p>\bar{V}_k is required for the serviceability check (see A.3.3).</p>										
<p>3.2 3.2.1</p>	<p>A.3.2 Wind profile The tower is situated on level ground, therefore 3.2.1 of Part 1 is used to obtain the wind profile. NOTE An example of calculating the wind profile for a site on a hill is given in A.7.1. Using</p> $\bar{V}_z = 35.5 \left(\frac{z}{10} \right)^{0.14} \text{ for } z \geq 10 \text{ m}$ <p>and</p> $\bar{V}_z = 17.75 \left(1 + \frac{z}{10} \right) \text{ for } z < 10 \text{ m}$ <p>The values of \bar{V}_z given in Table A.3.1 are obtained for typical levels.</p> <p style="text-align: center;">Table A.3.1 — Mean wind speed, \bar{V}_z</p> <table border="1" data-bbox="359 1608 1121 1697"> <thead> <tr> <th>Panel height, z (m)</th> <th>1.0</th> <th>12.5</th> <th>21.5</th> <th>27.5</th> </tr> </thead> <tbody> <tr> <td>\bar{V}_z (m/s)</td> <td>19.5</td> <td>36.6</td> <td>39.5</td> <td>40.9</td> </tr> </tbody> </table>	Panel height, z (m)	1.0	12.5	21.5	27.5	\bar{V}_z (m/s)	19.5	36.6	39.5	40.9
Panel height, z (m)	1.0	12.5	21.5	27.5							
\bar{V}_z (m/s)	19.5	36.6	39.5	40.9							
<p>3.3</p>	<p>A.3.3 Serviceability Serviceability is dealt with after the derivation of loads and strength (safety) assessment and the appropriate details are given in A.6.3.</p>										
<p>3.4</p>	<p>A.3.4 Fatigue life assessment Fatigue life assessment is dealt with after the derivation of loads and strength (safety) assessment and the appropriate details are given in A.6.4.</p>										

Reference in Part 1	Worked example 1
3.5	A.3.5 Ice loading
3.5.1	<p>a) <i>Wind speed</i>. The site reference speed to be used with ice, \bar{V}_i, is given by:</p> $\bar{V}_i = 0.8 \gamma_v K_d K_R \bar{V}_B$ $= 0.8 \times 1.15 \times 0.85 \times 1.1 \times 28.1$ $= 24.2 \text{ m/s} = 0.68 \bar{V}_r$
3.5.2	<p>The variation of \bar{V}_i with height follows that of \bar{V}_r, with \bar{V}_{zi} being $0.68 \times \bar{V}_z$, where values of \bar{V}_z are given in Table A.3.1.</p>
3.5.2.1	<p>b) <i>Basic ice thickness</i></p> <p>1) In the absence of wind:</p>
Figure 3.9	$r_{Bo} = k_i \left\{ r_o + \left(\frac{a - 200}{25} \right) \right\} \geq k_i r_o$
3.5.2.2	<p>where</p> $k_i = \left(\frac{2}{3} + \frac{4}{D} \right)$ <p>D varies from 21.3 mm to 76.1 mm; $a = 200$ m (site is at 170 m AMSL); $r_o = 60$ mm.</p> <p>2) With wind:</p>
Figure 3.9	$r_{Bw} = k_i \left\{ r_w + \left(\frac{a - 200}{25} \right) \right\} \geq k_i r_w$
4.8	<p>where</p> $r_w = 10 \text{ mm}$
3.5.3	<p>There are no gaps of less than 75 mm, and hence there are no significant areas that need to be considered as completely filled with ice.</p> <p>c) <i>Reference ice thickness</i>. The reference ice thickness is given by:</p> $r_r = \gamma_v K_C r_B$ $= 1.15 \times 1.0 \times r_B$ <p>i.e. $r_{ro} = 69 k_i \text{ mm}$; $r_{rw} = 11.5 k_i \text{ mm}$</p>
3.5.4	<p>This gives design values as shown in Table A.3.2.</p> <p>d) <i>Ice weight</i>. The unit weight of ice is:</p> $\rho_{io} = 5 \text{ kN/m}^3 \text{ for no wind;}$ $\rho_{iw} = 9 \text{ kN/m}^3 \text{ for wind and compression;}$ $\rho_{iw} = 5 \text{ kN/m}^3 \text{ for wind and uplift.}$ <p>Ice loads are then calculated on the basis of:</p> $I = \pi \rho_i r_r (d + r_r) \text{ kN/m}$ <p>with r_r and member diameter, d, in metres, using $\rho_{iw} = 9 \text{ kN/m}^3$ for I_w. Where required, these values can then be factored by 0.56 for uplift consideration. Values of I_o and I_w are given in Table A.3.2.</p>

Reference in Part 1	Worked example 1								
	Table A.3.2 — Ice thickness and weight for typical members								
	Member diameter	k_i	Member weight	No wind			With wind		
	mm		kN/m	r_{Bo}	r_{ro}	I_o	r_{Bw}	r_{rw}	I_w
				mm	mm	kN/m	mm	mm	kN/m
	21.3	0.85	0.014	51	59	0.074	9	10.0	0.009
	33.7	0.79	0.024	47	54	0.074	8	9.1	0.011
	76.1	0.72	0.086	43	50	0.099	7	8.3	0.020
4.1	A.4 Wind resistance								
4.1.1	A.4.1 General								
	For analysis, the tower is divided into 24 panels using leg/bracing intersections. The tower is mounted with a cylindrical shroud whose resistance should be calculated separately. Each lattice panel encompassing one set of primary bracing has been considered for the purposes of calculating wind resistance. For such a simple tower some of these panels may in practice be aggregated, but in this example full panel divisions are retained to demonstrate the calculation procedure more generally.								
Note to 4.1.3	The ancillaries consist of two small cable trays and a small ladder. The small cable trays and ladder are reasonably symmetrical in each face and can hence be treated as structural members for the purposes of wind resistance, as can the cylindrical shroud, and hence wind resistance can be determined by means of the overall drag coefficients given in 4.2 of Part 1, i.e.:								
4.1.2	$\Sigma R_w = R_T = K_\theta C_N A_F$								
4.2.1 a)	The crosswind resistance ΣR_x for a tower which is symmetric can be considered as the same as the in-line wind resistance, ΣR_w .								
4.2.1 b)									
4.2	A.4.2 Cylindrical shroud								
4.5	The overall resistance for this is derived in accordance with 4.5 of Part 1, using Table 4.1 of Part 1.								
Table 4.1	The effective Reynolds number is given by:								
	$R_e = \frac{1.5 \bar{V}_z D}{\nu} = \frac{1.5 \times 42 \times 0.7}{1.46 \times 10^{-5}} = 30 \times 10^5$								
	This is greater than 10×10^5 and hence for supercritical flow:								
	$C_N = 0.7$ (ice free) or 1.0 (iced);								
	$K_A = 1.0$;								
	$A_A \sin^2 \psi = 0.7 \times 3.0 = 2.1 \text{ m}^2$								
	$\Sigma R_W = R_{AW} = C_N K_A A_A \sin^2 \psi$								
	$= 0.7 \times 1.0 \times 2.1 = 1.47 \text{ m}^2$ (ice free)								
	or								
	$= 1.0 \times 1.0 \times 2.1 = 2.10 \text{ m}^2$ (iced)								
	The maximum ice-free resistance for subcritical flow will occur when $R_e = 2 \times 10^5$ compatible with a wind speed of about 3 m/s. Clearly this will not be a governing condition.								

Reference in Part 1	Worked example 1
<p>4.2.1</p>	<p>A.4.3 Panels 1 to 24, lattice sections</p> <p>The flow around the circular-section members has to be checked to see which flow regime exists. At the tower top:</p> $\bar{V}_z = 41.3 \text{ m/s}$ <p>Hence minimum D for supercritical flow:</p> $D \geq R_e \nu / 1.5 \bar{V}_z = 94 \text{ mm}$ <p>At a height of 12 m (top of 76 mm section) $\bar{V}_z = 36 \text{ m/s}$:</p> $D \geq 108 \text{ mm for supercritical flow}$ <p>Since all panel members are smaller than these limiting values, all circular-section members may be taken as having subcritical flow, and no reduction can be made for supercritical flow.</p> <p>Resistance without ice</p>  $A_c = 1.0 \times 0.42 \times 2 + (1.0 + 1.414) \times 0.021 = 0.134 \text{ m}^2$ $\phi = \frac{1.05 \times 0.134}{1.0 \times 1.0} = 0.14$ <p>Resistance with ice</p>  $A_c = 1.0 \times (0.042 + 2 \times 0.009) \times 2 + (1.0 + 1.414) \times (0.021 + 2 \times 0.01) = 0.218 \text{ m}^2$ $\phi = \frac{1.05 \times 0.218}{1.0 \times 1.0} = 0.23$ <p>Panels 4 to 9</p> $A_c = 1.0 \times 0.060 \times 2 + 1.414 \times 0.0213 = 0.150 \text{ m}^2$ $\phi = \frac{1.05 \times 0.151}{1.0 \times 1.0} = 0.16$ $A_c = 1.0 \times (0.060 + 2 \times 0.009) \times 2 + 1.414 (0.021 + 2 \times 0.010) = 0.214 \text{ m}^2$ $\phi = \frac{1.05 \times 0.215}{1.0 \times 1.0} = 0.23$ <p>This process is repeated in turn for each panel. Typical results have been tabulated in Table A.4.1. The ancillaries make up approximately 5 % of the tower area in this case, and are all flat-sided members. Since they are reasonably identical on each face, they may be treated as structural members and the tower resistance calculated in accordance with 4.2 of Part 1.</p>
4.2	

Reference in Part 1	Worked example 1																																																																																																																																																																																																																											
<p>4.2.1</p> <p>4.2.2</p> <p>Figure 4.2</p> <p>Figure 4.3</p>	<p>Values of A_c, A_f and $A_s (= A_c + A_f)$ are given in Table A.4.1, and the resistances of each panel are set out in Table A.4.2 derived from:</p> $R_w = K_\theta C_N A_s$ <p>Where</p> $C_N = \frac{A_f}{A_s} C_{Nf} + \frac{A_c}{A_s} C_{Nc} + \frac{A_c'}{A_s} C_{Nc'};$ <p>$K_\theta = 1.0$ from Figure 4.2 of Part 1;</p> <p>C_{Nf}, C_{Nc} from Figure 4.3 b) of Part 1.</p> <p style="text-align: center;">Table A.4.1 — Typical projected areas of tower panels</p> <table border="1" style="width:100%; border-collapse: collapse; text-align: center;"> <thead> <tr> <th rowspan="2">Panel no.</th> <th rowspan="2">Member</th> <th rowspan="2">Length</th> <th colspan="2">Width</th> <th rowspan="2">Panel no.</th> <th colspan="3">Projected area</th> </tr> <tr> <th>Uniced</th> <th>Iced</th> <th>Type</th> <th>Uniced</th> <th>Iced</th> </tr> </thead> <tbody> <tr> <td></td> <td></td> <td>m</td> <td>m</td> <td>m</td> <td></td> <td></td> <td>m²</td> <td>m²</td> </tr> <tr> <td rowspan="3">3</td> <td>Leg</td> <td>1.00</td> <td>0.042</td> <td>0.060</td> <td rowspan="3">3</td> <td>A_c</td> <td>0.114</td> <td>0.178</td> </tr> <tr> <td>Diag.</td> <td>1.41</td> <td>0.021</td> <td>0.041</td> <td>A_f</td> <td>0.006</td> <td>0.009</td> </tr> <tr> <td>Horiz.</td> <td>NA</td> <td>—</td> <td>—</td> <td>—</td> <td>—</td> <td>—</td> </tr> <tr> <td></td> <td></td> <td></td> <td></td> <td></td> <td>A_s</td> <td><u>0.120</u></td> <td><u>0.187</u></td> </tr> <tr> <td rowspan="3">9</td> <td>Leg</td> <td>1.00</td> <td>0.060</td> <td>0.078</td> <td rowspan="3">9</td> <td>A_c</td> <td>0.150</td> <td>0.214</td> </tr> <tr> <td>Diag.</td> <td>1.41</td> <td>0.021</td> <td>0.041</td> <td>A_f</td> <td>0.007</td> <td>0.011</td> </tr> <tr> <td>Horiz.</td> <td>NA</td> <td>—</td> <td>—</td> <td>—</td> <td>—</td> <td>—</td> </tr> <tr> <td></td> <td></td> <td></td> <td></td> <td></td> <td>A_s</td> <td><u>0.157</u></td> <td><u>0.225</u></td> </tr> <tr> <td rowspan="3">18</td> <td>Leg</td> <td>1.01</td> <td>0.060</td> <td>0.076</td> <td rowspan="3">18</td> <td>A_c</td> <td>0.177</td> <td>0.246</td> </tr> <tr> <td>Diag.</td> <td>2.07</td> <td>0.027</td> <td>0.045</td> <td>A_f</td> <td>0.009</td> <td>0.012</td> </tr> <tr> <td>Horiz.</td> <td>NA</td> <td>—</td> <td>—</td> <td>—</td> <td>—</td> <td>—</td> </tr> <tr> <td></td> <td></td> <td></td> <td></td> <td></td> <td>A_s</td> <td><u>0.186</u></td> <td><u>0.258</u></td> </tr> <tr> <td rowspan="3">24</td> <td>Leg</td> <td>2.01</td> <td>0.076</td> <td>0.092</td> <td rowspan="3">24</td> <td>A_c</td> <td>0.605</td> <td>0.796</td> </tr> <tr> <td>Diag.</td> <td>3.53</td> <td>0.042</td> <td>0.060</td> <td>A_f</td> <td>0.030</td> <td>0.040</td> </tr> <tr> <td>Horiz.</td> <td>NA</td> <td>—</td> <td>—</td> <td>—</td> <td>—</td> <td>—</td> </tr> <tr> <td></td> <td></td> <td></td> <td></td> <td></td> <td>A_s</td> <td><u>0.635</u></td> <td><u>0.836</u></td> </tr> </tbody> </table> <p style="text-align: center;">Table A.4.2 — Resistance of typical tower panels</p> <table border="1" style="width:100%; border-collapse: collapse; text-align: center;"> <thead> <tr> <th>Panel no.</th> <th>ϕ</th> <th>C_{Nf}</th> <th>C_{Nc}</th> <th>C_N</th> <th>R_w</th> </tr> </thead> <tbody> <tr> <td></td> <td></td> <td></td> <td></td> <td></td> <td>m²</td> </tr> <tr> <td colspan="6">Ice free</td> </tr> <tr> <td>3</td> <td>0.12</td> <td>2.80</td> <td>1.60</td> <td>1.66</td> <td>0.20</td> </tr> <tr> <td>9</td> <td>0.16</td> <td>2.70</td> <td>1.55</td> <td>1.60</td> <td>0.25</td> </tr> <tr> <td>18</td> <td>0.11</td> <td>2.85</td> <td>1.65</td> <td>1.71</td> <td>0.32</td> </tr> <tr> <td>24</td> <td>0.10</td> <td>2.90</td> <td>1.65</td> <td>1.71</td> <td>1.09</td> </tr> <tr> <td colspan="6">Iced</td> </tr> <tr> <td>3</td> <td>0.19</td> <td>2.60</td> <td>1.50</td> <td>1.55</td> <td>0.29</td> </tr> <tr> <td>9</td> <td>0.23</td> <td>2.45</td> <td>1.45</td> <td>1.50</td> <td>0.34</td> </tr> <tr> <td>18</td> <td>0.15</td> <td>2.75</td> <td>1.60</td> <td>1.66</td> <td>0.43</td> </tr> <tr> <td>24</td> <td>0.16</td> <td>2.70</td> <td>1.60</td> <td>1.66</td> <td>1.38</td> </tr> </tbody> </table> <p>Full tabulation of these produces total tower resistances as follows.</p> <p>Ice free: $\Sigma R_w = 13 \text{ m}^2$;</p> <p>Iced: $\Sigma R_w = 17 \text{ m}^2$.</p>	Panel no.	Member	Length	Width		Panel no.	Projected area			Uniced	Iced	Type	Uniced	Iced			m	m	m			m ²	m ²	3	Leg	1.00	0.042	0.060	3	A_c	0.114	0.178	Diag.	1.41	0.021	0.041	A_f	0.006	0.009	Horiz.	NA	—	—	—	—	—						A_s	<u>0.120</u>	<u>0.187</u>	9	Leg	1.00	0.060	0.078	9	A_c	0.150	0.214	Diag.	1.41	0.021	0.041	A_f	0.007	0.011	Horiz.	NA	—	—	—	—	—						A_s	<u>0.157</u>	<u>0.225</u>	18	Leg	1.01	0.060	0.076	18	A_c	0.177	0.246	Diag.	2.07	0.027	0.045	A_f	0.009	0.012	Horiz.	NA	—	—	—	—	—						A_s	<u>0.186</u>	<u>0.258</u>	24	Leg	2.01	0.076	0.092	24	A_c	0.605	0.796	Diag.	3.53	0.042	0.060	A_f	0.030	0.040	Horiz.	NA	—	—	—	—	—						A_s	<u>0.635</u>	<u>0.836</u>	Panel no.	ϕ	C_{Nf}	C_{Nc}	C_N	R_w						m ²	Ice free						3	0.12	2.80	1.60	1.66	0.20	9	0.16	2.70	1.55	1.60	0.25	18	0.11	2.85	1.65	1.71	0.32	24	0.10	2.90	1.65	1.71	1.09	Iced						3	0.19	2.60	1.50	1.55	0.29	9	0.23	2.45	1.45	1.50	0.34	18	0.15	2.75	1.60	1.66	0.43	24	0.16	2.70	1.60	1.66	1.38
Panel no.	Member				Length	Width		Panel no.	Projected area																																																																																																																																																																																																																			
		Uniced	Iced	Type		Uniced	Iced																																																																																																																																																																																																																					
		m	m	m			m ²	m ²																																																																																																																																																																																																																				
3	Leg	1.00	0.042	0.060	3	A_c	0.114	0.178																																																																																																																																																																																																																				
	Diag.	1.41	0.021	0.041		A_f	0.006	0.009																																																																																																																																																																																																																				
	Horiz.	NA	—	—		—	—	—																																																																																																																																																																																																																				
					A_s	<u>0.120</u>	<u>0.187</u>																																																																																																																																																																																																																					
9	Leg	1.00	0.060	0.078	9	A_c	0.150	0.214																																																																																																																																																																																																																				
	Diag.	1.41	0.021	0.041		A_f	0.007	0.011																																																																																																																																																																																																																				
	Horiz.	NA	—	—		—	—	—																																																																																																																																																																																																																				
					A_s	<u>0.157</u>	<u>0.225</u>																																																																																																																																																																																																																					
18	Leg	1.01	0.060	0.076	18	A_c	0.177	0.246																																																																																																																																																																																																																				
	Diag.	2.07	0.027	0.045		A_f	0.009	0.012																																																																																																																																																																																																																				
	Horiz.	NA	—	—		—	—	—																																																																																																																																																																																																																				
					A_s	<u>0.186</u>	<u>0.258</u>																																																																																																																																																																																																																					
24	Leg	2.01	0.076	0.092	24	A_c	0.605	0.796																																																																																																																																																																																																																				
	Diag.	3.53	0.042	0.060		A_f	0.030	0.040																																																																																																																																																																																																																				
	Horiz.	NA	—	—		—	—	—																																																																																																																																																																																																																				
					A_s	<u>0.635</u>	<u>0.836</u>																																																																																																																																																																																																																					
Panel no.	ϕ	C_{Nf}	C_{Nc}	C_N	R_w																																																																																																																																																																																																																							
					m ²																																																																																																																																																																																																																							
Ice free																																																																																																																																																																																																																												
3	0.12	2.80	1.60	1.66	0.20																																																																																																																																																																																																																							
9	0.16	2.70	1.55	1.60	0.25																																																																																																																																																																																																																							
18	0.11	2.85	1.65	1.71	0.32																																																																																																																																																																																																																							
24	0.10	2.90	1.65	1.71	1.09																																																																																																																																																																																																																							
Iced																																																																																																																																																																																																																												
3	0.19	2.60	1.50	1.55	0.29																																																																																																																																																																																																																							
9	0.23	2.45	1.45	1.50	0.34																																																																																																																																																																																																																							
18	0.15	2.75	1.60	1.66	0.43																																																																																																																																																																																																																							
24	0.16	2.70	1.60	1.66	1.38																																																																																																																																																																																																																							

Reference in Part 1	Worked example 1
<p>5.1.1</p>	<p>A.5 Structural response to wind</p> <p>A.5.1 General</p> <p>a) <i>Check for use of the static method.</i> The equivalent static method may be used if:</p> $\frac{7 m_T}{\rho_s R_{WT} \sqrt{(d_B \tau_o)} \left(\frac{5}{6} - \frac{h_T}{H} \right)^2} < 1$ <p>Total tower resistance, $\Sigma R_w = 13 \text{ m}^2$.</p> <p>$R_{WT} \leq \frac{\Sigma R_w}{3} = 4.3 \text{ m}^2$, which from a full version of Table A.4.2 corresponds with panels 0 to 12 inclusive for which $R_{WT} = 4.23 \text{ m}^2$, $m_T = 400 \text{ kg}$ and $h_T = 13.5 \text{ m}$, but not greater than $H/3$. $H/3 = 11 \text{ m}$, hence $h_T = 11 \text{ m}$; $\rho_s = 7\,850 \text{ kg/m}^3$; $\tau_o = 0.001 \text{ m}$; $d_B = 0.75 \times 3 = 2.25 \text{ m}$. Thus</p> $\frac{7 \times 400}{7850 \times 4.23 \times \sqrt{(0.001 \times 2.25)} \left(\frac{5}{6} - \frac{11}{33} \right)^2} = 0.44 < 1$ <p>Therefore the equivalent static method may be used.</p>
5.1.2	<p>b) <i>Procedure to be used.</i> The tower panels comply with the constraints of 4.1.3 of Part 1, thus maximum member forces can be derived in accordance with 5.2 of Part 1. Since there are no large ancillaries on the tower (other than those treated as structural members), the only analyses required are under total mean hourly wind load. The total load effects are obtained after the analyses are completed by factoring the forces in each member according to the appropriate gust factors, G, derived according to the height and member type [see d)].</p> <p>Two wind load cases are considered:</p> <ol style="list-style-type: none"> 1) with wind normal to a face to produce maximum leg compression (or tension) in the opposite leg; 2) with wind parallel to a face to produce maximum bracing forces. <p>Dead load and ice load have to be dealt with separately, so that due allowance can be made for reversal of derived forces for maximum tension or compression, and for incorporation of alternative values of γ_{DL} in the determination of dead load effects, and of ρ_{iw} in the determination of ice load effects, as well as to ensure that the gust factor, G, is applied only to forces due to wind effects.</p> <p>NOTE If the analyses are carried out by a computer program with automatic self weight procedure, care will be required in the combinations produced to ensure that the appropriate factored load effects are obtained.</p>
5.2.1	<p>c) <i>Mean wind load.</i> Values of the maximum mean wind load, $\bar{P}_{TW} = (\rho_a/2) \bar{V}_z^2 \Sigma R_w$ are given in Table A.5.1 for typical panels taking $\rho_a = 1.22 \text{ kg/m}^3$.</p>

Reference in Part 1	Worked example 1																																																												
	<p>Table A.5.1 — Mean wind loads on typical panels</p> <table border="1" style="width: 100%; border-collapse: collapse;"> <thead> <tr> <th style="text-align: center;">Panel no.</th> <th style="text-align: center;">Height</th> <th style="text-align: center;">\bar{V}_z</th> <th style="text-align: center;">R_w</th> <th style="text-align: center;">\bar{P}_{TW}</th> </tr> <tr> <td></td> <td style="text-align: center;">m</td> <td style="text-align: center;">m/s</td> <td style="text-align: center;">m²</td> <td style="text-align: center;">kN</td> </tr> </thead> <tbody> <tr> <td colspan="5" style="text-align: center;">Ice free</td> </tr> <tr> <td style="text-align: center;">3</td> <td style="text-align: center;">27.5</td> <td style="text-align: center;">40.9</td> <td style="text-align: center;">0.20</td> <td style="text-align: center;">0.205</td> </tr> <tr> <td style="text-align: center;">9</td> <td style="text-align: center;">21.5</td> <td style="text-align: center;">39.5</td> <td style="text-align: center;">0.25</td> <td style="text-align: center;">0.238</td> </tr> <tr> <td style="text-align: center;">18</td> <td style="text-align: center;">12.5</td> <td style="text-align: center;">36.6</td> <td style="text-align: center;">0.32</td> <td style="text-align: center;">0.261</td> </tr> <tr> <td style="text-align: center;">24</td> <td style="text-align: center;">1.0</td> <td style="text-align: center;">19.5</td> <td style="text-align: center;">1.09</td> <td style="text-align: center;">0.253</td> </tr> <tr> <td colspan="5" style="text-align: center;">Iced</td> </tr> <tr> <td style="text-align: center;">3</td> <td style="text-align: center;">27.5</td> <td style="text-align: center;">27.8</td> <td style="text-align: center;">0.29</td> <td style="text-align: center;">0.137</td> </tr> <tr> <td style="text-align: center;">9</td> <td style="text-align: center;">21.5</td> <td style="text-align: center;">26.9</td> <td style="text-align: center;">0.34</td> <td style="text-align: center;">0.150</td> </tr> <tr> <td style="text-align: center;">18</td> <td style="text-align: center;">12.5</td> <td style="text-align: center;">24.9</td> <td style="text-align: center;">0.43</td> <td style="text-align: center;">0.163</td> </tr> <tr> <td style="text-align: center;">24</td> <td style="text-align: center;">1.0</td> <td style="text-align: center;">13.3</td> <td style="text-align: center;">1.38</td> <td style="text-align: center;">0.149</td> </tr> </tbody> </table>	Panel no.	Height	\bar{V}_z	R_w	\bar{P}_{TW}		m	m/s	m ²	kN	Ice free					3	27.5	40.9	0.20	0.205	9	21.5	39.5	0.25	0.238	18	12.5	36.6	0.32	0.261	24	1.0	19.5	1.09	0.253	Iced					3	27.5	27.8	0.29	0.137	9	21.5	26.9	0.34	0.150	18	12.5	24.9	0.43	0.163	24	1.0	13.3	1.38	0.149
Panel no.	Height	\bar{V}_z	R_w	\bar{P}_{TW}																																																									
	m	m/s	m ²	kN																																																									
Ice free																																																													
3	27.5	40.9	0.20	0.205																																																									
9	21.5	39.5	0.25	0.238																																																									
18	12.5	36.6	0.32	0.261																																																									
24	1.0	19.5	1.09	0.253																																																									
Iced																																																													
3	27.5	27.8	0.29	0.137																																																									
9	21.5	26.9	0.34	0.150																																																									
18	12.5	24.9	0.43	0.163																																																									
24	1.0	13.3	1.38	0.149																																																									
<p>(C.3.5.1 of this part of BS 8100)</p> <p>5.2.2.2 Figures 5.1 and 5.2</p> <p>5.2.2.3 Figure 5.3</p>	<p>NOTE 1 Inspection of Table A.5.1 shows that the wind under ice-free conditions governs throughout. This agrees with the general guidance given in C.3.5.1, as follows:</p> $\frac{r_{rw}}{D} = \frac{10}{21} \approx 48\% \text{ at the top of the tower for the bracings}$ <p>or</p> $\frac{9}{42} \approx 21\% \text{ at the top of the tower for the legs.}$ <p>Hence, since in all cases $r_{rw}/D < 60\%$, wind with ice is not likely to govern.</p> <p>The loads \bar{P}_{TW} given in Table A.5.1 are used for both load cases:</p> <ol style="list-style-type: none"> 1) face on to wind; 2) face parallel to wind; <p>since K_θ is identical (= 1.0) for both these conditions for circular-section members (see Figure 4.2 of Part 1).</p> <p>NOTE 2 For flat-sided members or square towers, the loadings would need to be factored to allow for differing K_θ values.</p> <p>d) <i>Gust response factors.</i> Gust response factors are determined as follows.</p> <ol style="list-style-type: none"> 1) The basic gust response factor is calculated using $G_B = Bj$ as given in 5.2.2.1 of Part 1, using Figures 5.1 and 5.2 of Part 1; typical results are tabulated in Table A.5.2. The value of $(H - z)$ is limited in the upper part of the tower to the minimum value of 10 m when obtaining B, and the consequent value of $(H - z)/H = 10/33 = 0.30$ when obtaining j; these values of $(H - z)$ are given in parenthesis in Table A.5.2. 2) Alternatively, the simplified method, as given in 5.2.2.3 of Part 1, could be used giving G_B from Figure 5.3 of Part 1 as 0.98 for $H = 33$ m which is a slight upper bound on the values given in 5.2.2.2 of Part 1, i.e. the general method. 																																																												

Reference in Part 1	Worked example 1																																																																		
<p>5.2.4 Figure 5.4</p> <p>(C.5.2.4 of this BS 8100)</p>	<p>3) For bracings, the factor K_q is taken from Figure 5.4 of Part 1, according to $1/ f_q$ where f_q is the proportion of the mean hourly wind shear carried by the bracings at the level considered. For the upper part of the tower with parallel legs, $f_q = 1.0$ since no shear is transmitted through the legs. For the lower part of the tower with sloping legs, f_q is obtained from the analyses under mean wind loading, using:</p> $f_q = \frac{q_b}{\Sigma q}$ <p>where</p> <p>q_b is shear carried by the bracings; Σq is the total shear.</p> <p>Both q_b and Σq are taken appropriate to the level considered and the load direction in each analysis.</p>																																																																		
<p>5.2.3</p>	<p>4) The resulting leg and bracing gust factors are tabulated in Table A.5.2, where</p> $G_1 \text{ is given by } G_B \left\{ 1 + 0.2 \left(\frac{z}{H} \right)^2 \right\}$																																																																		
<p>5.2.4</p>	$G_b \text{ is given by } K_q G_B \left\{ 1 + 0.2 \left(\frac{z}{H} \right)^2 \right\} = K_q G_1$ <p style="text-align: center;">Table A.5.2 — Gust response factors</p> <table border="1" data-bbox="496 1122 1417 1368"> <thead> <tr> <th>Panel</th> <th>z</th> <th>$H-z$</th> <th>$\frac{z}{H}$</th> <th>B</th> <th>j</th> <th>G_B</th> <th>f_q</th> <th>k_q</th> <th>G_1</th> <th>G_b</th> </tr> </thead> <tbody> <tr> <td>1</td> <td>29.5</td> <td>(10)</td> <td>0.89</td> <td>1.20</td> <td>0.80</td> <td>0.96</td> <td>1</td> <td>1</td> <td>1.11</td> <td>1.11</td> </tr> <tr> <td>3</td> <td>27.5</td> <td>(10)</td> <td>0.83</td> <td>1.20</td> <td>0.80</td> <td>0.96</td> <td>1</td> <td>1</td> <td>1.09</td> <td>1.09</td> </tr> <tr> <td>9</td> <td>21.5</td> <td>11.5</td> <td>0.65</td> <td>1.16</td> <td>0.83</td> <td>0.96</td> <td>1</td> <td>1</td> <td>1.04</td> <td>1.04</td> </tr> <tr> <td>18</td> <td>12.5</td> <td>20.5</td> <td>0.38</td> <td>1.06</td> <td>0.92</td> <td>0.97</td> <td>0.348</td> <td>1.14</td> <td>1.00</td> <td>1.14</td> </tr> <tr> <td>24</td> <td>1.0</td> <td>32.0</td> <td>0.03</td> <td>0.98</td> <td>1.00</td> <td>0.98</td> <td>0.337</td> <td>1.18</td> <td>0.98</td> <td>1.15</td> </tr> </tbody> </table>	Panel	z	$H-z$	$\frac{z}{H}$	B	j	G_B	f_q	k_q	G_1	G_b	1	29.5	(10)	0.89	1.20	0.80	0.96	1	1	1.11	1.11	3	27.5	(10)	0.83	1.20	0.80	0.96	1	1	1.09	1.09	9	21.5	11.5	0.65	1.16	0.83	0.96	1	1	1.04	1.04	18	12.5	20.5	0.38	1.06	0.92	0.97	0.348	1.14	1.00	1.14	24	1.0	32.0	0.03	0.98	1.00	0.98	0.337	1.18	0.98	1.15
Panel	z	$H-z$	$\frac{z}{H}$	B	j	G_B	f_q	k_q	G_1	G_b																																																									
1	29.5	(10)	0.89	1.20	0.80	0.96	1	1	1.11	1.11																																																									
3	27.5	(10)	0.83	1.20	0.80	0.96	1	1	1.09	1.09																																																									
9	21.5	11.5	0.65	1.16	0.83	0.96	1	1	1.04	1.04																																																									
18	12.5	20.5	0.38	1.06	0.92	0.97	0.348	1.14	1.00	1.14																																																									
24	1.0	32.0	0.03	0.98	1.00	0.98	0.337	1.18	0.98	1.15																																																									

Reference in Part 1	Worked example 1																																																		
<p>5.2.6 (C.5.2.6 of this Part of BS 8100)</p>	<p>A.5.2 Member forces</p> <p>a) <i>General.</i> Member forces are derived in accordance with 5.2.6 of Part 1 from the summation of $\bar{F}_{TW} + F'_{TW}$. For reasonably symmetric towers (see C.5.2.6) and as discussed in A.5.1, this can be taken as $\bar{F}_{TW \max} (1 + G)$, where $F_{TW \max}$ is the maximum mean hourly wind load from either case (1) or (2) wind directions [see A.5.1 b)], plus dead load effects. Only the ice-free conditions need be considered from inspection of Table A.5.1. The tower has the same make-up over several panels, and since the gust factors vary only slightly over a series of panels, member forces under mean hourly loads need only be determined at the lower section of each group of panels. Also, since the tower is of construction such that the compression strength will govern, only the maximum compressive forces need be determined, as follows.</p> <table border="1" data-bbox="384 792 1054 1055"> <thead> <tr> <th colspan="5" data-bbox="384 792 1054 853">b) Bracings: $\Sigma F_{\max} \leq (1 + G_{\max}) \bar{F}_{\max}$</th> </tr> <tr> <th data-bbox="384 853 520 913">Panels</th> <th data-bbox="520 853 683 913">Type (CHS)</th> <th data-bbox="683 853 815 913">\bar{F}_{\max}</th> <th data-bbox="815 853 948 913">$1 + G_{\max}$</th> <th data-bbox="948 853 1054 913">ΣF_{\max}</th> </tr> </thead> <tbody> <tr> <td data-bbox="384 913 520 958">1 to 9</td> <td data-bbox="520 913 683 958">mm 21.3 × 3.2</td> <td data-bbox="683 913 815 958">kN 2.61</td> <td data-bbox="815 913 948 958">2.11</td> <td data-bbox="948 913 1054 958">kN 5.5</td> </tr> <tr> <td data-bbox="384 958 520 1003">10 to 18</td> <td data-bbox="520 958 683 1003">26.9 × 3.2</td> <td data-bbox="683 958 815 1003">1.98</td> <td data-bbox="815 958 948 1003">2.30</td> <td data-bbox="948 958 1054 1003">4.6</td> </tr> <tr> <td data-bbox="384 1003 520 1055">19 to 24</td> <td data-bbox="520 1003 683 1055">42.4 × 3.2</td> <td data-bbox="683 1003 815 1055">3.11</td> <td data-bbox="815 1003 948 1055">2.15</td> <td data-bbox="948 1003 1054 1055">6.7</td> </tr> </tbody> </table> <p>c) Legs: $\Sigma F_{\max} \leq (1 + G_{\max}) \bar{F}_{\max} + F_{DEAD}$</p> <table border="1" data-bbox="384 1115 1054 1357"> <thead> <tr> <th data-bbox="384 1115 520 1176">Panels</th> <th data-bbox="520 1115 683 1176">Type (CHS)</th> <th data-bbox="683 1115 815 1176">\bar{F}_{\max}</th> <th data-bbox="815 1115 948 1176">$1 + G_{\max}$</th> <th data-bbox="948 1115 1054 1176">ΣF_{\max}</th> </tr> </thead> <tbody> <tr> <td data-bbox="384 1176 520 1220">1 to 3</td> <td data-bbox="520 1176 683 1220">mm 42.4 × 4.0</td> <td data-bbox="683 1176 815 1220">kN 9.4</td> <td data-bbox="815 1176 948 1220">2.11</td> <td data-bbox="948 1176 1054 1220">kN 20.4</td> </tr> <tr> <td data-bbox="384 1220 520 1265">4 to 9</td> <td data-bbox="520 1220 683 1265">60.3 × 4.0</td> <td data-bbox="683 1220 815 1265">27.0</td> <td data-bbox="815 1220 948 1265">2.08</td> <td data-bbox="948 1220 1054 1265">56.9</td> </tr> <tr> <td data-bbox="384 1265 520 1310">10 to 18</td> <td data-bbox="520 1265 683 1310">60.3 × 5.0</td> <td data-bbox="683 1265 815 1310">41.2</td> <td data-bbox="815 1265 948 1310">2.03</td> <td data-bbox="948 1265 1054 1310">85.6</td> </tr> <tr> <td data-bbox="384 1310 520 1357">19 to 24</td> <td data-bbox="520 1310 683 1357">76.1 × 5.0</td> <td data-bbox="683 1310 815 1357">66.9</td> <td data-bbox="815 1310 948 1357">2.00</td> <td data-bbox="948 1310 1054 1357">137.8</td> </tr> </tbody> </table>	b) Bracings: $\Sigma F_{\max} \leq (1 + G_{\max}) \bar{F}_{\max}$					Panels	Type (CHS)	\bar{F}_{\max}	$1 + G_{\max}$	ΣF_{\max}	1 to 9	mm 21.3 × 3.2	kN 2.61	2.11	kN 5.5	10 to 18	26.9 × 3.2	1.98	2.30	4.6	19 to 24	42.4 × 3.2	3.11	2.15	6.7	Panels	Type (CHS)	\bar{F}_{\max}	$1 + G_{\max}$	ΣF_{\max}	1 to 3	mm 42.4 × 4.0	kN 9.4	2.11	kN 20.4	4 to 9	60.3 × 4.0	27.0	2.08	56.9	10 to 18	60.3 × 5.0	41.2	2.03	85.6	19 to 24	76.1 × 5.0	66.9	2.00	137.8
b) Bracings: $\Sigma F_{\max} \leq (1 + G_{\max}) \bar{F}_{\max}$																																																			
Panels	Type (CHS)	\bar{F}_{\max}	$1 + G_{\max}$	ΣF_{\max}																																															
1 to 9	mm 21.3 × 3.2	kN 2.61	2.11	kN 5.5																																															
10 to 18	26.9 × 3.2	1.98	2.30	4.6																																															
19 to 24	42.4 × 3.2	3.11	2.15	6.7																																															
Panels	Type (CHS)	\bar{F}_{\max}	$1 + G_{\max}$	ΣF_{\max}																																															
1 to 3	mm 42.4 × 4.0	kN 9.4	2.11	kN 20.4																																															
4 to 9	60.3 × 4.0	27.0	2.08	56.9																																															
10 to 18	60.3 × 5.0	41.2	2.03	85.6																																															
19 to 24	76.1 × 5.0	66.9	2.00	137.8																																															
<p>2.5</p> <p>2.5</p>	<p>A.6 Strength assessment</p> <p>A.6.1 General</p> <p>a) <i>Required reliability.</i> To achieve the required reliability with respect to strength:</p> $\Sigma F_{\max} \leq Q_d$ <p>where</p> <p>ΣF_{\max} is the maximum total force in the member;</p> <p>Q_d is the design strength of the member given by:</p> Q_k / γ_m <p>where</p> <p>Q_k is the characteristic strength of the member.</p> <p>b) <i>Design strengths.</i> The values of Q_k, and hence Q_d, may be obtained from appropriate characteristic strengths, or may be conservatively obtained from DD 133, according to type and slenderness, as follows.</p> <p>NOTE The detailed calculations on the interpretation of DD 133 are not given here as the document is a Draft for Development.</p>																																																		

Reference in Part 1	Worked example 1																																																																																																			
	<table border="1" data-bbox="504 443 1256 768"> <thead> <tr> <th>Member</th> <th>Member type</th> <th>Q_k</th> <th>γ_m</th> <th>Q_d</th> </tr> </thead> <tbody> <tr> <td rowspan="3">Bracings</td> <td>mm</td> <td>kN</td> <td></td> <td>kN</td> </tr> <tr> <td>21.3×3.2</td> <td>8.8</td> <td>1.1</td> <td>8.0</td> </tr> <tr> <td>26.9×3.2</td> <td>9.8</td> <td>1.1</td> <td>8.9</td> </tr> <tr> <td></td> <td>42.4×3.2</td> <td>15.3</td> <td>1.1</td> <td>13.9</td> </tr> <tr> <td rowspan="4">Legs</td> <td>42.4×4.0</td> <td>35</td> <td>1.1</td> <td>32</td> </tr> <tr> <td>60.3×4.0</td> <td>95</td> <td>1.1</td> <td>86</td> </tr> <tr> <td>60.3×5.0</td> <td>138</td> <td>1.1</td> <td>125</td> </tr> <tr> <td>76.1×5.0</td> <td>214</td> <td>1.1</td> <td>195</td> </tr> </tbody> </table> <p data-bbox="504 786 1493 846">c) <i>Strength check.</i> The safety assessment in the form of a strength check is most conveniently set out in the form of stress ratios, SR, where:</p> $SR = \frac{\Sigma F_{\max}}{Q_d}$ <p data-bbox="504 931 1519 1055"><i>The required reliability is then achieved provided $SR \leq 1.0$.</i> The levels of SR also indicate the capacity of the tower for carrying extra loadings, either in the form of ancillary attachments, aerials, dishes, etc., or alternative sitings, such as on hills or in more severe meteorological zones. The SR values are as follows.</p> <table border="1" data-bbox="504 1077 1256 1514"> <thead> <tr> <th>Panels</th> <th>Member (CHS)</th> <th>ΣF_{\max}</th> <th>Q_d</th> <th>Maximum stress ratio (SR)</th> </tr> </thead> <tbody> <tr> <td></td> <td>mm</td> <td>kN</td> <td>kN</td> <td></td> </tr> <tr> <td><i>Bracings</i></td> <td></td> <td></td> <td></td> <td></td> </tr> <tr> <td>1 to 9</td> <td>21.3×3.2</td> <td>5.5</td> <td>8.0</td> <td>0.69</td> </tr> <tr> <td>10 to 18</td> <td>26.9×3.2</td> <td>4.6</td> <td>8.9</td> <td>0.52</td> </tr> <tr> <td>10 to 24</td> <td>42.4×3.2</td> <td>6.7</td> <td>13.9</td> <td>0.48</td> </tr> <tr> <td><i>Legs</i></td> <td></td> <td></td> <td></td> <td></td> </tr> <tr> <td>1 to 3</td> <td>42.4×4.0</td> <td>20.4</td> <td>32</td> <td>0.64</td> </tr> <tr> <td>4 to 9</td> <td>60.3×4.0</td> <td>56.9</td> <td>86</td> <td>0.66</td> </tr> <tr> <td>10 to 18</td> <td>60.3×5.0</td> <td>85.6</td> <td>125</td> <td>0.68</td> </tr> <tr> <td>19 to 24</td> <td>76.1×5.0</td> <td>137.8</td> <td>195</td> <td>0.71</td> </tr> </tbody> </table> <p data-bbox="504 1532 1519 1621">Hence the tower is satisfactory for the intended use at the site considered. There is a lower bound limit of about 40 % increase in load before the size of the members would need to be increased.</p>					Member	Member type	Q_k	γ_m	Q_d	Bracings	mm	kN		kN	21.3×3.2	8.8	1.1	8.0	26.9×3.2	9.8	1.1	8.9		42.4×3.2	15.3	1.1	13.9	Legs	42.4×4.0	35	1.1	32	60.3×4.0	95	1.1	86	60.3×5.0	138	1.1	125	76.1×5.0	214	1.1	195	Panels	Member (CHS)	ΣF_{\max}	Q_d	Maximum stress ratio (SR)		mm	kN	kN		<i>Bracings</i>					1 to 9	21.3×3.2	5.5	8.0	0.69	10 to 18	26.9×3.2	4.6	8.9	0.52	10 to 24	42.4×3.2	6.7	13.9	0.48	<i>Legs</i>					1 to 3	42.4×4.0	20.4	32	0.64	4 to 9	60.3×4.0	56.9	86	0.66	10 to 18	60.3×5.0	85.6	125	0.68	19 to 24	76.1×5.0	137.8	195	0.71
Member	Member type	Q_k	γ_m	Q_d																																																																																																
Bracings	mm	kN		kN																																																																																																
	21.3×3.2	8.8	1.1	8.0																																																																																																
	26.9×3.2	9.8	1.1	8.9																																																																																																
	42.4×3.2	15.3	1.1	13.9																																																																																																
Legs	42.4×4.0	35	1.1	32																																																																																																
	60.3×4.0	95	1.1	86																																																																																																
	60.3×5.0	138	1.1	125																																																																																																
	76.1×5.0	214	1.1	195																																																																																																
Panels	Member (CHS)	ΣF_{\max}	Q_d	Maximum stress ratio (SR)																																																																																																
	mm	kN	kN																																																																																																	
<i>Bracings</i>																																																																																																				
1 to 9	21.3×3.2	5.5	8.0	0.69																																																																																																
10 to 18	26.9×3.2	4.6	8.9	0.52																																																																																																
10 to 24	42.4×3.2	6.7	13.9	0.48																																																																																																
<i>Legs</i>																																																																																																				
1 to 3	42.4×4.0	20.4	32	0.64																																																																																																
4 to 9	60.3×4.0	56.9	86	0.66																																																																																																
10 to 18	60.3×5.0	85.6	125	0.68																																																																																																
19 to 24	76.1×5.0	137.8	195	0.71																																																																																																
<p>3.4.2.1</p> <p>5.1.5</p> <p>5.5</p>	<p>A.6.2 Vortex excitation</p> <p>a) <i>Overall response.</i> The cylindrical fibreglass shroud may cause vortex-excited vibrations and this needs to be checked in accordance with 5.5 of Part 1.</p>																																																																																																			

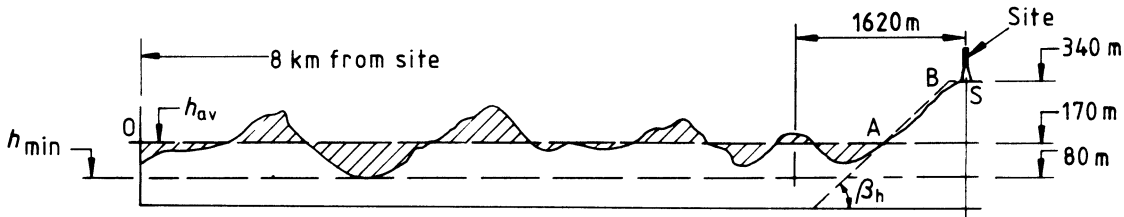
Reference in Part 1	Worked example 1
5.5.1	<p>b) <i>Critical wind speed in fundamental mode.</i> The lowest critical wind speed occurs at:</p> $V_{cr1} = \frac{n_1 D}{S}$ <p>For</p> <p>$n_1 = 1.9$ Hz (from an initial estimate of frequency); $S = 0.2$ for circular cylinders; $V_{cr1} = 6.6$ m/s.</p> <p>This is less than $1.3 \bar{V}_z (= 55$ m/s), thus the tower is subject to vibrations induced through vortex shedding.</p>
5.5.2	<p>The amplitudes and hence member forces so induced can be estimated by considering the tower under the influence of aerodynamic loads given by:</p> $.9\rho_a \bar{V}_e^2 k_e C' D_z \sin 2 \pi n t$ <p>per unit height</p>
Figure 5.8	<p>In order to obtain the largest force, the value $\bar{V}_e^2 k_e$ has to be maximized. This can be done using Figure 5.8 of Part 1 for various values of k_e. The maximum value occurs at $k_e = 0.75$, giving:</p> $\frac{1.3 \bar{V}_e}{V_{cr1}} = 1.2$ $\bar{V}_e = \frac{1.2}{1.3} \times 6.6$ $= 6.1 \text{ m/s}$ <p>Hence the maximum value that the fluctuating aerodynamic load can have in the fundamental mode is:</p> $0.9 \times 1.22 \times 6.1^2 \times 0.75 \times 0.3 \times 0.7 \times 1.0 = 6.5 \text{ N/m}$ <p>This is equivalent to a total load on the cylinder of 0.019 kN. The aerodynamic load effects may be assessed initially using the periodic dynamic magnifier $\pi/\Sigma\delta$. For crosswind response, aerodynamic damping, $\delta_a = 0$. Using Table E.1 and Table E.2 of Part 1, δ_T is taken as 0.06 and $K_\delta = 2$, for spread footing on medium soil. Hence $\Sigma\delta = K_\delta \delta_T = 0.12$</p> <p>Hence the effective dynamic load $\simeq \frac{\pi}{0.12} \times 0.019 = 0.5$ kN.</p> <p>The total equivalent static load on the cylinder is given by:</p> $(1 + G) \bar{P}_{TW} = (1 + 1.15) \times 1.56 = 3.35 \text{ kN}$ <p>Hence vortex shedding forces are approximately 15 % of this and may be neglected.</p>

Reference in Part 1	Worked example 1																										
<p>3.4.2.1</p> <p>3.3</p> <p>3.4.2.2</p>	<p>c) <i>Further modes.</i> Due to the low \bar{V}_{cr} in the fundamental mode, the tower has to be checked for higher modes. The next two modes of the tower have frequencies estimated as:</p> $n_2 = 6.9 \text{ Hz}$ $n_3 = 20.4 \text{ Hz}$ <p>Thus</p> $V_{cr2} = \frac{6.9 \times 0.7}{0.2} = 24 \text{ m/s} < 1.3 \bar{V}_z (= 55 \text{ m/s})$ <p>and</p> $\bar{V}_{e\max} = \frac{1.2}{1.3} \times 24 = 22 \text{ m/s for } K_e = 0.75$ <p>The maximum value of fluctuating aerodynamic force in the second mode is $0.9 \times 1.22 \times 22.0^2 \times 0.75 \times 0.3 \times 0.7 \times 1.0 = 84 \text{ N/m}$, which is equivalent to a total effective dynamic load of $\approx 3 \times 0.084 \times \pi/0.12 = 6.6 \text{ kN}$, which is approximately twice the total equivalent static load on the cylinder. However, this force (and to a lesser extent that from the fundamental frequency) will be reduced by mode shape considerations, when comparing with the equivalent static loads applied to the tower. Consequently, the effects of vortex shedding may be a governing criterion for the design of the strength of the tower, and a simple dynamic analysis should be made to derive load effects [see f)]. For the third frequency of vibration:</p> $V_{cr3} = 71 \text{ m/s} > 1.3 \bar{V}_z (= 55 \text{ m/s})$ <p>Thus vortex excitation should not occur in this or any higher mode, but this should also be checked by dynamic analysis in this case [see f)].</p> <p>d) <i>Fatigue.</i> The effect of the first and second modes of vortex excitation may need consideration for fatigue, in accordance with 3.4.2 of Part 1, and for serviceability, in accordance with 3.3 of Part 1 (see A.6.3).</p> <p>e) <i>Individual member response.</i> Slender tubular members may be subject to vortex shedding at low wind speeds. The slenderness of the members in this tower are such that the resulting stresses will be relatively small, but may need to be considered for fatigue.</p> <p>f) <i>Results from simple dynamic analysis.</i> The results from simple dynamic analysis are as follows.</p> <table border="1" data-bbox="504 1576 1283 1839"> <thead> <tr> <th rowspan="2">Mode</th> <th rowspan="2">Frequency</th> <th rowspan="2">V_{cr}</th> <th rowspan="2">δ</th> <th colspan="2">Ratio dynamic/static</th> </tr> <tr> <th>Shear</th> <th>Moment</th> </tr> </thead> <tbody> <tr> <td>Mode 1</td> <td>1.7 Hz</td> <td>6.1 m/s</td> <td>13 mm</td> <td>0.08</td> <td>0.09</td> </tr> <tr> <td>Mode 2</td> <td>7.4</td> <td>26.0</td> <td>5</td> <td>0.35</td> <td>0.40</td> </tr> <tr> <td>Mode 3</td> <td>18.9</td> <td colspan="4">66.1 \rightarrow exceeds $1.3 \bar{V}_z$</td> </tr> </tbody> </table> <p>The maximum load effects are less than 40 % of the static design criteria, and hence will not govern.</p>	Mode	Frequency	V_{cr}	δ	Ratio dynamic/static		Shear	Moment	Mode 1	1.7 Hz	6.1 m/s	13 mm	0.08	0.09	Mode 2	7.4	26.0	5	0.35	0.40	Mode 3	18.9	66.1 \rightarrow exceeds $1.3 \bar{V}_z$			
Mode	Frequency					V_{cr}	δ	Ratio dynamic/static																			
		Shear	Moment																								
Mode 1	1.7 Hz	6.1 m/s	13 mm	0.08	0.09																						
Mode 2	7.4	26.0	5	0.35	0.40																						
Mode 3	18.9	66.1 \rightarrow exceeds $1.3 \bar{V}_z$																									

Reference in Part 1	Worked example 1
2.6	A.6.3 Serviceability
3.3	a) <i>General</i> . The serviceability criteria have been specified as a limiting deflection of 50 mm, not to be exceeded for more than 20 h per year, i.e. $\Delta_s = 50$ mm, the specified deflection limit.
5.1.4	b) <i>Downwind deflections</i> . From the analysis under mean hourly loading, the maximum deflection, $\delta = 78$ mm at the level of the shroud.
5.2.5	From 5.2.5 of Part 1 $\Delta = (1 + G_{B \text{ base}}) \times \delta = 1.98 \times 78 = 154 \text{ mm}$
	Hence
3.3.2	$\frac{\bar{V}_s}{V_k} = \gamma_v \sqrt{\left(\frac{\Delta_s}{\Delta}\right)} = 1.15 \sqrt{\left(\frac{50}{154}\right)} = 0.66$
Figure 3.6	This limiting deflection is independent of the angle of wind incidence, hence from Figure 3.6 of Part 1, the number of hours per year that the aerial will be out of service is 18 h and hence the criteria are satisfied, and the wind speed \bar{V}_s at which the limit occurs = $0.66 \times 30.9 = 20.4$ m/s.
3.1.5	
3.3.3	a) <i>Crosswind deflections (vortex shedding)</i> . The forces due to vortex excitation have been derived from a simple dynamic analysis, the results giving the crosswind deflection, as
5.5.2	$\delta_1 = 13$ mm in the first mode
	$\delta_2 = 5$ mm in the second mode [see A.6.4 b)]
	i.e. $\Delta'_{\text{max}} = 13$ mm and hence $\Delta_s (= 50$ mm) is never exceeded.
	Therefore it is satisfactory.
	NOTE If an aerial, more sensitive to deflection, was proposed such that $\Delta_s = 12$ mm, but the period of unavailability were increased to 600 h per year, the following results would be obtained.
	1) Downwind:
	$\frac{\bar{V}_s}{V_k} = 1.15 \sqrt{\left(\frac{12}{154}\right)} = 0.32$
Figure 3.6	The period out of service (see Figure 3.6 of Part 1) = 2 100 h per year.
	2) Crosswind:
	$\bar{V}_s = 6.1$ m/s in the first mode, for which $\Delta' = 13$ mm is greater than Δ_s (12 mm), giving:
Figure 3.8 b)	$\frac{\bar{V}_s}{V_k} = \frac{6.1}{30.9} = 0.20$
3.3.3	From Figure 3.8 of Part 1, at 240° annual occurrence = 290 h, and total time out of service = $290 \times 6.5 = 1\ 880$ h/year
	For higher modes, $\delta < \Delta_s$ and need not be considered.
	3) Total period out of service = 3 980 h = 5 months which is unsatisfactory.

Reference in Part 1	Worked example 1
<p>3.4.1</p> <p>3.4.2</p> <p>3.4.2.1</p> <p>3.3.3</p> <p>3.4.2.2</p>	<p>A.6.4 Fatigue</p> <p>a) <i>In-line vibrations</i>. Since the tower is of steel grade 43 complying with BS 4360, i.e. yield stress ≤ 355 N/mm², the fatigue life can be assumed to exceed 50 years if bolted connections are used. If welded, the fatigue life may still be assumed to be 30 years, without further checks, and is therefore satisfactory for the intended service life.</p> <p>b) <i>Vortex-excited vibrations</i>. The vortex-excited vibrations are as follows.</p> <p>1) <i>Overall response</i>. Duration of first mode of vibration:</p> $\frac{\bar{V}_s}{\bar{V}_k} = \frac{6.6}{30.9} = 0.21$ <p>Number of hours per year = $6.5 \times 290 = 1\ 890$ h/year But stress levels $< 10\%$ of maximum equivalent static stress. Duration of second mode of vibration:</p> $\frac{\bar{V}_s}{\bar{V}_k} = \frac{22}{30.9} = 0.71$ <p>Number of hours per year = $6.5 \times 13 = 85$ h/year But stress levels $\leq 40\%$ of maximum equivalent static stress. These values can be checked against the appropriate fatigue criteria, but should not result in any reduction on the 30 year life.</p> <p>2) <i>Individual member response</i>. The stress range will be small, and need not be considered further for this particular tower.</p> <p>A.6.5 Summary</p> <p>A.1 to A.6.4 complete the design process for the intended use of the tower at the particular site. However this tower may also need to be assessed for use on a hill site and for use abroad. The preliminary calculations required are set out in A.7 and the results are summarized as follows.</p>
<p>Figures 3.4 and 3.5</p> <p>3.2.2</p>	<p>a) <i>Alternative site on hill</i>. The comparison of wind loads shows that, for the particular hill site chosen, the wind loads (and hence member forces) increase by an overall factor greater than two, and hence a full redesign would be required for such a site. The maximum increase in wind speed due to a hill that could be accommodated by the present design is only of the order of $\sqrt{1.4} = 1.2$. Inspection of Figures 3.4 and 3.5 of Part 1 and use of 3.2 of Part 1 show that the factor on wind speed at any height z is given by:</p> $\left(\frac{K_\mu}{z}\right)^\mu$ <p>This can be used to check initially the acceptability of any hill site, e.g. for a 30 m high hill of slope $\beta = 6^\circ$, at a height of 20 m:</p> $\left(\frac{K_\mu}{z}\right)^\mu \approx \frac{1.27}{2^{0.007}} = 1.21$ <p>This may be shown to be satisfactory with further detailed study.</p> <p>b) <i>Alternative overseas site</i>. This shows an increase in wind load of about 1.6 and the basic tower could only be used with most members increased as required following further analyses.</p>

Reference in Part 1	Worked example 1
	<p>A.7 Alternative sites</p> <p>A.7.1 Alternative site on hill</p> <p>For an alternative site on a hill the following preliminary calculations are required.</p> <p>a) Assume the tower was sited on a nearby hill as shown in the following figure with the site level = 340 m.</p>



Appendix D

$h_{av} = 170 \text{ m}, h_{min} = 80 \text{ m}$
 $18 (h_{av} - h_{min}) = 1\ 620 \text{ m}$
 The hill is defined by OABS.
 Hence the height of the hill, $H = 340 - 170 = 170 \text{ m}$

Slope = $\sin^{-1} \left(\frac{170}{1000} \right) = 9.8^\circ; x \approx 80 \text{ m}$

Hence:

$K_\mu = 1.64; K_{\mu x} = 1.64 - \frac{80 \times 0.64}{18 \times 170} = 1.62$

$\mu = 0.101; \mu_x = 0.101 \left(1 - \frac{80}{18 \times 170} \right) = 0.098$

so $\bar{V}_r K_{\mu x} = 57.5 \text{ m/s}; \alpha - \mu_x = 0.042$
 and $\bar{V}_z = 57.5 (z/10)^{0.042}$ for $z \geq 10$
 $28.8 (1 + z/10)$ for $z < 10$

b) A comparison can be made with that for the level site. Table A.7.1 gives the ratio of factored wind speeds and also the ratio of wind speeds squared to give an indication of the increase in loading.

Table A.7.1 — Comparison of wind profiles

Height z	\bar{V}_{zh} (hill)	\bar{V}_{zf} (flat)	$\frac{\bar{V}_{zh}}{\bar{V}_{zf}}$	$\left(\frac{\bar{V}_{zh}}{\bar{V}_{zf}} \right)^2$
m	m/s	m/s		
27.5	60.0	40.9	1.47	2.15
21.5	59.4	39.5	1.50	2.26
12.5	58.0	36.6	1.59	2.51
1.0	31.8	19.5	1.63	2.66

c) Inspection of column 5 of Table A.7.1 indicates that for the identical tower situated on the hill, member forces will increase by a factor of approximately **2.3**. Since resistances and gust factors are unchanged, the total member forces will be likewise factored by **2.3**. Inspection of the strength checks given in **A.6.1 c)** indicates that the tower members will be under-strength, and increased sizes are required.

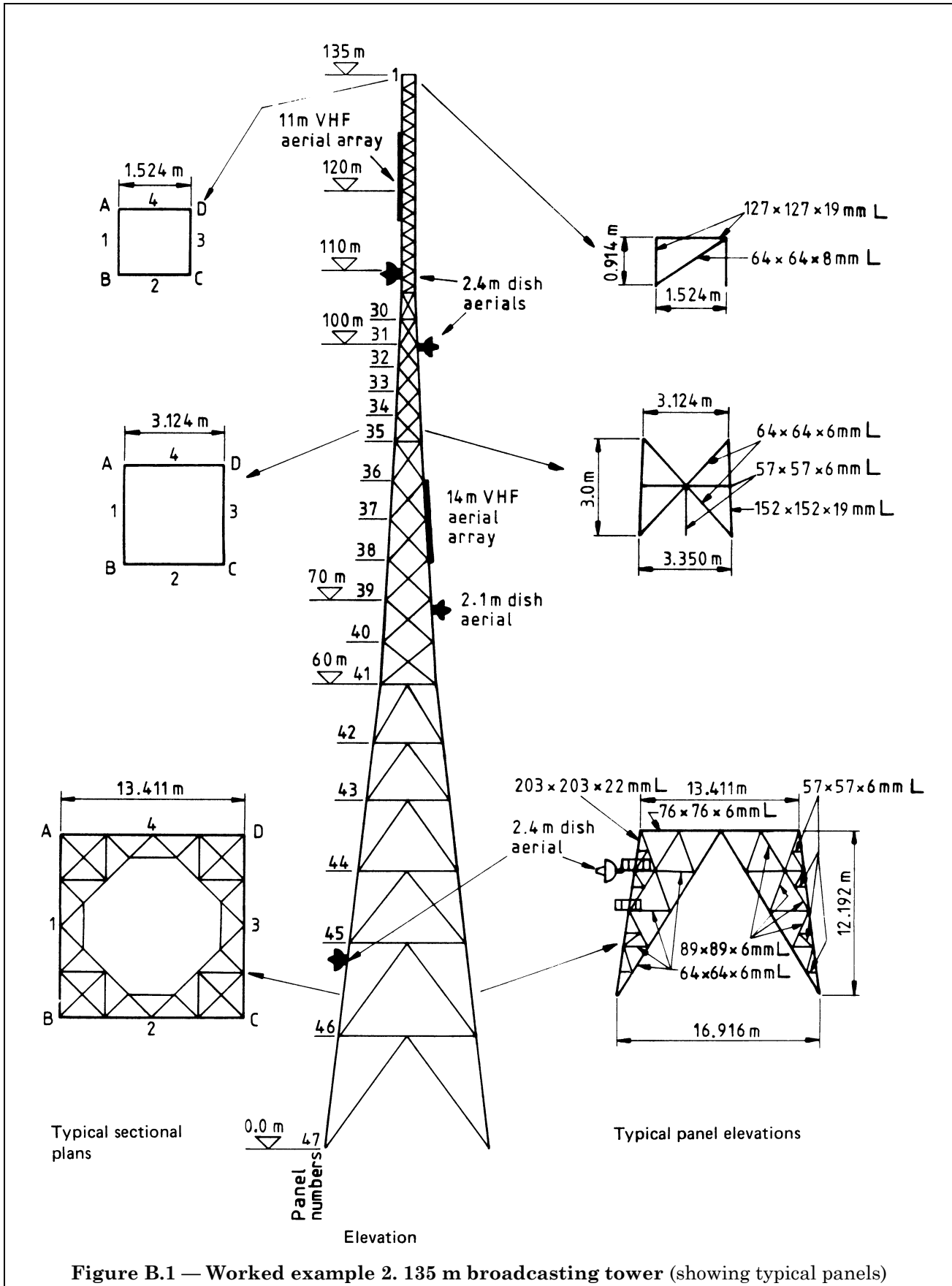
The deflections will also increase, and hence the serviceability criteria will need to be reassessed. Additional analyses should be made, as required.

Reference in Part 1	Worked example 1
<p>3.1.1</p> <p>3.1.2</p> <p>A.1.5</p> <p>(C.3.1.2 of this Part of BS 8100)</p> <p>A.1.6</p> <p>Appendix C C.2</p> <p>Figure C.2</p> <p>(Table C.3.2 of this Part of BS 8100) Figure A.1</p>	<p>A.7.2 Alternative site with limited wind data</p> <p>The tower is a standard design developed for use both in the UK and overseas. An example of an alternative location with limited wind data is as follows.</p> <p><i>Basic wind speed</i></p> <p>a) \bar{V}_B has to be derived from a statistical analysis since there are no appropriate official Meteorological Office wind maps of the site. The site is near a local airport where the mean hourly wind speed data has been recorded for only 13 years, consequently a coefficient of variation of 0.2 has been taken. Thus for the recording station, for a height of 10 m:</p> $\bar{V}_{av} = 32.0 \text{ m/s}, \nu = 0.20$ $\frac{\bar{V}_{max}}{\bar{V}_{av}} = 1 + 2.6\nu \text{ (50 year return period)}$ <p>Hence:</p> $\bar{V}_{max} = 1.52 \times 32.0$ $= 48.6 \text{ m/s}$ <p>The airport terrain is category II thus \bar{V}_{max} has to be divided by the appropriate value of K_R to obtain \bar{V}_B, the basic wind speed:</p> $\bar{V}_B = \bar{V}_{max}/K_R$ $= 48.6/1.10 = \underline{44.2} \text{ m/s}$ <p>No correction for altitude is required since the airport and site are the same height above sea level.</p> <p>b) Data from similar climatic zones have been examined and a gradient wind speed of 70 m/s has been used as a probable value. The gradient wind height was 1 000 m for the zone data.</p> <p>Using Figure C.2 of Part 1, a value for the gradient wind speed reduction factor, K_g, is obtained.</p> $K_g = 0.57 \text{ (for site 10 km from the coast and gradient wind height of 1 000 m)}$ <p>Thus:</p> $\bar{V}_B = 0.57 \times 70$ $= \underline{39.9} \text{ m/s}$ <p>c) An additional data source is a code for which a design wind speed of 69 m/s is appropriate.</p> <p>This is a 2 s to 3 s gust wind speed, and the terrain category of that code corresponds with the basic terrain category of Part 1.</p> $V_t/\bar{V} = 1.55 \text{ for 2 s to 3 s gust, giving:}$ $\bar{V} = \bar{V}_B = 69/1.55 = \underline{44.5} \text{ m/s}$ <p>d) Thus \bar{V}_B has been adopted as that obtained from site measurements since the value has been approximately confirmed using wind speeds from remote stations and gradient wind data.</p> <p>Consequently, the predicted value from a) will be used, and \bar{V}_B is taken as 44.2 m/s.</p>

Reference in Part 1	Worked example 1																														
<p>3.1.3 3.1.4 Table 3.1</p> <p>Figure 2.1 3.2.5</p> <p>3.2.1</p>	<p>e) The terrain for the site in category IV and the ground is essentially flat. A wind profile may be developed for the site using the parameters from Part 1. $K_d = 1.0$ (for no icing)</p> <p>Terrain category IV, therefore: $K_R = 0.86$; $h_e = 2$; $\alpha = 0.19$. $\gamma_v = 1.15$ (using the same criteria as the East Riding site)</p> <p>NOTE There may need to be a modification to γ_m (see notes in A.2.3)</p> $\bar{V}_T = \gamma_v K_d K_H \bar{V}_B$ $= 1.15 \times 1.0 \times 0.86 \times 44.2$ $= 43.7 \text{ m/s}$ <p>The wind profile is:</p> $\bar{V}_z = 43.7 \left(\frac{z-2}{10} \right)^{0.19} \text{ for } z \geq 12 \text{ m};$ $= 21.85 \left(1 + \frac{z}{12} \right) \text{ for } z < 12 \text{ m}.$ <p>A comparison between the wind speeds at the alternative site and at East Riding is as follows.</p> <table border="1" style="width: 100%; border-collapse: collapse; text-align: center;"> <thead> <tr> <th>Height</th> <th>\bar{V}_{zT} (alternative)</th> <th>\bar{V}_{zR} (E.Riding)</th> <th>$\frac{\bar{V}_{zT}}{\bar{V}_{zR}}$</th> <th>$\left(\frac{\bar{V}_{zT}}{\bar{V}_{zR}} \right)^2$</th> </tr> </thead> <tbody> <tr> <td>m</td> <td>m/s</td> <td>m/s</td> <td></td> <td></td> </tr> <tr> <td>27.5</td> <td>53</td> <td>40.9</td> <td>1.29</td> <td>1.66</td> </tr> <tr> <td>21.5</td> <td>50</td> <td>39.5</td> <td>1.27</td> <td>1.62</td> </tr> <tr> <td>12.5</td> <td>41</td> <td>36.6</td> <td>1.16</td> <td>1.35</td> </tr> <tr> <td>1.0</td> <td></td> <td>19.5</td> <td></td> <td></td> </tr> </tbody> </table> <p>f) The tower has been designed as a standard tower which can be used in several locations. At its East Riding site, it is approximately 70 % fully stressed. Thus at the alternative site, the same tower could only be used by strengthening critical members since the increased wind loading would produce a stress increase of about 60 %, giving a maximum stress ratio $\approx 1.6 \times 0.7 = 1.12$.</p>	Height	\bar{V}_{zT} (alternative)	\bar{V}_{zR} (E.Riding)	$\frac{\bar{V}_{zT}}{\bar{V}_{zR}}$	$\left(\frac{\bar{V}_{zT}}{\bar{V}_{zR}} \right)^2$	m	m/s	m/s			27.5	53	40.9	1.29	1.66	21.5	50	39.5	1.27	1.62	12.5	41	36.6	1.16	1.35	1.0		19.5		
Height	\bar{V}_{zT} (alternative)	\bar{V}_{zR} (E.Riding)	$\frac{\bar{V}_{zT}}{\bar{V}_{zR}}$	$\left(\frac{\bar{V}_{zT}}{\bar{V}_{zR}} \right)^2$																											
m	m/s	m/s																													
27.5	53	40.9	1.29	1.66																											
21.5	50	39.5	1.27	1.62																											
12.5	41	36.6	1.16	1.35																											
1.0		19.5																													

Appendix B Worked example 2

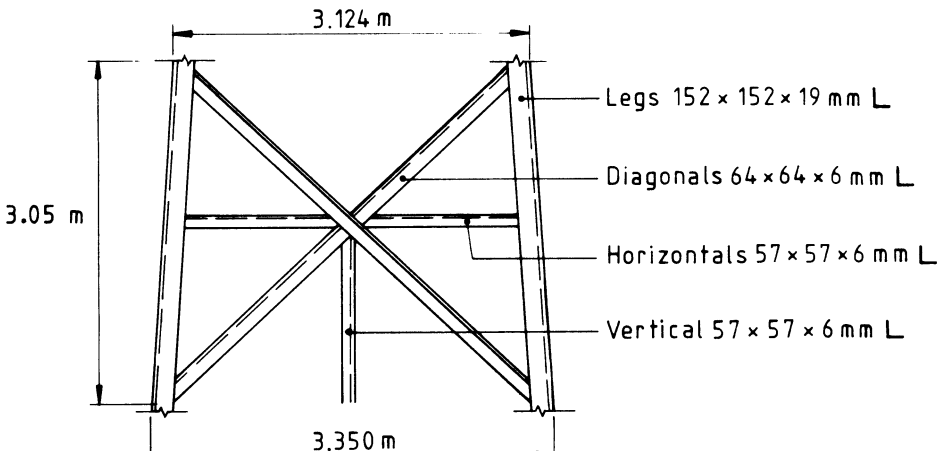
Reference in Part 1	Worked example 2
	<p>B.1 Site and tower details</p> <p>B.1.1 General The tower is an existing structure and is located in the New Forest in a wooded area. The ground is gently undulating and may be treated as level ground. The altitude of the site is 60 m AMSL. The structure is a square tower 135 m high and is to be considered as a manned broadcasting tower. It is located alongside a railway, but otherwise is away from any form of habitation. The tower is to be checked with both existing and proposed dishes and aerials mounted on it.</p> <p>B.1.2 Form of structure The general form of the tower is shown in Figure B.1, which also indicates the panels for which specific calculations are made in relation to this example. All sections used are equal angles of various sizes as shown.</p>
<p>2.1</p> <p>2.1.2</p>	<p>B.2 Performance requirements</p> <p>B.2.1 Service life and safety factors Long-term planning will lead to a replacement for this tower in about 20 years time. Allowing for some change in planning times, the required service life is taken as 25 years. The safety factors appropriate to the required reliability of the tower are derived as given in B.2.2 to B.2.4.</p>
<p>2.2</p> <p>2.2.2</p> <p>2.2.3.2</p> <p>2.2.3.3</p>	<p>B.2.2 Classification of required reliability</p> <p>a) <i>Environmental conditions</i>. The environmental category is that of “adjacent to railway”.</p> <p>b) <i>Economic consequences or usage</i>. A value of $g = 4.5$ has been determined for the ratio of consequential costs of failure to present costs, taking account of the costs of replacement, removal of the failed tower, loss of revenue during inoperation and contingency costs such as third-party claims. The alternative usage category is “broadcasting”.</p>
<p>2.3</p> <p>2.3.2</p> <p>Appendix F</p>	<p>B.2.3 Classification of quality The tower complies with all the recommendations of 2.3.2 of Part 1 in that it had been designed and fabricated in accordance with the appropriate British Standards and is being independently appraised and inspected. The construction and quality control of materials was in accordance with the relevant British Standards. The tower is inspected every 2 years for damage, corrosion or other defects. As a result the tower is deemed to be class A. NOTE Appendix F of Part 1 may also be used to assess the tower class (see Appendix A for a typical example).</p>
<p>2.4</p> <p>2.4.1</p> <p>Figure 2.1</p>	<p>B.2.4 Safety factors</p> <p>a) <i>Wind speed and ice thickness factors</i>. From Figure 2.1 of Part 1: 1) from the environmental category of “adjacent to railway”: $\gamma_v = 1.21$</p>



Reference in Part 1	Worked example 2
<p>Figure 2.1 (C.2.5 of this Part of BS 8100) 2.4.2 Figure 2.1 (or Table C.2.2 of this Part of BS 8100) 2.5 Figure 2.1</p>	<p>2) from the economic consequences: $\log_{10}(gi_s) = (4.5 \times 25) = 2.05$ which gives $\gamma_v = 1.17$ to 1.22 (This is further to the right than “broadcasting” usage which gives $\gamma_v = 1.15$) In this case (1) and (2) give similar values, and the wind speed factor will be taken as $\gamma_v = \underline{1.21}$. b) <i>Dead load factors</i>. Again using the same governing performance requirement from a), the dead load factors from Figure 2.1 of Part 1 are: $\gamma_{DL} = 1.06$ when dead load effects increase wind load effects; 0.90 when dead load effects decrease wind load effects. c) <i>Partial safety factor on strength</i>. From Figure 2.1 of Part 1: $\gamma_m = \underline{1.10}$ for quality class A.</p>
<p>3.1 3.1.2 Figure 3.1 3.1.3 3.1.4 Note 3 to Table 3.1 Note 4 to Table 3.1 (C.3.7 of this Part of BS 8100) (Figure C.3.33 of this Part of BS 8100) (Figure C.3.31 of this Part of BS 8100) (Figure C.3.32 of this Part of BS 8100) Table 3.1</p>	<p>B.3 Meteorological parameters B.3.1 General a) <i>Basic wind speed</i>. Using Figure 3.1 of Part 1 wind speed is given as 21.4 m/s at 10 m AMSL. The site is 60 m AMSL and hence the basic mean hourly wind speed is: $\bar{V}_B = 21.4 \times 1.06 = \underline{22.7}$ m/s b) <i>Wind direction factor</i>. The site is such that there is no marked difference in terrain with direction near the site nor are there topographic effects requiring factoring of wind speed in any particular direction. Also, the structural configuration of the tower is symmetrical, and the overall wind resistance will be sensibly constant for each face or diagonal wind direction. Hence, for wind without ice, K_d will be taken as 1.0, and for wind with ice K_d will be taken as 0.85. c) <i>Terrain roughness parameters</i>. The wooded terrain surrounding the site extends generally 10 km in the westerly, northerly and easterly directions, but the coast is situated 3 km away to the south at one point. Also there is an area of cleared farmland extending approximately 2 km, starting 2 km away to the north-west, and hence the effects of terrain roughness should be considered, since the site has rougher terrain within a few kilometres upwind, than that outside this area for upwind directions to the north-west and to the south. Using C.3.7 which gives guidance on terrain changes, the effect of the open farmland to the north-west can be neglected since the extent of the open area is less than the distance to the site with category V terrain both inside and outside, i.e. complying with situation b) of Figure C.3.33 of this Part of BS 8100. For the coastal effect to the south, use can be made of Figure C.3.31 and Figure C.3.32 of this Part of BS 8100. For a 3 km distance to the change of terrain, the mean hourly ABL is well above the top of the tower, and the gust ABL intersects the tower at a level of 120 m (see Figure C.3.32 of this Part of BS 8100). Hence the tower is virtually entirely encompassed by the wind profile of terrain category V and this is used for design. From Table 3.1 of Part 1 the terrain parameters are: $K_R = 0.72$; $\alpha = 0.23$ $h_e = 10$ m</p>

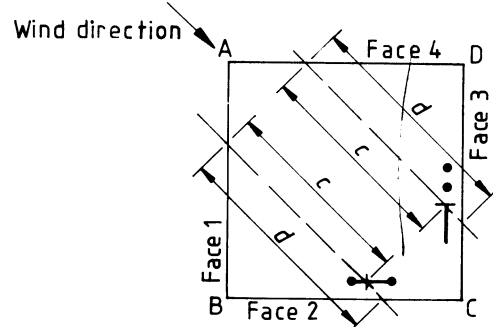
Reference in Part 1	Worked example 2
<p>3.2.1 Figure 3.3 Table 3.1 (Figure C.3.1 of this Part of BS 8100)</p> <p>3.1.5</p>	<p>Part 1 permits interpolation for values of h_e and K_R through the use of Figure 3.3 of Part 1. The terrain description given in Table 3.1 of Part 1 for category V describes the site conditions suitably, so Figure 3.3 of Part 1 has not been used; the parameters and terrain description are confirmed from Figure C.3.1 of this Part of BS 8100.</p> <p>d) <i>Site reference wind speed.</i> The mean hourly wind speed at the site at a height of 20 m, i.e. 10 m above the effective level of surface obstructions, is:</p> $\bar{V}_r = \gamma_v K_d K_R \bar{V}_B$ $= 1.21 \times 1.0 \times 0.72 \times 22.7 = \underline{19.8} \text{ m/s}$ <p>For serviceability, if required:</p> $\bar{V}_r = K_R \bar{V}_B$ $= 0.72 \times 22.7 = \underline{16.3} \text{ m/s}$
<p>3.2 3.2.1</p>	<p>B.3.2 Wind profile</p> <p>The site is on level ground, therefore 3.2.1 of Part 1 is used to obtain the wind profile. The mean wind speed \bar{V}_z at any required height z above the site ground level, i.e. the base of the tower, is determined for ice-free conditions from:</p> $\bar{V}_z = 19.8 \left(\frac{z}{10} - 1 \right)^{0.23} \quad \text{for } z \geq 20 \text{ m;}$ $= 9.9 \left(1 + \frac{z}{20} \right) \quad \text{for } z < 20 \text{ m.}$
<p>3.3 5.5</p>	<p>B.3.3 Serviceability</p> <p>Serviceability is dealt with in 3.3 of Part 1 and is considered independently from the derivation of loads and strength (safety) assessment. This calculation is carried out after the analyses are made together with any assessment of vortex shedding (see 3.3.3 and 5.5 of Part 1). These checks have not been carried out for this tower, but would be similar to those detailed in Appendix A, A.6.3.</p>
<p>3.4 5.5</p>	<p>B.3.4 Fatigue</p> <p>Fatigue is dealt with in 3.4 of Part 1 and is considered independently from the derivation of loads and strength (safety) assessment. This calculation is carried out after the analyses are made together with any assessment of vortex shedding (see 3.4.2 and 5.5 of Part 1). These checks have not been carried out for this tower, but would be similar to those detailed in Appendix A, A.6.4.</p>
<p>3.5 3.5.2 Figure 3.9</p> <p>3.5.3 3.5.4 3.5.1</p>	<p>B.3.5 Ice loading</p> <p>a) <i>Basic ice thickness.</i> The ice thickness appropriate to the site are taken from the map in Figure 3.9 of Part 1. At the site of the tower in the New Forest, the following thicknesses are obtained:</p> $r_o = 50 \text{ mm (in the absence of wind);}$ $r_w = 0 \text{ (with wind).}$ <p>The altitude of the tower top is $a_T = a_o + H$, giving $a_T = 60 + 135 = 195 \text{ m}$, which is less than 200 m and hence there is no increase on r_o and r_w.</p> <p>Also $k_i = 1.0$ since all sections are angles, and $r_B = r_o$ or r_w, as appropriate.</p> <p>b) <i>Reference ice thickness, ice weight and combinations.</i> For the case of wind with ice, $r_r = 0$, and hence no further considerations of wind with ice are required, and the only combination to be considered is wind only (ice free).</p>

Reference in Part 1	Worked example 2
<p>4.1</p> <p>4.1.1</p>	<p>B.4 Wind resistance</p> <p>B.4.1 General</p> <p>The tower has already been divided into 47 panels in the reference data provided, such that each panel encompasses a set of primary diagonal cross-bracing.</p> <p>NOTE More typically, however, some of the upper panels would be aggregated up, to about 6 m heights of tower, since $0.05 \times 135 = 6.75$ m, halving the total number of panels for the purposes of wind resistance calculation from 47 to about 23.</p> <p>Three panels have been selected to demonstrate the use of Part 1. These three panels (numbers 1, 35 and 46 as indicated in Figure B.1) show the effects of the various ancillaries which are likely to be encountered in the full analysis of the tower.</p> <p>The panels have been selected so as to demonstrate the three different methods of calculating panel resistances and tower response.</p>
<p>4.1.2</p> <p>4.2</p>	<p>B.4.2 Panel 1</p> <p>There are no ancillaries on panel 1, thus it complies with 4.1.2 of Part 1. Consequently the total resistance can be derived in accordance with 4.2 of Part 1.</p>
<p>4.2.1</p> <p>Figure 4.1</p> <p>Figure 4.2</p>	<div data-bbox="571 952 1295 1236" data-label="Diagram"> </div> <p>The panel is composed of flat sections only, so:</p> $A_s = A_f = (0.127 \times 0.914 \times 2) + \{(1.524 - 0.254) \times 0.127\} + (1.494 \times 0.064) = \underline{0.49 \text{ m}^2}$ $\phi = \frac{A_s}{ht} = \frac{0.49}{0.914 \times 1.524} = \underline{0.35}$
<p>4.2.2</p> <p>Figure 4.3 a)</p>	<p>The wind incidence factor, K_θ, is derived from Figure 4.2 of Part 1 for $A_f/A_F = 1.0$ and $\phi = 0.35$.</p> <p>For wind on face ($\theta = 0^\circ$), $K_\theta = 1.0$.</p> <p>For wind on diagonal ($\theta = 45^\circ$), $K_\theta = 1.19$.</p> <p><i>Drag coefficients</i></p> <p>From $C_N = C_{Nf} \frac{A_f}{A_F} + C_{Nc} \frac{A_c}{A_F} + C_{Nc'} \frac{A_{c'}}{A_F}$</p> $A_c = A_{c'} = 0, \text{ and } A_f = A_F$
<p>4.2.1 a)</p> <p>4.2.1 b)</p>	<p>Hence $C_N = C_{Nf} = 2.36$</p> $R_w = R_T = K_\theta C_N A_s$ <p>For $\theta = 0^\circ$</p> $R_w = 1.0 \times 2.36 \times 0.49 = \underline{1.16 \text{ m}^2}$ <p>and $R_x = R_w = 1.16 \text{ m}^2$</p> <p>For $\theta = 45^\circ$</p> $R_w = 1.19 \times 2.36 \times 0.49 = \underline{1.39 \text{ m}^2}$ <p>and $R_x = R_w = 1.39 \text{ m}^2$</p>

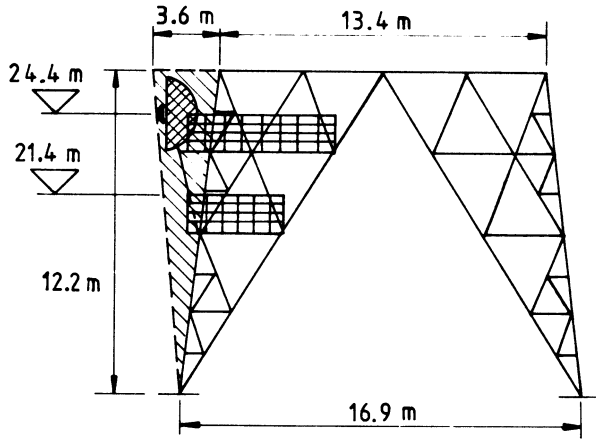
Reference in Part 1	Worked example 2
4.1.2	<p>B.4.3 Panel 35 Panel 35 contains several ancillaries in the form of ladders and feeder trays, etc. and hence the panel resistances cannot be derived in accordance with 4.2 of Part 1.</p>
4.1.3	<p>NOTE The ancillaries are not reasonably identical on each face, and hence cannot be treated as structural members in accordance with 4.2 of Part 1.</p>
4.1.3	<p>However, approximate calculation of face areas shows the following.</p>
4.1.3	<p>a) Maximum projected area of ancillaries in any face is less than 0.9 m²; minimum area of structural members in any face is greater than 1.3 m², and hence:</p>
4.1.3	$\frac{\Sigma A_A}{\Sigma A_F} \leq \frac{0.9}{1.3} = 0.69 < 1.0$
4.1.3	<p>Therefore the panel complies with 4.1.3 a) of Part 1.</p>
4.1.3	<p>b) Gross face area $\approx 10 \text{ m}^2$, and $\frac{A_{A \text{ max}}}{A_g} \leq \frac{0.9}{10} = 0.09 < 0.5$</p>
4.1.3	<p>Therefore the panel complies with 4.1.3 b) of Part 1.</p>
4.1.3	<p>c) No ancillaries extend outside the legs.</p>
4.1.3	<p>Therefore the panel complies with 4.1.3 c) of Part 1.</p>
4.3.1	<p>Hence, the total resistance may be derived in accordance with 4.3 of Part 1 without recourse to the recommendations of 4.4 of Part 1.</p>
4.3.1	<p>The total panel resistance, ΣR_w is given by:</p>
4.3.1	$\Sigma R_w = R_T + R_{AW}$
4.3.1	<p>The bare tower is composed of flat sections only, and is identical in each face. Its resistance, R_T, can thus be dealt with in an identical manner to panel 1 (see B.4.2).</p>
4.2.1 a)	 <p>The diagram shows a square tower section with a height of 3.05 m. The top width is 3.124 m and the bottom width is 3.350 m. The tower is composed of flat sections: legs, diagonals, horizontals, and a vertical member. The labels for the members are: Legs 152 x 152 x 19 mm L, Diagonals 64 x 64 x 6 mm L, Horizontals 57 x 57 x 6 mm L, and Vertical 57 x 57 x 6 mm L.</p>
4.2.1 a)	$A_s = A_f = (0.152 \times 3.05 \times 2) + (4.445 \times 0.064 \times 2) + (3.124 \times 0.057) + (1.524 \times 0.057) = 1.76 \text{ m}^2$
Figure 4.1	$\phi = \frac{2A_s}{h(b_1 + b_2)} = \frac{2 \times 1.76}{3.05(3.12 + 3.35)} = 0.18 \text{ i.e. that appropriate to the bare tower.}$
Figure 4.2	<p>The wind incidence factor, K_θ, is derived from Figure 4.2 of Part 1 for $A_f/A_F = 1.0$ and $\phi = 0.18$:</p>
Figure 4.2	<p>For wind on face ($\theta = 0^\circ$), $K_\theta = 1.0$;</p>
Figure 4.2	<p>For wind on diagonal ($\theta = 45^\circ$), $K_\theta = 1.11$.</p>

Reference in Part 1	Worked example 2
Figure 4.3 a)	<p><i>Drag coefficients</i> $A_s A_f = A_F$ For $\phi = 0.18$, $C_N = C_{Nf} = 2.95$: $R_T = K_\theta C_N A_s$</p>
4.2.1 a)	<p>For $\theta = 0^\circ$: $R_T = 1.0 \times 2.95 \times 1.76 = 5.19 \text{ m}^2$</p>
4.2.1 b)	<p>For $\theta = 45^\circ$: $R_T = 1.11 \times 2.95 \times 1.76 = 5.76 \text{ m}^2$</p>
Figure 4.1	<p>The ancillaries are all linear, comprising a ladder, feeders and a cable tray. Hence their wind resistance may be derived in accordance with 4.5 of Part 1.</p>
4.5	<p>The resistance is evaluated in accordance with 4.5 of Part 1, i.e.</p> $R_{AW} = C_N K_A A_A \sin^2 \psi$ <p>where</p> $K_A = K_A' \left\{ 1 - \frac{c}{2d} + \frac{2}{3} \left(\frac{c}{d} \right)^2 \right\}$
Table 4.2	<p>The following items are constant for all faces:</p> <ol style="list-style-type: none"> $K_A' = 0.6$ for ancillaries internal to the section for a square tower; $d = 3.24 \text{ m}$ (mean value at mid-height); $\sin^2 \psi \approx 1.0$ since all ancillaries are close to vertical.
Table 4.1	<p>All circular items are subcritical since the Reynolds number is less than the critical value.</p> $R_e = 1.5 \frac{\bar{V}_z D}{\nu} = \frac{1.5 \times 32.0 \times 0.05}{1.46 \times 10^{-5}} = 1.64 \times 10^5 < 2 \times 10^5$
	<p>Using $A_{A(f)}$ for flat items and $A_{A(c)}$ for circular items:</p>
	<p>Ladder on faces 1,3:</p> $A_{A(f)} = (3.05 \times 0.050) = 0.153 \text{ m}^2$
	<p>Faces 2, 4:</p> $A_{A(f)} = (3.05 \times 0.006) \times 2 = 0.037 \text{ m}^2$
	$A_{A(c)} = \left(\frac{3.05}{0.254} \right) \times 0.016 \times 0.254 = 0.049 \text{ m}^2$

Reference in Part 1	Worked example 2																																																																																														
<p>Table 4.1</p> <p>4.3.2</p>	<p>Feeders, trays on faces 1,3: $A_{A(f)} = 0.150 \times 3.050 = 0.458 \text{ m}^2$ $A_{A(c)} = 0.050 \times 3.050 \times 2 = 0.305 \text{ m}^2$</p> <p>Faces 2, 4: $A_{A(c)} = 0.050 \times 3.050 = 0.153 \text{ m}^2$</p> <p><i>Drag coefficients</i> The drag coefficients are taken from Table 4.1 of Part 1: for ladder and cable trays $C_{N(f)} = 2.0$; for feeders (and ladder rungs) $C_{N(c)} = 1.2$.</p> <p>This allows for cables being of type b), c) or d) in Table 4.1 of Part 1. The equivalent C_{NA} is given by: $C_{NA} = C_{N(f)}A_{A(f)} + C_{N(c)}A_{A(c)}$</p> <p>Hence the total resistance of ancillaries for wind normal to each face can be tabulated as follows.</p> <table border="1" data-bbox="359 958 1109 1601"> <thead> <tr> <th>Face</th> <th>Ancillary</th> <th>c</th> <th>C_{NA}</th> <th>K_A</th> <th>R_{AW} m²</th> </tr> </thead> <tbody> <tr> <td rowspan="2">1</td> <td>Ladder</td> <td>2.49</td> <td>0.31</td> <td>0.61</td> <td>0.19</td> </tr> <tr> <td>Feeders (and trays)</td> <td>3.14</td> <td>1.28</td> <td>0.69</td> <td>0.89</td> </tr> <tr> <td colspan="5"></td> <td style="border-top: 1px solid black;">1.08</td> </tr> <tr> <td rowspan="2">2</td> <td>Ladder</td> <td>0.13</td> <td>0.133</td> <td>0.59</td> <td>0.08</td> </tr> <tr> <td>Feeders (and trays)</td> <td>0.50</td> <td>0.184</td> <td>0.56</td> <td>0.10</td> </tr> <tr> <td colspan="5"></td> <td style="border-top: 1px solid black;">0.18</td> </tr> <tr> <td rowspan="2">3</td> <td>Ladder</td> <td>0.50</td> <td>0.31</td> <td>0.56</td> <td>0.17</td> </tr> <tr> <td>Feeders (and trays)</td> <td>0.05</td> <td>1.28</td> <td>0.60</td> <td>0.76</td> </tr> <tr> <td colspan="5"></td> <td style="border-top: 1px solid black;">0.93</td> </tr> <tr> <td rowspan="2">4</td> <td>Ladder</td> <td>3.06</td> <td>0.133</td> <td>0.68</td> <td>0.09</td> </tr> <tr> <td>Feeders (and trays)</td> <td>2.54</td> <td>0.184</td> <td>0.61</td> <td>0.12</td> </tr> <tr> <td colspan="5"></td> <td style="border-top: 1px solid black;">0.21</td> </tr> </tbody> </table> <p>The resulting total resistance of the tower normal to each face is then:</p> <table border="1" data-bbox="359 1675 813 1892"> <thead> <tr> <th>Face</th> <th>R_T</th> <th>R_{AW}</th> <th>ΣR_W m²</th> </tr> </thead> <tbody> <tr> <td>1</td> <td>5.19</td> <td>1.08</td> <td>6.27</td> </tr> <tr> <td>2</td> <td>5.19</td> <td>0.18</td> <td>5.37</td> </tr> <tr> <td>3</td> <td>5.19</td> <td>0.93</td> <td>6.12</td> </tr> <tr> <td>4</td> <td>5.19</td> <td>0.21</td> <td>5.40</td> </tr> </tbody> </table>	Face	Ancillary	c	C_{NA}	K_A	R_{AW} m ²	1	Ladder	2.49	0.31	0.61	0.19	Feeders (and trays)	3.14	1.28	0.69	0.89						1.08	2	Ladder	0.13	0.133	0.59	0.08	Feeders (and trays)	0.50	0.184	0.56	0.10						0.18	3	Ladder	0.50	0.31	0.56	0.17	Feeders (and trays)	0.05	1.28	0.60	0.76						0.93	4	Ladder	3.06	0.133	0.68	0.09	Feeders (and trays)	2.54	0.184	0.61	0.12						0.21	Face	R_T	R_{AW}	ΣR_W m ²	1	5.19	1.08	6.27	2	5.19	0.18	5.37	3	5.19	0.93	6.12	4	5.19	0.21	5.40
	Face	Ancillary	c	C_{NA}	K_A	R_{AW} m ²																																																																																									
1	Ladder	2.49	0.31	0.61	0.19																																																																																										
	Feeders (and trays)	3.14	1.28	0.69	0.89																																																																																										
					1.08																																																																																										
2	Ladder	0.13	0.133	0.59	0.08																																																																																										
	Feeders (and trays)	0.50	0.184	0.56	0.10																																																																																										
					0.18																																																																																										
3	Ladder	0.50	0.31	0.56	0.17																																																																																										
	Feeders (and trays)	0.05	1.28	0.60	0.76																																																																																										
					0.93																																																																																										
4	Ladder	3.06	0.133	0.68	0.09																																																																																										
	Feeders (and trays)	2.54	0.184	0.61	0.12																																																																																										
					0.21																																																																																										
Face	R_T	R_{AW}	ΣR_W m ²																																																																																												
1	5.19	1.08	6.27																																																																																												
2	5.19	0.18	5.37																																																																																												
3	5.19	0.93	6.12																																																																																												
4	5.19	0.21	5.40																																																																																												

Reference in Part 1	Worked example 2																						
	<p>The resistance needs to be calculated for wind incidence at 45° to a face. The calculations for wind into leg A have been given here only (this direction will give the highest resistance).</p>  <p style="text-align: right;">$K_{A'}$ and C_N are unchanged from the normal to face calculation.</p> <p>Projected area of ladder: $A_{A(f)} = 0.242 \text{ m}^2$; $A_{A(e)} = 0.035 \text{ m}^2$.</p> <p>Projected area of feeders and tray: $A_{A(f)} = 0.388 \text{ m}^2$ $A_{A(e)} = 0.305 \text{ m}^2$.</p> <table border="1" data-bbox="478 1131 1181 1489"> <thead> <tr> <th>Ancillary</th> <th>cd</th> <th>$C_N A_A$</th> <th>$K_A \sin^2 \psi$</th> <th>R_{AW} m²</th> </tr> </thead> <tbody> <tr> <td rowspan="2">Ladder</td> <td>3.70</td> <td rowspan="2">0.53</td> <td rowspan="2">0.68</td> <td rowspan="2">0.36</td> </tr> <tr> <td>3.88</td> </tr> <tr> <td rowspan="2">Feeders and trays</td> <td>3.89</td> <td rowspan="2">1.14</td> <td rowspan="2">0.69</td> <td rowspan="2">0.79</td> </tr> <tr> <td>3.96</td> </tr> <tr> <td></td> <td></td> <td></td> <td></td> <td><u>1.15</u></td> </tr> </tbody> </table> <p>Wind resistance at 45° to faces 1 and 2 is then: $\Sigma R_w = 5.76 + 1.15 = \underline{6.91} \text{ m}^2$</p> <p>NOTE This calculation should be repeated for each diagonal wind as required.</p>	Ancillary	cd	$C_N A_A$	$K_A \sin^2 \psi$	R_{AW} m ²	Ladder	3.70	0.53	0.68	0.36	3.88	Feeders and trays	3.89	1.14	0.69	0.79	3.96					<u>1.15</u>
Ancillary	cd	$C_N A_A$	$K_A \sin^2 \psi$	R_{AW} m ²																			
Ladder	3.70	0.53	0.68	0.36																			
	3.88																						
Feeders and trays	3.89	1.14	0.69	0.79																			
	3.96																						
				<u>1.15</u>																			

Reference in Part 1	Worked example 2																				
4.1.2	B.4.4 Panel 46																				
4.1.3	Panel 46 contains several different types of ancillaries, such as dish aerials, platforms, ladders and feeders, hence the resistance of the panel cannot be derived in accordance with 4.2 of Part 1.																				
4.1.4	A quick check of the dimensions of the dish aerial reveals that it protrudes almost 4 m beyond the tower, i.e.:																				
4.4.1	$\frac{\text{length of aerial past tower}}{\text{width of tower}} = \left(\frac{4}{14}\right) \approx 30\% > 10\%$																				
4.4.2	This does not comply with 4.1.3 c) of Part 1, and the resistance is derived in accordance with 4.4 of Part 1.																				
4.6	<p>The total resistance is built up from the effective individual face resistances, R_1 to R_4, which are derived allowing for the total combined resistance of the bare tower and all ancillaries and discrete attachments in each face of the tower.</p> <p>a) <i>Area of structural members.</i> Since the tower is symmetrical, and all members are flat sided, for all faces:</p> $A_s = Af;$ $C_n = C_{nf}$ <p>A_f can be determined in a similar way to panel 35 (see B.4.3) for all members on the face, i.e. excluding all hip and plan bracing, giving:</p> $A_s = 13.04 \text{ m}^2$ <p>C_{nf} for the tower face cannot be determined until the areas of ancillaries are calculated, and the consequent solidity ratio for each face determined.</p> <p>b) <i>Areas of ancillaries and attachments</i></p> <p>1) <i>Dish aerial</i> at 24.4 m (faces 1 and 4). Data provided by supplier (or wind tunnel tests):</p> $A_A = 4.71 \text{ m}^2 \text{ and } C_n = 1.46.$ <p>This is situated on leg A, and to allow possible directional orientation is taken as applying equally to face 1 and face 4.</p> <p>2) <i>Platforms and ladder</i> (faces 1 and 4). These are all virtually symmetrical about leg A, and can be summed together to give areas appropriate to both faces 1 and 4, and ϕ_A relevant to each attachment.</p>																				
4.4.2	$A_s = Af;$ $C_n = C_{nf}$																				
4.6	<p>A_f can be determined in a similar way to panel 35 (see B.4.3) for all members on the face, i.e. excluding all hip and plan bracing, giving:</p> $A_s = 13.04 \text{ m}^2$ <p>C_{nf} for the tower face cannot be determined until the areas of ancillaries are calculated, and the consequent solidity ratio for each face determined.</p> <p>b) <i>Areas of ancillaries and attachments</i></p> <p>1) <i>Dish aerial</i> at 24.4 m (faces 1 and 4). Data provided by supplier (or wind tunnel tests):</p> $A_A = 4.71 \text{ m}^2 \text{ and } C_n = 1.46.$ <p>This is situated on leg A, and to allow possible directional orientation is taken as applying equally to face 1 and face 4.</p> <p>2) <i>Platforms and ladder</i> (faces 1 and 4). These are all virtually symmetrical about leg A, and can be summed together to give areas appropriate to both faces 1 and 4, and ϕ_A relevant to each attachment.</p>																				
	<table border="1" data-bbox="403 1541 1043 1751"> <thead> <tr> <th data-bbox="403 1541 762 1585">Item</th> <th data-bbox="762 1541 858 1585">$A_{A(f)}$</th> <th data-bbox="858 1541 954 1585">$A_{A(e)}$</th> <th data-bbox="954 1541 1043 1585">ϕ_A</th> </tr> </thead> <tbody> <tr> <td data-bbox="403 1585 762 1619">(i) Platform at 24.4 m</td> <td data-bbox="762 1585 858 1619">1.36</td> <td data-bbox="858 1585 954 1619">0.69</td> <td data-bbox="954 1585 1043 1619">0.36</td> </tr> <tr> <td data-bbox="403 1619 762 1653">(ii) Platform at 21.3 m</td> <td data-bbox="762 1619 858 1653">1.10</td> <td data-bbox="858 1619 954 1653">0.44</td> <td data-bbox="954 1619 1043 1653">0.32</td> </tr> <tr> <td data-bbox="403 1653 762 1686">(iii) Ladder and other items</td> <td data-bbox="762 1653 858 1686">2.11</td> <td data-bbox="858 1653 954 1686">0.13</td> <td data-bbox="954 1653 1043 1686">0.24</td> </tr> <tr> <td data-bbox="403 1686 762 1720"></td> <td data-bbox="762 1686 858 1720">4.57</td> <td data-bbox="858 1686 954 1720">1.26</td> <td data-bbox="954 1686 1043 1720"></td> </tr> </tbody> </table>	Item	$A_{A(f)}$	$A_{A(e)}$	ϕ_A	(i) Platform at 24.4 m	1.36	0.69	0.36	(ii) Platform at 21.3 m	1.10	0.44	0.32	(iii) Ladder and other items	2.11	0.13	0.24		4.57	1.26	
Item	$A_{A(f)}$	$A_{A(e)}$	ϕ_A																		
(i) Platform at 24.4 m	1.36	0.69	0.36																		
(ii) Platform at 21.3 m	1.10	0.44	0.32																		
(iii) Ladder and other items	2.11	0.13	0.24																		
	4.57	1.26																			
	$\Sigma A_A = \underline{5.83} \text{ m}^2$																				

Reference in Part 1	Worked example 2												
<p>4.5</p> <p>Figure 4.5</p> <p>4.4.2</p> <p>Table 4.1</p> <p>Figure 4.1</p>	<p>The diameters of all circular elements are not large enough for supercritical regime.</p> <p>Hence from 4.4.2 of Part 1, the corresponding C_n are:</p> <table border="1" data-bbox="608 524 1015 683"> <thead> <tr> <th>Item</th> <th>C_{nf}</th> <th>C_{nc}</th> </tr> </thead> <tbody> <tr> <td>(i)</td> <td>1.65</td> <td>1.04</td> </tr> <tr> <td>(ii)</td> <td>1.68</td> <td>1.04</td> </tr> <tr> <td>(iii)</td> <td>1.75</td> <td>1.06</td> </tr> </tbody> </table> <p>Hence equivalent C_n</p> $= \frac{1}{5.83} ((1.65 \times 1.36) + (1.68 \times 1.10) + (1.75 \times 2.11) + (1.05 \times 1.26))$ $= \underline{1.56}$ <p style="text-align: right; margin-right: 100px;">↑ [average C_{nc}]</p> <p>3) <i>Feeders and trays</i> (faces 2 and 3)</p> <p>Face 2: $A_{A(e)} = 0.61 \text{ m}^2$; $C_n = 1.2$</p> <p>Face 3: $A_{A(e)} = 1.22 \text{ m}^2$; $C_n = 1.2$</p> <p>$A_{A(f)} = 1.83 \text{ m}^2$; $C_n = 2.0$</p> <p>$\Sigma A_A = 3.05 \text{ m}^2$</p> <p>c) <i>Solidity ratios</i>. Solidity ratios are based on all elements within a face, with due allowance in the enveloping area for those items protruding significantly past the face width:</p> $\phi = \frac{A_s + \Sigma A_A}{h \times b_e}$ <p>where</p> <p>b_e is an equivalent face width to cater for dish projections, etc. where appropriate e.g.:</p> 	Item	C_{nf}	C_{nc}	(i)	1.65	1.04	(ii)	1.68	1.04	(iii)	1.75	1.06
Item	C_{nf}	C_{nc}											
(i)	1.65	1.04											
(ii)	1.68	1.04											
(iii)	1.75	1.06											

Reference in Part 1	Worked example 2																																								
	<table border="1"> <thead> <tr> <th>Face</th> <th>A_S m²</th> <th>ΣA_A m²</th> <th>h m</th> <th>b_e m</th> <th>ϕ</th> <th>C_{nf}</th> </tr> </thead> <tbody> <tr> <td>1</td> <td>13.04</td> <td>10.54</td> <td>12.2</td> <td>16.95</td> <td>0.12</td> <td>1.83</td> </tr> <tr> <td>2</td> <td>13.04</td> <td>0.61</td> <td>12.2</td> <td>15.15</td> <td>0.07</td> <td>1.93</td> </tr> <tr> <td>3</td> <td>13.04</td> <td>3.05</td> <td>12.2</td> <td>15.15</td> <td>0.09</td> <td>1.88</td> </tr> <tr> <td>4</td> <td>13.04</td> <td>10.54</td> <td>12.2</td> <td>16.95</td> <td>0.12</td> <td>1.83</td> </tr> </tbody> </table>	Face	A_S m ²	ΣA_A m ²	h m	b_e m	ϕ	C_{nf}	1	13.04	10.54	12.2	16.95	0.12	1.83	2	13.04	0.61	12.2	15.15	0.07	1.93	3	13.04	3.05	12.2	15.15	0.09	1.88	4	13.04	10.54	12.2	16.95	0.12	1.83					
Face	A_S m ²	ΣA_A m ²	h m	b_e m	ϕ	C_{nf}																																			
1	13.04	10.54	12.2	16.95	0.12	1.83																																			
2	13.04	0.61	12.2	15.15	0.07	1.93																																			
3	13.04	3.05	12.2	15.15	0.09	1.88																																			
4	13.04	10.54	12.2	16.95	0.12	1.83																																			
4.4.2 Figure 4.5	<p>d) <i>Total face resistance</i> The total face resistance can now be obtained using ϕ from c) for tower drag coefficient: $C_n = C_{nf}$</p>																																								
4.4.1	<p>and $R = C_n A_s + \Sigma (C_{nA} A_A)$ $R_1 = (1.83 \times 13.04) + (1.46 \times 4.71) + (1.56 \times 5.83)$ $= 23.9 + 6.9 + 9.0 = R_4 = \underline{39.8} \text{ m}^2$ $R_2 = (1.93 \times 13.04) + (1.2 \times 0.61) = \underline{25.9} \text{ m}^2$ $R_3 = (1.88 \times 13.04) + (1.2 \times 1.22) + (2.0 \times 1.83)$ $= 24.5 + 1.5 + 3.6 = \underline{29.6} \text{ m}^2$</p>																																								
4.4.1 Figure 4.2	<p>e) <i>Wind resistance according to direction</i> For wind normal to face, $\theta = 0^\circ$ $\Sigma R_w = R_e = (R_F + \eta_F R_B)$, since $K_\theta = 1$ For wind on corner, $\theta = 45^\circ$, and using a mean K_θ $\Sigma R_w = \epsilon K_\theta (R_{F1} + R_{F2} + \eta_{F1} R_{B1} + \eta_{F2} R_{B2})$ where suffixes F and B refer to front and back faces, respectively. From Figure 4.2 of Part 1, we have averaged K_θ thus:</p>																																								
Figure 4.2	<table border="1"> <thead> <tr> <th>Corner</th> <th>ΣA_f m²</th> <th>ΣA_F m²</th> <th>$\Sigma A_f / \Sigma A_F$</th> <th>ϕ_{AV}</th> <th>K_θ</th> </tr> </thead> <tbody> <tr> <td>1/2</td> <td>26.08</td> <td>37.23</td> <td>0.70</td> <td>0.10</td> <td>1.12</td> </tr> <tr> <td>2/3</td> <td>26.08</td> <td>29.74</td> <td>0.88</td> <td>0.08</td> <td>1.11</td> </tr> <tr> <td>3/4</td> <td>26.08</td> <td>39.67</td> <td>0.66</td> <td>0.11</td> <td>1.12</td> </tr> <tr> <td>4/1</td> <td>26.08</td> <td>47.16</td> <td>0.55</td> <td>0.12</td> <td>1.14</td> </tr> </tbody> </table>						Corner	ΣA_f m ²	ΣA_F m ²	$\Sigma A_f / \Sigma A_F$	ϕ_{AV}	K_θ	1/2	26.08	37.23	0.70	0.10	1.12	2/3	26.08	29.74	0.88	0.08	1.11	3/4	26.08	39.67	0.66	0.11	1.12	4/1	26.08	47.16	0.55	0.12	1.14					
Corner	ΣA_f m ²	ΣA_F m ²	$\Sigma A_f / \Sigma A_F$	ϕ_{AV}	K_θ																																				
1/2	26.08	37.23	0.70	0.10	1.12																																				
2/3	26.08	29.74	0.88	0.08	1.11																																				
3/4	26.08	39.67	0.66	0.11	1.12																																				
4/1	26.08	47.16	0.55	0.12	1.14																																				
	<p>NOTE K_θ values here are very similar due to the low values of ϕ; this will <i>not</i> be the case when $\phi \geq 0.2$ (see Figure 4.2 of Part 1). For this panel, for all corner wind directions, $0.5 K_\theta$ could be taken as 0.57, but more generally, the value according to each corner should be used.</p>																																								
	<p>f) <i>Shielding factors</i>. Now $A_c = A_c' = 0$ (all structural members are flat sided). Then $\eta' = \eta_f \left(\frac{A_f + A_A}{A_F} \right) = \eta_f$ Also for square-section towers $\omega = 1$ Therefore $\eta = \eta' = \eta_f$, giving: faces 1 and 4: $\phi = 0.12$; $\eta = 0.78$; face 2: $\phi = 0.07$; $\eta = 0.87$; face 3: $\phi = 0.09$; $\eta = 0.83$.</p>																																								

Reference in Part 1	Worked example 2																																																																																																														
	<p>g) <i>Total panels resistances</i> The total panel resistance can now be determined using the data in a) to f):</p> <table border="1"> <thead> <tr> <th>Wind direction on to</th> <th>R_F</th> <th>R_B</th> <th>ηF</th> <th>K_θ</th> <th>ΣR_W</th> </tr> </thead> <tbody> <tr> <td></td> <td>m^2</td> <td>m^2</td> <td></td> <td></td> <td>m^2</td> </tr> <tr> <td>Face 1</td> <td>39.8</td> <td>29.6</td> <td>0.78</td> <td>1.0</td> <td>62.9</td> </tr> <tr> <td>Face 2</td> <td>25.9</td> <td>39.8</td> <td>0.87</td> <td>1.0</td> <td>60.5</td> </tr> <tr> <td>Face 3</td> <td>29.6</td> <td>39.8</td> <td>0.83</td> <td>1.0</td> <td>62.6</td> </tr> <tr> <td>Face 4</td> <td>39.8</td> <td>25.9</td> <td>0.78</td> <td>1.0</td> <td>60.0</td> </tr> <tr> <td></td> <td colspan="2">$\Sigma R_F + \Sigma (R_B \eta_F)$</td> <td colspan="2">$0.5 K_\theta$</td> <td>$\Sigma R_W$</td> </tr> <tr> <td>Corner 1/2</td> <td colspan="2">$\equiv (62.9 + 60.5)$</td> <td>0.56</td> <td></td> <td>69.1</td> </tr> <tr> <td>Corner 2/3</td> <td colspan="2">$\equiv (60.5 + 62.6)$</td> <td>0.55</td> <td></td> <td>67.7</td> </tr> <tr> <td>Corner 3/4</td> <td colspan="2">$\equiv (62.6 + 60.0)$</td> <td>0.56</td> <td></td> <td>68.7</td> </tr> <tr> <td>Corner 4/1</td> <td colspan="2">$\equiv (60.0 + 62.9)$</td> <td>0.57</td> <td></td> <td>70.1</td> </tr> </tbody> </table> <p>NOTE These resistances do not differ greatly between directions, but in cases where $\phi > 0.1$ and $\Sigma A_A \geq A_F$, there will be greater differences.</p> <p>B.4.5 General summary (resistance) In a similar way to the methods detailed in B.4.2 to B.4.4, all the panel resistances can be determined in accordance with 4.2, 4.3 or 4.4 of Part 1, as required. For all panels with resistances determined in accordance with 4.4 of Part 1, as well as ΣR_W, the contribution due to ancillaries and cables will be required, ($\Sigma R_{AW} + \Sigma R_c$), since these are needed for determining loads on the "equivalent bare tower" in deriving fluctuating loads and gust response factors in accordance with B.5. Thus for panel 46, $\Sigma R_c = 0$ and $\Sigma R_{AW} = \Sigma (C_{nA} A_A)$ see B.4.4 d).</p> <table border="1"> <thead> <tr> <th>Wind direction</th> <th>ΣR_W</th> <th>ΣR_{AW}</th> <th>R_{TE}</th> </tr> </thead> <tbody> <tr> <td></td> <td>m^2</td> <td>m^2</td> <td>m^2</td> </tr> <tr> <td>Face 1</td> <td>62.9</td> <td>15.9 + 5.1</td> <td>41.9</td> </tr> <tr> <td>Face 2</td> <td>60.5</td> <td>0.7 + 15.9</td> <td>43.9</td> </tr> <tr> <td>Face 3</td> <td>62.6</td> <td>5.1 + 15.9</td> <td>41.6</td> </tr> <tr> <td>Face 4</td> <td>60.0</td> <td>15.9 + 0.7</td> <td>43.4</td> </tr> <tr> <td>Corner 1/2</td> <td>69.1</td> <td>6.9 + (1.41 × 14.1)</td> <td>42.5</td> </tr> <tr> <td>Corner 2/3</td> <td>67.7</td> <td>(9.7 × 1.41) + 6.9</td> <td>47.2</td> </tr> <tr> <td>Corner 3/4</td> <td>68.7</td> <td>(14.1 × 1.41) + 6.9</td> <td>42.1</td> </tr> <tr> <td>Corner 4/1</td> <td>70.1</td> <td>6.9 + (1.41 × 9.7)</td> <td>49.6</td> </tr> </tbody> </table> <p>NOTE An approximate check on the tower-only resistance can be derived from: $R = A_s C_n (1 + \eta)$ which using typical face values from the above gives: $R \approx 13.04 \times 1.9 \times (1 + 0.8) = 44.6 m^2$.</p>					Wind direction on to	R_F	R_B	ηF	K_θ	ΣR_W		m^2	m^2			m^2	Face 1	39.8	29.6	0.78	1.0	62.9	Face 2	25.9	39.8	0.87	1.0	60.5	Face 3	29.6	39.8	0.83	1.0	62.6	Face 4	39.8	25.9	0.78	1.0	60.0		$\Sigma R_F + \Sigma (R_B \eta_F)$		$0.5 K_\theta$		ΣR_W	Corner 1/2	$\equiv (62.9 + 60.5)$		0.56		69.1	Corner 2/3	$\equiv (60.5 + 62.6)$		0.55		67.7	Corner 3/4	$\equiv (62.6 + 60.0)$		0.56		68.7	Corner 4/1	$\equiv (60.0 + 62.9)$		0.57		70.1	Wind direction	ΣR_W	ΣR_{AW}	R_{TE}		m^2	m^2	m^2	Face 1	62.9	15.9 + 5.1	41.9	Face 2	60.5	0.7 + 15.9	43.9	Face 3	62.6	5.1 + 15.9	41.6	Face 4	60.0	15.9 + 0.7	43.4	Corner 1/2	69.1	6.9 + (1.41 × 14.1)	42.5	Corner 2/3	67.7	(9.7 × 1.41) + 6.9	47.2	Corner 3/4	68.7	(14.1 × 1.41) + 6.9	42.1	Corner 4/1	70.1	6.9 + (1.41 × 9.7)	49.6
Wind direction on to	R_F	R_B	ηF	K_θ	ΣR_W																																																																																																										
	m^2	m^2			m^2																																																																																																										
Face 1	39.8	29.6	0.78	1.0	62.9																																																																																																										
Face 2	25.9	39.8	0.87	1.0	60.5																																																																																																										
Face 3	29.6	39.8	0.83	1.0	62.6																																																																																																										
Face 4	39.8	25.9	0.78	1.0	60.0																																																																																																										
	$\Sigma R_F + \Sigma (R_B \eta_F)$		$0.5 K_\theta$		ΣR_W																																																																																																										
Corner 1/2	$\equiv (62.9 + 60.5)$		0.56		69.1																																																																																																										
Corner 2/3	$\equiv (60.5 + 62.6)$		0.55		67.7																																																																																																										
Corner 3/4	$\equiv (62.6 + 60.0)$		0.56		68.7																																																																																																										
Corner 4/1	$\equiv (60.0 + 62.9)$		0.57		70.1																																																																																																										
Wind direction	ΣR_W	ΣR_{AW}	R_{TE}																																																																																																												
	m^2	m^2	m^2																																																																																																												
Face 1	62.9	15.9 + 5.1	41.9																																																																																																												
Face 2	60.5	0.7 + 15.9	43.9																																																																																																												
Face 3	62.6	5.1 + 15.9	41.6																																																																																																												
Face 4	60.0	15.9 + 0.7	43.4																																																																																																												
Corner 1/2	69.1	6.9 + (1.41 × 14.1)	42.5																																																																																																												
Corner 2/3	67.7	(9.7 × 1.41) + 6.9	47.2																																																																																																												
Corner 3/4	68.7	(14.1 × 1.41) + 6.9	42.1																																																																																																												
Corner 4/1	70.1	6.9 + (1.41 × 9.7)	49.6																																																																																																												
4.2																																																																																																															
4.3																																																																																																															
4.4																																																																																																															
4.4																																																																																																															
5.3.1																																																																																																															

Reference in Part 1	Worked example 2
<p>5.1</p> <p>5.1.1</p> <p>5.1.2</p> <p>5.3.1</p> <p>3.2.1</p> <p>5.2.1</p>	<p>B.5 Structural response to wind</p> <p>B.5.1 General</p> <p>a) <i>Check for use of the static method.</i> The equivalent static method may be used to assess the maximum member forces in the tower if:</p> $\frac{7 m_T}{\rho_s R_{WT} \sqrt{(d_B \tau_o)}} \left(\frac{5}{6} - \frac{h_T}{H} \right)^2 < 1$ <p>The minimum total tower resistance including ancillaries:</p> $\Sigma R_W = 433 \text{ m}^2$ <p>Therefore</p> $\frac{\Sigma R_W}{3} = 144 \text{ m}^2$ <p>The panel resistance summation just less than this, corresponds to panels 1 to 40 inclusive, for which:</p> $R_{WT} = 141.2 \text{ m}^2$ <p>The height to the underside of panel 40 = 65 m.</p> <p>Therefore, the height of panels 1 to 40 = 135 – 65 = 70 m = h'_t</p> $h_t = 70 \text{ or } H/3, \text{ whichever is less}$ $= 70 \text{ m or } 45 \text{ m}$ <p>Therefore</p> $h_t = 45 \text{ m};$ $H = 135 \text{ m}$ $d_B = 21.3 \text{ m};$ $\tau_o = 0.001 \text{ m};$ $\rho_s = 7\,850 \text{ kg/m}^3$ $m_T = 28\,870 \text{ kg, including all ancillaries for panels 1 to 40.}$ <p>Therefore</p> $\frac{7 \times 28870}{7850 \times 141.2} \frac{1}{\sqrt{(0.001 \times 21.3)}} \left(\frac{5}{6} - \frac{1}{3} \right)^2 = 0.31 < 1$ <p>Therefore the equivalent static method may be used.</p> <p>b) <i>Procedure to be used.</i> Although panels 1 and 35 (and many other panels) comply with the constraints of 4.1.3 of Part 1, the forces cannot be evaluated using 5.2 of Part 1, since several panels do not comply with those recommendations (e.g. panel 46). Hence the wind loading for analysis and the member forces so derived have to be determined in accordance with 5.3 of Part 1.</p> <p>c) <i>Mean wind loads</i></p> <p><i>Panel 1</i></p> <p>For wind blowing normal to each face:</p> <p>for $H = 135 \text{ m}$: $\bar{V}_z = 19.8 \times (12.5)^{0.23} = 35.4 \text{ m/s}$</p> $R_{TE} = \Sigma R_W - (R_{AW} + R_{CW}) = 1.16 - 0 = 1.16$ <p>Therefore</p> $\bar{P}_{TW} = \frac{1.22}{2} \times \frac{35.4^2}{1000} \times 1.16 = 0.89 \text{ kN}$

Reference in Part 1	Worked example 2																																																		
<p>5.2.1</p> <p>3.2.1</p> <p>4.3.2 a)</p> <p>5.3</p>	<p>Similarly, for wind on any diagonal:</p> $\bar{P}_{\text{TW}} = 0.89 \times \frac{1.39}{1.16} = \underline{1.06} \text{ kN}$ <p><i>Panel 35</i></p> <p>The method of calculating the loads with resistances determined in accordance with 4.3 of Part 1 is similar to that for panel 1, but the total loads will differ for each face direction:</p> <p>for $H = 91 \text{ m}$: $\bar{V}_z = 19.8 \times (8.1)^{0.23} = \underline{32.0} \text{ m/s}$</p> <p>Since $R_{\text{TE}} \equiv \Sigma R_{\text{W}}$, the loads can be tabulated thus, using:</p> $\bar{P}_{\text{TW}} = \frac{1}{2} \rho_a \bar{V}_z^2 \times R_{\text{TE}} = 0.625 R_{\text{TE}} \text{ (kN)}$ <p>NOTE The R_{AW} term used in determining ΣR_{W} in accordance with 4.3 of Part 1, is not subtracted, since ΣR_{W} is an "effective total tower resistance", R_{TE}</p> <table border="1" data-bbox="480 846 922 1093"> <thead> <tr> <th>Direction</th> <th>R_{TE}</th> <th>\bar{P}_{TW}</th> </tr> </thead> <tbody> <tr> <td></td> <td>m²</td> <td>kN</td> </tr> <tr> <td>Face 1</td> <td>6.27</td> <td>3.92</td> </tr> <tr> <td>Face 2</td> <td>5.37</td> <td>3.35</td> </tr> <tr> <td>Face 3</td> <td>6.12</td> <td>3.82</td> </tr> <tr> <td>Face 4</td> <td>5.40</td> <td>3.37</td> </tr> <tr> <td>Diagonal 1/4</td> <td>6.91</td> <td>4.32</td> </tr> </tbody> </table>	Direction	R_{TE}	\bar{P}_{TW}		m ²	kN	Face 1	6.27	3.92	Face 2	5.37	3.35	Face 3	6.12	3.82	Face 4	5.40	3.37	Diagonal 1/4	6.91	4.32																													
Direction	R_{TE}	\bar{P}_{TW}																																																	
	m ²	kN																																																	
Face 1	6.27	3.92																																																	
Face 2	5.37	3.35																																																	
Face 3	6.12	3.82																																																	
Face 4	5.40	3.37																																																	
Diagonal 1/4	6.91	4.32																																																	
<p>3.2.1</p> <p>5.2.1 and 5.3.2</p>	<p><i>Panel 46</i></p> <p>Again the loads can be set down in a similar form to panel 35, but with separate items for \bar{P}_{TE} and \bar{P}_{AW} as follows:</p> <p>$H = 19.6 \text{ m} < 20 \text{ m}$</p> $\bar{V}_z = 9.9 \left(1 + \frac{19.6}{20} \right) = 19.6 \text{ m/s}$ $\bar{P} = \frac{1}{2} \rho_a \bar{V}_z^2 \times R = 0.234 \times R \text{ (kN)}$ <table border="1" data-bbox="480 1406 1238 1749"> <thead> <tr> <th>Direction</th> <th>R_{TE}</th> <th>ΣR_{AW}</th> <th>\bar{P}_{TE}</th> <th>\bar{P}_{AW}</th> </tr> </thead> <tbody> <tr> <td></td> <td>m²</td> <td>m²</td> <td>kN</td> <td>kN</td> </tr> <tr> <td>Face 1</td> <td>41.9</td> <td>21.0</td> <td>9.81</td> <td>4.91</td> </tr> <tr> <td>Face 2</td> <td>43.9</td> <td>16.6</td> <td>10.23</td> <td>3.88</td> </tr> <tr> <td>Face 3</td> <td>41.6</td> <td>21.0</td> <td>9.73</td> <td>4.91</td> </tr> <tr> <td>Face 4</td> <td>43.4</td> <td>16.6</td> <td>10.16</td> <td>3.88</td> </tr> <tr> <td>Corner 1/2</td> <td>42.5</td> <td>26.6</td> <td>9.95</td> <td>6.22</td> </tr> <tr> <td>Corner 2/3</td> <td>47.2</td> <td>20.5</td> <td>11.05</td> <td>4.80</td> </tr> <tr> <td>Corner 3/4</td> <td>42.1</td> <td>26.6</td> <td>9.85</td> <td>6.22</td> </tr> <tr> <td>Corner 4/1</td> <td>49.6</td> <td>20.5</td> <td>11.61</td> <td>4.80</td> </tr> </tbody> </table>	Direction	R_{TE}	ΣR_{AW}	\bar{P}_{TE}	\bar{P}_{AW}		m ²	m ²	kN	kN	Face 1	41.9	21.0	9.81	4.91	Face 2	43.9	16.6	10.23	3.88	Face 3	41.6	21.0	9.73	4.91	Face 4	43.4	16.6	10.16	3.88	Corner 1/2	42.5	26.6	9.95	6.22	Corner 2/3	47.2	20.5	11.05	4.80	Corner 3/4	42.1	26.6	9.85	6.22	Corner 4/1	49.6	20.5	11.61	4.80
Direction	R_{TE}	ΣR_{AW}	\bar{P}_{TE}	\bar{P}_{AW}																																															
	m ²	m ²	kN	kN																																															
Face 1	41.9	21.0	9.81	4.91																																															
Face 2	43.9	16.6	10.23	3.88																																															
Face 3	41.6	21.0	9.73	4.91																																															
Face 4	43.4	16.6	10.16	3.88																																															
Corner 1/2	42.5	26.6	9.95	6.22																																															
Corner 2/3	47.2	20.5	11.05	4.80																																															
Corner 3/4	42.1	26.6	9.85	6.22																																															
Corner 4/1	49.6	20.5	11.61	4.80																																															
<p>5.3.1</p>	<p>NOTE The partition of loads between \bar{P}_{TE} and \bar{P}_{AW} is not crucial and any reasonable assumption for the partition of ΣR can be made, provided:</p> <ol style="list-style-type: none"> 1) ΣR_{AW} is any upper bound to the total resistance of all discrete attachments excluding shielding effects; 2) $R_{\text{TE}} + \Sigma R_{\text{AW}} = \Sigma R_{\text{W}}$. 																																																		

Reference in Part 1	Worked example 2																																																																																													
<p>5.2.2</p> <p>5.2.3</p> <p>5.2.4</p> <p>Figure 5.4</p> <p>Figures 5.2, 5.3 and 5.4</p> <p>5.2.4</p> <p>5.2.2.3</p> <p>5.2.2.2</p> <p>5.3.2</p> <p>Figures 5.1 and 5.2</p> <p>5.3.2</p>	<p>d) <i>Gust response factors</i></p> <p>1) <i>For tower loads.</i></p> <p>For legs:</p> $G_l = B j \left\{ 1 + 0.2 \left(\frac{z}{H} \right)^2 \right\}$ <p>For bracings:</p> $G_b = K_q G_l$ <p>where</p> <p>K_q is derived from the mean hourly analyses on the partially shielded tower body, using Figure 5.4 of Part 1 according to the ratio $1/f_q$, where f_q is the proportion of the shear carried by the bracings to the total at the level considered.</p> <p>These are required for each level up the tower, but are the same regardless of direction.</p> <p>For lower sections of the tower with complex bracing arrangements, it may be easier to determine the proportion of shear carried by the bracing system by resolving the leg member forces under mean wind on the effective tower body and subtracting this from the total.</p> <p>Typical gust factors, for members in the panels considered above, are as follows:</p> <table border="1" style="width: 100%; border-collapse: collapse; text-align: center;"> <thead> <tr> <th>Panel</th> <th>z</th> <th>$H - z$</th> <th>z/H</th> <th>B</th> <th>j</th> <th>G_B</th> <th>f_q</th> <th>K_q</th> <th>G_l</th> <th>G_b</th> </tr> </thead> <tbody> <tr> <td>1</td> <td>135</td> <td>(13.5)</td> <td>1.00</td> <td>3.19</td> <td>0.53</td> <td>1.69</td> <td>1.00</td> <td>1.00</td> <td>2.03</td> <td>2.03</td> </tr> <tr> <td>35</td> <td>91</td> <td>44</td> <td>0.67</td> <td>2.30</td> <td>0.72</td> <td>1.66</td> <td>0.42</td> <td>1.17</td> <td>1.80</td> <td>2.10</td> </tr> <tr> <td>46</td> <td>20</td> <td>115</td> <td>0.15</td> <td>1.72</td> <td>0.96</td> <td>1.65</td> <td>0.11^a</td> <td>2.72</td> <td>1.66</td> <td>4.51</td> </tr> </tbody> </table> <p>^a $1/f_q = 9.1 (> 8)$, so $K_q = 1 + \frac{115^{0.4}}{23.6} (9.1 - 3) = 2.72$</p> <p>NOTE 1 \bar{G}_B from the “simple method” (see 5.2.2.3 of Part 1) gives $G_B = 1.65$.</p> <p>NOTE 2 Figures in parentheses indicate use of minimum value of $0.1 H$ when $H > 100$ m; G_B applies to all levels above 121.5 m.</p> <p>2) <i>For loads on attachments.</i> There are no cables, so 5.3.3 of Part 1 is not required and appropriate gust factors can be derived in accordance with 5.3.2 of Part 1, using:</p> $G_A = B_A j_A [1 + 0.2 (Z_A/H)^2]$ <p>Unlike G_B, these do not relate to the level of the members being considered, but solely to the size and level of the ancillary, and hence are determined for each major attachment as follows, using Figure 5.1 and Figure 5.2 of Part 1:</p> <table border="1" style="width: 100%; border-collapse: collapse; text-align: center;"> <thead> <tr> <th>Item^a</th> <th>z_A</th> <th>e_A^b</th> <th>e_A/z_A^c</th> <th>BA</th> <th>j_A</th> <th>G_A</th> </tr> </thead> <tbody> <tr> <td>1. 11 m long VHF</td> <td>123</td> <td>12.3</td> <td>0.10</td> <td>3.17</td> <td>0.53</td> <td>1.96</td> </tr> <tr> <td>2. 2.4 m ϕ dish</td> <td>110</td> <td>11.0</td> <td>0.10</td> <td>3.22</td> <td>0.53</td> <td>1.93</td> </tr> <tr> <td>3. 2.4 m ϕ dish</td> <td>98</td> <td>10.0</td> <td>0.10</td> <td>3.30</td> <td>0.53</td> <td>1.93</td> </tr> <tr> <td>4. 14 m long VHF</td> <td>78</td> <td>14.0</td> <td>0.18</td> <td>3.08</td> <td>0.62</td> <td>2.04</td> </tr> <tr> <td>5. 2.1 m ϕ dish</td> <td>70</td> <td>10.0</td> <td>0.14</td> <td>3.30</td> <td>0.58</td> <td>2.02</td> </tr> <tr> <td>6. 2.4 m ϕ dish</td> <td>24</td> <td>10.0</td> <td>0.42</td> <td>3.30</td> <td>0.77</td> <td>2.56</td> </tr> </tbody> </table> <p>^a Includes associated platforms, etc.</p> <p>^b e_A should not be taken as less than 10 m or $0.1 z_A$.</p> <p>^c e_A/z_A should not be taken as less than $10/z_A$ or 0.1, i.e. value e_A/z_A.</p>	Panel	z	$H - z$	z/H	B	j	G_B	f_q	K_q	G_l	G_b	1	135	(13.5)	1.00	3.19	0.53	1.69	1.00	1.00	2.03	2.03	35	91	44	0.67	2.30	0.72	1.66	0.42	1.17	1.80	2.10	46	20	115	0.15	1.72	0.96	1.65	0.11 ^a	2.72	1.66	4.51	Item ^a	z_A	e_A ^b	e_A/z_A ^c	BA	j_A	G_A	1. 11 m long VHF	123	12.3	0.10	3.17	0.53	1.96	2. 2.4 m ϕ dish	110	11.0	0.10	3.22	0.53	1.93	3. 2.4 m ϕ dish	98	10.0	0.10	3.30	0.53	1.93	4. 14 m long VHF	78	14.0	0.18	3.08	0.62	2.04	5. 2.1 m ϕ dish	70	10.0	0.14	3.30	0.58	2.02	6. 2.4 m ϕ dish	24	10.0	0.42	3.30	0.77	2.56
Panel	z	$H - z$	z/H	B	j	G_B	f_q	K_q	G_l	G_b																																																																																				
1	135	(13.5)	1.00	3.19	0.53	1.69	1.00	1.00	2.03	2.03																																																																																				
35	91	44	0.67	2.30	0.72	1.66	0.42	1.17	1.80	2.10																																																																																				
46	20	115	0.15	1.72	0.96	1.65	0.11 ^a	2.72	1.66	4.51																																																																																				
Item ^a	z_A	e_A ^b	e_A/z_A ^c	BA	j_A	G_A																																																																																								
1. 11 m long VHF	123	12.3	0.10	3.17	0.53	1.96																																																																																								
2. 2.4 m ϕ dish	110	11.0	0.10	3.22	0.53	1.93																																																																																								
3. 2.4 m ϕ dish	98	10.0	0.10	3.30	0.53	1.93																																																																																								
4. 14 m long VHF	78	14.0	0.18	3.08	0.62	2.04																																																																																								
5. 2.1 m ϕ dish	70	10.0	0.14	3.30	0.58	2.02																																																																																								
6. 2.4 m ϕ dish	24	10.0	0.42	3.30	0.77	2.56																																																																																								

Reference in Part 1	Worked example 2
(C.5.3.4 of this Part of BS 8100)	<p>According to the values of G_A, separate sets of mean hourly analyses are required for each ancillary item. However, as demonstrated here, for ancillaries of virtually any size, the value of G_A will generally depend on the level of attachment, and provided the resulting G_A values are similar, the number of analyses can be reduced by grouping together.</p> <p>Hence for the attachments, only three sets of analyses are required:</p> <ul style="list-style-type: none"> i) items 1, 2 and 3, for which $G_{A1} \approx 1.95$ can be used; ii) items 4 and 5, for which $G_{A2} = 2.03$ can be used; iii) item 6, for which $G_{A3} = 2.56$ is used.
5.3.4 (C.5.3.4 of this Part of BS 8100)	<p>B.5.2 Member forces</p> <p>Having undertaken the appropriate elastic analyses under mean hourly wind loading for the shielded tower and for each set of attachments, together with an analysis under dead load, the member forces can be obtained using 5.3.4 of Part 1 (see C.5.3.4).</p> <p>Thus in general terms;</p> $\Sigma F_{\max} = F_{DL} + \Sigma \bar{F}_W + \Sigma F_{W'} \sqrt{1 + \left(\frac{\Sigma F_{x'}}{\Sigma F_W} \right)^2}$ <p>where</p> $\Sigma \bar{F}_W = (\bar{F}_{TE} + \bar{F}_{A1} + \bar{F}_{A2} + \bar{F}_{A3})_{\max}$ $\Sigma F_{W'} = G \bar{F}_{TE} + G_{A1} \bar{F}_{A1} + G_{A2} \bar{F}_{A2} + G_{A3} \bar{F}_{A3}$ $\Sigma F_{x'} = \frac{1}{2} [G \bar{F}_{TEX} + G_{A1} \bar{F}_{A1X} + G_{A2} \bar{F}_{A2X} + G_{A3} \bar{F}_{A3X}]$ <p>where suffix X indicates \bar{F} due to mean hourly loads normal to the maximum down-wind direction.</p>
(C.5.3.4 of this Part of BS 8100)	<p>The simplified procedure discussed in C.5.3.4 may be used for this tower leading to:</p> $\Sigma F_{\max} = F_{DL} + \bar{F}_{TE \max} (1 + 1.12 G) + \sum_{1 \text{ to } 3} \bar{F}_{An} (1 + 1.12 G_{An})$ $\simeq F_{DL} + (\bar{F}_{TE} + \sum_{1 \text{ to } 3} \bar{F}_{An})_{\max} (1 + 1.12 G)$ <p>since at high levels on the tower $G_A \approx G$, and at lower levels $\Sigma \bar{F}_A \ll \Sigma \bar{F}_{TE}$ for this tower.</p>
5.1.4 5.3.5 3.3.2 5.2.5	<p>B.5.3 Deflections for serviceability checks</p> <p>The maximum mean hourly deflection, δ, should be obtained from each set of analyses.</p> <p>The required Δ for use in 3.3.2 of Part 1 is then obtained as follows:</p> $\Delta_a = (1 + G_B) \delta_{TE} + \sum_{1 \text{ to } 3} (1 + G_{An}) \delta_{An} \text{ in accordance with 5.2.5 a) of Part 1}$ $\Delta_b = \delta_{TE} + \sum_{1 \text{ to } 3} \delta_{An} \text{ in accordance with 5.2.5 b) of Part 1}$
5.1.4	<p>The serviceability check would then be carried out in the same manner as in Appendix A.</p>
2.5	<p>B.6 Safety assessment</p> <p>The maximum member loads are checked against the design strength thus to achieve the required reliability with respect to strength:</p> $\Sigma F_{\max} \leq \frac{Q_k}{\gamma_m} \text{ for each member}$ <p>where</p> <p>Q_k is obtained in accordance with DD 133, or equivalent.</p> <p>See A.6.1 of Appendix A for typical calculations.</p>

Appendix C Background to the use of Part 1

C.1 General

C.1.1 *Introduction and philosophy*

The scope of Part 1 was specified in a brief prepared by the British Standards Code of Practice Committee for Lattice Towers and Masts. Part 1 is intended to provide a rational basis for estimating loading for free-standing towers of lattice construction with due allowance for dynamic response to gusty winds. Guyed masts and offshore-mounted lattice towers are not fully covered by BS 8100 at present, for the reasons discussed in C.1.2.

Part 1 is suited to worldwide application and is so written that use may be made of the best meteorological information available. In view of the common practice to allow competitive design for strength and in the absence of a structural design code for lattice towers written in limit state format, safety factors on design loadings and on characteristic values of strength are given. DD 133 [1.1] provides a means of deriving characteristic strengths of members fabricated, erected and maintained to good practice. By use of the partial factors contained in Part 1, appropriate design strengths can be derived for other less well-controlled structures. Such strengths may need to be assessed when dealing with the appraisal of existing structures, or in work overseas. In this way it has been possible to overcome the problem of choice of load factor which followed the publication of CP 3: Chapter V: Part 2 [1.2]. The probabilistic nature of the primary loadings demanded statistical models. Thus, limit state principles and the partial load factor method of design have been adopted.

C.1.2 *Application to guyed masts and offshore-mounted lattice towers*

C.1.2.1 *Guyed masts.* The provisions in Part 1 for assessing the meteorological parameters to be used in design (section three) and wind resistance (section four) are also applicable to the design of guyed masts. However, the gust response of free-standing towers in which the first mode of vibration predominates, is inapplicable to guyed masts where many modes can contribute to the peak loading. In addition, correlation of gusts over lengths between stays affects the peak forces in the members. For these reasons, the gust response factors given in section five of Part 1 are inappropriate for guyed masts and recourse should be made to published sources to determine their response. Theoretical guidance is given in a CIRIA publication [1.3] and recommendations for the design and analysis of guyed masts are contained in recommendations published by the International Association for Shell and Spatial Structures [1.4].

In addition, the safety factors set out in section two of Part 1 have been based on calibration studies of lattice towers only, and on the provisions of the strength Draft for Development DD 133 [1.1] which was developed for lattice tower type construction. For these reasons, the provisions of section two of Part 1 may be inappropriate for guyed mast design, although they may be used for general guidance purposes.

It is intended to extend the scope of Part 1 to incorporate the recommendations for guyed masts at a future date.

C.1.2.2 *Offshore-mounted lattice towers.* Lattice towers mounted on offshore platforms are not covered by Part 1 as far as the meteorological parameters (section three) and safety factors (section two) are concerned. The gust response factors are inappropriate for inclined flare booms, and for booms supported other than solely at their base. Interference effects from the platform itself have a major influence on the wind loading and no provisions are contained in Part 1 to assess these effects. The provisions of section five of Part 1 are also related to land terrain and the figures in Part 1 would need to be extended for offshore conditions. Guidance on how Part 1 could be extended for application to these structures has been developed for the Department of Energy [1.5], and it is hoped that Part 1 will be extended to incorporate the necessary amendments covering all of these aspects, at a future date.

C.1.3 *References in C.1*

1.1 BRITISH STANDARDS INSTITUTION. *Strength assessment of members for towers of lattice construction*, 1st ed., 1985, DD 133.

1.2 BRITISH STANDARDS INSTITUTION. *Code of basic data for the design of buildings: Chapter V Loading: Part 2 Wind loads*, 4th ed., 1972, CP 3: Chapter V: Part 2.

1.3 CONSTRUCTION INDUSTRY RESEARCH AND INFORMATION ASSOCIATION. *The modern design of wind sensitive structures*, 1971.

1.4 INTERNATIONAL ASSOCIATION FOR SHELL AND SPATIAL STRUCTURES, WORKING GROUP NO. 4. *Recommendations for the Analysis and Design of Guyed Masts*, 1981.

1.5 FLINT AND NEILL PARTNERSHIP. *Extension of the Lattice Tower Code to Offshore Mounted Structures*, Final Report for the Department of Energy, No. 605/1, 1983 (unpublished).

C.2 Performance requirements

C.2.1 Safety and service life

Performance requirements for towers are stated in terms of the relevant limit states broadly in accordance with ISO/DIS 2394 [2.1]. These aim to provide acceptable reliability related to the particular usage and location of the tower.

Lattice towers can be used for a wide variety of purposes and in differing environmental conditions. It follows that the consequences of a tower's failure can differ significantly, and it is logical to provide higher margins of safety in design in those towers for which collapse could have significant economic consequences or would be likely to cause loss of life.

The safety provisions of Part 1 are partially based on the probabilistic approach since by this means safety factors for use in design may be selected in a rational way and adjusted for any chosen level of reliability. A statistical model has been used to define safety calibrated against existing practice, as recommended by the CIRIA Study Committee on Structural Safety [2.2].

The safety factors appropriate to any required reliability levels are related to corresponding values of notional failure probability, calculated as described in C.2.7. The failure probability is notional in the sense that it relates only to random variabilities of the loads and structural strength which are considered in the design, no allowance being made for gross error or unforeseen (accidental) loadings.

The range of values of notional annual failure probability for the categories of tower covered by Part 1 is about 10^{-2} to 5×10^{-4} which embraces the range recommended for transmission towers in the draft recommendations prepared by the International Electrotechnical Commission (IEC) [2.3] which considers three reliability classes with annual probabilities of failure from 10^{-2} to 10^{-3} . The lower value of probability has commonly been considered to be appropriate to structures of inhabited buildings. (See, for example, the draft Nordic safety code [2.4].)

C.2.2 Classification of required reliability

C.2.2.1 General. No additional guidance.

C.2.2.2 Environmental conditions. The safety margins chosen for the design of a tower should reflect the potential risk to life in the event of its failure. A basis for selecting a target level of reliability is discussed in CIRIA Report 63 [2.5]. It is suggested that the target notional annual failure probability for towers should not exceed $10^{-4}/N_1$ where N_1 is the likely number of fatalities in the event of a failure. Thus the target value should depend on the environment in which the structure is built.

In considering this number, it is suggested in CIRIA Report 63 [2.5] that allowance be made for the degree of correlation between the loading leading to failure and the number of people likely to be close to or on the structure. Since failure, if it occurs, is most likely to occur under extreme wind speeds, it may be assumed that there will be no one climbing a tower at the time and that people will not be in its vicinity unless there are buildings near its base. Thus for unmanned towers in open countryside the value of N_1 may be of the order of 0.03 to 0.01, i.e. there would be a chance of less than 1 in 30 of a death in the event of a collapse. It is of interest to note that no deaths have resulted from the collapse due to wind loading of a number of transmission towers during the past 25 years.

At the other extreme will be a tower located on an industrial or residential site or adjacent to a building housing personnel operating systems mounted on the tower. In such cases the value of N_1 may lie in the range 0.1 to 10, with due regard to the average periods of occupation of the buildings, their proximity and the direction of their position relative to the structure in relation to the prevailing wind (see the wind roses in Figure 3.8 of Part 1).

The performance requirements are related to the environment of a tower as shown in Figure 2.1 of Part 1, the categories given being considered to correspond to the following likely number of fatalities:

Environment	Number of fatalities assumed
Unmanned towers in open country or sea	0.01 to 0.04
Manned towers in open country or sea	0.04 to 0.06
Tower adjacent to major road or railway	0.06 to 0.1
Towers in suburban or industrial area	0.1 to 0.2
Major towers in urban environment	≥ 0.2

C.2.2.3 Economic consequences or usage. When a tower is to be located at a site for which the risk of loss of life in the event of a failure is slight or when the function of the structure is of great economic importance, the safety margins used in design should reflect the financial consequences of collapse. In such circumstances, the method proposed by Bea [2.6] may be used to determine the target level of notional reliability which will provide the least total of initial cost and potential future costs consequent upon a failure. The latter may be expressed as the present value of the estimated consequential costs multiplied by the notional failure probability during the design service life.

In deriving the optimum probability, it has been assumed that the weight of the design is governed only by wind loading, i.e. that the dead load is only a negligible fraction of the live load. In such circumstances, Ryles' formula may be used to express the weight of a structure, W , of given height and configuration as approximately:

$$W = \text{constant} \sqrt{\gamma_G}$$

where γ_G is the global factor on wind loading given in C.2.4.1.

The initial cost of the superstructure may then be taken to be proportional to $K_j W$ where K_j is a factor to allow for the relative cost of design, fabrication, control and maintenance. It has been assessed that the factor K_j may change by 5 % when transferring from one quality class to the next.

On this basis, the relationships between the relative initial costs and the notional failure probability may be obtained by use of the values of safety factors derived for the different classes. These are plotted in Figure C.2.1 from which it may be seen that there is little difference in initial costs of the three quality classes for a given reliability, since the lower global safety factors of a higher quality class balance the increased cost factor, K_j , required for the improved quality. It was therefore considered unnecessary to differentiate between the three quality classes.

The present value of the potential consequential costs may be expressed as:

$$E_1 P_1 \frac{\{1 - e^{-(U_j - U_1) i_s}\}}{U_j - U_1}$$

where

U_j is the appropriate interest rate on capital;

U_1 is the rate of inflation;

i_s is the design life;

E_1 is the estimated consequential cost of failure including the cost of replacement;

P_1 is the notional probability of failure.

By taking various ratios, g , of the consequential costs to initial cost, the present value of the total potential costs may be derived for different failure probabilities and values of the effective interest rate ($U_j - U_1$). Since the inflation and interest rates over the design life cannot be accurately predicted, it has been assumed that the economic optima may be judged assuming that $U_j - U_1$ is between 10 % and zero. The resulting total costs for a design life of 50 years are plotted in Figure C.2.2 for a class A structure for both effective interest rates of zero and 10 %.

It will be seen that in each case there is an optimum notional failure probability for least total cost which corresponds to a particular value of γ_v , the partial safety factor on wind speed. These results have been used to produce the economic categories shown in Figure 2.1 of Part 1, represented therein as a band covering the range of effective interest rates.

Where the economic consequences of failure are not readily assessable, the wind speed factors should be chosen as appropriate to the function of the tower within the suggested usage ranges indicated in Figure 2.1 of Part 1, which have been based on an assessment of the economic importance of typical structures. It is, however, recommended that, when possible, the consequences be evaluated for each design, location and function.

C.2.3 Classification of quality

Part 1 is written to apply to towers designed and constructed in accordance with best practice in the UK to levels of materials and workmanship comparable with those specified in relevant British Standards and the safety factors given have been derived by reference to results of tests on towers of such quality. It is, however, recognized that the reliability of a given design may be influenced by errors in the design and detailing. In consequence there is justification for permitting lower safety margins in instances in which such errors are controlled either by appraisal of the final design by an experienced engineer working independently of the designer, or by testing of the kind commonly undertaken on prototype transmission towers.

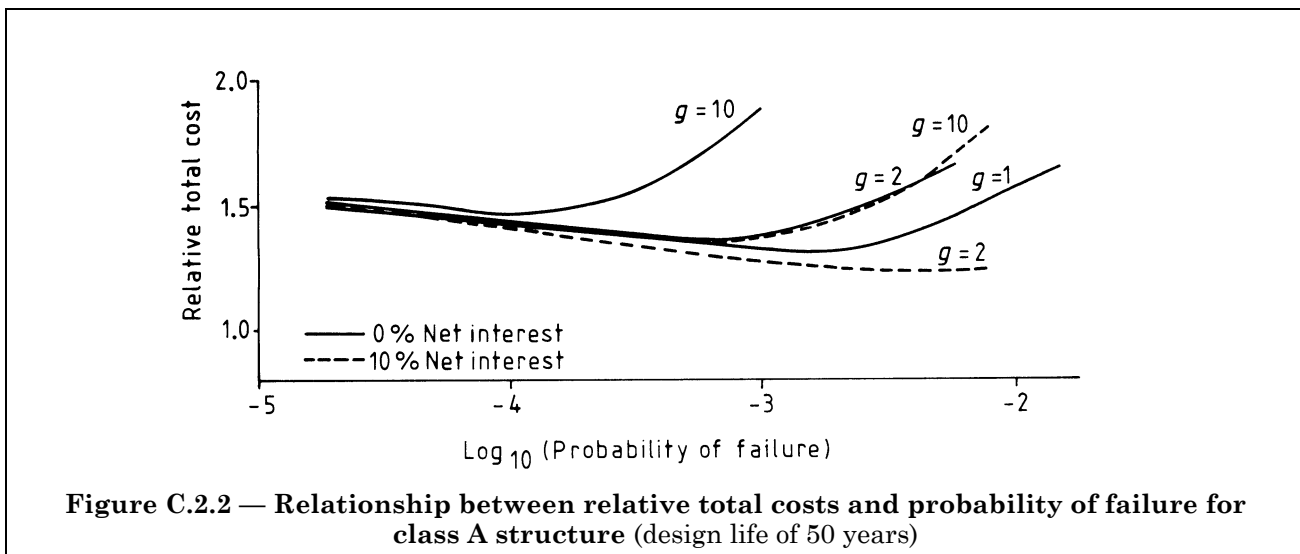
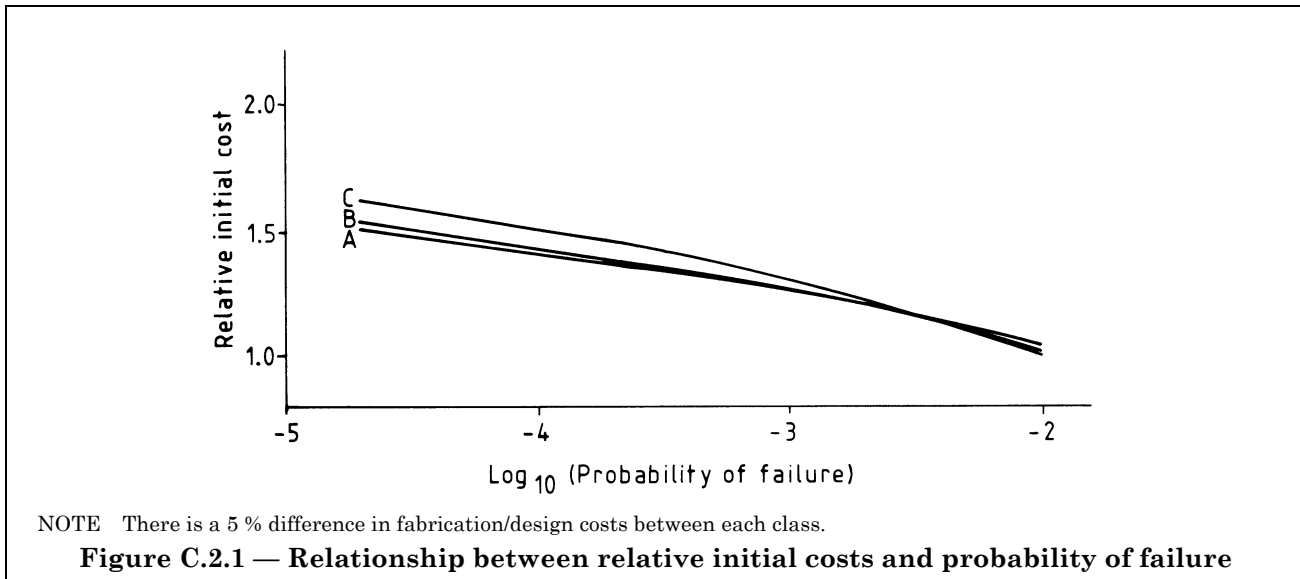
Furthermore, it has been considered to be desirable to recommend the use of higher margins of safety for towers for which errors in fabrication and erection are not to be controlled by independent inspection and which are not to be subject to regular inspection and maintenance in service.

The statistical models used to represent the strengths of towers employed log normal frequency distributions with mean values and coefficients of variation related to quality classification. In order to assess the likely strengths of towers in relation to their design strengths, the CEGB and Balfour Beatty & Co. Ltd. have made available the results of full-scale tests carried out at their testing stations. For transmission line structures, type tests are carried out under specified loadings and records are kept of failures where these occur at less than the specified load. Thus a statistical sample of results arising was available for analysis to assess the likely distribution of strengths. Unfortunately, most of the tests considered apply to conditions outside the scope of Part 1, due to the loading cases used in the tests. For example, in broken wire conditions the critical members may be governed by a loading pattern specific to transmission type towers or for line deviation towers the main loading is from conductor tensions where part of the uncertainty associated with the difference between predicted and observed failure is due to the analytical method used to determine the forces in the members. In addition, after a premature failure the designer will try to identify the cause of failure and provide an economic solution within the limitations imposed by the geometry of the tower. If such efforts are unsuccessful, these additional tests are each recorded as a further failure. Strictly, they should be regarded as design development tests or experimental efforts to eliminate the identified weakness.

The most relevant tests are those associated with the latest designs for transmission towers. The results of nine such tests are shown in Table C.2.1 for both towers as submitted for testing, and for those to which remedial improvements were made after premature failure had occurred.

It was considered that the towers used for testing, prior to any strengthening that may have been found necessary as a result of the tests, represent typical tower construction in the UK and that they typify quality class B or C structures. As the conditions of service of the towers at the time of testing would be unknown, they could not be considered categorically as class B structures [see item f) of 2.3.2 of Part 1]. Those towers which have been tested and which in consequence may be considered to have had gross errors and design shortcomings eliminated may be considered to be class A structures. Such towers would invariably be subject to high standards of maintenance.

From Table C.2.1 it may thus be seen that the mean failure loads, as a percentage of the design load, would be 105 % for a class A tower and 94 % for the classes B and C. For codification purposes, i.e. for the application of the theory into the form of Part 1, it was assumed that the mean failure load for class B was 100 % and for class C was 95 % of the design load. The coefficients of variation from the test results were found to be 3 % and 15 % for the two categories. The 3 % figure was considered to be difficult to achieve in general design practice, and test results on other towers indicated that, even after strengthening, a coefficient of variation of perhaps 10 % would be more appropriate. For classes B and C, coefficients of 15 % and 20 %, respectively, were assumed.



The parameters for the three quality classes are thus:

Class	A	B	C
Mean failure load/design load	1.05	1.00	0.95
Coefficient of variation	0.10	0.15	0.20
Characteristic strength	0.90	0.75	0.60

The equivalent values for the CEGB tests on unmodified and modified towers are:

	Modified after test	Unmodified
Mean failure load/design load	1.05	0.94
Coefficient of variation	0.03	0.15
Characteristic strength	1.00	0.70

The adopted class C category is compatible with tests on unproven design configurations, where existing experience was not necessarily of benefit and could be representative of general tower designs, unchecked by others and fabricated or erected without supervision and rectification of errors.

The tower test results for leg failure and bracing failure separately analysed have not disclosed any significant differences in their statistical characteristics, and it has, therefore, been acceptable to adopt a single distribution for all members of a given quality class.

The IEC Technical Committee for transmission line design [2.3] recommend, for transmission line towers only, a range of characteristic strengths from 0.87 to 0.94 of the mean value with a corresponding range of coefficient of variation of between 0.05 and 0.1. This is broadly in line with the adopted class A tower parameters.

A study was also undertaken of existing practice in assessing the strengths of individual members of lattice towers. Whilst towers contain large numbers of members, only a few are tightly designed for a given critical loading direction, as a result of member standardization and geometric constraints. This emerged clearly from the calibration studies undertaken for the BBC et al [2.7] in developing Part 1. In view of this, the overall structural strength characteristics of the tower classes adopted may be considered to be consistent with the characteristics of the individual members.

For all reliability analyses it is necessary to define a strength model. Even in the case of the tested towers, their design strengths are not known and may be based on different strength/slenderness relationships and using different assumptions concerning effective lengths. There has, therefore, been no clear definition of design strength. The most relevant British Standards (BS 449, which is obsolescent, and BS 5950) do not define the relationship between design strength and characteristic strength. The general nature of both these documents, however, renders them inappropriate for the prediction of strengths for these specialized frameworks. Consequently, it was agreed to adopt the design proposal for lattice frames of ECCS task committee 7, which is based on results from transmission tower tests, and to produce these in the form of a design directive to be used in conjunction with Part 1. This directive is being published by BSI as a Draft for Development (DD 133) and should be used as the basis for predicting directly member characteristic strengths. The design strengths are then obtained by dividing these characteristic strengths by the appropriate partial safety factor on strength (see 2.5 of Part 1).

In order to provide guidance on the delineation between the proposed quality classes of tower, conditions are recommended which, if all are complied with, would ensure a class A structure. These conditions cover design, checking (either by testing or by an independent appraisal), material quality, workmanship inspection and maintenance. Class B towers should comply with all these conditions, other than the recommendation for testing or independent checks. Towers that comply with the design recommendations of Part 1, with materials and workmanship in accordance with British Standards, but without independent checking, testing or inspection, are deemed to be class C structures. Whilst such structures are not to be recommended for use in the UK, conditions abroad may dictate that erection checks and maintenance are out of the control of the designer and in such cases it may be advisable to assume class C structures with a consequent weight penalty. Class C towers may also need to be assumed when appraising existing structures.

C.2.4 Safety factors

C.2.4.1 Wind speed and ice thickness factors. The reliability analysis outlined in C.2.7 has been used to derive global factors of safety between the 50 year return wind load and the mean strengths, for the three classes of structure. The global factor, γ_G , under wind loading, was partitioned to provide partial factors on wind loading, γ_{wL} , and partial factors on design strength, γ_m , such that:

$$\gamma_G = \gamma_{wL} \gamma_m$$

The partial wind load factor was further modified to be applicable to wind speed, γ_v , as the factored speed, rather than load, is the relevant parameter to consider for various criteria in Part 1, such as Reynolds number (see 4.2.1 of Part 1), wind speed to avoid aerodynamic excitation (see 5.5.1 of Part 1) and the spectral analytical formulae (see Appendix E of Part 1). In addition, the factors on ice load were found to coincide with those for wind speed (see C.3.5.3).

The analysis thus provided a curve of partial factors on wind speed, for elements loaded by wind only, against notional probabilities of failure, p_1 . These values of p_1 were related to the two criteria for performance requirements described in C.2.2.2 and C.2.2.3, namely:

- a) environment;
- b) economic consequences or usage.

Figure 2.1 of Part 1 was developed accordingly and its use is described in C.2.5.

Table C.2.1 — Analysis of test data for CEGB D type towers

a) Percentage of design ultimate load at failure for tower as first offered for test.				
Tower test	Percentage ultimate design load			Remarks
	Transverse	Vertical	Leg load	
	%	%	%	
1	100	100	100	Single circuit
2	105	100	104	
3	95	100	96	
4	75	90	83	
5	105	100	104	
6	70	90	80	Single circuit
7	70	70	65 ^a	Single circuit
8	110	100	108	
9	105	105	105	
Mean failure load		= 93.9 %		
Standard deviation		= 13.8 %		
Coefficient of variation		= 14.7 %		
Characteristic strength		= 93.9 (1 - 1.64 × 0.147)		
		= 72 %		
^a Bracing failure				
b) Percentage of design ultimate load at failure on destruction test after remedial improvement where premature failure had occurred.				
Tower test	Percentage ultimate design load			Remarks
	Transverse	Vertical	Leg load	
	%	%	%	
1	100	100	100	
2	105	100	104	
3	103	100	102	
4	104	100	103	
5	105	100	104	
6	106	100	105	
7	110	110	110	
8	110	100	108	
9	105	105	105	
Mean failure load		= 104.5 %		
Standard deviation		= 2.8 %		
Coefficient of variation		= 2.7 %		
Characteristic strength		= 104.5(1 - 1.64 × 0.027)		
		= 100 %		

The uncertainties which are taken into account in the determination of the values γ_G (and thus γ_v) to obtain the notional probabilities of failure, p_1 , are discussed in C.2.7.2. There is a clear distinction between the equivalent static method (see 5.1.2 of Part 1) and the spectral analytical method (see 5.1.3 of Part 1), in that the latter makes specific allowance for dynamic magnification of the response, taking account of the dynamic properties of the tower considered. An allowance based on typical values of dynamic magnification is included in the equivalent static method, but the variability of the dynamic effects over the range of structures to which the static method may be applied, i.e. noting the limitation imposed, in 5.1.1 of Part 1 (see C.2.7.3), is included in the respective reliability analysis.

The use of both the static and spectral analysis methods in Part 1 required careful consideration of the appropriate safety factors to be used. The variability of dynamic effects results in the static procedure leading to the design of towers which, if examined by the spectral analysis procedure, could be shown to have varying notional probabilities of failure. To provide compatibility with the greater consistency and lower variability of the spectral analytical procedure, a marginal allowance (2 % on wind speed) would be required in application of the spectral analytical procedure, relative to the values which would give the target overall notional probability of failure (integrated across the whole range of towers) selected for application of the static procedure.

The static procedure includes an allowance for dynamic amplification, in the factor applied in 5.2.3 and 5.2.4 of Part 1 and in the augmented peak factor (see C.5.7.3.4). The notional probability of failure using the dynamic procedure is approximately the same as the average value for that half of the structures envisaged as being designed by the static procedure which are the least favourable in terms of dynamic properties. The reduction factor 0.97 applied to γ_v thus gives an overall economy in use of the dynamic procedure.

C.2.4.2 Dead load factors. The reliability analysis outlined in C.2.7 was repeated for two ratios of dead to wind load to enable partial dead load factors to be derived. These were also obtained for the range of notional failure probabilities and corresponding values to the relevant figures were plotted on Figure 2.1 of Part 1. Two sets of figures are provided, the first where dead load effects are additive to the wind load effects, in which case higher partial factors on dead load are required to achieve the required reliability. For dead load effects reducing wind load effects, it was found that the factor was insensitive to the range of notional failure probability considered and a constant value of 0.9 has been adopted.

C.2.5 Safety assessment

Figure 2.1 of Part 1 should be used by first selecting the performance requirement of the tower appropriate to both:

- a) the environmental conditions in which the tower is to be built; and
- b) the economic consequences of failure of the tower (if these cannot be defined, then the usage of the tower should be considered within the range defined in Figure 2.1 of Part 1).

Part 1 requires the more onerous performance requirement to be used so that a manned broadcasting tower in open countryside would have a γ_v value (see Figure C.2.3, based on Figure 2.1 of Part 1) of between 1.11 and 1.16. The range is appropriate to the relative importance of the structure; the actual level should be specified by the client unless he would accept the minimum value which would be 1.11. However, if the broadcasting tower were to be erected adjacent to a main road, the minimum value of γ_v would be 1.16 and the upper recommended value 1.20.

This example excludes the economic consequences criteria but would be appropriate for a tower whose design life was 30 years and whose consequences of failure would be between about 1.7 and 3.8 of its initial cost, when designed between the limits of “manned in open countryside”.

An alternative presentation of Figure 2.1 of Part 1 is shown in Table C.2.2 in which the range of γ_v for each combination of usage and environment is provided. The economic consequences criteria are also included in this form of presentation, but are not necessarily linked to the usage criteria, i.e. civil telecommunications towers do not necessarily have economic consequences of failure given by $60 < gi_s < 160$. In both Figure 2.1 of Part 1 and Table C.2.2, once the value of γ_v has been selected, i.e. appropriate to the abscissa in the graph of Figure 2.1 of Part 1, then the corresponding values of γ_{DL} and γ_m can be selected. The partial factor on dead load depends on whether the dead load effects increase or decrease the wind load effects. The partial factor γ_m depends on the quality class of the tower.

C.2.6 Serviceability

The serviceability requirements for a tower are invariably related to limiting deflections or rotations to acceptable levels under moderate wind speeds. Generally, broadcasting or radar towers are required to deflect within defined constraints for a given proportion of the time. Traditionally, the criterion has been for a given rotation, e.g. 0.5° , not to be exceeded at a fraction, e.g. 0.75, of the full design wind speed. This was intended to ensure that for a high percentage of time this limit is satisfied. Floodlighting towers are required to remain sensibly rigid and towers supporting stacks should not allow large movements to occur, to prevent breakdown of the stack joints. Part 1 provides more comprehensive information than has been available hitherto, to enable the designer to calculate the periods for which specified deflections are exceeded, incorporating direction factors to cater for where deflections are directionally critical.

C.2.7 Background to statistical basis

C.2.7.1 Reliability theory

C.2.7.1.1 General. The theoretical (notional) probability of failure p_1 of any one of an identical family of structures, all assumed to be located at the same site, may be defined in terms of the statistical distribution of extreme loads and of the frequency distribution of the strength of the structures in relation to the value of strength assumed in design. In its simplest form:

$$p_1 = \int_0^{\infty} p(W) \left\{ \int_0^W p(Q) dQ \right\} dW$$

where

$p(W)$ is the probability density of the load function;

W is the load;

$p(Q)$ is the probability density of the strength function;

Q is the strength.

If the distributions of the loading and strength functions are known, the risk of failure can be varied by modifying the relative locations of these distributions, i.e. adjusting the load factor. This is shown diagrammatically in Figure C.2.4.

The uncertainty in the structural strength, leading to the probability density function $p(Q)$, is discussed in C.2.3.

With regard to the factors taken into account in the assessment of uncertainty in loading, recognition of differences in the nature and origin of uncertainties may be helpful; in particular the distinction between physical uncertainty, statistical uncertainty and model uncertainty [2.8].

Physical uncertainty is particularly well exemplified by wind loading. Even if all the required input data were exactly determined, the actual maximum wind load occurring during the intended lifetime of the structure (or in any other predetermined period) would be uncertain, because of the random nature of the occurrence of extreme wind storms. The probability of occurrence of a wind speed of, for example, 25 % higher than the highest speed which on average will occur once in the lifetime of the structure is small, but nonetheless significant in relation to the target level of reliability for most structures.

The Fisher-Tippett type 1 (Gumbel) extremal distribution has been widely accepted for the analysis of extreme winds (see C.3.1.2). The distribution has been based on the analysis of annual maximum speeds, but it has recently been recognized that it is better applied to the square of the speed, i.e. pressure, q , than the speed itself. If the annual maxima are Gumbel distributed, the probability distribution of the maximum value of q in a predetermined period takes the same form.

However, there is also statistical uncertainty. In this context, this means that there will be some uncertainty in selection of the values of the parameters of the Gumbel distribution, i.e. the mode and the dispersion, applicable to the given site. The mode is the value having a return period equal to the design life. Most commonly this will be estimated from a map such as Figure 3.1 of Part 1, generally requiring interpolation to the site, and correction for terrain and topography. The statistical uncertainty of the mode has been treated as Gaussian, with a coefficient of variation of 0.15 appropriate to a 60 m high tower. Since the effect of the terrain and topography corrections diminish with height, the values used for the relevant coefficient of variation diminish with height. Marginal adjustments were made for higher and lower towers.

The dispersion is expected to be broadly in proportion to the mode. A special investigation of this relationship was made by the Building Research Establishment, giving data on the variation of the ratio of the dispersion to the mode deduced from records of annual maxima at sites in the UK. Corrected to the longer periods representative of the design life, these results indicated an uncertainty in the dispersion/mode ratio for any arbitrarily-selected site corresponding to a log normal distribution with coefficient of variation 0.13.

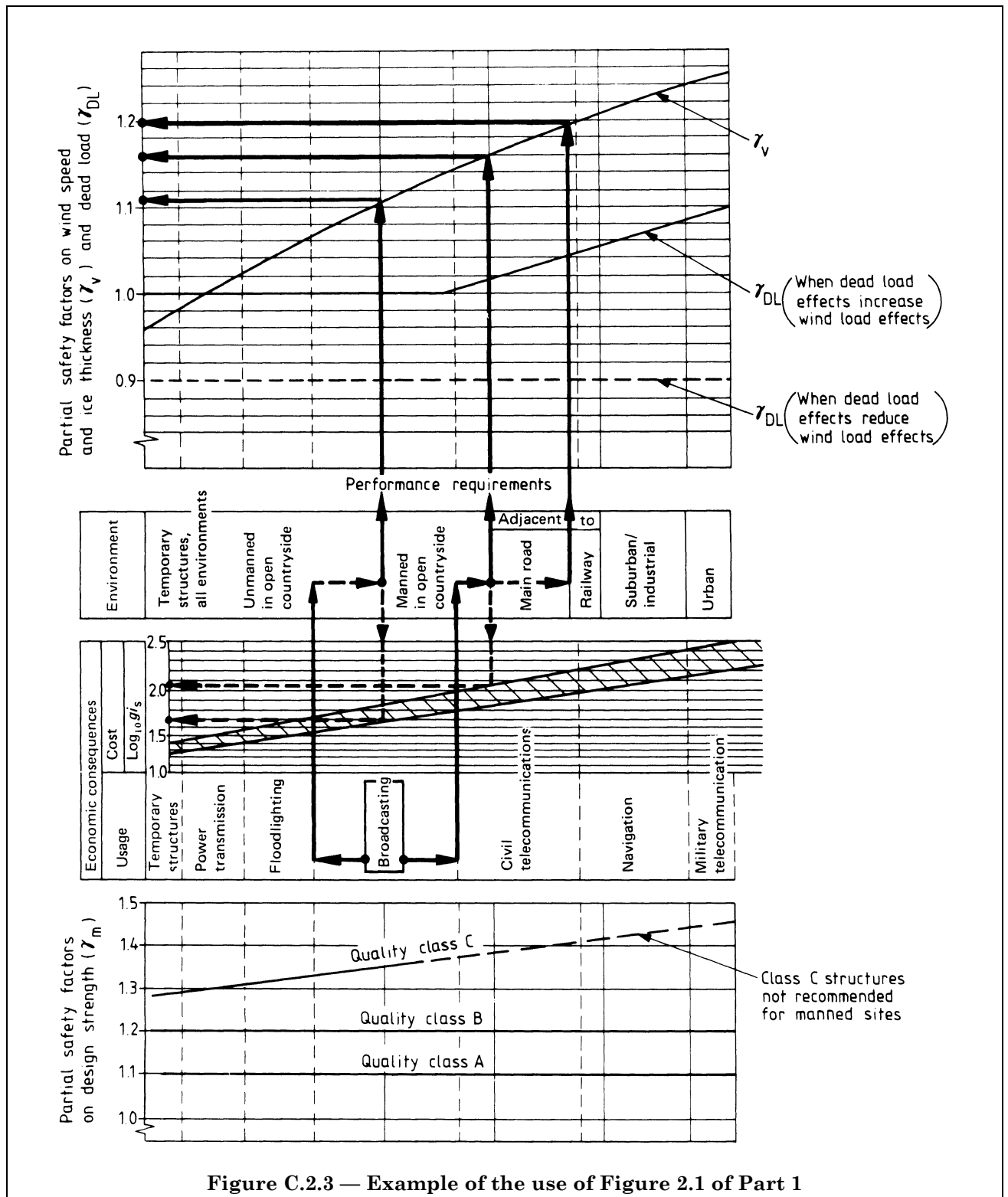


Figure C.2.3 — Example of the use of Figure 2.1 of Part 1

Table C.2.2 — Alternative presentation of Figure 2.1 of Part 1

a) Partial safety factors on wind speed and ice thickness, γ_v																		
Economic consequences		Environment																
Either Usage	Or Cost, g_{i_s}	Unmanned in open countryside	Manned in open countryside	Adjacent to main road	Adjacent to railway	Suburban/ industrial	Urban											
Temporary structures	15 to 25	0.96 to 0.98	0.96 to 0.98	0.96 to 0.98	0.96 to 0.98	0.96 to 0.98	0.96 to 0.98											
Power transmission	20 to 35	0.98 to 1.03	1.11 to 1.15	1.15 to 1.20	1.20 to 1.21	1.21 to 1.24	1.24 to 1.26											↑ Environment governs ↓
Floodlighting	25 to 50	1.03 to 1.06	1.11 to 1.16	1.16 to 1.20	1.20 to 1.21	1.21 to 1.24	1.24 to 1.26											
Broadcasting	30 to 70	1.06 to 1.11	1.11 to 1.16	1.16 to 1.20	1.20 to 1.21	1.21 to 1.24	1.24 to 1.26											
	50 to 90	1.11 to 1.14																
Civil telecommunications	60 to 100	1.14 to 1.16	1.16 to 1.20	1.20 to 1.21	1.21 to 1.24	1.24 to 1.26												
	70 to 160	1.16 to 1.20																
Navigation	90 to 180	1.20 to 1.21	1.20 to 1.21	1.20 to 1.21	1.20 to 1.21	1.24 to 1.26												
	100 to 250	1.21 to 1.24	1.21 to 1.24	1.21 to 1.24	1.21 to 1.24													
Military telecommunications	130 to 300	≥ 1.24	≥ 1.24	≥ 1.24	≥ 1.24	≥ 1.24	≥ 1.24											
← Usage governs →																		
b) Partial safety factors on dead load, γ_{DL} , and on design strength, γ_m																		
γ_v [selected from a)]	0.94	0.96	0.98	1.00	1.02	1.04	1.06	1.08	1.10	1.12	1.14	1.16	1.18	1.20	1.22	1.24	1.26	
γ_{DL} (dead load effects increase wind load effects)	1.0											1.02	1.03	1.05	1.07	1.09	1.10	
γ_{DL} (dead load effects decrease wind load effects)	0.9																	
γ_m	Class A	1.1																
	Class B	1.2																
	Class C	1.27	1.28	1.29	1.30	1.31	1.32	1.33	1.34	1.35	Class C not recommended							

The prediction of the maximum load effect, given the basic speed pressure, is based on the stochastic analysis and the associated mean (expected) values of the relevant wind structure parameters, etc., as set out by Wyatt [2.9]. As already pointed out (see C.2.4.1), if the design is based on the equivalent static method, there is an additional uncertainty in the value of the margin between the maximum load effect and the strength, resulting from the range of dynamic properties that can be anticipated in structures so designed. This requires a major addition to the reliability analysis, based on a study of the basic structural parameters which influence the dynamic properties, which is discussed in C.2.7.2.

C.2.7.1.2 Influence of parameters on reliability. Consideration has to be given to the following uncertainties.

a) *Wind structure.* There is considerable uncertainty in the values of the scale parameters for gusts in strong winds. Fortunately, however, the prediction of maximum values of load effect in tower-type structures is relatively insensitive to the values taken.

It is also fortunate that the reliability analysis can broadly be viewed as summing variabilities by addition of variances (mean-square deviations), and thus factors which have r.m.s. deviations less than, for example, one-quarter of the dominant term have a very weak influence on the result. A study of the complex interactions of scale parameters, power spectrum, co-spectrum and turbulence intensity by means of parametric studies of the effect of various input values, suggested that it was sufficient to apply a small additional variability to the overall result. For the intermediate steps of comparison of quasi-static and dynamic components to study the dynamic magnification, the quasi-static component could adequately be represented as a deterministic multiple of the corresponding mean hourly load effect, the value of the multiplier being predetermined as a function of terrain and structure height.

The basic case was taken as terrain category III ($z_0 = 0.03$ m) and an appropriately factored wind speed was taken. For this case, the r.m.s. quasi-static response for 60 m high towers was considered to be about 0.3 times the mean hourly value. This quantity increases slightly according to the height above ground of the location considered, and decreases considerably with increasing overall height of tower.

b) *Wind resistance.* The basic reliability study was focused on cases where the wind resistance is dominated by the structure itself in combination with linear or quasi-linear ancillaries, possibly including simple arrays of small antennae or floodlights. For such cases, the uncertainty in the resistance can be postulated to be fairly small; a normal distribution with a coefficient of variation of 0.10 was assumed.

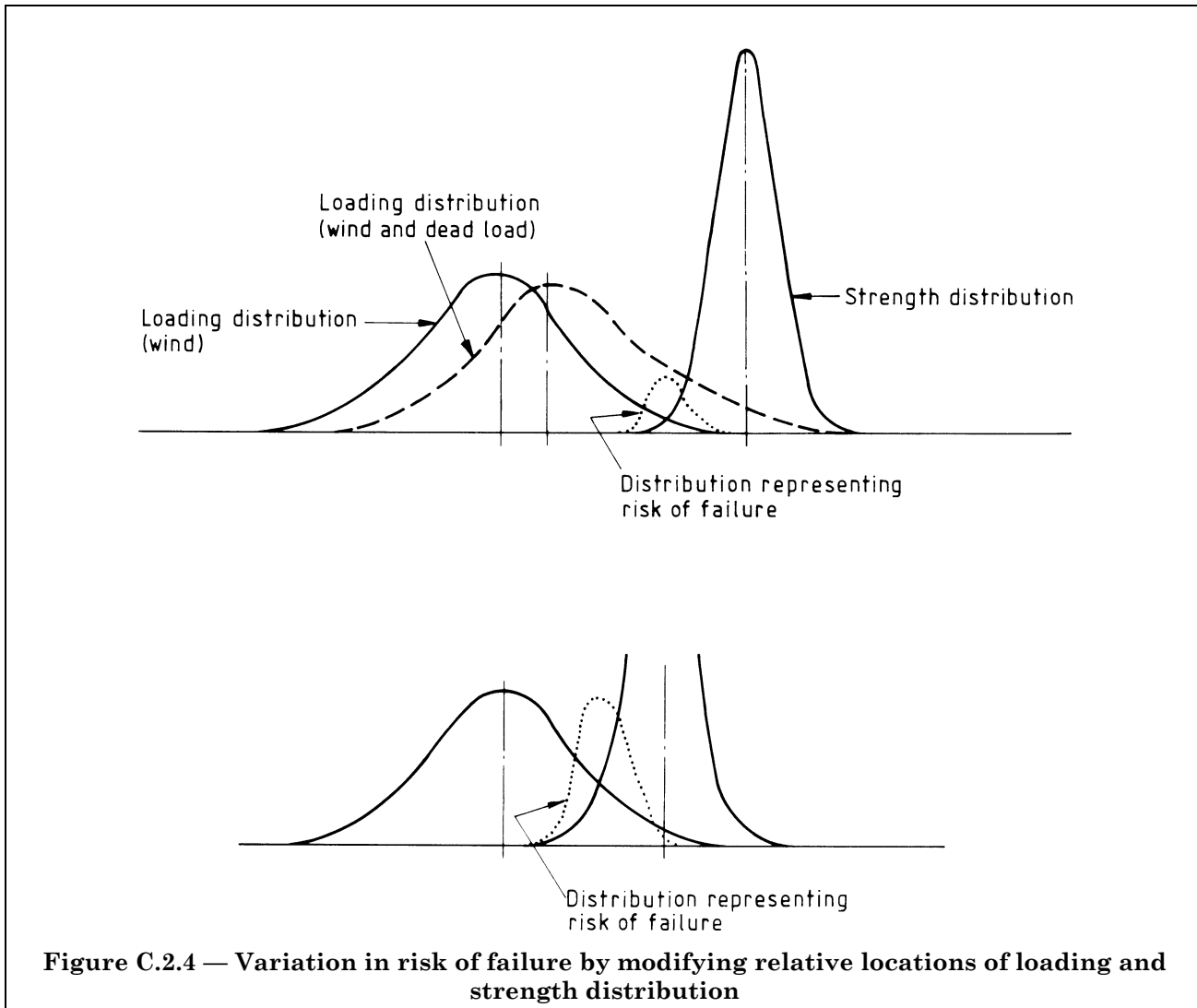
c) *Model uncertainty.* It has been shown that natural frequency calculations for tower structures give generally good accuracy, because the elastic structure is clearly defined, with the possible exception of foundation compliance. Structural damping is uncertain, but this has relatively little impact because the additional damping action resulting from the wind forces themselves is relatively large and can be well estimated (see C.5.11).

The stochastic analysis procedure is believed to give good results in very strong winds. No allowance has been made for any enhancement of structural tolerance of dynamic response that may result from yielding or other non-linearity in the structure. The model uncertainty is thus small. The overall effect of wind structure and dynamic analysis uncertainties (statistical and model), as expressed in terms of the ratio of the r.m.s. resonant contribution to the corresponding mean hourly value of the load effect, was conservatively taken as giving a coefficient of variation of 0.15. The distribution was assumed to be log normal; the expected values are discussed in C.2.7.1.3.

d) *Gust response multiplier.* The maximum value of a response process of the type treated by the stochastic analysis is obtained from a multiplier applicable to the overall r.m.s. fluctuation of load effect and represented by the peak factor, g , (see C.5.6.3). The variability associated with this factor can also be evaluated [2.8], and was included in the overall evaluation of the notional probability of failure.

e) *Dead load.* The dead load was considered to be normally distributed, with a mean value equal to the evaluated nominal dead load, and a coefficient of variation 0.05.

C.2.7.1.3 Combination of uncertainties. Computation of the notional probability of failure arising from the combination of the uncertainties discussed in C.2.7.1.2 was then carried out for a range of values of the global load factor, γ_G . This procedure had to be repeated for a range of relative influence of dead load and live load, for members at different locations in the tower, for the various quality classes, and for towers of various heights. Specifically, results were computed for wind load only, and for wind load plus and minus dead load of nominal magnitude one-half of the wind load; and for tower heights of 25 m, 60 m and 240 m. These results were plotted, and the partitioning of the load factor between wind speed, γ_v , dead load, γ_{DL} and strength, γ_m , was performed by trial. The results achieved represent a satisfactory fit within practical limits; the specified values being independent of tower height, taller towers will have a superior nominal reliability than shorter towers.



C.2.7.2 Reliability analysis applied to the quasi-static procedure. The lowest natural frequency of any practical lattice tower lies in the upper tail of the wind speed power spectrum. This means that the fluctuating wind load contains only relatively weak components in the vicinity of a natural frequency of the structure. However, the damping is relatively small, so there may be a significant resonant response, which can be treated as an addition to the total variance of the fluctuation of stress in any member.

The area affected by a gust, the gust size, is also clearly related to the duration of its effect on a structure as it is carried past by the mean wind. In practice, the size of the resonant gust is very small compared with the size of the structure. For example, the scale length of the 1 Hz gust component in a wind speed of 27 m/s will be about 3 m, whereas a natural frequency of 1 Hz would be typical of towers about 60 m high. Clearly, the lower the natural frequency, the more effective will be the resonant gust component.

Fortunately, a lower natural frequency also implies a more effective aerodynamic damping action (see C.5.11), although this too is not a simple relationship, as the formula makes further use of the ratio of mass to resistance, and there is a strong negative correlation between this ratio and the natural frequency.

The stresses arising due to the resonant component of response can be thought of as in static equilibrium with an inertial loading represented by the product of mass and acceleration at all points on the tower. Since the resonant response of a lightly-damped system follows the natural mode shape, at the natural frequency of free vibrations, the distribution of this load is in proportion to the product of the mass and mode shape function. This implies that the resultant inertia load acts relatively high up the tower, and the relative importance of the stresses so caused in comparison to the static stressing generally increases as the height above ground of the member increases.

It is convenient to group these influences and focus on the following, while recognizing that these effects are not independent:

- a) lowest natural frequency;
- b) aerodynamic damping;
- c) member sensitivity to dynamic loading.

Fortunately, the design of lattice towers is highly systemized, with a relatively small number of basic configurations. Assuming that members are generally designed to come close to the permitted stress under the design wind loading, the natural frequency and other required properties can thus be consistently related to a number of basic variables, which include:

- 1) structural form (square, triangular; sharp edged, tubular members);
- 2) payload and other non-structural elements (especially the ratio of wind resistance to mass thereof);
- 3) slenderness (height/width ratio);
- 4) profile (taper, linear or Eiffelized);
- 5) design wind speed and design stress levels.

The way in which these basic variables can be manipulated to indicate their influence on the natural frequency and aerodynamic damping has been described by Wyatt [2.10]. The variability of the r.m.s. narrow-band (resonant) contribution to response, resulting from the effect of these basic variables on the frequency and damping, has been evaluated in a parametric study.

The number of variables can be reduced by bringing together the factors influencing the ratio of the wind resistance, R_{WT} , to the mass in the upper parts of the tower, m_T . This can be expressed using the parameter τ_T given by:

$$\tau_T = m_T / \rho_s R_{WT}$$

where

ρ_s is the density of the material of the tower structure.

τ_T is a multiple of the parameter t_{av} used in C.5.11.2, the factor depending on the type of construction or tower function, typically as given in Table C.2.3 for cases without significant payloads.

The value of τ_T tends to increase with increasing height of tower, but there is no evidence of a corresponding trend in its relative variability (coefficient of variation).

Appropriate values of the basic variables were derived from parametric studies and compared with values from about 20 actual towers with good agreement.

The resulting parameters are shown in Table C.2.4, for the case of a 60 m high tower, square plan form, sharp-edged members (angles). The analysis for this case, using the previously defined relationships [2.10], predicted a coefficient of variation of 0.27 applicable to the ratio of the r.m.s. narrow-band response to the hourly mean value.

In addition, this ratio is subject to variability as a result of variation of the member sensitivity to dynamic loading, and to uncertainty in the wind structure parameters. These are deemed to correspond to a coefficient of variation of 0.1 in each case, and to be mutually independent. The overall coefficient of variation in this ratio is thus 0.30, by root-sum-square. It was found that this value could reasonably be used throughout the range of tower size and structural form.

The corresponding values of the dynamic parameters and the consequent values of the ratio of the r.m.s. narrow-band response to the mean hourly value are given in Table C.2.5, for towers in terrain category III, expressed in terms of a factor K_m . This factor indicates the variation of dynamic sensitivity with location on the tower. The value of K_m input to the reliability analysis is shown in Figure C.2.5, together with computed values for leg members in seven specific towers of varying type.

The notional probability of failure was then evaluated for arbitrary values of overall load factor, for the wide range of cases described in C.2.7.1.3 These showed that for the 60 m tower in category III terrain, to obtain equal notional probabilities of member failure at different levels in the tower, the global load factor should be 3 % higher for leg members at half-height, and 11 % higher for leg members near the top of the tower, by comparison with values for leg members near the base, assuming a standard basis of the static loading as the mean value plus 4.1 times the r.m.s. quasi-static fluctuation (c.f. C.5.7.3.4).

To allow for this increased dynamic sensitivity using a uniform load factor, the fluctuating part of the load effect has to be increased by about 5 % and 16 %, respectively, for this structure. This has been codified by incorporating the multiplication factor $\{1 + 0.2 (z/H)^2\}$ in the gust response factors in section five of Part 1. Near the top of a tower, higher modes of oscillation may make a further significant contribution to the dynamic magnification, which has not been included in the reliability analysis. The simple codified factor is less conservative in rougher terrain categories, but the overall population of towers is so distributed that it is considered that further complexity would not be justified by marginal benefits in uniformity of notional reliability of structures designed in accordance with Part 1.

Table C.2.3 — Ratio τ_T to t_{av}

Tower type		Ratio τ_T to t_{av}		
		$\phi = 0.1$	$\phi = 0.3$	$\phi = 0.5$
Square	Flats, angles CHS	1.6	2.1	2.7
		4.4	5.6	6.4
Triangular	Flats, angles CHS	1.4	1.9	2.3
		3.8	4.8	5.3

Table C.2.4 — Parameter variability (60 m; square; sharp-edged)

Parameter	Distribution type	Assumed mean	Coefficient of variation
Tower height/base width	Normal	9	0.33
Taper parameter	Normal		0.17
Eiffelization and shear effects	Normal	See (2.10)	0.19
Mass/resistance parameter τ_T (see 2.7.2)	Log normal	20 mm	0.35
Basic wind pressure q /axial stress	Normal	17×10^{-6}	0.30

Table C.2.5 — Typical values of dynamic parameters

Tower height	Mean wind speed, \bar{V}_H	Natural frequency, n_1	Aerodynamic damping, δ_a	Total damping, δ	Mass/resistance parameter, τ_T	Ratio $\sigma_1 (F)/\bar{F}$
m	m/s	Hz			mm	
25	34	1.58	0.105	0.15	14	$0.12 K_m$
60	38	0.93	0.135	0.18	20	$0.095 K_m$
240	50	0.38	0.24	0.28	30	$0.06 K_m$

Table C.2.6 — Examples of comparison of static and dynamic stress predictions

Example	Height	Base width	Cross section	Mass/resistance parameter, τ_T	Natural frequency, n_1	Stress ratio ^a
A	m	m		mm	Hz	
A	40	3.5	Δ	12	1.21	1.03
B	49	4.3	Δ	9	1.40	0.97
C	72	19.0	Δ	50	1.08	1.01
D	76	7.3	\square	12	1.25	0.98
E	85	7.5	\square	58	0.52	1.14
F	155	18.0	Δ	27	0.66	0.96
G	255	40.0	\square	20	0.46	0.95

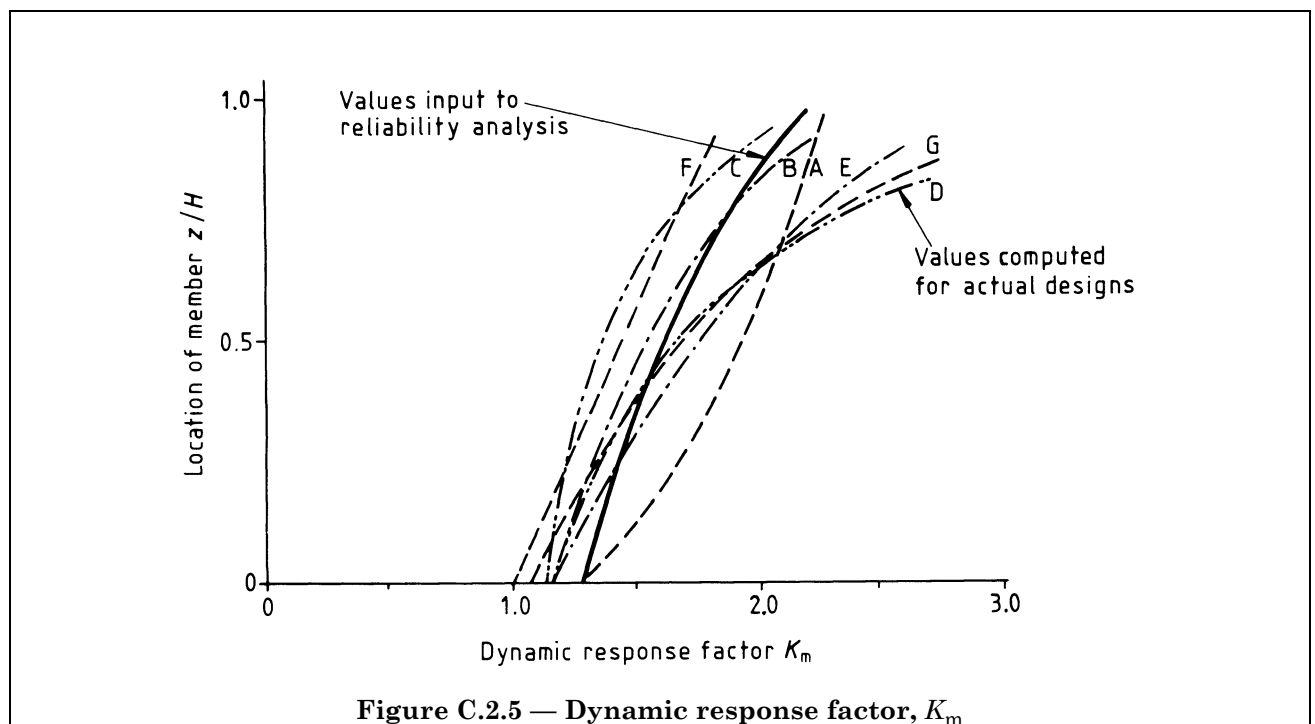
^a Ratio of expected value of maximum stress in leg member at location $z = 0.7 H$ by dynamic analysis to value by equivalent static procedure.

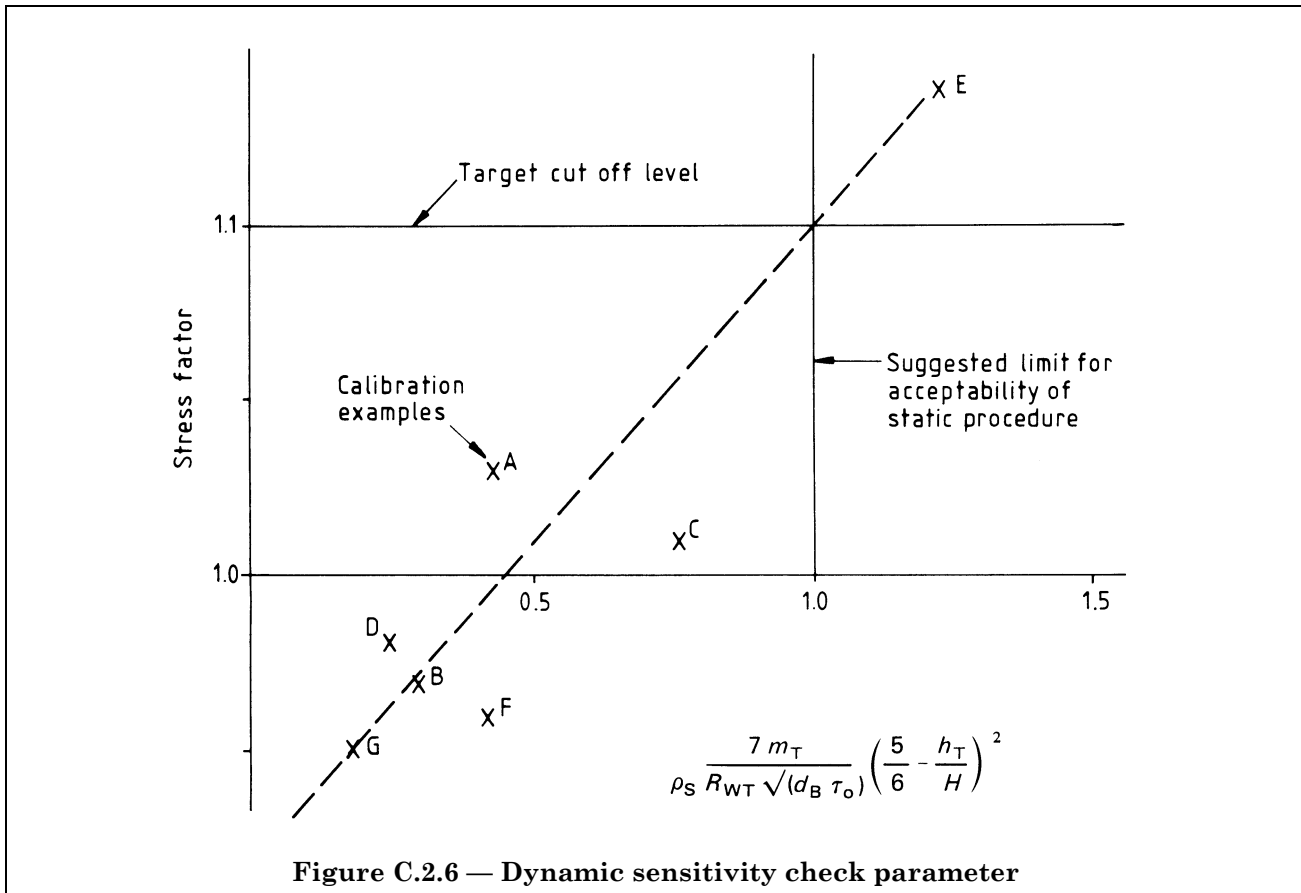
Bracing members for which the K_q effect (see 5.2.5 of Part 1) is small, e.g. $K_q < 1.15$, are subject to smaller values of K_m than the adjacent leg members, but it is considered that any economies that could result therefrom would be more than offset by additional complexity. It has not proved possible to generalize the dynamic analysis for members where K_q is large, and some caution should be exercised in cases where $f_q \rightarrow 0$.

C.2.7.3 Dynamic sensitivity. The reliability analysis also considered a range of towers in terms of dynamic sensitivity, in order to assess whether the equivalent static method could be used, or whether full spectral analysis was necessary. It is clear that the mass/resistance parameter, τ_T , exercises a dominant role, and it has further been observed that there are consistent trends in the value of this parameter according to the function of the tower. Flare towers, for example, commonly have relatively unfavourable values. It would be undesirable to permit methods that led to a substantial consistent short-fall in reliability of identifiable classes of structure, and hence be undesirable to permit a design or an identifiable class of structures resulting from the static procedure which could be shown by more detailed analysis to be expected to have an unacceptably high risk of failure.

In view of the observed importance of the mass/resistance ratio which is expressed by τ_T , together with the effect of the slenderness (height/width ratio), and the tower height, combinations of these parameters were investigated empirically in order to produce a simple check for dynamically-sensitive towers, for which the spectral analysis would be required. The ratio of τ_T to the square root of the base width was found to be the most useful measure. The target was set to exclude cases where the expected maximum stress in a leg member at location $z = 0.7 H$ should not exceed the corresponding value predicted by the equivalent static method by more than 10 %. A selection of results from actual towers used to calibrate the formula given in 5.1.1 of Part 1 is shown in Figure C.2.6; the principal parameters of these towers are set out in Table C.2.6. It is expected that dynamic analysis will only be called for in a very small proportion of towers as designed in current practice.

Caution should be exercised when the tower payload has a high mass/resistance factor (as with flare tips), or when high leg forces occur within the top 20 % of the tower height (as when tower width is severely constrained, for example to permit compact antenna configurations).





C.2.8 References in C.2

- 2.1 INTERNATIONAL STANDARDS ORGANIZATION. *General principles on reliability for structures*, 1984, ISO/DIS 2394.
- 2.2 CONSTRUCTION INDUSTRY RESEARCH AND INFORMATION ASSOCIATION. *The report of the CIRIA Study Committee on Structural Safety*, CIRIA Report 30, April 1971.
- 2.3 INTERNATIONAL ELECTROTECHNICAL COMMISSION, STUDY COMMITTEE NO. 11. *RECOMMENDATIONS FOR OVERHEAD LINES. Recommendations for the calculation of wind loading*.
- 2.4 NORDIC COMMITTEE ON BUILDING REGULATIONS. *Recommendation for loading — and safety regulations for structural design*, NKB Report No. 36, Nov. 1978.
- 2.5 CONSTRUCTION INDUSTRY RESEARCH AND INFORMATION ASSOCIATION. *Rationalisation of Safety and Serviceability Factors in Structural Codes*, CIRIA Report 63, July 1977.
- 2.6 BEA, R.G. *Development of Safe Environmental Criteria for Offshore Structures*. *Oceanology International*, 1975.
- 2.7 FLINT AND NEILL PARTNERSHIP. *Report on the Results of the Calibration Studies Draft Lattice Tower Code*, May 1982 (unpublished).
- 2.8 THOFT-CHRISTENSEN, P. and BAKER, M.J. *Structural Reliability Theory and its Applications*, Section 1.2, Springer-Verlag, 1982.
- 2.9 WYATT, T.A. *Evaluation of gust response in practice*. *Wind engineering in the eighties*, CIRIA, London, 1981.
- 2.10 WYATT, T.A. *Comportement dynamique des pylons à treillis sous l'effet du vent*. *Construction Metallique*, 3, Sept. 1981. (in French: English version in *Diului Sfintesco 70: the engineer and the man*, Valbert, Paris 1980).

C.3 Meteorological parameters

C.3.1 Wind speed data

C.3.1.1 General. Part 1 is based on standardized interpretation of meteorological data in order to rationalize the design basis for towers in the UK (and overseas) and to encourage stations to provide records of use to a designer. Wind speeds to be used for structural design are dependent on the following naturally occurring aspects [3.1]:

- a) global climatic regions;
- b) local climatic factors;
- c) wind direction;
- d) topographic effects (hills, valleys, etc.);
- e) terrain characteristics.

All of these items can affect the derivation of a reference design wind speed appropriate to any site. Part 1 provides data for the UK in terms of a basic mean hourly wind speed, which can be obtained from a map or from suitable wind speed records. By use of simple factors, the site reference wind speed may be obtained at a standardized reference height taking account of the aspects listed in a) to e). Guidance is given on how to determine the equivalent data for overseas sites.

Since the effect of terrain is of great significance, there is an alternative approach to derive site reference wind speeds working downwards from the gradient wind height at which the frictional influence of the ground becomes negligible. However, there are still limitations in this approach, particularly with regard to quoted values of gradient wind height, which has been variously reported as being between 300 m and 3 000 m and is still terrain dependent. Hence this approach is not recommended where suitable adequate wind records or wind maps are available, but Part 1 permits the use of gradient wind speeds as a design basis for structures located remotely from recording stations.

Data for overseas sites are not given explicitly in Part 1 and relevant data should be obtained from the appropriate national Meteorological Office or code of practice. Sources of data for wind speeds outside the UK are given in ESDU item 82026 [3.2]. The design wind speeds will not necessarily be mean hourly values, and the comments in **C.3.1.2** should be followed in order to obtain mean hourly values. A source list of world codes and other advisory documents, as well as an indication of locations likely to fall into the atmospheric regions of type a), b) or c) of **3.1.1** of Part 1 are also given by Cook [3.1]. All of the UK, Europe, most of North America and Asia, Chile, Argentina, Tasmania and New Zealand can generally be considered to be well conditioned regions of type a), for which **3.1** and **3.2** of Part 1 can be used for deriving wind data. The exceptions for North America and Asia are the eastern coastal areas. These and all remaining regions may, therefore, be subject to hurricanes or typhoons and should be considered of type b), and hence include all polar regions, Central and South America (other than Chile and Argentina), Australia, Pacific Islands, Africa and all Tropical and Equatorial regions.

Regions of type c) where local intense storms may occur cannot be readily defined and may require consideration in any climatic region, but subtropical areas will always be at risk where the intensity of tornadoes is greater than in temperate regions, and the tornadoes grow to a larger size. An increase in severity of localized storms may occur in coastal areas, near mountains and (for tornadoes) in areas of plains. Cook [3.1] gives further guidance on this, and notes on interpretation of data for regions of types b) and c).

C.3.1.2 Basic wind speed. A 50 year return wind period has been adopted to define basic values of speed as being that in common use (see Table C.3.1). This also conforms with the return period in use for the majority of structures in the current UK wind code, CP 3: Chapter V: Part 2 [3.3].

The time averaging period adopted in the past and in different codes has varied considerably (see Table C.3.2). However, an averaging period of 1 h is now recommended, since following the work of Van der Hoven, Davenport, Vickery and others, it is now accepted that there is a clear advantage in choosing an averaging period of about 1 h, so that the wind fluctuations can be separated into the macro- and micro-meteorological ranges, and hence provide a satisfactory base for spectral analysis [3.4]. In addition, 1 h is the period adopted for wind data collection by a majority of the national meteorological services and has been specified as being that favoured by the UK Meteorological Office. In European practice, a 10 min period is sometimes adopted [3.5], and the USA uses the “fastest mile of wind”, which implies a varying time averaging period (see Table C.3.2). Hence a method of converting speeds of shorter averaging periods to equivalent hourly mean values may be required, and this is given in Appendix A of Part 1 (see Figure A.1 of Part 1).

The standard height of 10 m above ground and the use of open level countryside with terrain roughness parameter, z_0 , of 0.03 m have been adopted for reference as representing common practice and permitting the least correction to data from the majority of meteorological stations. It is known that the simple power law velocity profile may not accurately apply below 20 m [3.6], and hence it is recommended in Appendix A of Part 1 that anemometers should be sited at a height of at least 10 m and clear of obstructions.

The values of 50 year return mean speeds given in Figure 3.1 of Part 1 have been based on records produced by the Meteorological Office [3.7] for use for sites in open level country, i.e. terrain category III, with the effects of regional topography removed by relating to a height of 10 m above a ground level reduced to that of mean sea level. It is to be noted that the corresponding map shown in Figure 1 of CP 3: Chapter V-2:1972 [3.3] is related to the altitude of the countryside in the regions of the anemometers providing the data, and no adjustment can be made for variation in altitude. The data from Figure 3.1 of Part 1 can however be adjusted for altitude by means of the 10 % addition per 100 m altitude AMSL as noted on the figure. For sites on hills, the reference altitude should be to that of the surrounding terrain only, and not that of the top of the hill, the effect of the hill being allowed for separately (see C.3.2.2). The altitude allowance is as derived by Cook [3.1] and is compatible with the fitting of data used to produce the basic wind speed map for the UK. It is to be noted, in addition, that the speeds shown on the map are appropriate to a terrain roughness characterized by a gust ratio of maximum gust speed to mean hourly speed of about 1.6 at an effective height of 10 m, whereas Figure 1 of CP 3: Chapter V-2:1972 [3.3] relates to a 50 year extreme *gust* ratio of 1.5 (a smoother reference site), now reckoned to be of terrain roughness of $z_0 \approx 0.010$ m, i.e. terrain category II (see C.3.1.4). The gust period as recorded by the anemometer is generally in the range of 1 s to 5 s, according to the anemometer, but is typically about 2 s. A method for deriving or rechecking the averaging period of an anemometer is given in A.2 of Part 1.

Recent work by Greenway (see ESDU item 83045 [3.8]) has shown that for typical standard cup anemometers and their recording equipment, the relationship between the time constant of the equipment τ_i and the maximum gust velocity of short duration averaged over t seconds, V_t , is given by $\tau_i \approx 20/V_t$. Thus τ_i varies from 4 s for low wind speeds down to about 1 s or less for extreme winds; this lower value may be limited by the response time of the associated recorder.

The derivation of the data used in the production of Figure 3.1 of Part 1 has been carried out by Cook [3.1], and is also used in ESDU item 82026 [3.2]. The fitting of data is based on the statistics of extremes, and in particular the analytical method of fitting data initiated by Gumbel [3.9], which is now accepted as that most appropriate for the fitting of extreme wind data [3.1, 3.10, 3.11, 3.12, 3.13]. In some countries the Fréchet distribution has been used [3.11, 3.12] (see Table C.3.1), but it is now generally agreed that the Gumbel distribution applied to pressures is the most appropriate and acceptably accurate model for extreme winds regardless of meteorological origin [3.12]. Summaries of the properties of the Gumbel distribution (also known as Fisher-Tippet type I) and the Fréchet distribution (also known as Fisher-Tippet type II) are readily available [3.1, 3.11, 3.13]. In producing the basic wind speed map for the UK (see Figure 3.1 of Part 1), data has been assessed from a large number of closely spaced sites, and some of the previous bias introduced in earlier wind maps, such as in CP 3: Chapter V-2 [3.3] and ESDU item 72026 [3.14], has now been removed. This has been achieved by analysing the extreme from every storm in a 10 year period, using the method of Jensen and Franck [3.15] as developed by Cook [3.16]. This method is about as accurate with 6 years data, as annual extremes with 50 years data.

Table C.3.1 — Mean return period, \bar{T} , of annual climatic maxima in other codes of practice [3.11]

Country	Mean return period \bar{T} (years)	Type of distribution	Observations
Australia	50 for all structures, except as follows 100 for structures presenting an unusually high degree of hazard to life and property in the case of failure and for structures which have special functions 25 for structures presenting a low degree of hazard to life and property in the case of failure 5 for structures used only during construction operations and for structures of low replacement cost	—	—
Canada	30 for the design of structural members for strength 10 for the design of structural members for deflection and vibration 100 for building essential for post-disaster services	Gumbel	—
Denmark	50	—	—
UK	50 for all structures with the exception of temporary structures or structures where greater than normal safety is required, where \bar{T} may be varied	Gumbel	For other values of \bar{T} see Appendix C of CP 3: Chapter V-2:1972 [3.3]
Soviet Union	10 to 15 for normal structures 20 for special structures	Fréchet	Code also gives values for $\bar{T} = 3$ years, 5 years, 30 years and 50 years
USA	50 for all permanent structures, except as follows 100 for structures presenting an unusually high degree of sensitivity to climatic loads and an unusually high degree of risk to life and property in the case of failure 25 for structures that have no human occupants or where there is a negligible risk to human life	Fréchet	Code also gives values for $\bar{T} = 2.5$ years and 10 years

Table C.3.2 — Time averaging interval for basic wind speed [3.11]

Country	Time averaging interval
Australia	2 s to 3 s
Canada	1 h
Denmark	10 min
France Extreme winds	2 s to 5 s
UK Units of cladding, glazing and roofing	3 s 5 s
Buildings and structures where neither the greatest horizontal nor vertical dimension exceeds 50 m	15 s
Buildings and structures whose greatest horizontal or vertical dimensions exceed 50 m	
Romania, Soviet Union	~2 min
USA Basic wind speed is fastest-mile speed i.e. for speed of 120 m.p.h. (54.5 m/s)	30 s
for speed of 60 m.p.h. (27.0 m/s)	1 min
for speed of 30 m.p.h. (13.5 m/s)	2 min

When following the statistical procedures outlined in Appendix A of Part 1, the Fisher-Tippet type I (Gumbel) extremal distribution should therefore be used. This can effectively be reduced to the following for the prediction of maximum mean hourly wind speed, \bar{V}_{\max} :

$$\bar{V}_{\max} = \bar{V}_{\text{av}} - \left[\frac{\ln \{1.785 p(V)\}}{1.2825} \right] \bar{V}_{\sigma} \quad (3.1)$$

where

\bar{V}_{av} and \bar{V}_{σ} are the average and standard deviation, respectively, of the distribution of mean hourly wind speeds (annual maxima):

$p(V)$ is the annual probability of occurrence, i.e. the probability that the wind speed exceeds \bar{V}_{\max} in any given year, which should be $\ll 1$ for use in the simplified expression in equation (3.1).

For $p(V) = 0.02$, i.e. 1 in 50 year return, this further reduces to:

$$\frac{\bar{V}_{\max}}{\bar{V}_{\text{av}}} = 1 + 2.6v \quad (3.2)$$

where

v is the coefficient of variation, i.e. $\bar{V}_{\sigma}/\bar{V}_{\text{av}}$.

It is considered that at least 15 annual maxima should be analysed to provide a reliable statistical basis for extreme value prediction, and this has therefore been used. The alternative, permitting the use of a multiple of the average of at least 10 values, assumes that the coefficient of variation, v , of annual maxima is 0.2, thus producing a 50 year value from the Gumbel distribution of $\bar{V}_{\max} = 1.5\bar{V}_{\text{av}}$

Since the alternative will only be used for countries for which few records are available, the coefficient of variation has been assumed to be higher than the range of $0.10 < v < 0.18$ typically obtained, but is necessary to ensure an upper bound value of design wind speed is derived. It is however noted that a value of 0.25 has been assumed as a basis for the National Building Code of Canada [3.45], but some sample checks on UK data from stations with 10 years or more of records have produced values generally in the range of 0.12 to 0.18, but with only occasional values less than 0.1 or greater than 0.2.

It should further be noted that in using Appendix A of Part 1 for deriving basic wind speed, care is required in the interpretation of anemometer records, as errors can easily be introduced in the data provided (see C.3.1.4) and a suitably modified wind map should also be used in preference when available.

C.3.1.3 Wind direction. The variation of extreme wind speed as a function of direction was derived by Cook [3.17]. Values of the recorded wind speeds for each 30° sector were obtained from 50 sites distributed throughout the UK. The values were reduced to non-dimensional form using contours of pressure integrated to produce uniformly distributed directional risk equal to the selected overall risk independent of direction [3.1, 3.17]. An envelope of all contours then gave the highest value of wind speed ratio as a function of direction, and is plotted in Figure 3.2 of Part 1. An earlier analysis using the envelope of the ratios obtained by dividing the maximum windspeed for each direction by the overall maximum for a reduced sample of 11 stations produced similar but obviously less accurate results. In addition, it should be noted that the use of the Gumbel distribution in this context is not ideal due to the yearly variation of the number of hours in each sector producing variable results from the extreme value analysis, unless specific corrections are made. As in the case of the derivation of data for sites with limited records, use of a modified form of the Jensen and Franck method [3.15] is required.

As the data used covered periods of at least 10 years duration, it has been considered probable that the extreme wind speed profile will not be significantly changed as more measurements become available and it has therefore been applied to the 50 year return period wind speed. However, some additional evidence studied by British Telecommunications has indicated that the direction of maximum gust in Scotland, North-west England and Northern Ireland only, centred on 300°. Hence, until further data has been assessed, it has been thought prudent to apply the ± 30° variation for present use of Part 1. Similarly, stations close to the east coast were excluded as it was noted that highest measured wind speeds were frequently not from the south-west. For sites near the east coast (within 16 km), the maximum wind speed was considered as likely to blow from any direction. There was, however, some correlation for east coast areas, but further work is required before the direction factor can be produced for these areas. Some information on aspects of variation of maximum wind with direction are given in BRE publications relating to gale damage in the UK [3.18, 3.19, 3.20].

The comments on the use of statistical interpretation of data given in C.3.1.2 and C.3.1.4 should be noted when Appendix A of Part 1 is being followed for directional analysis.

Use of the wind direction factor, K_d , in the context of coincident wind plus ice combination is discussed in C.3.5.1 and C.3.5.2.

C.3.1.4 Terrain roughness. For the purposes of Part 1, a range of terrain categories have been provided (see Table 3.1 of Part 1) covering all types of terrain ranging from large flat areas of tarmac or open sea to forested areas or suburban environment. The characteristics of the terrain are primarily defined by the terrain aerodynamic roughness parameter, z_0 . Once this parameter has been assessed, the parameters required by the designer for deriving the site reference wind speed (see C.3.1.5) and the appropriate wind profile variation with height (see C.3.2) can readily be assessed. For this reason Table 3.1 of Part 1 sets out all the relevant parameters, i.e. z_0 , K_R and h_e . The parameters α and h_e relate to the wind variation with height, and are discussed further in C.3.2. The parameter z_0 is not used explicitly in Part 1, but is now the accepted cornerstone of atmospheric boundary layer technology, and has been used for terrain classification and the consequent definition of wind characteristics in all the primary sources of data. In particular these include Davenport [3.10], Harris [3.4, 3.21], Cook [3.1, 3.13] and ESDU [3.2, 3.8, 3.14, 3.22], and for this reason a summary of the significance of this parameter is set out in B.1 of Part 1. The current theories of wind profile variation with height based on the log law (see C.3.2) utilize z_0 directly in their formulation.

The terrain roughness factor, K_R , is, by definition, given by the ratio of the mean hourly wind speed over any terrain to that over the reference terrain, which is taken in Part 1 as category III ($z_{0B} = 0.03$ m), i.e. $K_R = \bar{V}_{10}/\bar{V}_B$. This same relationship is used by Cook [3.1], and ESDU [3.2, 3.8, 3.14]. K_R can be expressed explicitly in log law terms [3.1, 3.2] in relation to the terrain roughness parameter, z_0 , and the gradient wind height, z_g , and can be closely approximated by:

$$K_R = \frac{\ln(10^5/z_{or}) \ln(10/z_0)}{\ln(10^5/z_0) \ln(10/z_{or})} \quad (3.3)$$

For reference terrain $z_{or} = z_{oB} = 0.03$ m, this reduces to:

$$K_R = 2.5855 \left[\frac{\ln(10/z_o)}{\ln(10^5/z_o)} \right] \quad (3.4)$$

Some earlier work of Caton [3.23], Shellard [3.24], Harris [3.4], see [3.7] and ESDU item 72026 [3.14] developed K_R values via gust ratios, and where comparisons are possible these are given in Table C.3.3.

There has in the past been some variation in the correlation of terrain type by description with an appropriate z_o and resulting K_R , α and h_e value. However, Davenport [3.10], Harris and Deaves [3.21], Cook [3.1] and ESDU [3.2, 3.8] are now virtually all in agreement, and early data given by Caton [3.23] and ESDU [3.14] are not significantly different. Thus Table 3.1 of Part 1 has been based primarily on data derived by Cook [3.1] and ESDU [3.2], with appropriate modifications to suit the presentation of Part 1, as this now represents a sound basis.

As a further aid to the classification of site terrain categories, a modified form of the ESDU terrain description chart is given in Figure C.3.1. This should be used for confirmation of the results obtained from interpretation of wind data, particularly where Appendix A of Part 1 is used for the calibration of a site.

Part 1 stated that K_R may alternatively be derived by the procedure given in Appendix A of Part 1 utilizing recorded ratios of gust speed to mean hourly speed. Figure A.1 of Part 1 allows for an averaging period for the gust from the typical 1 s to 5 s through to 60 s, and also for 10 min as noted in C.3.1.2. This figure is also based on the data of Cook [3.1] and ESDU [3.2, 3.8]. Some comparisons with the other aforementioned K_R to gust ratio relationships [3.4, 3.7, 3.14, 3.24] are given in Figure C.3.2, together with comparisons of alternative relationships for gust averaging periods given by Vellozzi and Cohen [3.25], Mackey et al [3.26], and CP 3: Chapter V-2 [3.3].

In many situations overseas there may be little or no recorded data available close to the site. In such cases, gross interpolation based on distant wind data and global meteorological advice may be the only alternative. The design wind data derived and the consequent site calibration should be checked against any such available data. Even in cases where wind data is available for use with Appendix A of Part 1, errors may exist due to instrument error, poor location of the instrument, changes in terrain and local obstructions over the life of the anemometer, or even changes and errors in the calibration of the instrument. When the instrument is located at a height other than the standard 10 m reference height, reduction of the recorded data to this height may introduce further error. In consequence, the estimation of K_R via site calibration following the procedures of Appendix A of Part 1 should always be confirmed wherever possible by aerial photographs or similar, if available, or at least be checked against the data of Table 3.1 of Part 1 or Figure C.3.1.

In using Appendix A of Part 1, it may be necessary to adopt a power law relationship with height for gust wind speeds. These have not been given in Part 1, but may be taken as the values given in Figure C.3.3, which have been extracted from ESDU item 72026 [3.14].

The intensity of turbulence, in terms of the r.m.s. value of the fluctuating wind speed $\sigma(V)$, used in the derivation of gust loading factors (see C.5), is terrain dependent and can be related to K_R (or z_o for log law relationships). Guidance on the value adopted, including comparisons with other data, is given in C.3.6. This data is not required for use in Part 1, other than for use in spectral analytical methods.

Part 1 states that a reasonably constant terrain roughness should apply for several kilometres upwind of the site, resulting in the adoption of the chosen roughness category for the site. However, frequently there may be significant changes in terrain surrounding the tower site, and changes at a distance of as far as 50 km can affect the wind profile at the site. In fact for high towers, the terrain in the region from 5 km to 20 km upwind may be more significant on the overall loads on the tower, than a different terrain within 5 km of the site, since the former will be relevant to loading in the upper part of the structure. Further guidance on the effects of change of terrain roughness, including choice of appropriate terrains for the mean hourly wind and gust factor aspects, is given in C.3.7.

Table C.3.3 — Comparisons of power law index, α , gust factor, G , and terrain factor, K_R

Values from Part 1	Category		I	II	III	IV	V		
	Table 3.1 Figure A.1	}	z_0	0.003	0.01	0.03	0.10	0.30	0.80
K_R			1.20	1.10	1.00	0.86	0.72		
α			0.125	0.14	0.165	0.19	0.23		
}		G_1	1.46	1.53	1.61	1.74	1.93		
		G_3	1.41	1.47	1.54	1.65	1.80		
		G_5	1.37	1.43	1.49	1.60	1.75		
Caton [3.23]	α	0.11	0.13	0.14	0.17	0.18	0.21	0.22	0.23
	G	0.35	0.45	0.50	1.60	1.65	1.85	2.00	2.10
Shellard [3.24] ^a	α	(No power law values)							
	average G	1.56		1.64		1.81		2.13	
Deacon [3.7] ^a	α	(No power law values)							
	G_3	1.51		1.66		1.81			
ESDU item 72026 [3.14] ^a	α	0.13	0.15	0.165	0.19	0.23	0.26	0.29	
	G_4	1.50			1.80		2.10		
CP 3: Chapter V-2 [3.3] ^a	(No mean hourly power law values provided)								
	G	1.50			1.70		1.90		2.10
Cook [3.1]	0 to 50 m α	0.12	0.14	0.16	0.20	0.24	0.32		
	0 to 300 m α	0.12	0.14	0.16	0.18	0.22	0.27		
	G_1	1.46	1.53	1.61	1.74	1.92	2.22		
	G_4	1.39	1.44	1.51	1.61	1.77	2.01		
Cook [3.1]	K_R	1.211	1.108	1.000	0.861	0.711	0.554		
ESDU item 72026 [3.14]	K_R	1.17	1.10	1.00	0.88	0.74	0.59		
Harris [3.4] ^b	G	1.48	1.51	1.56	1.65	1.78			
	K_R	1.17	1.10	1.03	0.95	0.84			
Shellard [3.24] and ^b	G	1.47	1.51	1.56	1.66	1.78	1.99		
Deacon [3.7]	K_R	1.09	1.05	1.02	0.97	0.90	0.80		
NOTE A suffix to G indicates the gust averaging period, in seconds, when defined.									
^a These references do not contain K_R or z_0 data; they have been aligned to the categories I to V of Part 1 by means of terrain description and Figure C.3.1.									
^b These are as modified by Harris in 1976 using asymptotic similarity theory, for terrain conversions [3.21].									

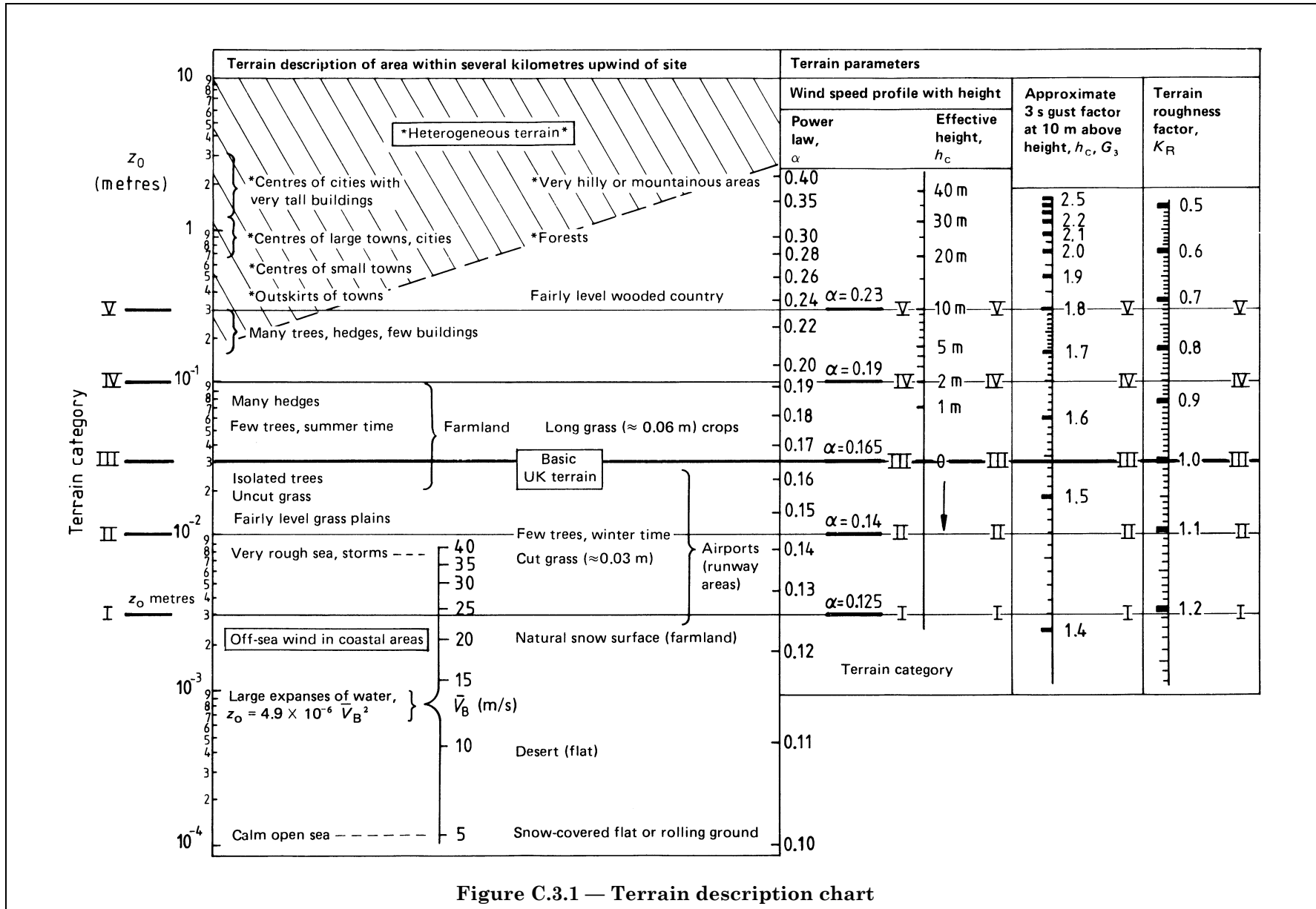


Figure C.3.1 — Terrain description chart

C.3.1.5 Site reference wind speed. The site reference wind speed, \bar{V}_r , is the resulting direction-dependent factored wind speed appropriate to the terrain over several kilometres upwind from the site, at a reference height (at the site) of $(10 + h_e)$ metres.

The characteristic site wind speed, \bar{V}_k , which is unfactored, is a maximum regardless of direction, and is identical to \bar{V}_{10} referred to in C.5, i.e.:

$$\bar{V}_{10} = \bar{V}_k = K_R \bar{V}_B \quad (3.5)$$

As stated in C.3.1.1, gradient wind speed data may be used where there are no other sources of data. As an example of the form of gradient wind data required, the appropriate map for the UK is given in Figure C.1 of Part 1 together with the typical range of values of the gradient wind speed reduction factor, K_g , as obtained by Caton [3.23], where $K_g = \bar{V}_B / \bar{V}_g$, i.e. the reference wind speed at 10 m for the standard roughness condition divided by the 900 m gradient wind speed. K_g depends more on large-scale topography than on local terrain as may be seen by reference to Figure C.3.4 which shows the variation of K_g in the UK calculated by Caton [3.23]. The value of K_g derived by Cook [3.1] is 0.41, regardless of large-scale topography, but is related to a gradient height of 2 550 m. Correction to a height of 900 m, as assumed by Caton, would lead to approximately 19 % decrease in gradient wind speed implying an equivalent K_g of 0.49.

C.3.2 Variation of wind speed with height

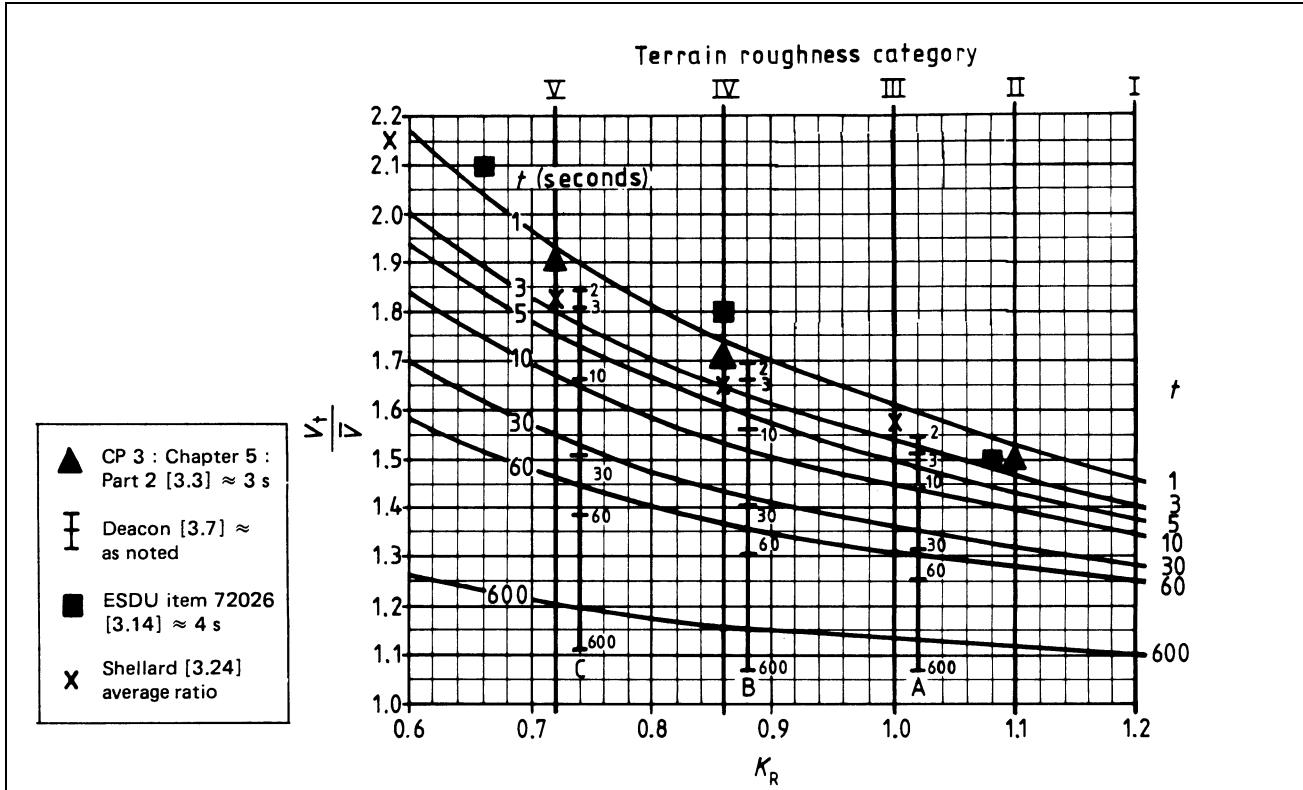
C.3.2.1 Sites on level terrain. The power law variation of wind speed with height, α , has been adopted in Part 1 for ease of use, as well as being a familiar concept more easily utilized in practical design [3.27]. The difference between the power law profile and the equivalent log law is not great, but the form of the log law is terrain-dependent, and needs height correction terms for use above 30 m [3.21]. Cook [3.1] and ESDU [3.2] give tables or graphs and the relevant log law formulae. Some typical comparisons using values derived from the theory of Harris and Deaves [3.21] are given in Figure C.3.5, where full account of the effects of wind speed on the power law, and terrain on the log law formulae are taken into account. However, Table C.3.4 shows how the adopted power law agrees very closely with the simplified log law data tabulated for design purposes by Cook [3.1].

Figure C.3.6 shows the relationship between α and K_R adopted in Part 1 compared with the indices proposed by others [3.1, 3.2, 3.6, 3.10, 3.11, 3.14, 3.23, 3.28] for the terrain categories. It will be seen that some of the values differ from those previously in use and those evaluated by Davenport [3.10, 3.28] in a survey of a number of observations, the discrepancy arising mainly due to values of a zero plane level assumed in built-up areas, i.e. terrain category V.

The velocity profile adopted has been based on a power law related to a reference level at 10 m above a zero plane h_e , taken to be 10 m above ground in terrain category V and 2 m above ground for terrain category IV, and at ground level for terrain categories I to III. A linear variation in speed has been assumed between the ground and the reference level. Figure C.3.7 gives sample Part 1 comparisons with that in CP 3: Chapter V-2 [3.3] which is based on a linear relationship of wind pressure below a level of $(10 + h_e)$ metres and with Cook [3.1] which continues the log law profile, but has a cut off at $1.5 h_e$ metres, to ensure an upper bound wind speed in urban terrain.

It had been suggested by Caton [3.23] that the profile index could be related to $K_R K_g$ (see C.3.1.5). The suggested relationship between $K_R K_g$, and the mean velocity index is also given in Figure C.3.6. For open coastal sites and sites in the sea, $K_R K_g$ is reasonably constant at 0.6 and 0.7, respectively, and the value of α from this approach agrees reasonably with that given in Part 1. For inland sites, particularly in the central highlands of Scotland and the London area, the aforementioned values of K_g vary and would suggest the use of no fixed value of α for a given terrain type, which again sheds doubt on the use of gradient speeds.

However, the later work of Harris [3.4, 3.21], Cook [3.1] and ESDU [3.2] are now more relevant and thus form the basis of Figure 3.3 of Part 1 for relationship between K_R , α and h_e . The values on the terrain description chart, Figure C.3.1 discussed in C.3.1.4, are based on the same data. Davenport [3.10] now agrees generally with the adopted relationship between α and z_0 .

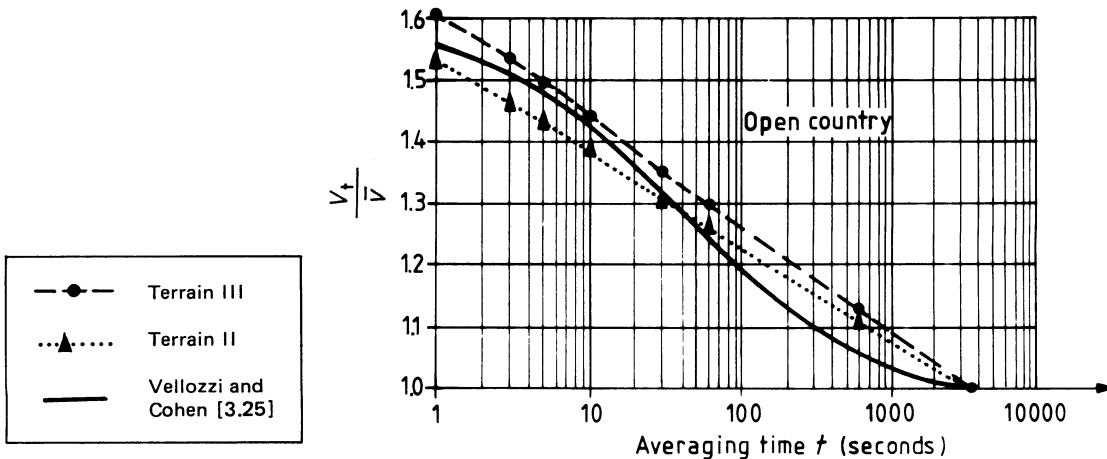


a) Gust ratio comparisons [3.3, 3.7, 3.14, 3.24] at 10 m height

Source	Terrain category, and intensity of turbulence $I_w = \sigma/\bar{V}$			Averaging time interval, t , (in s)								
				3 600	600	300	60	30	10	5	3	1
Mackey	cities	$\sigma/\bar{V} = 0.26$	(i)	1.00	1.202	1.279	1.461	1.538	1.662	1.738	1.797	1.922
	Open country	$\sigma/\bar{V} = 0.16$	(ii)	1.00	1.108	1.150	1.248	1.290	1.356	1.398	1.430	1.496
	Seacoast	$\sigma/\bar{V} = 0.08$	(iii)	1.00	1.047	1.062	1.102	1.120	1.147	1.164	1.177	1.205
Part 1	Terrain category V		(i)	1.00	1.20	—	1.46	1.54	1.67	1.75	1.80	1.93
	Terrain category III		(ii)	1.00	1.13	—	1.30	1.35	1.44	1.49	1.53	1.61
	Terrain category I		(iii)	1.00	1.10	—	1.24	1.28	1.34	1.37	1.41	1.46

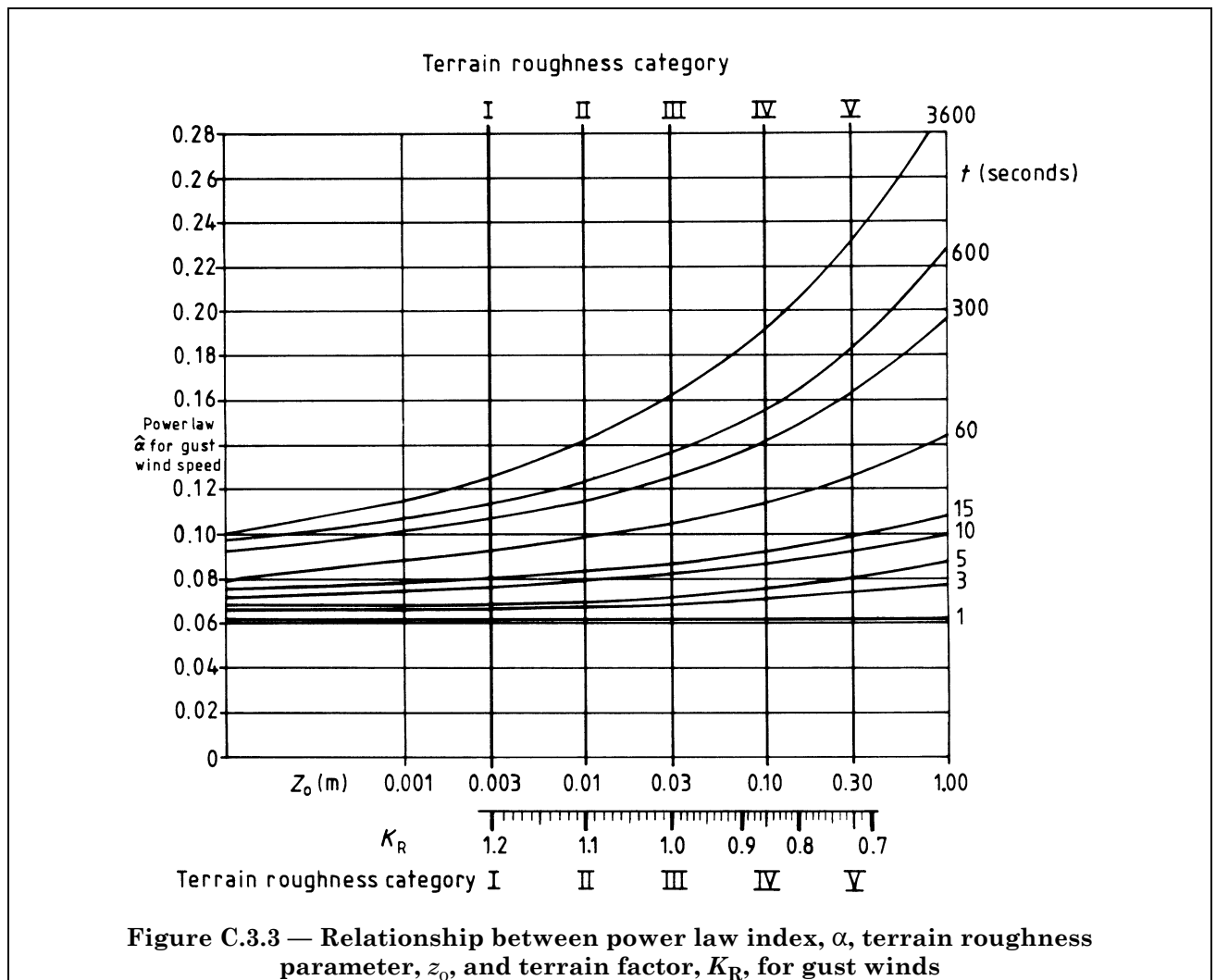
b) Conversion table for wind speed averaged over the interval t , V_t to that averaged over an hour V_{1h} . After Mackey et al [3.26].

$$\frac{V_t}{\bar{V}} = 1 - 0.6226 \left(\frac{a}{\bar{V}}\right)^{1.2716} \times \log \frac{t}{T}$$



c) Conversion of the wind speed averaged over an interval t , V_t into that averaged over 1 h \bar{V} . After Vellozzi and Cohen [3.25].

Figure C.3.2 — Comparison of gust ratios



C.3.2.2 Sites on hills

A) *General.* The presence of escarpments or hills will alter the mean speed profile and since tall transmission-type towers are often sited on hills it is important to estimate the resulting profile in such conditions.

Theoretical studies of this problem have been made in which boundary-layer theory has been applied with the molecular viscosity replaced by the eddy viscosity, which results from the turbulent mixing of the atmosphere. Simplifying assumptions made by Alexander and Coles [3.29] and extended by Deaves [3.30] consider the flow as taking place only in two dimensions, parallel to the wind direction and vertically. In this case, it is possible to define the stream function and vorticity in such a way that the system of equations is reduced to a pair of non-linear partial differential equations, continuity being automatically satisfied. Solution techniques utilize numerical relaxation methods and hence are not suitable for codification. An empirical relationship has therefore been derived which considers the effect of the hill to change the normal speed profile in the surrounding terrain to a profile with a power law index which is a function of both the hill slope and position of the structure with respect to the brow of the hill. Modification of the wind speed at 10 m is also necessary according to the height of the hill and the aforementioned parameters. Thus, away from the hill, the speed, \bar{V}_z , at height z metres is given by:

$$\bar{V}_z = \bar{V}_{10} \left(\frac{z - h_e}{10} \right)^\alpha \quad (3.6)$$

and on the hill:

$$\bar{V}_z = \bar{V}_{10} K_\mu \left(\frac{z - h_e}{10} \right)^{\alpha - \mu} \quad (3.7)$$

B) *Derivation of formulae.* The constants K_μ and μ were derived by equating the volumetric flow of air, at any instant, away from the hill to that over the brow of the hill assuming the flow to be laminar and incompressible. It was assumed that, at the brow of the hill, the effect of the hill was insignificant at a height of eight times its height, a value somewhat greater than that found by Onishi [3.31]. This assumption does significantly alter the values of \bar{V}_z but was chosen so that under no circumstances would the power law index ($\alpha - \mu$) become negative, which would imply that the wind speed exceeded the wind speed at the boundary-layer height. It was subsequently found to fit both experimental and theoretical data available.

The second assumption made in the derivation of these constants was in relation to the distance downwind of the brow of the hill at which the original profile was regained. In Part 1 this distance has been taken as 18 times the height of the hill, chosen on the basis of test results obtained by CERL [3.32]. It may be noted that CP 3: Chapter V-2 [3.3] assumes the effect of the hill to be negligible at a distance downwind of four times the height of the hill.

The effective boundary height, h_u , was then assumed to follow a linear variation from the foot of the hill to the point 18 H beyond the brow of the hill. Variations in this assumption only affect sites which are away from the brow of the hill and Part 1 overestimates the wind speed in this region if the assumption of 18 H is too large.

K_μ and μ were then derived, using the notation set out in Figure C.3.8, resulting in the following:

$$\mu = \alpha - \frac{(144 + 8 \cot \beta') - 18}{162 + \cot \beta'} \quad (3.8)$$

$$K_\mu = \left(\frac{1 + \alpha}{1 + \alpha - \mu} \right)^\alpha (0.8H_h)^\mu \quad (3.9)$$

At this stage $\beta' = \bar{\beta}_h$, the effective slope of the hill.

Following the results of the comparisons outlined in C), the formulation in equations (3.8) and (3.9) was found to generally indicate the right order of increase of wind speed on top of a hill, although the appropriate assumptions of α required for each comparison made exact comparison difficult.

A final comparison with results of Cook [3.1], which has been based on the approach of Jackson and Hunt [3.33], led to a final modification to allow for the separation effects that rapidly increase as $\bar{\beta}_h$ exceeds about 17° , leading to an empirical value of β' used in equation (3.8) given by:

$$\beta' = 1.22 (e^{0.22\beta_h} - 1) \quad (3.10)$$

C) *Comparisons with theoretical and experimental results.* Comparison was made between the theory of Deaves [3.30], the expressions given in Part 1 and field observations for a hill site at Sutton Coldfield, prior to the modification to β' . The results are shown in Figure C.3.9. Figure C.3.10 and Figure C.3.11 compare the same expression given in Part 1 for hills of two forms used in wind tunnel tests carried out by CERL [3.32], and show the improvement to the profile produced in relation to that in CP 3: Chapter V-2 [3.3]. Further comparisons with records obtained at a mast at Durris in Scotland are given in Figure C.3.12 to Figure C.3.14. A valuable comparison was made for another mast at Black Hill in Scotland, by means of coincident records at Abbotsinch Airport which is situated 36 km due east of Black Hill and could be treated as a reference site unaffected by hills. Part 1 here showed a reasonable prediction of the increased wind speed over the hill, far better than the gross underestimates produced by the procedure in CP 3: Chapter V-2 [3.3].

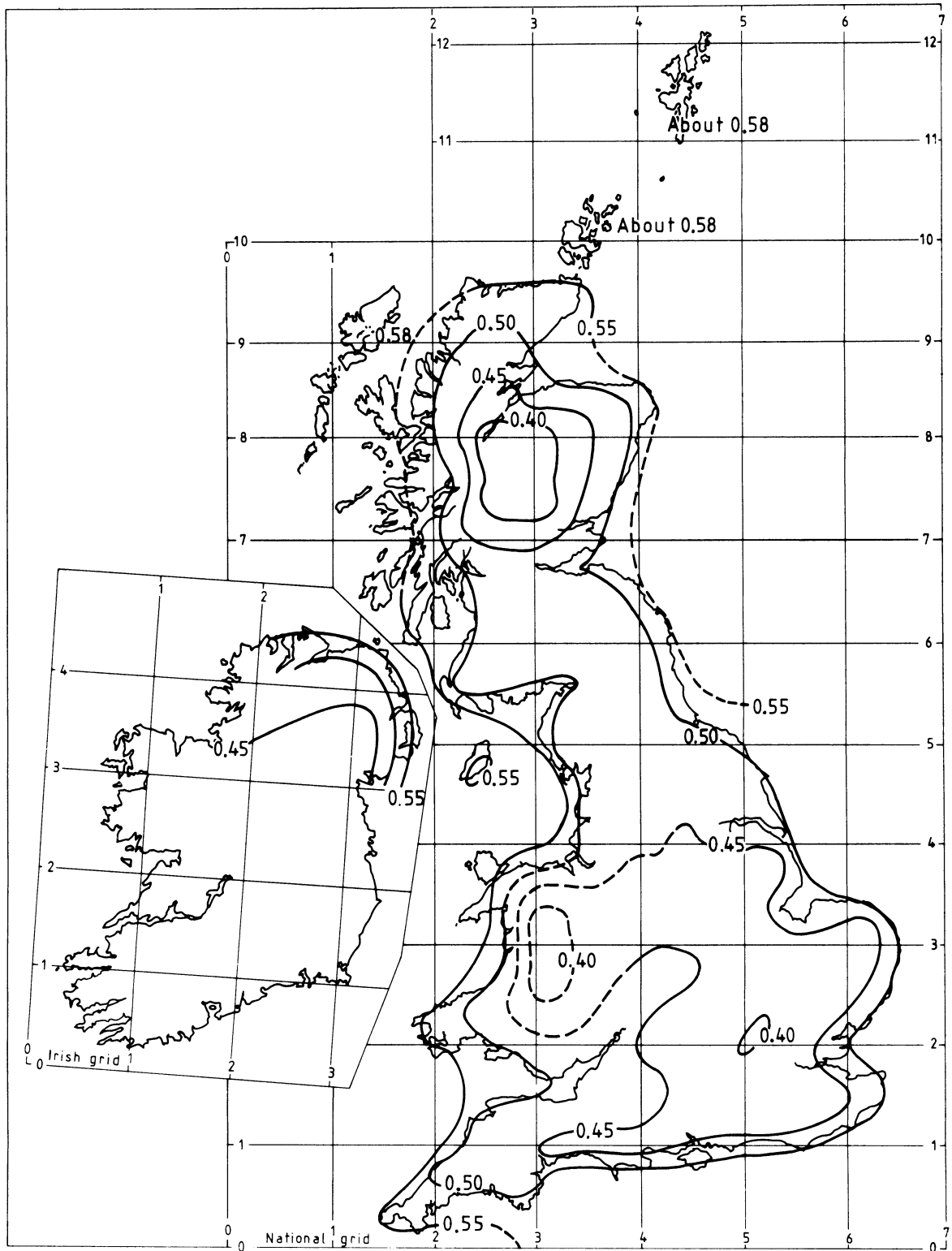


Figure C.3.4 — Values of gradient wind speed reduction factor, K_g [3.23]

Table C.3.4 — Comparison of $\bar{V}_z/\gamma_d V_B$ for (a) log law [3.1] (b) power law

Terrain category	I $\alpha = 0.125$		II $\alpha = 0.14$		III $\alpha = 0.165$		IV $\alpha = 0.19$		V $\alpha = 0.23$	
$z - h_e$	z_0									
	≈ 0.003 (m) $\bar{V}_z/\gamma_d \bar{V}_B$		0.01 (m) $\bar{V}_z/\gamma_d \bar{V}_B$		0.03 (m) Basic terrain $\bar{V}_z/\gamma_d \bar{V}_B$		0.10 (m) $\bar{V}_z/\gamma_d \bar{V}_B$		0.30 (m) $\bar{V}_z/\gamma_d \bar{V}_B$	
	(a)	(b)	(a)	(b)	(a)	(b)	(a)	(b)	(a)	(b)
m										
1	0.87	0.66	0.74	0.61	0.60	0.55	0.50 ^a	0.54	0.57 ^a	0.54
2	0.97	0.76	0.85	0.66	0.72	0.60	0.56	0.58	0.57 ^a	0.57
4	1.08	0.84	0.96	0.77	0.84	0.70	0.69	0.65	0.57 ^a	0.60
6	1.14	0.96	1.03	0.88	0.91	0.80	0.77	0.72	0.61	0.64
8	1.18	1.08	1.08	0.99	0.96	0.90	0.82	0.79	0.67	0.67
10	1.22	1.20	1.11	1.10	1.00	1.00	0.86	0.86	0.72	0.71
15	1.28	1.26	1.18	1.16	1.08	1.07	0.94	0.93	0.80	0.78
20	1.32	1.31	1.23	1.21	1.13	1.12	1.00	0.98	0.86	0.83
25	1.36	1.35	1.27	1.25	1.17	1.16	1.04	1.02	0.91	0.88
30	1.39	1.38	1.30	1.28	1.20	1.20	1.08	1.06	0.95	0.91
35	1.41	1.40	1.32	1.31	1.23	1.23	1.11	1.09	0.98	0.95
40	1.43	1.43	1.35	1.34	1.25	1.26	1.14	1.12	1.01	0.98
50	1.47	1.47	1.39	1.38	1.30	1.30	1.18	1.17	1.06	1.03
60	1.50	1.50	1.42	1.41	1.33	1.34	1.22	1.21	1.10	1.07
70	1.53	1.53	1.45	1.44	1.36	1.38	1.25	1.24	1.13	1.11
80	1.55	1.56	1.47	1.47	1.39	1.41	1.28	1.28	1.16	1.15
90	1.57	1.58	1.50	1.50	1.41	1.44	1.31	1.31	1.19	1.18
100	1.59	1.60	1.52	1.52	1.44	1.46	1.33	1.33	1.22	1.21
110	1.61	1.62	1.54	1.54	1.46	1.49	1.35	1.36	1.24	1.23
120	1.63	1.64	1.55	1.56	1.47	1.51	1.37	1.38	1.26	1.26
130	1.64	1.65	1.57	1.57	1.49	1.53	1.39	1.40	1.28	1.28
140	1.66	1.68	1.59	1.59	1.51	1.55	1.41	1.42	1.30	1.30
160	1.69	1.70	1.62	1.62	1.54	1.58	1.44	1.46	1.34	1.34
180	1.71	1.72	1.64	1.65	1.57	1.61	1.47	1.49	1.37	1.38
200	1.74	1.75	1.67	1.67	1.59	1.64	1.50	1.52	1.40	1.41
220	1.76	1.76	1.69	1.70	1.62	1.67	1.52	1.55	1.42	1.45
240	1.78	1.79	1.71	1.72	1.64	1.69	1.55	1.57	1.45	1.47
260	1.80	1.80	1.73	1.74	1.66	1.71	1.57	1.60	1.47	1.50
280	1.82	1.82	1.75	1.75	1.68	1.73	1.59	1.62	1.50	1.53
300	1.84	1.84	1.77	1.77	1.70	1.75	1.61	1.64	1.52	1.55

NOTE $\gamma_d \bar{V}_B = \gamma_v K_d \bar{V}_B = \bar{V}_r / K_R$ (see 3.1.5 of Part 1).

^a For log law values (a), values below $z - h_e = \frac{1}{2} h_e$ follow different relationship to Part 1 basis in (b) (see Figure C.3.7).

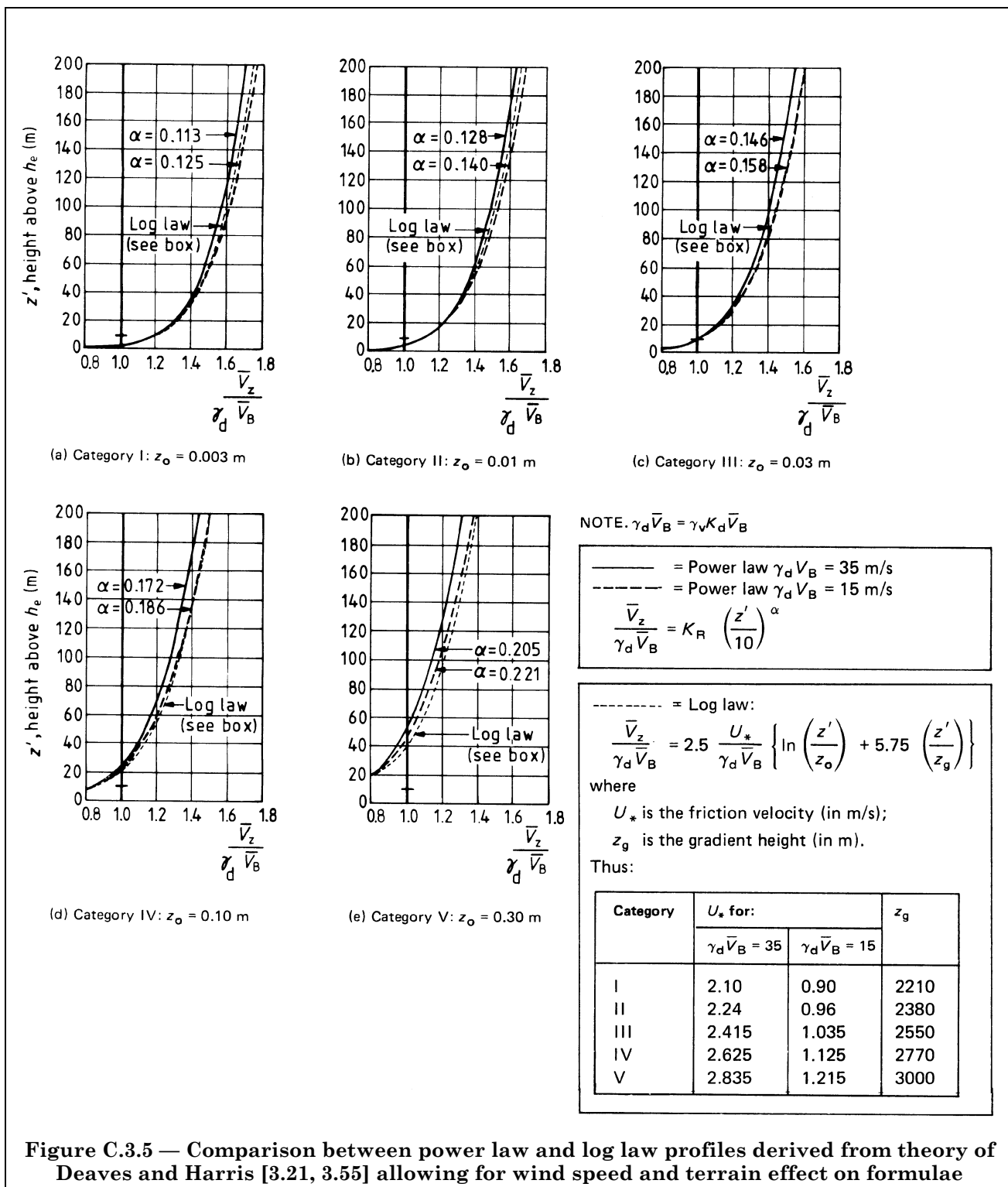


Figure C.3.5 — Comparison between power law and log law profiles derived from theory of Deaves and Harris [3.21, 3.55] allowing for wind speed and terrain effect on formulae

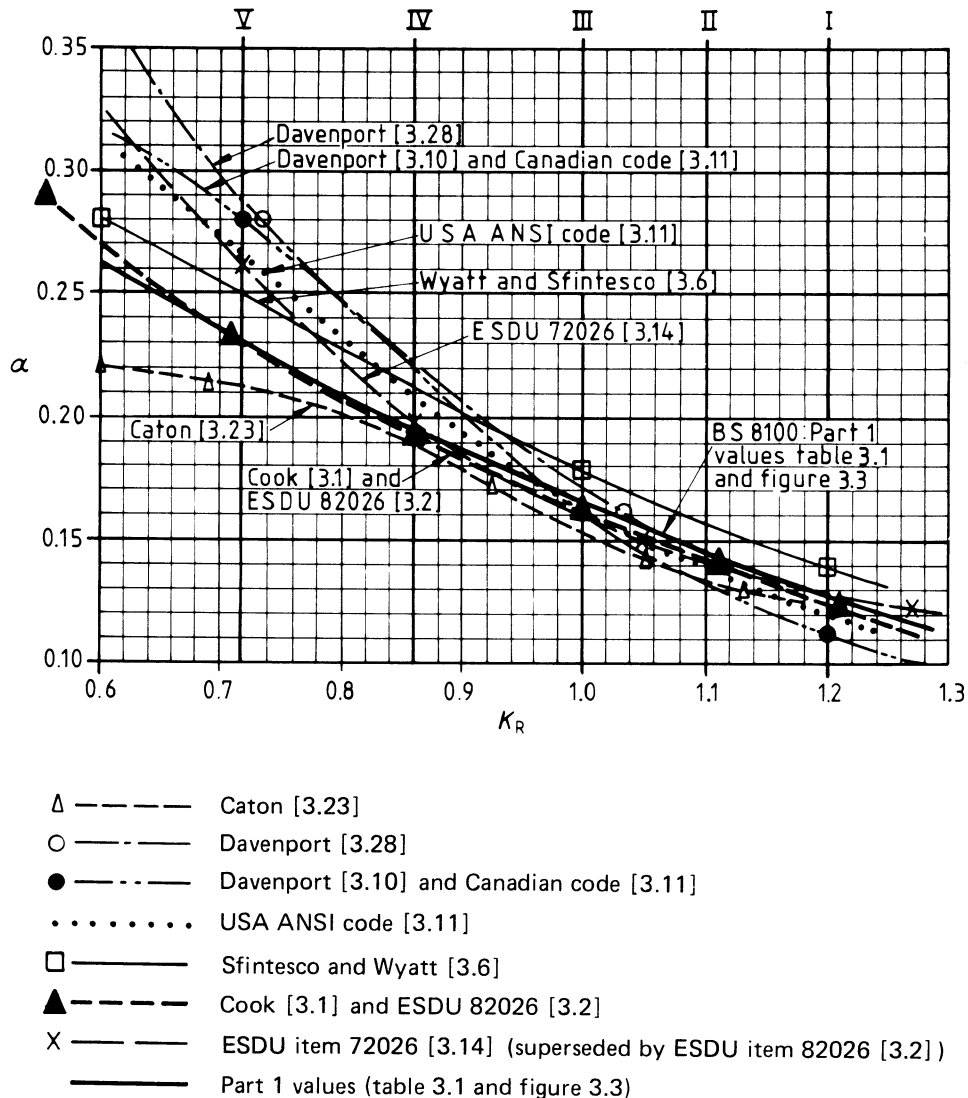


Figure C.3.6 — Variation of power law index of mean wind speed with terrain roughness

Although these comparisons are not entirely conclusive, it may be inferred that Part 1 predicts the increase in speed at hill sites reasonably accurately and certainly much better than the procedure in CP 3: Chapter V-2 [3.3].

Final comparisons made against the procedure developed by Cook [3.1] are given in Figure C.3.15 to Figure C.3.18, which show good agreement.

D) *Sites away from the crest of a hill.* This simplified formulation, given in B), applicable to the tops of hills may be extended to sites behind the hill on the assumption that μ and K_μ vary linearly with distance from the crest, with sites at a distance greater than $18 H_h$ behind the crest being unaffected by the slope of the hill.

Thus for sites downwind a distance x from the crest:

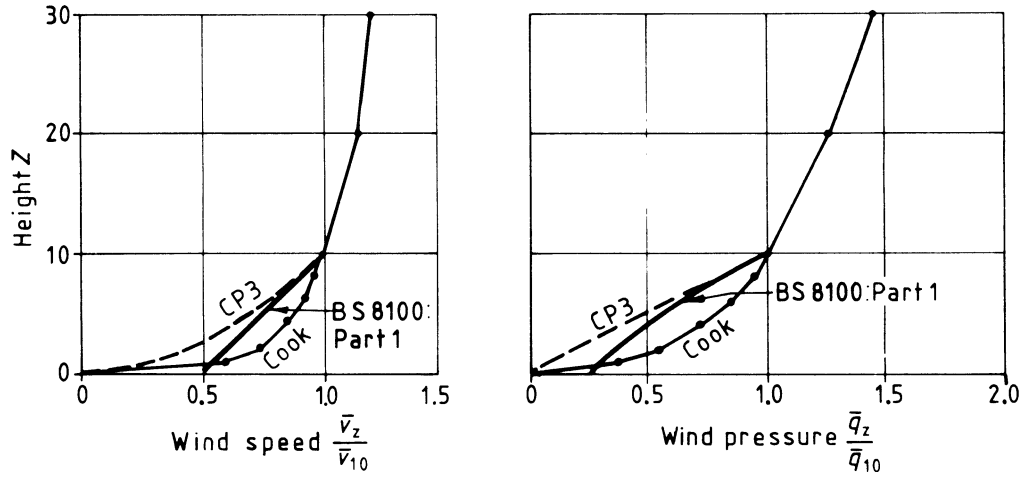
$$\mu_x = \mu \left(1 - \frac{x}{18 H_h} \right) \quad (3.11)$$

$$K_{\mu x} = K_\mu - \frac{x}{18 H_h} (K_\mu - 1) \quad (3.12)$$

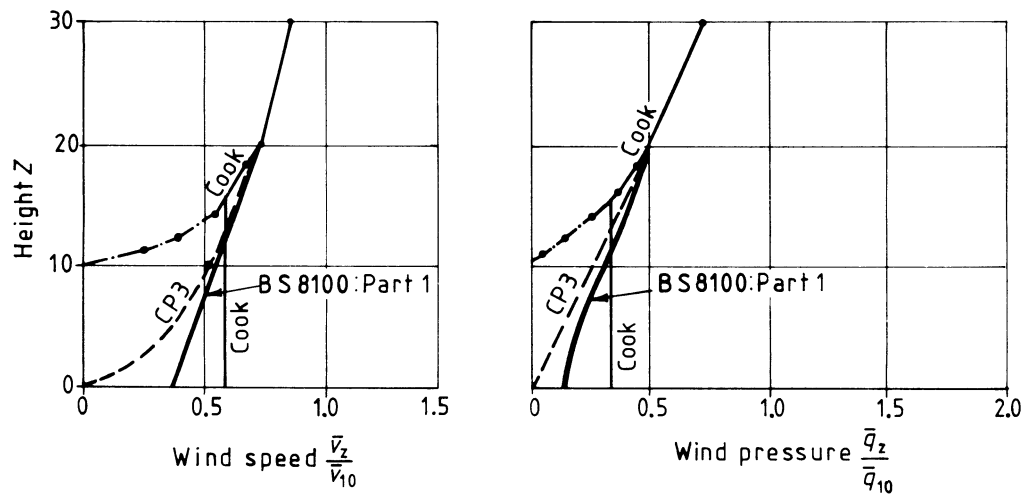
For a series of hills the comparison with the CERL results [3.32] showed that it is reasonable to assume that intermediate valleys may be ignored but that the value of x should be taken from the brow of the first hill in the line considered. The hill profile should be plotted for a region 8 km in front of the site and the mean level of the terrain be taken between this point and the valley of the hill immediately adjacent to the site. If there are no significant level regions between this point and the site hill, the effective height of the hill is then taken as the difference between this mean level and the site level [see Figure C.3.19(a)]. For sites where there is a significant upwind plateau, a value of x could be taken from the first hill behind the flat region to the site position [see Figure C.3.19(b)].

E) *Sites in undulating terrain.* For regions of undulating terrain, Appendix C of Part 1 sets out a procedure for assessing the hill parameters, so that complex terrain can be idealized for application of the recommendations.

This procedure has been applied to the case of Lowther Hill and the recommendations of Part 1 used to predict the mean flow on the hill, producing a ratio of wind speed on the hill to that in the surrounding low terrain of about 1.6. Records obtained from the Meteorological Office for a period of gales at Lowther Hill at which the mean wind speed at the site was 41 m/s have been obtained for sites at Hunterston and Prestwick. These showed that the coincident mean wind speed at the time of the gale at these sites was approximately 25 m/s giving a ratio to that on the hill of 1.64, showing good prediction by the combined procedure of section three of Part 1 and Appendix C of Part 1.



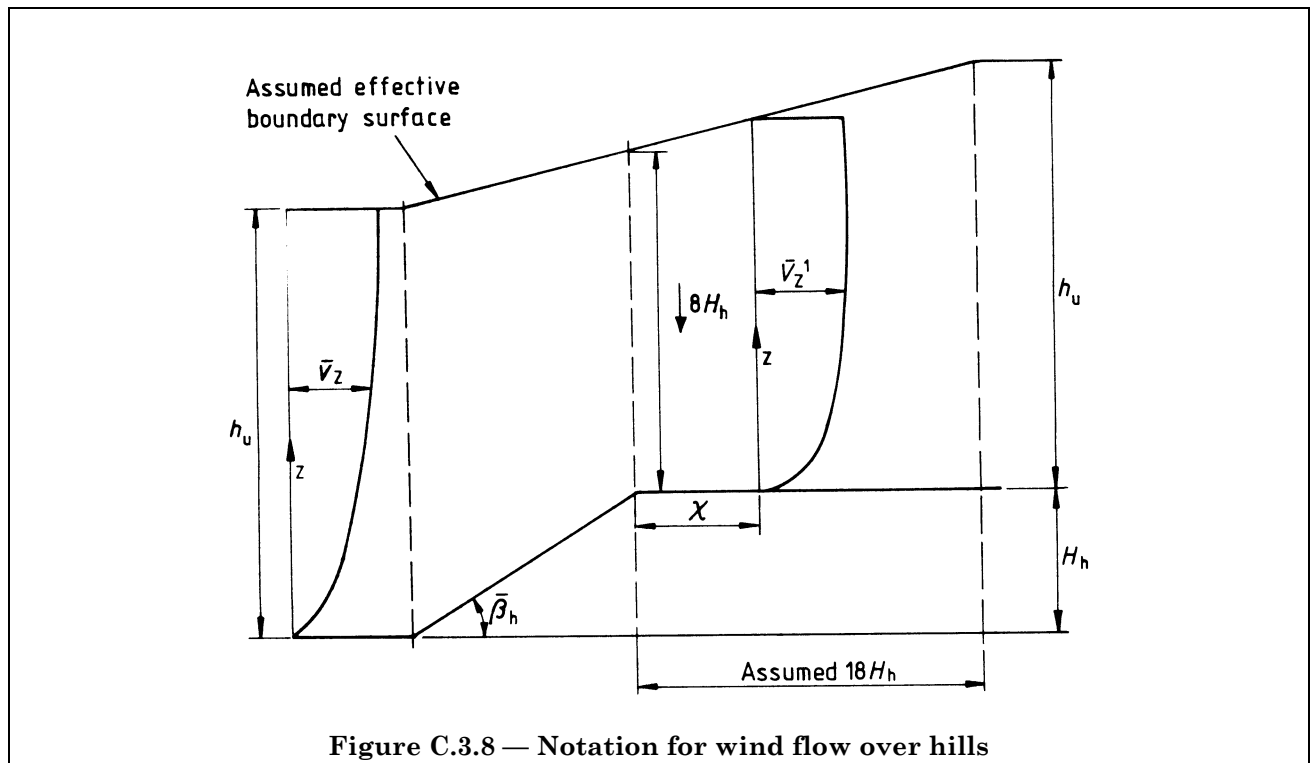
(a) $z_0 = 0.03$ m; $h_e = 0$, i.e. basic open terrain



(b) $z_0 = 0.30$ m; $h_e = 10$ m

- Cook [3.1]
- - - - - CP 3 [3.3]
- BS 8100 : Part 1

Figure C.3.7 — Comparison of wind and pressure profiles at low levels



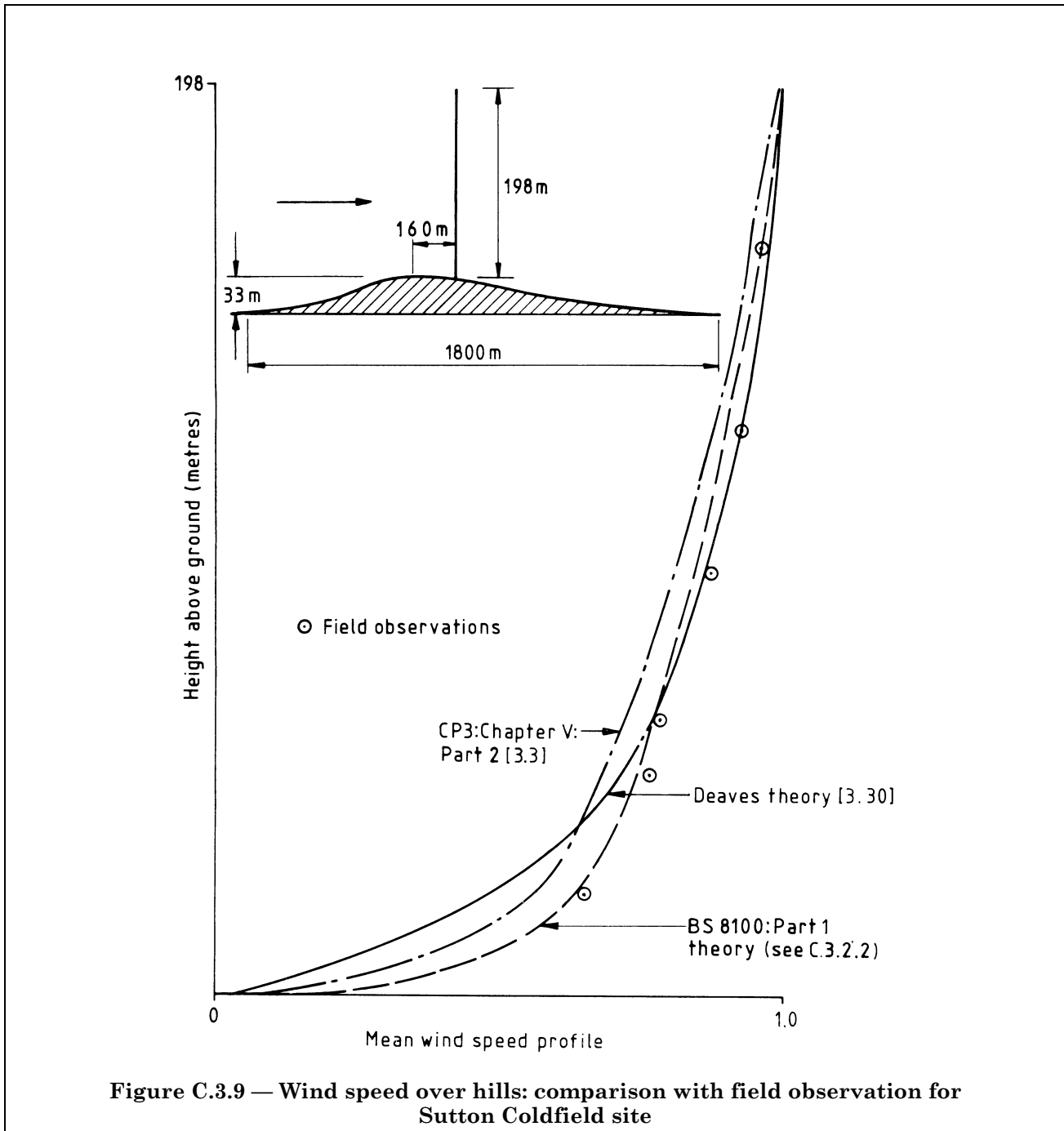
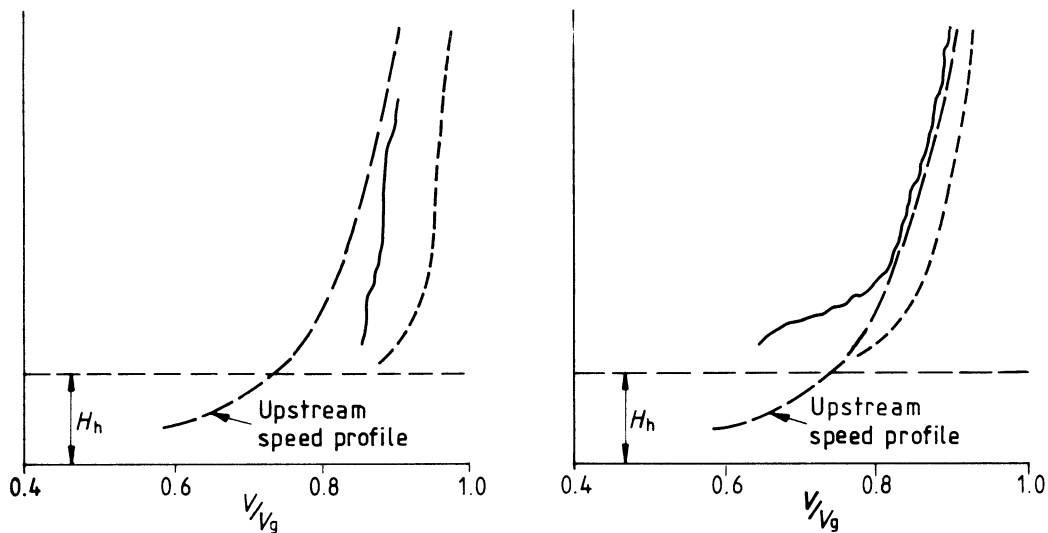
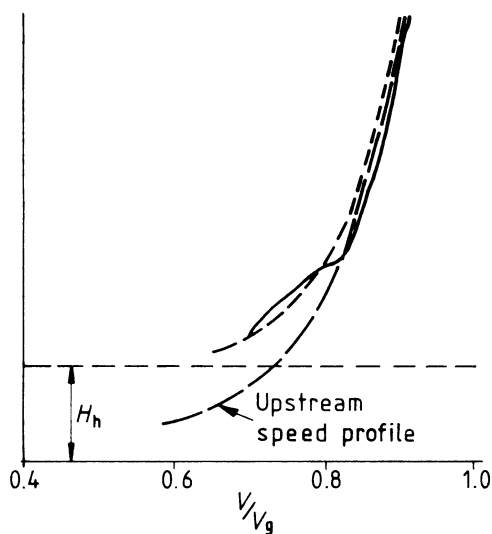


Figure C.3.9 — Wind speed over hills: comparison with field observation for Sutton Coldfield site


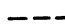


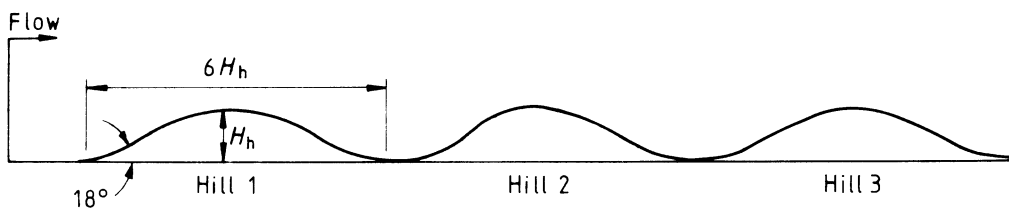
(a) Hill number 1

(b) Hill number 2



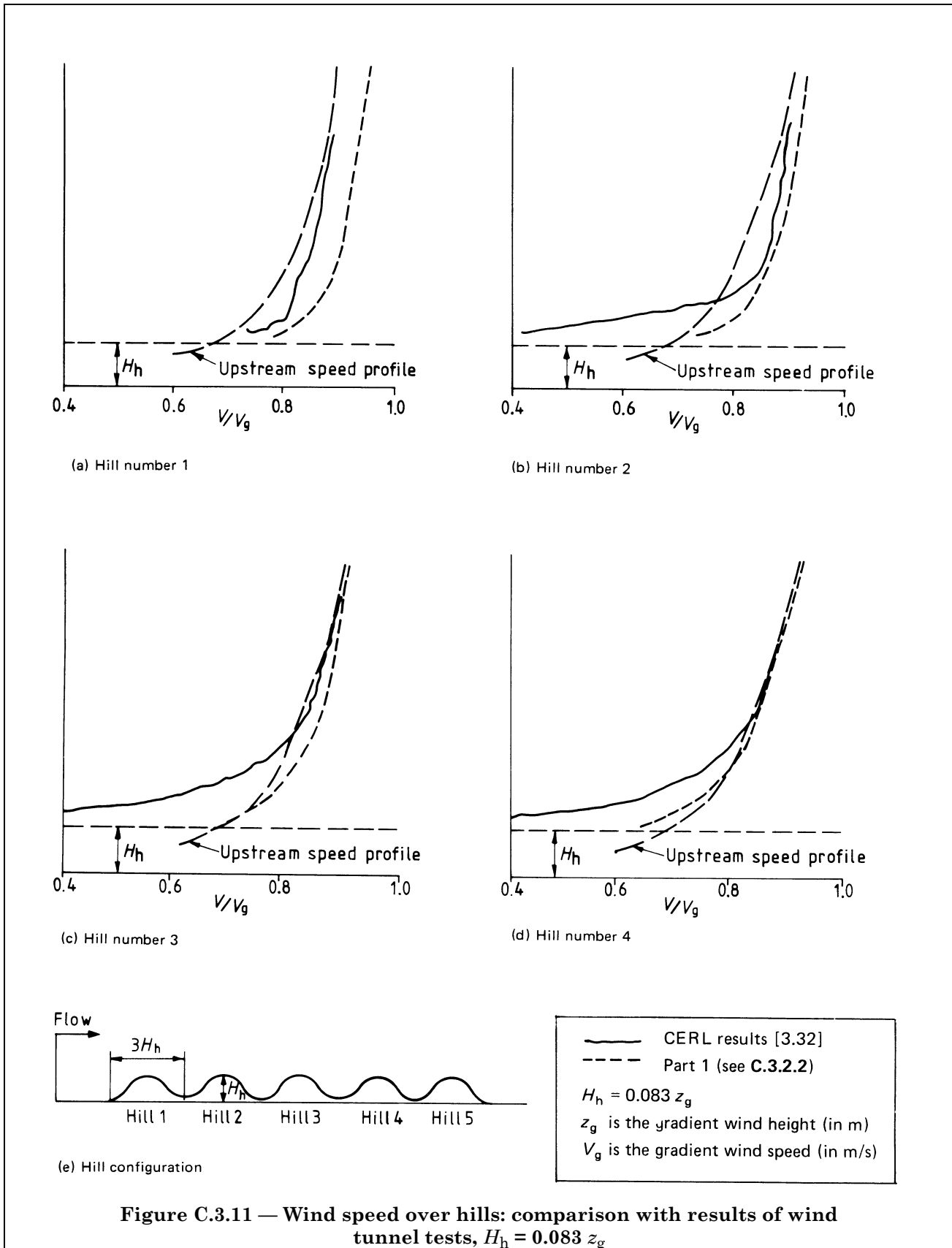
(c) Hill number 3

 CERL results [3.32]
 Part 1 (see C.3.2.2)
 $H_h = 0.125 z_g$
 z_g is the gradient wind height (in m)
 V_g is the gradient wind speed (in m/s)



(d) Hill configuration

Figure C.3.10 — Wind speed over hills: comparison with results of wind tunnel tests, $H_h = 0.125 z_g$



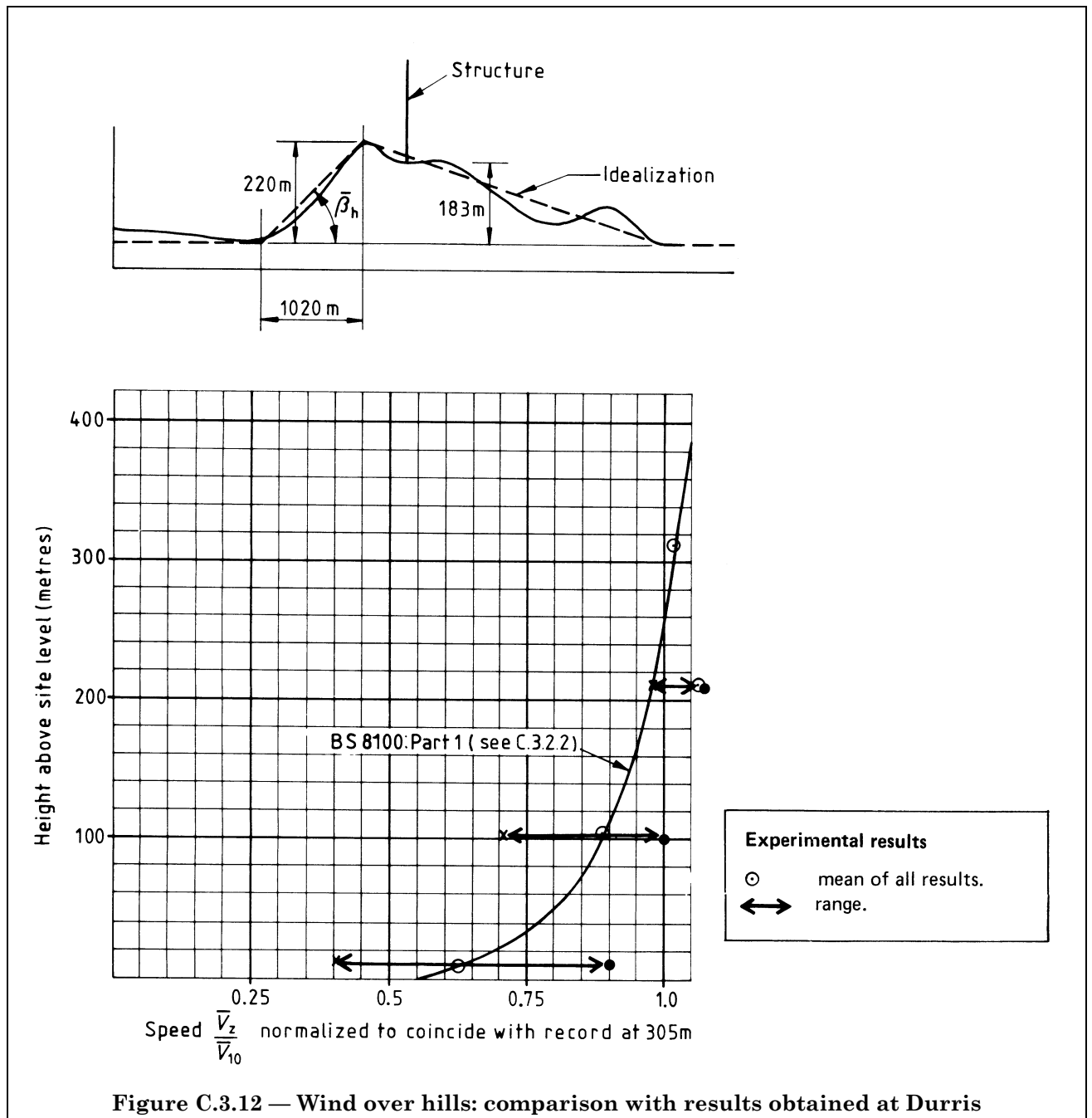
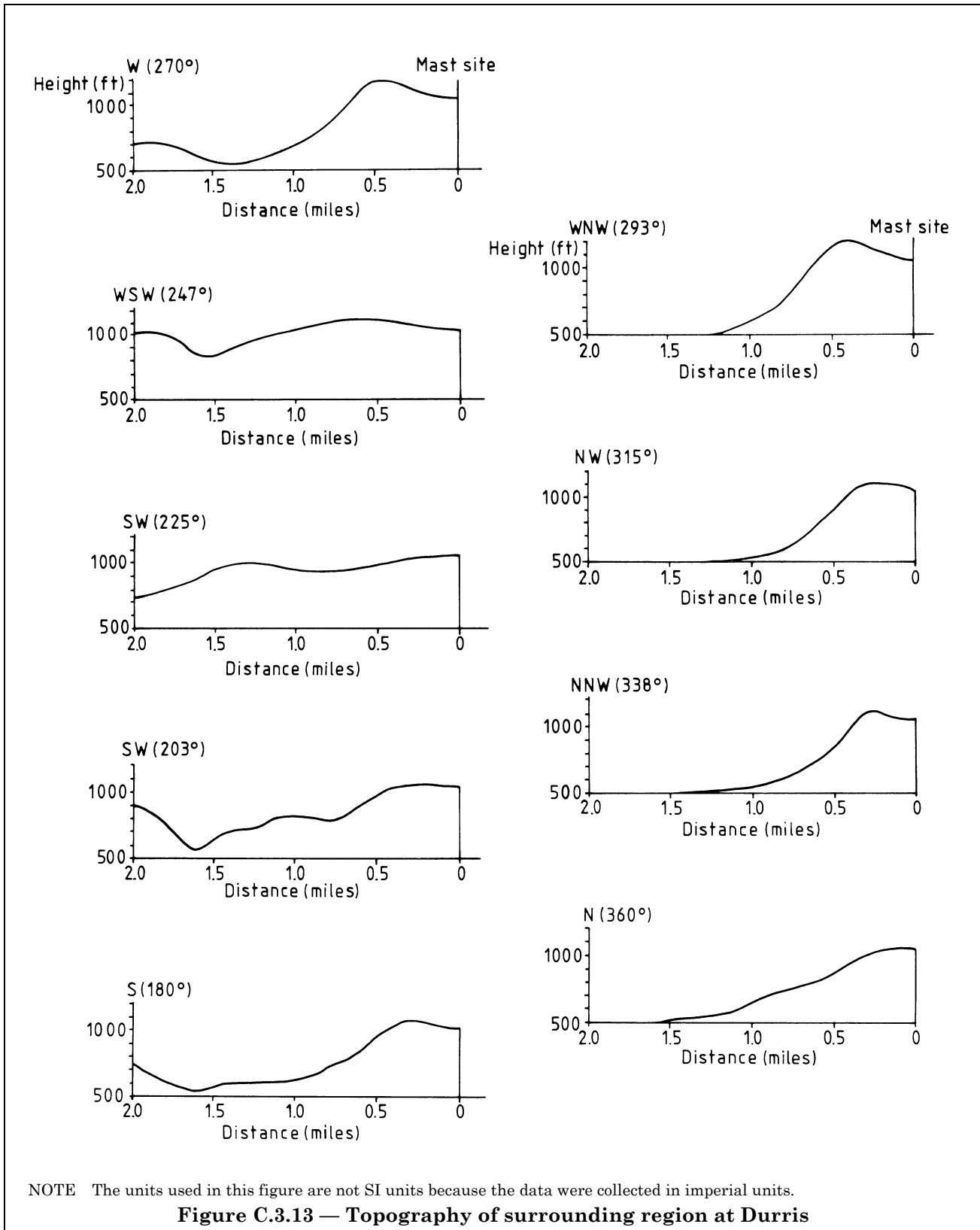
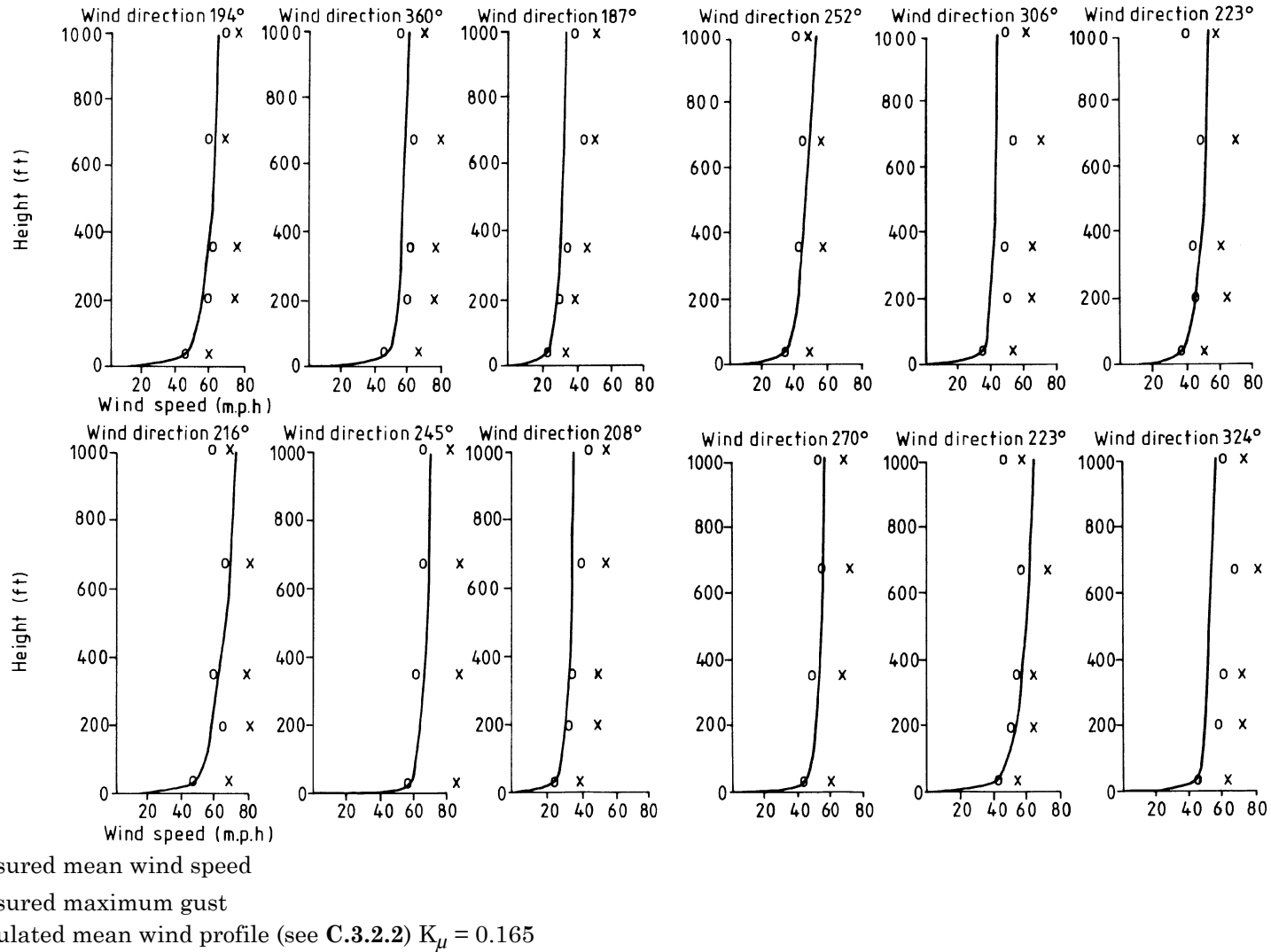


Figure C.3.12 — Wind over hills: comparison with results obtained at Durris





NOTE The units used in this figure are not SI units because the data were collected in imperial units.

Figure C.3.14 — Wind over hills: comparison with records from Durris mast

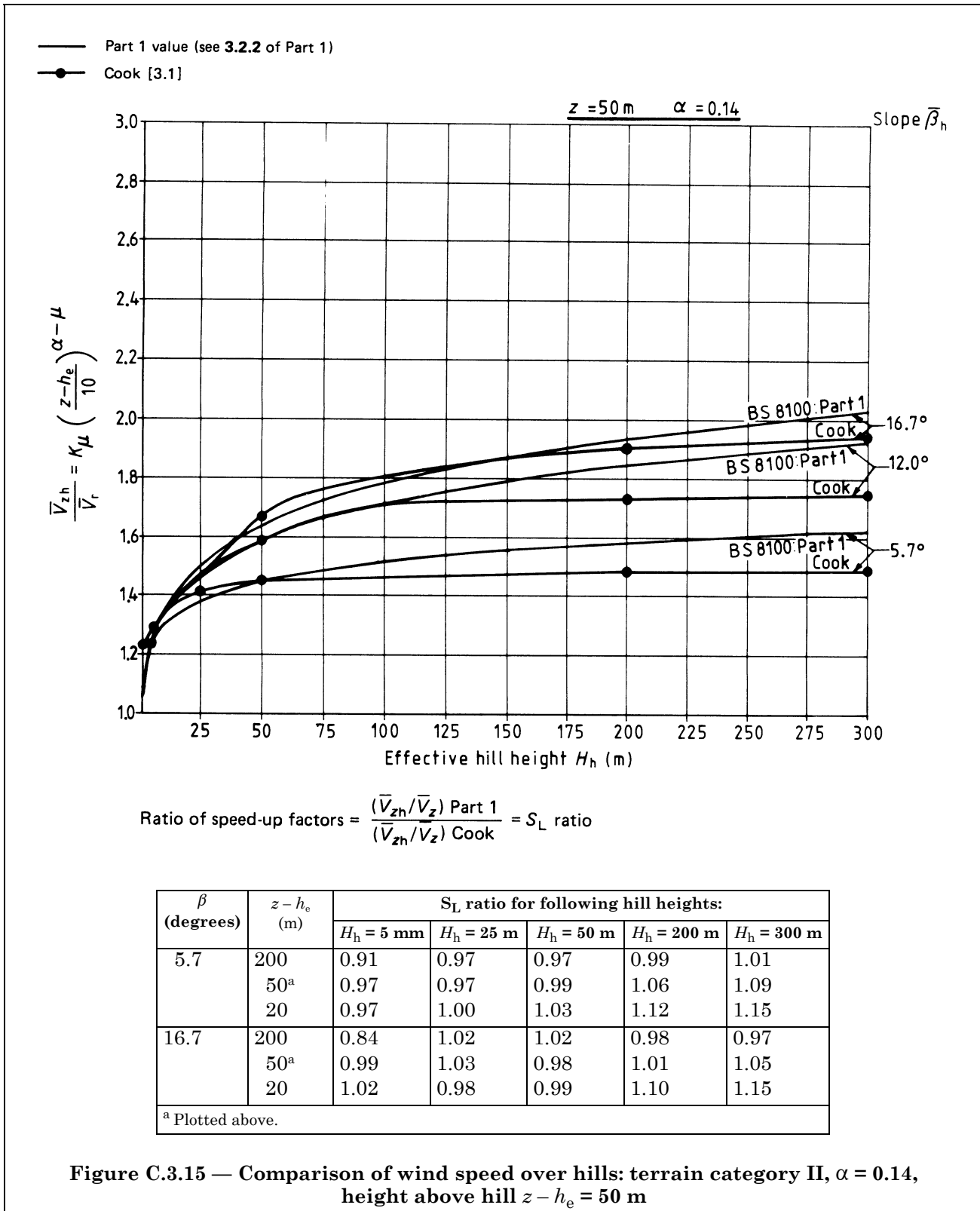


Figure C.3.15 — Comparison of wind speed over hills: terrain category II, $\alpha = 0.14$, height above hill $z - h_e = 50 \text{ m}$

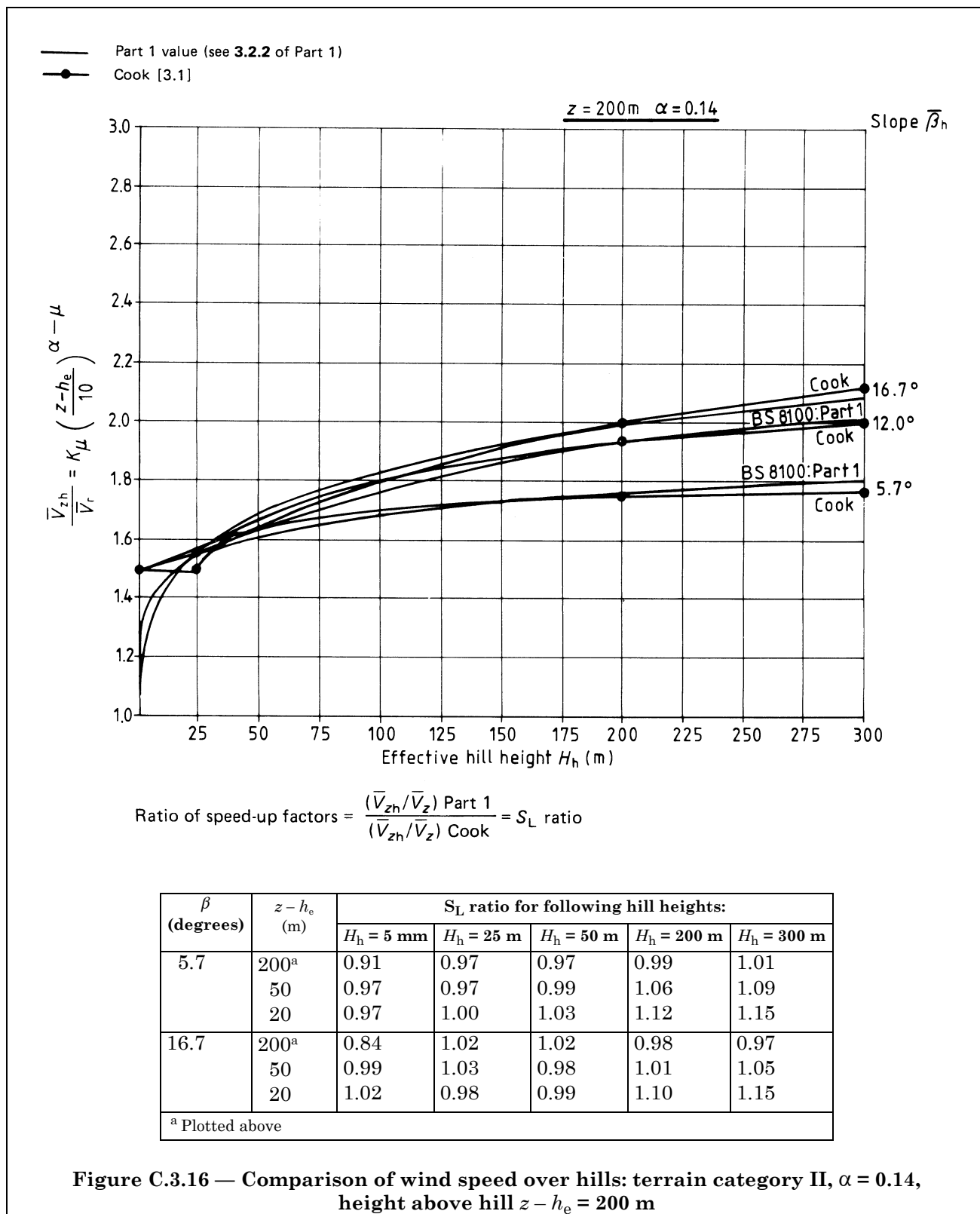


Figure C.3.16 — Comparison of wind speed over hills: terrain category II, $\alpha = 0.14$, height above hill $z - h_e = 200 \text{ m}$

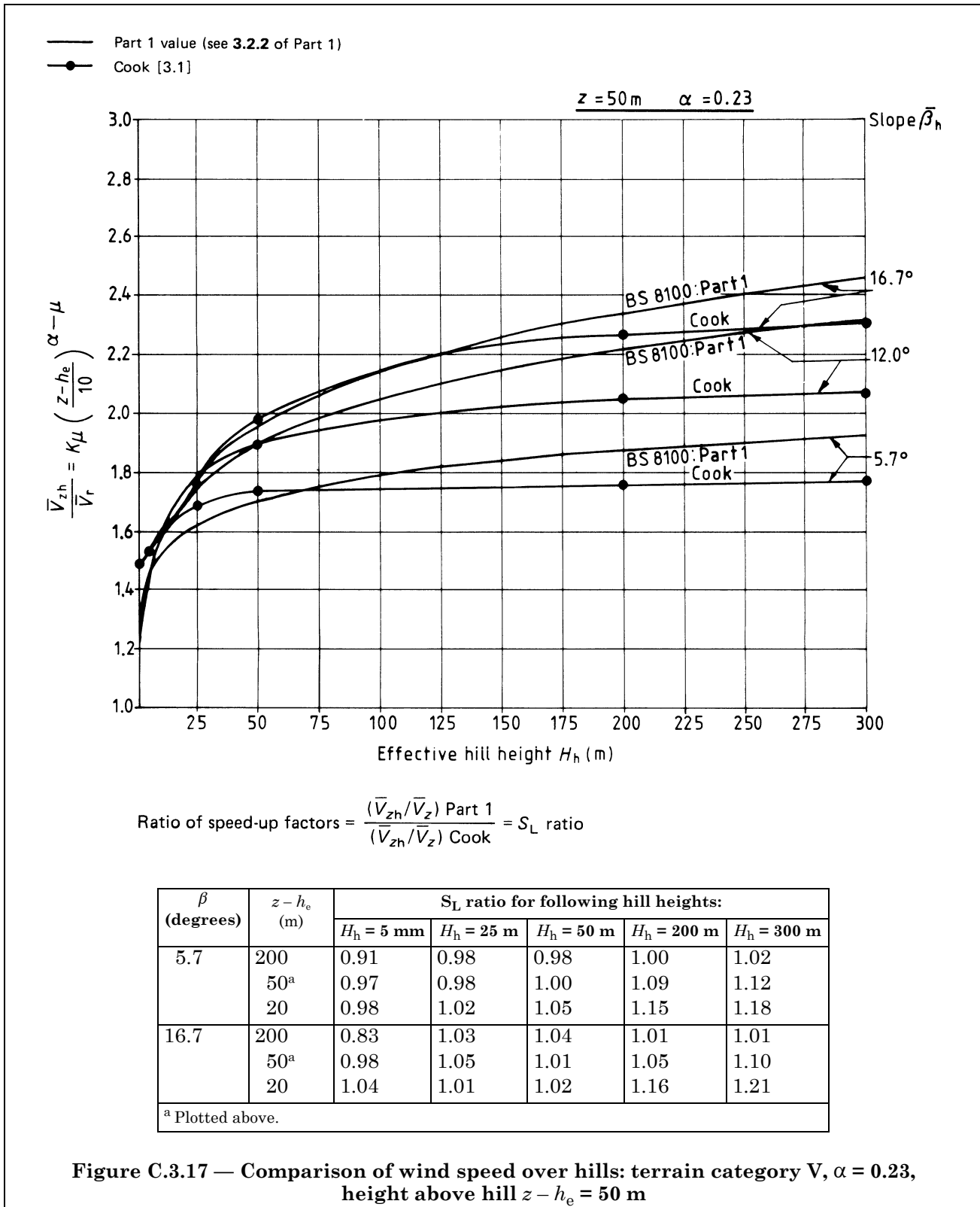
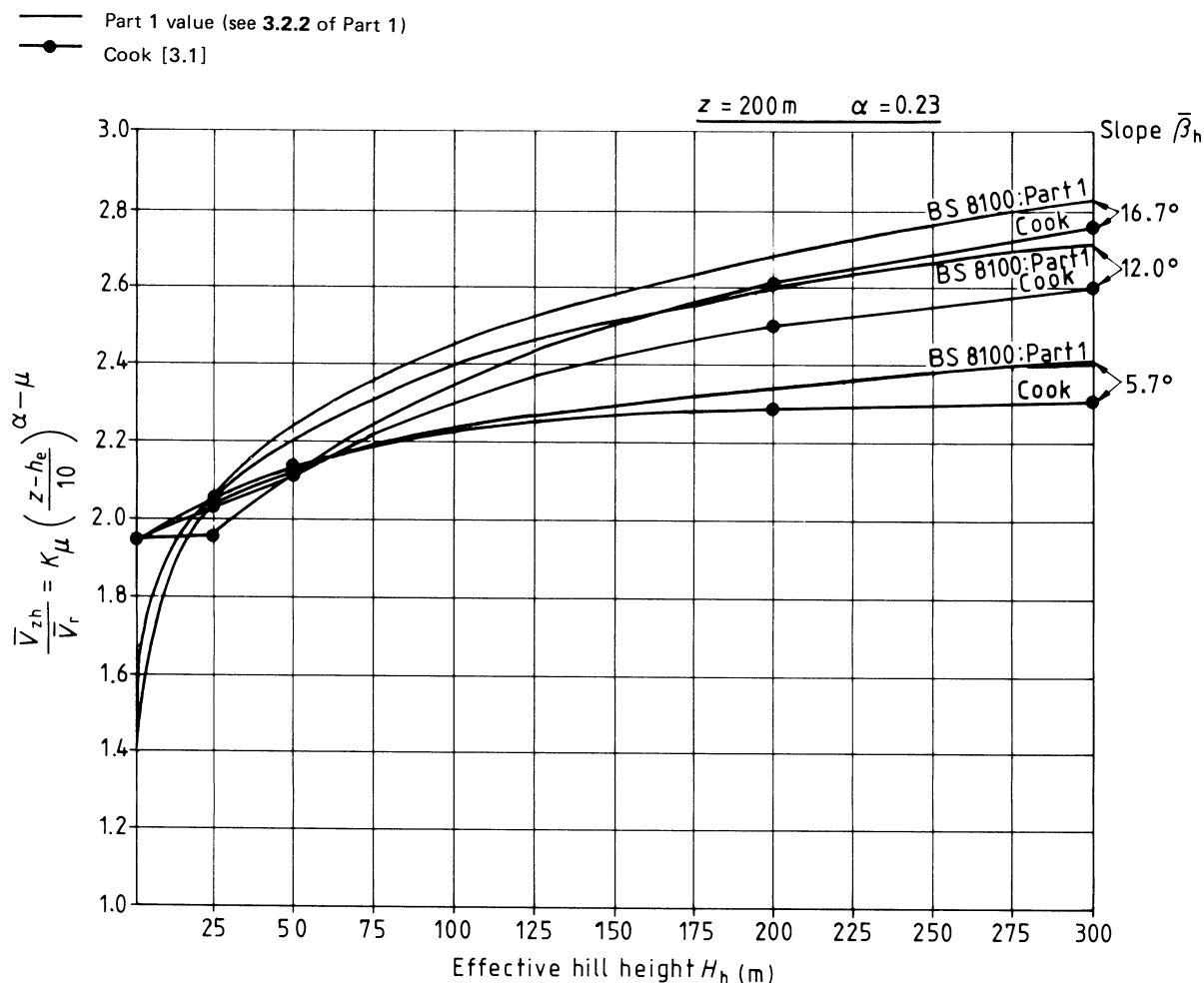


Figure C.3.17 — Comparison of wind speed over hills: terrain category V, $\alpha = 0.23$, height above hill $z - h_e = 50 \text{ m}$



$$\text{Ratio of speed-up factors} = \frac{(\bar{V}_{zh}/\bar{V}_z) \text{ Part 1}}{(\bar{V}_{zh}/\bar{V}_z) \text{ Cook}} = S_L \text{ ratio}$$

β (degrees)	$z - h_e$ (m)	S_L ratio for following hill heights:				
		$H_h = 5\text{ m}$	$H_h = 25\text{ m}$	$H_h = 50\text{ m}$	$H_h = 200\text{ m}$	$H_h = 300\text{ m}$
5.7	200 ^a	0.91	0.98	0.98	1.00	1.02
	50	0.97	0.98	1.00	1.09	1.12
	20	0.98	1.02	1.05	1.15	1.18
16.7	200 ^a	0.83	1.03	1.04	1.01	1.01
	50	0.98	1.05	1.01	1.05	1.10
	20	1.04	1.01	1.02	1.16	1.21

^a Plotted above.

Figure C.3.18 — Comparison of wind speed over hills: terrain category V, $\alpha = 0.23$, height above hill $z - h_e = 200\text{ m}$

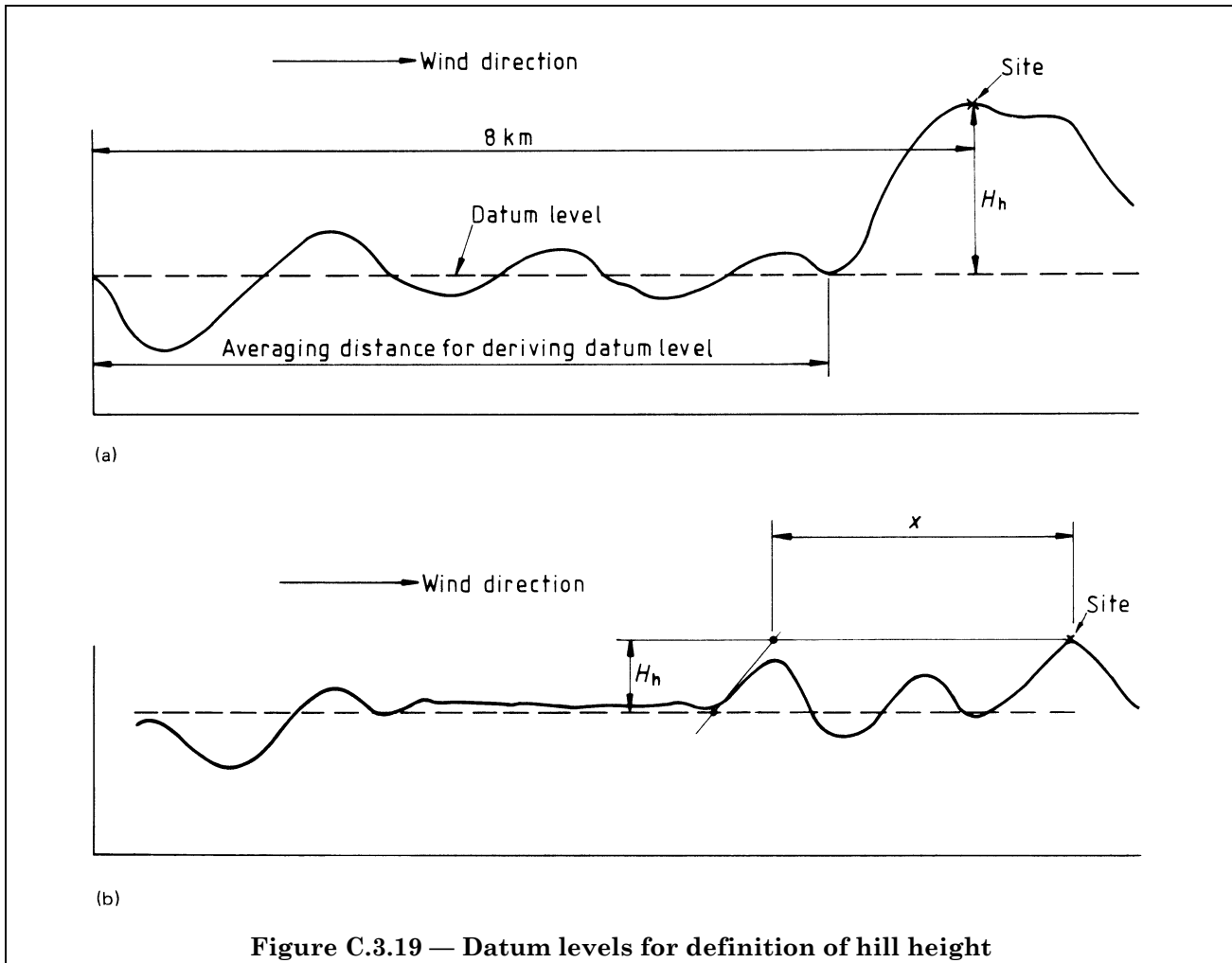


Figure C.3.19 — Datum levels for definition of hill height

C.3.3 Serviceability criteria

The frequency distributions of mean hourly wind speeds for five meteorological stations widely distributed throughout Britain obtained from 15 years of records are plotted in Figure C.3.20. The recorded mean distributions are plotted and, for comparison, a Gaussian distribution having a coefficient of variation of 0.15 is shown which fits the observations over the range of moderate speeds.

Using the distribution curve shown by the full line, the annual periods for which the mean wind speed exceeds various fractions of the 50 year return wind speed, shown in Figure C.3.20 have been obtained by integration. In the high wind speed range, it has been assumed that the annual periods diminish logarithmically from a period of 10 h/year for $\bar{V}_s = 0.7\bar{V}_k$ to a period of 0.1 h/year for $\bar{V}_s = \bar{V}_k$, i.e. equivalent to a 5 h storm of maximum intensity once in 50 years.

The Meteorological Office has examined records of extreme winds from more than 120 stations over periods of up to 20 years and provided tentative frequency distributions for sheltered and exposed sites as shown in Figure C.3.21. Data were not available for the variation of mean wind speed in the period of a typical storm and the distribution at the low frequency end may require review. Also shown in Figure C.3.21 is the distribution shown in Figure 3.6 of Part 1, which has therefore been made conservative in comparison with the observations.

The wind roses shown in Figure 3.8 of Part 1 have been derived by analysis of data from selected meteorological stations, the mean wind distributions being plotted for each of twelve 30° sectors from which the roses were compounded. Since these are relevant only to wind speeds of less than one-half of the 50 year return speed, the universal rose given in Figure 3.7 of Part 1 has been constructed as an envelope to the curves shown in Figure 3.8 of Part 1 to be used in conjunction with the speed distribution shown in Figure 3.6 of Part 1, and Figure 3.7 of Part 1 may be taken to apply to any wind speed. In each case the periods given are those during which the wind speed is predicted to be within a range of 5 % of the designated speed.

C.3.4 *Fatigue life assessment*

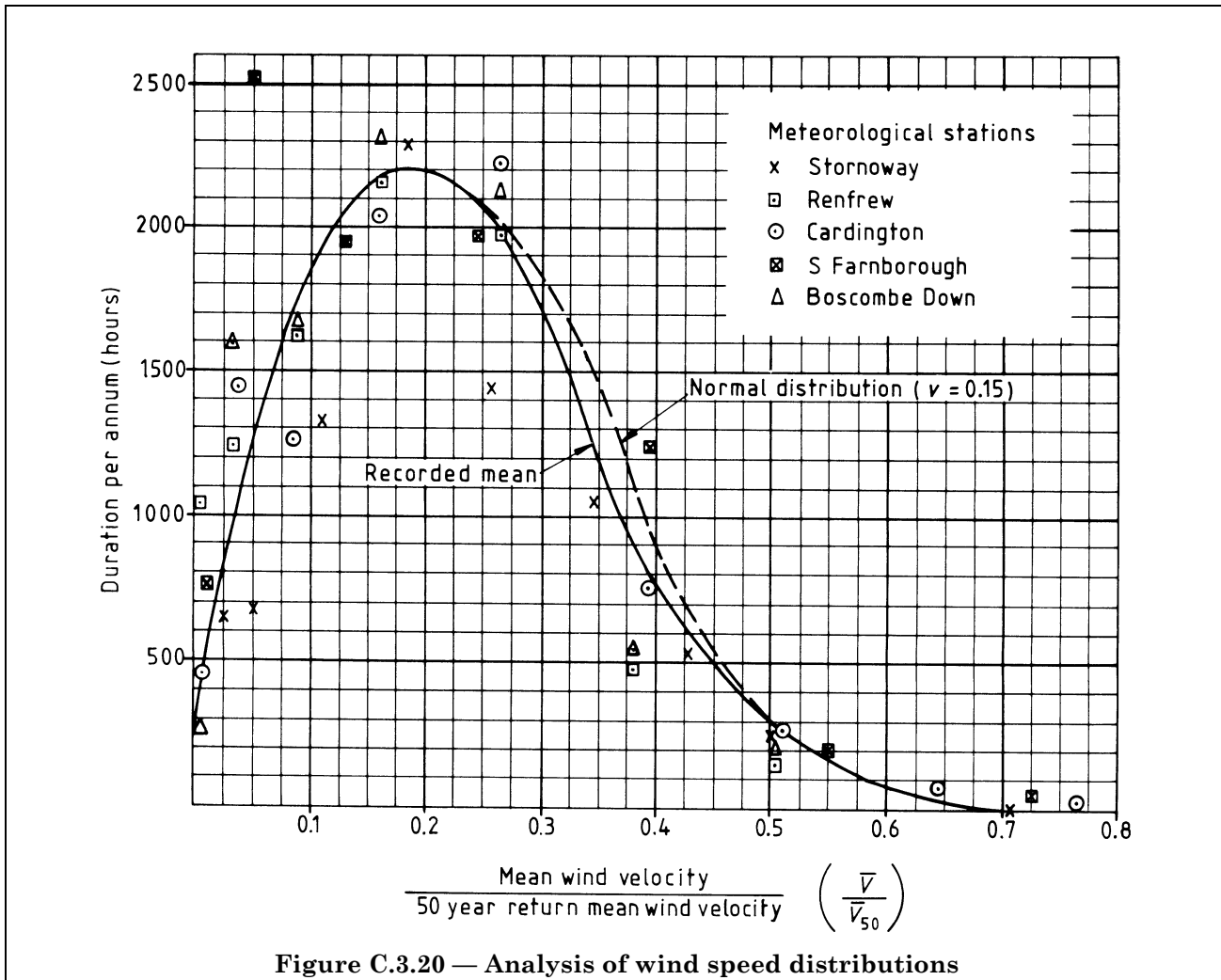
Consideration should be given to the risk of fatigue failure of a tower due to stress fluctuations resulting from gusts. It would appear, however, that with connections unlikely to have fatigue characteristics worse than those of class G in legs and class F in bracings in steels of Grade 50 or worse than class D in Grade 55 steels [3.34], the fatigue life of a tower free from aerodynamic instability is likely to exceed 50 years. To reach this conclusion, it has been assumed that the gust factor for legs will be of the order of 2.0 and may be very large for bracings. Thus the peak stress range may be assumed to be equal to the maximum stress for legs and twice the maximum for bracings. Adopting a normal distribution with the peak value taken as four standard deviations above the mean and taking the design stress on the gross section as a maximum of two-thirds of the yield stress under 50 year return conditions, the cumulative fatigue damage summation calculation may be undertaken by reference to the mean wind speed distribution shown in Figure 3.6 of Part 1. Due allowance may also be made for the variation in wind direction by reference to Figure 8. It is found that the major contribution to damage is that due to mean wind speeds of the order of one-half of the 50 year return values, with several hundred hours occurrence per annum. This implies that fatigue endurance is sensitive to the material fatigue characteristics at the low ends of the *S/N* curves which have been little explored. It also implies that the frequency distribution of high-intensity storms probably has little influence on fatigue endurance.

Hence, for the purposes of Part 1 it has been considered reasonable to discount the risk of fatigue, as is present practice, although the position should be reviewed for towers of welded construction, which should be subject to fatigue life appraisal if required to have a design life of more than 30 years, or if constructed from extra high yield material ($> 355 \text{ N/mm}^2$). In addition, in-line gust response of welded towers may lead to unsatisfactory fatigue life if the detailing or response of the structure are not compatible with these assumptions.

C.3.5 *Ice loading*

C.3.5.1 *General.* Loading due to ice and snow alone is unlikely to govern the design of self-supporting towers, but in combination with wind such loading may prove critical in the UK for some structures. Design allowances for ice have therefore been included which are applicable to all lattice structures. The appropriate combinations of ice thickness and density and wind speed to be assumed in design depend on the frequency of occurrence and duration of icing conditions, the interaction between thickness and speed during such conditions and on the meteorological characteristics of the region of the site. There are insufficient records of coincident conditions on which to base design rules and the provisions of 3.5.1 b) of Part 1 have been based on the following considerations.

The Meteorological Office, in their analysis of records to provide the basis for ice zoning prior to 1978 (see C.3.5.2) have examined wind speeds coincident with the conditions deemed to permit icing. From at least 10 years of records, the extreme coincident speeds did not exceed 70 % of the 50 year return speeds and this corresponds closely to 80 % of the 10 year return values appropriate to the extent of the records. The corresponding wind directions were also noted and are indicated in Figure C.3.22. Since these only apply to the extreme values, it has not been feasible yet to produce a wind rose for combinations of wind and ice, although the directions shown could be used as an interim basis for design when direction is critical. It has been considered reasonable to assume that since the directions noted lie broadly in the anticipated range of 0 to 150° it would generally be acceptable to use a direction factor not greater than 0.85 (see 3.1.3 a) 2) of Part 1 and Figure 3.2 of Part 1, thereby permitting the adoption of a resulting design wind speed of 68 % of the ice-free speed. This closely corresponds to the use of a wind speed of two-thirds of the full design value when treating combined loading, a basis sometimes used in the past in the design of guyed masts. Further work is being undertaken by the Meteorological Office on coincident wind and ice conditions.



The ice thicknesses selected for consideration in conjunction with the reduced 50 year return wind speed are intended to represent the mean annual maxima for two reasons. First, the combined probability of occurrence of this wind and the average maximum ice values amounts to 0.01 and this probability lies near to the point of maximum probability density in the reliability analysis for wind alone. Secondly, the conditions causing the most severe icing in the UK do not appear to be those for high wind, even from the north or east.

Typically, wind with ice conditions are only likely to govern when the factored reference ice thickness, r_r , exceeds about 60 % of the widths of the structural and ancillary parts. This percentage would decrease to about 30 % if full advantage can be taken of the direction factor, K_d , for the ice-free conditions, that is with the governing design wind direction being taken in the section 0 to 150° apart from sites within 16 km of the east coast where K_d has to be taken as 1.0. It should, however, be noted, that these percentages do not apply to towers with circular-section members in the supercritical regime under the wind only condition. There will be increased resistance under wind plus ice conditions since only subcritical regimes should be assumed for iced members (see C.4), with corresponding increases in drag coefficients. The percentage of ice thicknesses quoted for the ice plus wind condition to govern may be drastically reduced for such towers and this combination should always be checked in these circumstances, however small the value of the reference ice thickness, r_r . Additional problems may arise where there is the risk of ice filling gaps in closely-spaced lattices, as noted in 4.8 of Part 1, or where the weight of the ice could be a governing factor. Loading due to snow may be neglected as insignificant in the design of conventional towers. Special consideration of snow loads may, however, be needed for unusual towers in extreme climates.

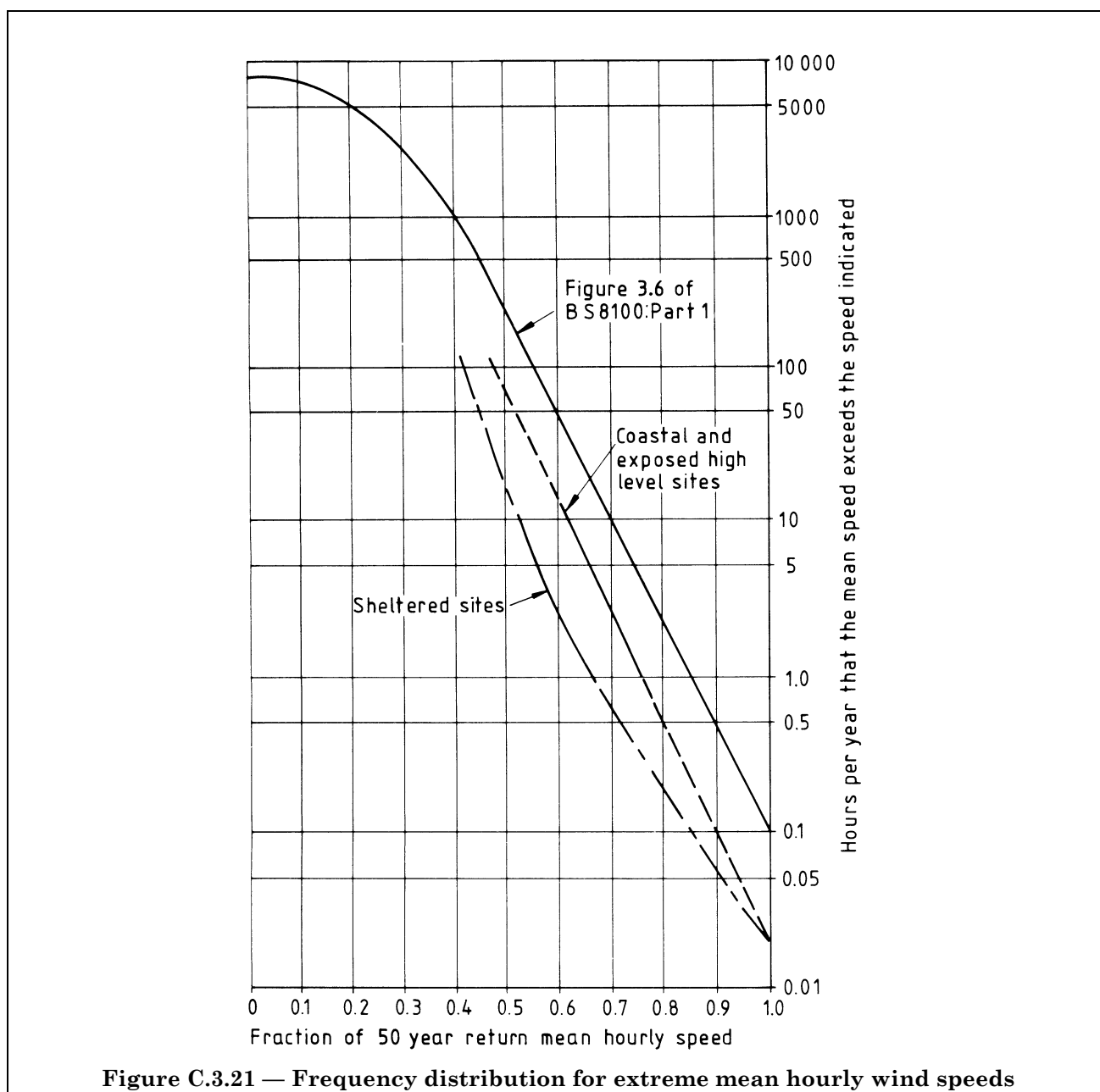


Figure C.3.21 — Frequency distribution for extreme mean hourly wind speeds

Part 1 gives no specific guidance on ice or snow load criteria for overseas sites, and recourse should be made to appropriate national codes. However, some references to such existing codes are given in this Part of BS 8100. In particular, **C.3.5.5** gives specific comments on data for France [3.35], Holland [3.36], Norway [3.37], Germany [3.38, 3.39], Czechoslovakia [3.40, 3.41], Romania [3.42, 3.43], USA [3.44] and Canada [3.45].

C.3.5.2 Basic ice thickness. Ice thicknesses to be assumed in design should ideally be based on statistical analysis of observations. Recommendations concerning such analysis as applied to overhead transmission lines have been drafted by the IEC [3.46]. However, there are no coordinated data available in the UK from which to derive mean annual maximum values and standard deviations, and hence the following basis has been used. Further observations and measurements are required to predict the design criteria more accurately.

Differences in climate within the UK make it appropriate to select loading in relation to the latitude at which the structure is sited, and with allowance for the altitude of the site.

A map (see Figure C.3.22) has been drawn up by the Meteorological Office on the basis of coincident records of temperature and humidity at 23 stations dividing the UK into three regions of varied expected severity of icing. The average annual duration of occurrence of relative humidity exceeding 97 %, in combination with minimum daily air temperature within the range -4°C to 0°C was examined from records over periods of over 10 years to provide a basis for the zoning given on this map. These regions are broadly compatible with height AMSL, distance from the coast, and latitude and do not conflict with qualitative data received from various sites. However, for purposes of codification, and to allow application to structures of various heights, the altitude effects were separated from the remainder. The regional zoning map (see Figure 3.9 of Part 1) has been derived such that, in conjunction with the altitude allowances, the severity of icing given corresponds with the Meteorological Office map. This is illustrated by Figure C.3.23 which shows contours of calculated radial ice thickness at ground level and which may be compared with Figure C.3.22.

Variation of ice thicknesses with height approximately follows the rules in the French code [3.35] with maximum values reached at 1 500 m above sea level. Figure C.3.24 shows the variation of ice thicknesses with height given in the French code compared with the simplified expression given in C.3.5.2 which is considered to be adequate for the altitude range in the UK.

There is further indication that icing should be more severe with increasing height, since tests in Germany [3.47] have shown that ice load measured at 16 m above the ground is two to three times as much as that at 2 m above ground level. During 13 years of observations on various mountains in Germany, icing has been found between limits of air temperatures from approximately $+2^{\circ}\text{C}$ to 25°C . Figure C.3.25 and Figure C.3.26 show, respectively, the days per year and ice load plotted against altitude for the seven sites considered. The IEC recommendations [3.46] suggest a variation in ice loading on conductors with height, amounting to 20 % increase from 10 m to 40 m height.

The draft Romanian loading code [3.42] also gives data for ice thickness increasing with height above ground. The ice thickness is given as 10 mm to 15 mm at 10 m above ground (depending on geographical location), increasing to 20 mm to 30 mm at 100 m above ground, and then to 35 mm at 200 m, 45 mm at 300 m and 60 mm at 400 m above ground, as discussed by Ghiocel and Lungu [3.11].

C.3.5.3 Reference ice thickness

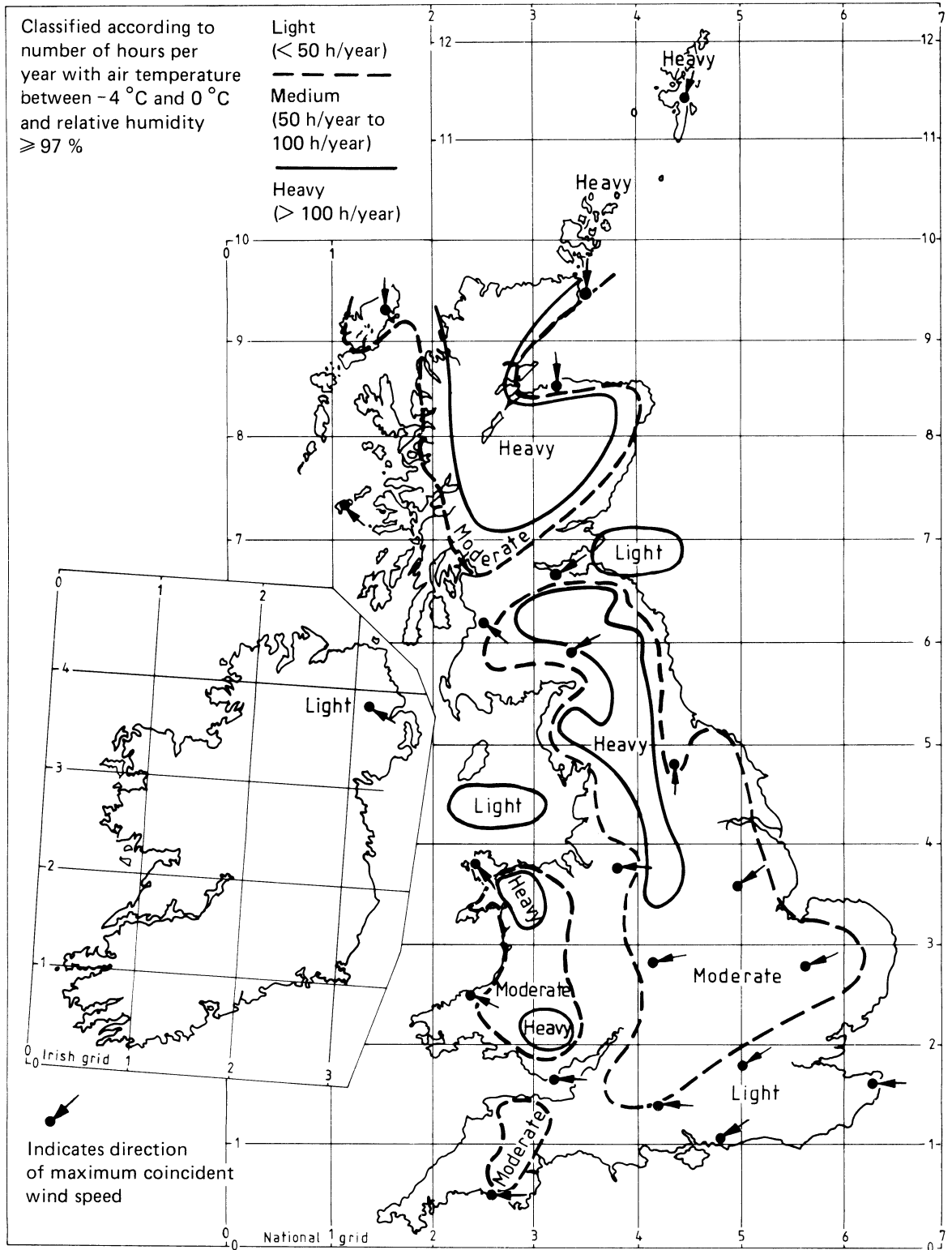
C.3.5.3.1 General. Reference values of ice loading are defined in terms of the average radial thickness of ice adhering to the member under consideration. No allowance is made for uneven distribution of ice nor for the different types of ice formation which occur, although it is recognized that glazed frost is heavily compacted with a more uniform adherence to the member compared with rime ice which forms banners in the windward direction and is of a lower density (see 3.5.4 of Part 1). Ice may also be deposited as melting snow which, in appearance, is midway between glazed frost and rime ice.

In any icing situation a combination of the three methods of deposition is possible and Part 1 quantifies in a realistic, although arbitrary, form the likely deposits of ice on both steelwork and cables taking account of the research work undertaken up to the time of drafting Part 1 both in this country and abroad.

It should be emphasized, however, that little quantifiable data exist on ice deposition and reliance has had to be made on the experience of the electricity supply boards and broadcasting companies to assess the order of ice thicknesses given. Negative experience has been relied upon such that by using the ice thicknesses recommended in conjunction with the appropriate wind velocity, existing structures in the more severely ice-loaded regions would not be predicted to collapse.

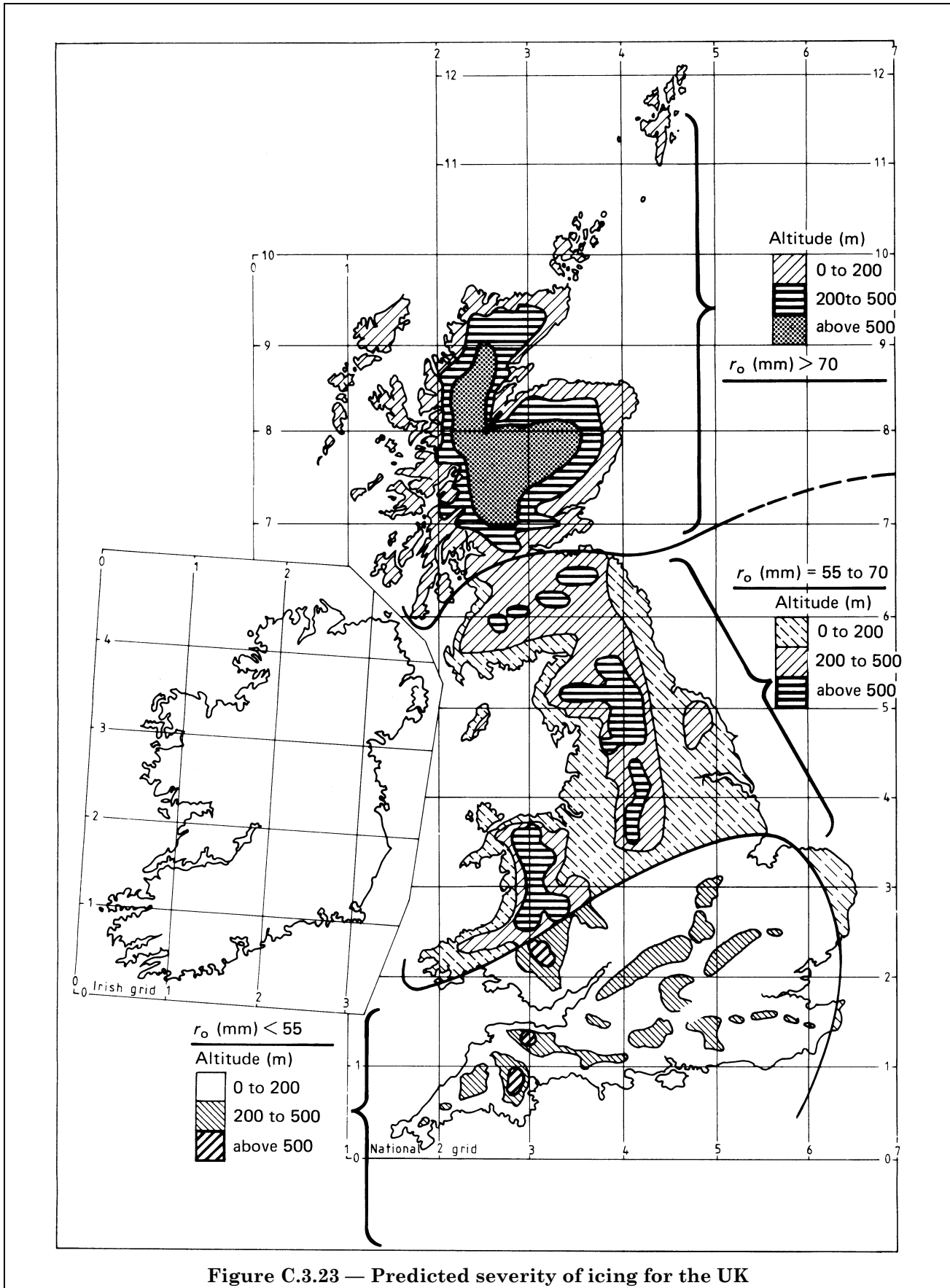
C.3.5.3.2 Partial safety factor. The dependence of ice intensity on member size and of the wind load on member size plus ice thickness implies that generalized reliability analysis cannot be extended to treat combinations of wind and ice or to treat ice loading in isolation. Moreover, the probability density functions are likely to be curtailed by the physical limits to the size of ice formation, although this is not apparent from the Czech observations discussed in C.3.5.4.

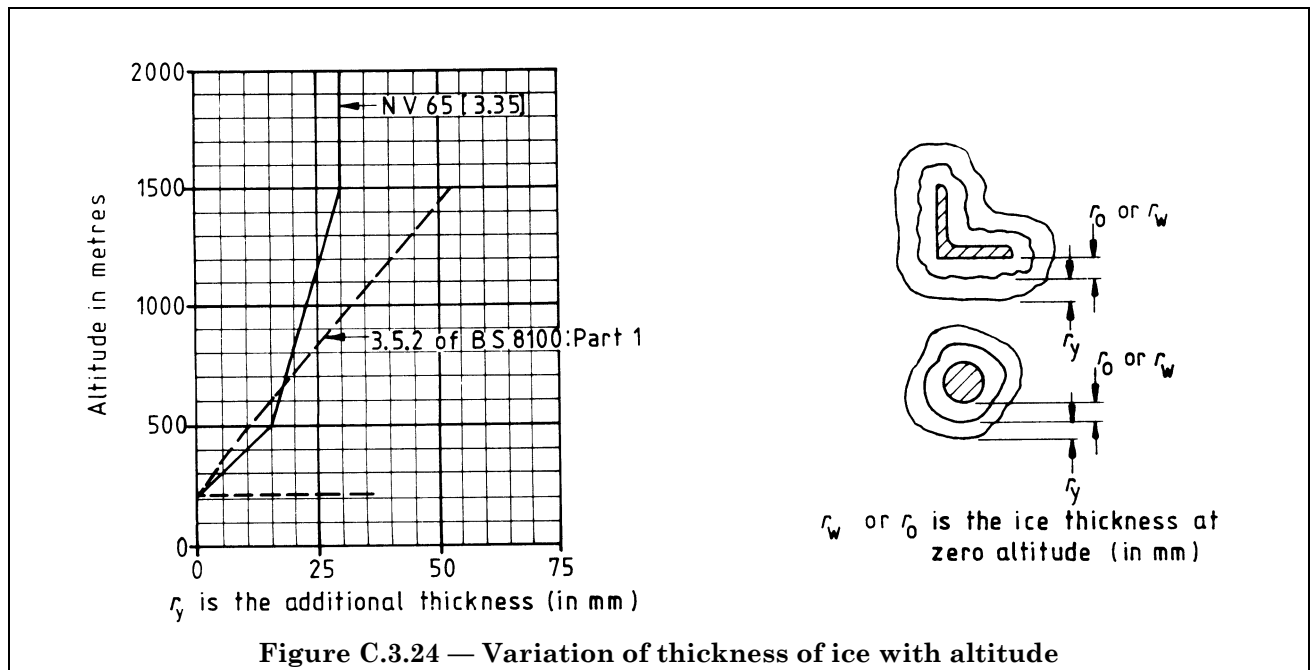
The ice thickness formed may be shown to vary exponentially with time for a circular-section member in constant icing conditions and this implies that the extreme thickness decreases with increasing member size. Consequently, the results obtained from the Czech observations (see C.3.5.4) may not be readily extrapolated to apply to other than 30 mm diameter bars. For circular-section members, the limit to the thickness of ice is approximately proportional to the square root of the wind speed. It has however been found that in Czechoslovakia ice formation becomes decreasingly severe at speeds in excess of 28 m/s due to decreasing humidity. This trend may not be assumed to apply necessarily to the UK.



Meteorological Office (MET 03) Sept. 1974.

Figure C.3.22 — Conditions conducive to icing severity





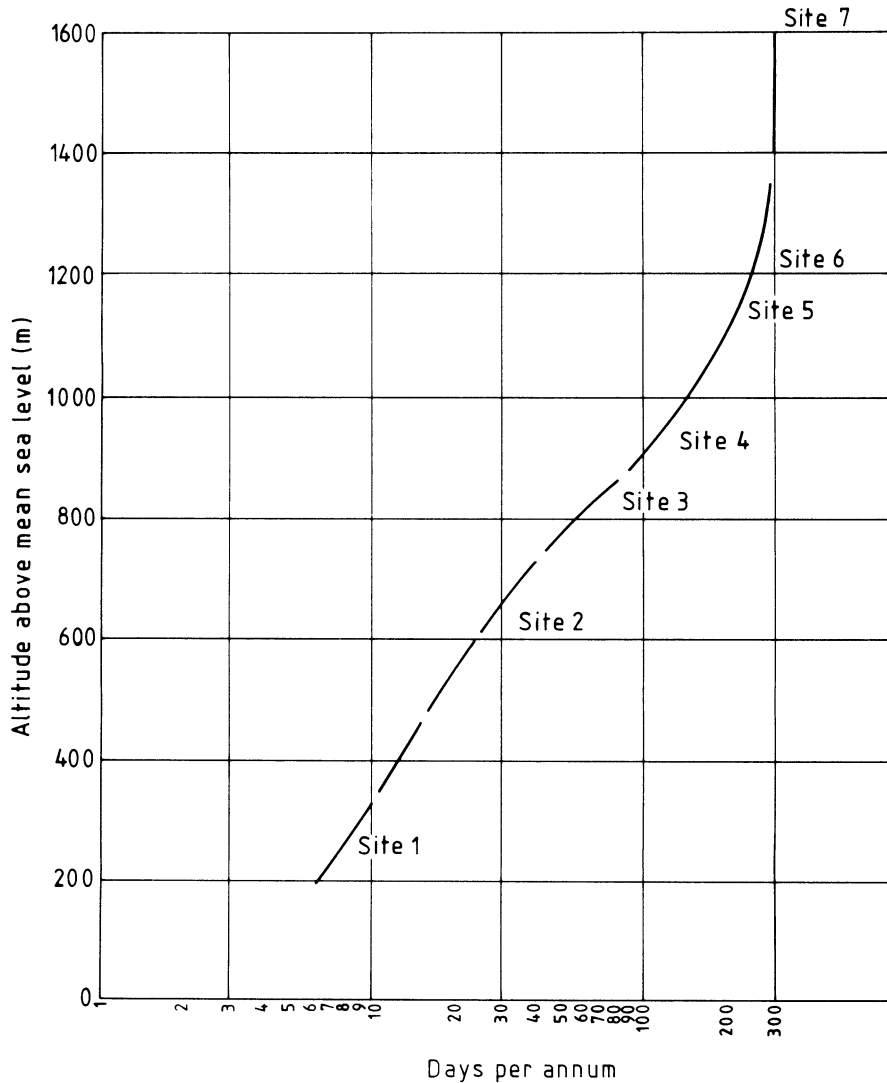


Figure C.3.25 — Frequency of icing in Germany [3.47]

For low wind conditions, the reference value given in Figure 3.9 of Part 1 represents 50 year return thickness, r_{02} , and those given for consideration in conjunction with 80 % of the 50 year return annual maximum wind speed represent average annual maximum thickness, r_{av} .

Using the Gumbel distribution (see equation (3.2)):

$$r_{02} = r_{av} + 2.6 \sigma_r \quad (3.13)$$

where

σ_r is the standard deviation of the annual maximum ice thickness.

The range of σ_r obtained from the Czech observations was 11.6 mm for the lowest altitude site to 34.4 mm for the highest. The constant value of σ_r implied in Figure 3.9 of Part 1 is 19.4 mm, since $r_{02} = r_0$ and $r_{av} = r_w$.

The coefficient of variation as derived from the values of r_0 and r_w in Figure 3.9 of Part 1 is not realistic due to the empirical derivation of the thicknesses. Clearly they are considerably higher than for wind speed and will vary with both latitude and altitude.

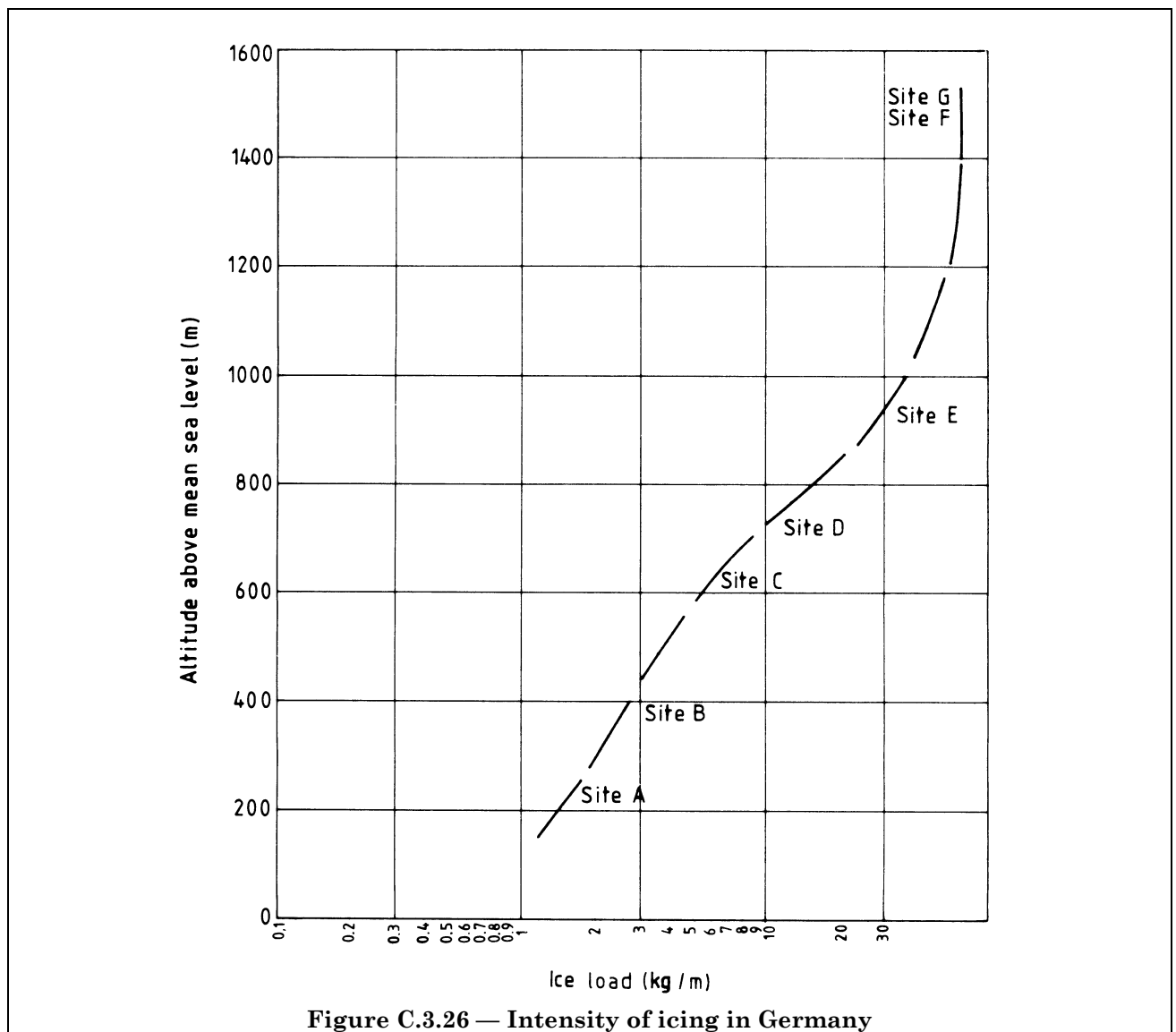


Figure C.3.26 — Intensity of icing in Germany

Reliability analysis for loads having a modified Gumbel distribution and coefficients of variation of up to 0.6 (appropriate to ice thickness at high altitudes) has shown the failure probability to be relatively insensitive to the dispersion when design is based on 50 year return values. In such cases, the maximum probability density occurs in the region of the design loadings. This being the case, the safety factors on ice thickness alone may be taken to be the same as those on wind speed for a given target failure probability.

Comparisons were made with the IEC recommendations for ice loading [3.46]. These recommendations give factors to be used on average annual maximum ice load for different notional failure probabilities and coefficients of variation of ice load on a conductor. It appeared that for a region such as central Scotland, Part 1 would provide factored design thicknesses similar to those intended by the IEC document. For sites further south, the IEC recommendations (which apply to wind-free conditions) may not be used since they only cover coefficients of variation of ice load of up to 0.7, which is exceeded for the majority of England and Wales.

C.3.5.3.3 Cables. Ice thicknesses for cables partly follow the principle stipulated by Staiger [3.47] that the radial thickness of ice is inversely proportional to the cross-sectional area of the cable.

It is noted that foreign specifications follow this principle, although for very small diameter cables they appear to suggest that only very light icing accumulates. Part 1 implies that ice thickness remains constant for cable diameters less than 7.5 mm.

Ice thickness for a 12 mm diameter cable in central England 250 m above sea level to be considered with wind corresponds approximately to the 12 mm thickness generally used in transmission line design and in the design of guyed masts, in the past.

Figure C.3.27 gives some comparisons with the Czech [3.40, 3.41] and Romanian [3.42] codes. Work undertaken by Ove Arup & Partners [3.48] suggests that the amount and type of ice caught on an object is a function of target size, droplet diameter, water content, wind speed and temperature. It may be shown that, because of a large deflection in the direction of air flowing around a large or bluff obstacle, drag effects are great and consequently droplet deflection is large, while for flow around a small or slender obstacle, the small deflection in the air flow results in little deviation in the paths of the droplets. Thus, the larger the cylinder, the lower the collection efficiency of the ice. Elliott [3.49] noted that measurements on spheres of various diameter show how strongly the diameter of an exposed object influences the amount of ice load. In the case of a sphere of 100 mm diameter, 5.4 cm³ of melted ice per hour were observed, whereas a sphere of 200 mm diameter supplied 11 cm³ of ice during the same time. For wires he states that the ice loads are approximately proportional to $D_c^{5/8}$. Thin cables, however, have a lower heat capacity, on which ice starts forming earlier, but the formations do not always adhere well, and may drop off more often than from very thick cables.

In treating ice loading on multiple cables, it has been considered appropriate to allow some diversity. The relationship is such that the reference thickness refers to a single cable and that this is reduced for groups so that for a large number, the reference values used without wind correspond to a mean annual maximum with a coefficient of variation of 0.6.

Experience with transmission towers in the north of England has included icing of at least 50 mm radial thickness on structural sections. For transmission lines of 28 mm diameter, Part 1 would require an extreme thickness allowance of 81 % of the values given in Figure 3.9 of Part 1, corresponding to about 50 mm radial in the north of England at an altitude of 250 m. Such thicknesses have been reported.

C.3.5.4 Ice weight. The weight of ice has been detailed as ranging from 9 kN/m³ relating to small thicknesses (which would invariably consist of glazed frost) to 5 kN/m³ relating to large deposits, which takes account of the open type of rime ice. Macklin [3.50] suggests a figure of 8.8 kN/m³ for glazed frost and Appendix F of CP 3: Chapter V-2:1972 [3.3] suggests 9.2 kN/m³. The German Meteorological Office [3.47] have measured values between 8 kN/m³ and 9 kN/m³ for glazed frost. For rime ice, Page [3.51] measured a weight of 6 kN/m³ on cables at Emley Moor, but recommends a value of 5 kN/m³ for these conditions. From Macklin's work, Page suggests a sharp reduction in density once a certain critical iced radius has been reached. This reduction depends on wind speed, air droplet size and temperature, and Figure C.3.28 shows a typical series of graphs showing density for various temperatures and wind speeds, all for an air droplet size of 20 µm. On the basis of this graph, the values of 9 kN/m³ and 5 kN/m³ appear reasonable limiting values to apply to thicknesses used in Part 1. Casper and Sandreczki [3.52] have plotted unit weights of ice deposits in Europe over a period of 4 years from which it is seen (see Figure C.3.29) that half of all specific gravities are below 2.8 kN/m³ with only 5 % exceeding 6.2 kN/m³. The US National Electrical Safety Code [3.44] and the Romanian code [3.43] detail the weight of ice formation as 9.1 kN/m³ and 9.0 kN/m³, respectively, [3.11].

The frequency distributions of ice weight independent of wind speed have been studied in Czechoslovakia [3.41] at three stations over a period of 28 years and were found to approximate to a Gumbel distribution. Figure C.3.30 shows the results converted to equivalent radial thickness of ice of assumed density 9 kN/m³ formed on 30 mm diameter rods 5 m above ground at the sites of different altitudes. The results exhibit differing ratios of dispersion/mode, decreasing with increasing mean values and altitude. Although these results may not be directly applicable to the UK, they appear to justify the use of increased coefficients of variation with reduced severity of icing, as discussed in **C.3.5.3.2**.

Coefficient k_i as function of the conductor or wire diameter compared with Romanian code [3.42]							
Conductor or wire diameter (mm)		5	10	20	30	50	70
k_i	[3.42]	1.1	1.0	0.9	0.8	0.7	0.6
	BS 8100-1	1.20	1.07	0.87	0.80	0.75	0.72

Czechoslovakia

- . — Ice load for overhead power lines Czech code [3.40]
- — — Ice load for czech code [3.41]

USA NESC [3.44]

- - - - - Heavy: $I_i = 0.0046 + 0.36 D_c$ (12.5 mm)
- Medium: $I_i = 0.0011 + 0.18 D_c$ (6 mm)

Romania [3.42]

- $I_i = 27.7 (D + rk_i) rk_i$
- $r = 60$ mm at 450 m AMSL
- $r = 35$ mm at 200 m AMSL
- $r = 12.5$ mm at 10 m AMSL

UK

- Ice load for cables in accordance with 3.5.2 of part 1
- I: 0 m to 200 m AMSL, SOUTH ($r_s = 50 + 0 = 50$ mm)
- II: 450 m AMSL, SOUTH ($r_s = 50 + 10 = 60$ mm)
- III: 0 m to 200 m AMSL, NORTH ($r_s = 70 + 0 = 70$ mm)
- IV: 450 m AMSL, NORTH ($r_s = 70 + 10 = 80$ mm)

Using $\rho_i = 9$ kN/m³
 $I_i = 28.3 k_i r_s (k_i r_s + D_c)$ kN/m where r_s and D are in m

In all expressions for I_i , the values D_c and r should be in metres to give I_i in kN/m.

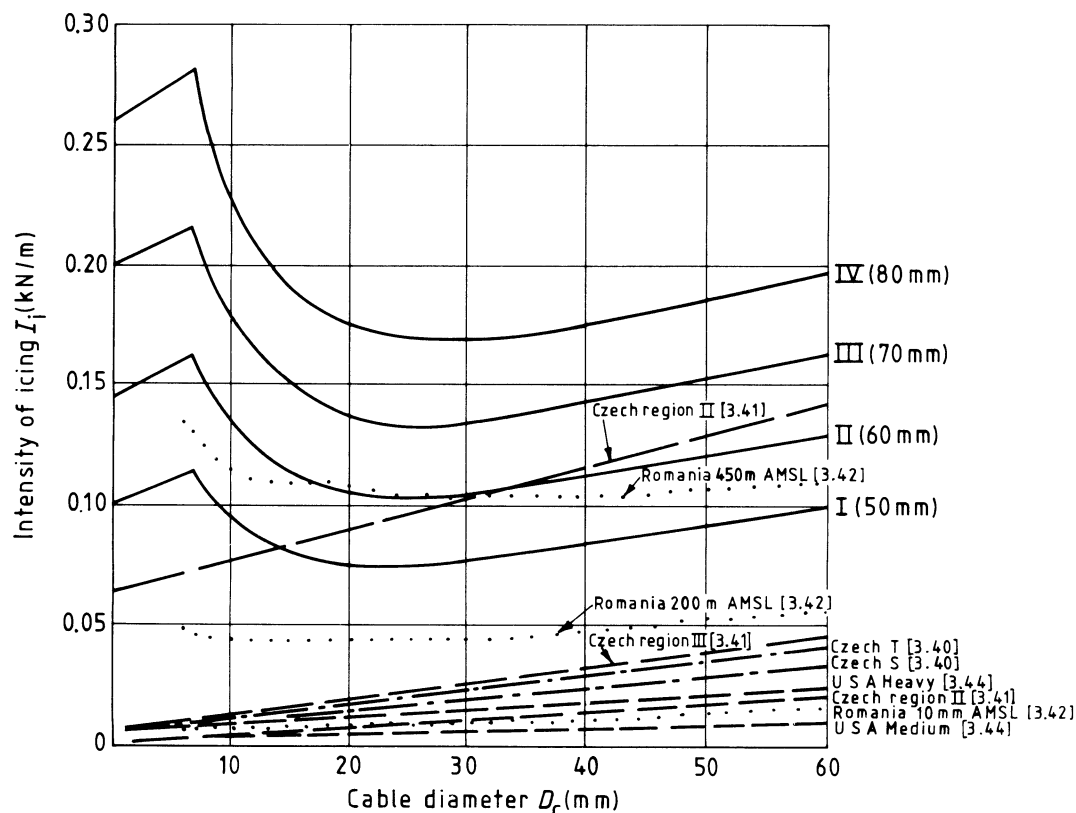


Figure C.3.27 — Variation of intensity of icing with cable diameter

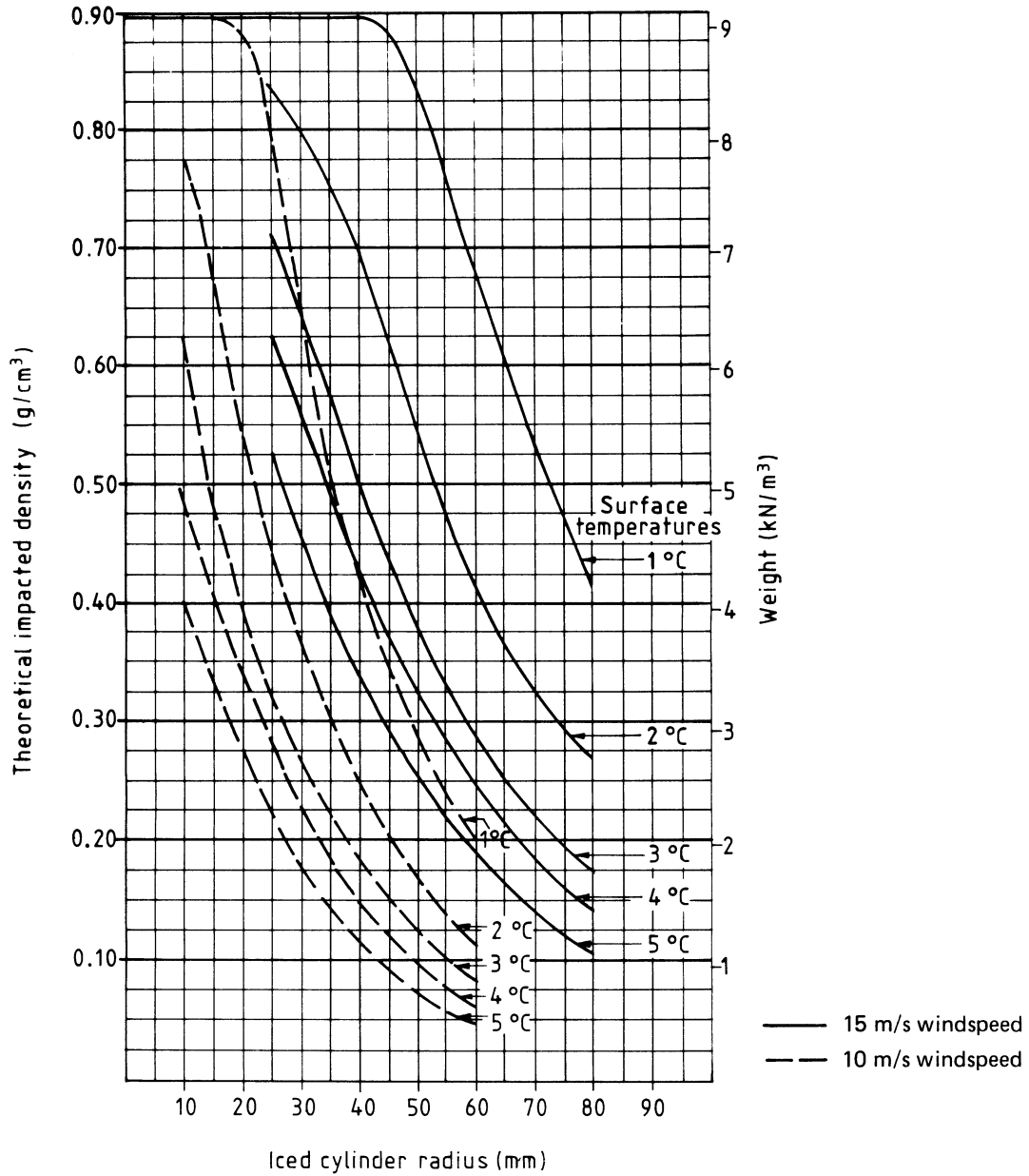


Figure C.3.28 — Typical theoretical densities of accreted ice based on the work of Macklin [3.50] and Page [3.51]

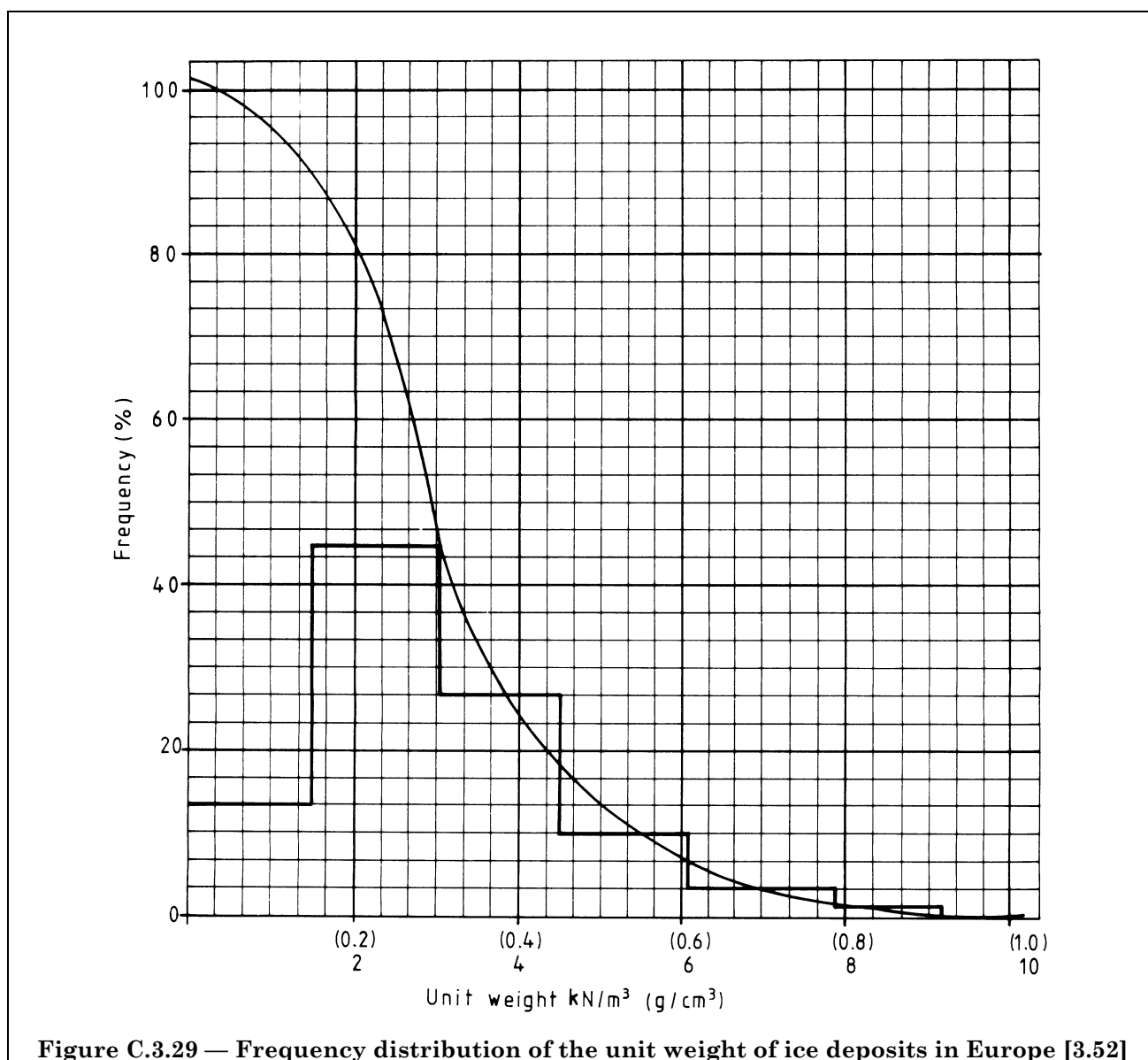
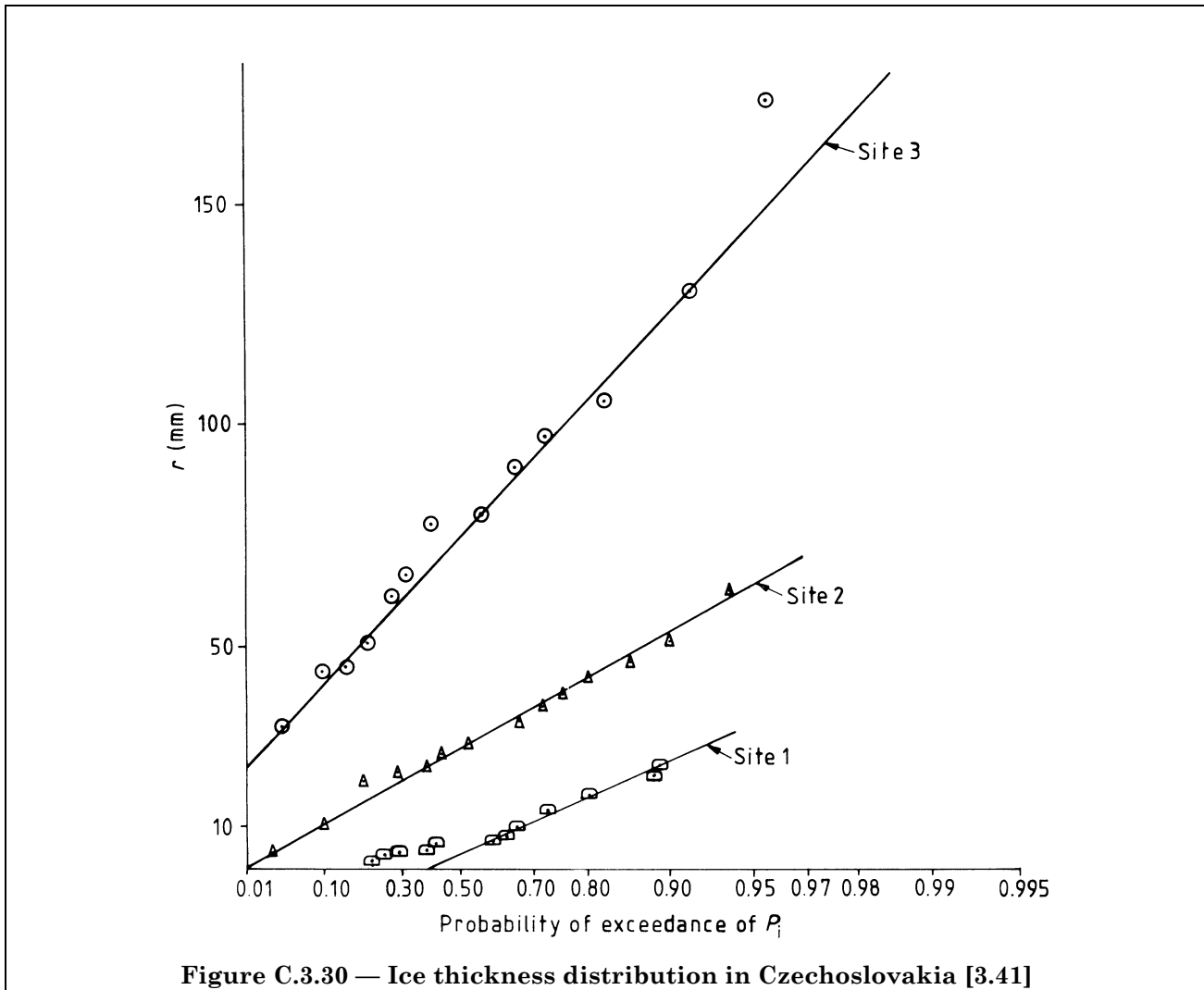


Figure C.3.29 — Frequency distribution of the unit weight of ice deposits in Europe [3.52]

C.3.5.5 Existing codes of practice. European codes of practice generally quantify snow loading. In the Dutch code [3.36] a basic snow load is given applicable throughout the country, whereas the Norwegian code [3.37] gives three regions of varying severity. The East German Code [3.38] recommends varying loads according to the site height, whilst the French code [3.35] accounts for variations in loading according to both regions and site height. In view of the different climatic conditions, quantitative comparison is of little significance. Ice loading is not covered in the French, Dutch or Norwegian codes. The East German code [3.38] considers various degrees of icing according to the region and site height, with minimum thicknesses of 20 mm, but for severe regions the degree of icing is to be decided in cooperation with the Meteorological Services.

The West German code [3.39] concedes that it is not possible to provide data concerning the occurrence of icing which would be generally valid; it is recommended that the degree of icing should be decided in the planning stage by the engineer in charge of the project in cooperation with the competent authority. The West German code does recommend, however, that where accurate data cannot be obtained an all round deposit of 20 mm ice should be assumed.



The Czechoslovakian code for transmission lines [3.40] details three regions of relative ice severity and Schaeffer and Feibicke [3.53] quote a further Czechoslovakian standard which specifies ice severity. These values are shown plotted in Figure C.3.27 together with the values in accordance with Part 1, as discussed in C.5.3.3. Draft IEC recommendations [3.46] indicate procedures which may be adopted in deriving design ice loading on transmission line conductors in the absence of wind. While leaving national committees to obtain and interpret ice loading observations, the recommendations indicate factors to be used to allow for the influence of conductor size and height above ground and give safety factors to be applied to ice weight for different target notional failure probability.

The draft Romanian loading code [3.42] recommends that the weight of ice is taken as 9 kN/m^3 and gives a coefficient k_i dependent on the conductor diameter, which is compared with the Part 1 value given in Figure C.3.27. The ice thickness is considered at 10 m above ground as 10 mm or 15 mm, depending upon the geographical location, and it increases with the height above ground to 60 mm at 400 m above ground.

The Romanian code [3.43] also gives data for the design of transmission lines. The unit weight of ice formations is taken as 9 kN/m^3 and the ice thickness is assumed to vary between 13 mm and 30 mm, depending upon the geographical location of the line.

In the USA data for ice formation on transmission lines is given in the National Electric Safety Code [3.44] which divides the USA into three loading zones. In the heavy zone, the conductors are designed for 12 mm of radial ice, in the medium zone for 6 mm, while in the light zone, no ice load is considered.

The Canadian Building Code [3.45] provides no quantified basis for ice thickness assessment but recommends that an allowance be based on meteorological evidence.

Table C.3.5 — Intensity of turbulence, I_w

Basis of calculation	Height	Intensity of turbulence, I_w				
		Terrain category				
		I	II	III	IV	V
Terrain reference data $\left\{ \begin{array}{l} z_0 \text{ (m)} \\ h_e \text{ (m)} \\ \alpha \\ K_R \end{array} \right.$	(m)	0.003	0.01	0.03	0.10	0.30
		0	0	0	2	10
		0.125	0.14	0.165	0.19	0.23
		1.20	1.10	1.00	0.86	0.72
Part 1 $I_w = \frac{\left(\frac{1.6}{K_R} - 1\right)}{3.3 \left(\frac{z - h_e}{10}\right)^\alpha}$	10	0.10	0.14	0.18	0.26	0.37
	100	0.08	0.10	0.12	0.17	0.22
	300	0.07	0.09	0.10	0.14	0.17
ESDU item 72026 [3.14]	10	0.15	0.17	0.20	0.23	0.28
	100	0.10	0.11	0.12	0.13	0.14
	300	0.06	0.07	0.08	0.08	0.09
ESDU item 83045 [3.8] (for $\bar{V}_B = 20\text{m/s}$)	10	0.14	0.16	0.18	0.22	0.28
	100	0.10	0.11	0.12	0.15	0.18
	300	0.06	0.07	0.08	0.10	0.13
Cook [3.1] (excluding topographic effects)	10	0.13	0.15	0.18	0.22	0.27
	100	0.10	0.11	0.13	0.15	0.18
	300	0.06	0.08	0.09	0.11	0.14
NOTE $I_w = \frac{\sigma(V)}{\bar{V}_z}$ where $\sigma(V)$ is the r.m.s. value of the fluctuating speed of turbulent wind; \bar{V}_z is the mean hourly wind speed at height z .						

C.3.6 Turbulence

The r.m.s. value of fluctuating speed of turbulent wind (in the direction of the wind), $\sigma(V)$, is an integral part of the formulation of the gust response factors, given in section five of Part 1. Hence assumed values of $\sigma(V)$ are inherent in the development and codification of the size factor, B , and the basic gust factor, G_B , (see C.5.6.4, C.5.7.2.1 and C.5.7.3.4) as well as the cable height (gust) factor, K_z , (see C.5.9.2). Generally, $\sigma(V)$ has been referred to in terms of the intensity of turbulence, I_w given by:

$$I_w = \frac{\sigma(V)}{\bar{V}_z} \quad (3.14)$$

where

\bar{V}_z is the relevant mean hourly wind speed at height z .

The intensity of turbulence, I , has always been known to vary considerably both with height and terrain, typically varying from about 0.06 at 300 m height in smooth terrain to about 0.30 at 10 m height in rough terrain. However, a major part of this variation results from relating $\sigma(V)$ to \bar{V}_z , which in itself varies with terrain and height, due to variation of the terrain roughness factor, K_R , (see C.3.1.4), and the power law variation with height, α , (see C.3.2.1). In the development of the gust factors required for design, which are correctly dependent on the value of turbulence, $\sigma(V)$, the procedure was simplified by removal of some of the variation. It had already been proposed by Davenport [3.54], that the variation of $\sigma(V)$ with height could be minimized by relating it to \bar{V}_{10} , the mean hourly wind speed at 10 m above the zero plane.

Table C.3.6 — Simplified expressions for $\sigma(V)/\bar{V}_B$, independent of height

Basis of calculation	Value of $\sigma(V)/\bar{V}_B$					
	Terrain category					
	I	II	III	IV	V	
Terrain reference data	z_0 (m)	0.003	0.01	0.03	0.10	0.30
	α	0.125	0.14	0.165	0.19	0.23
	K_R	1.20	1.10	1.00	0.86	0.72
a) Part 1 $\frac{K_R}{3.3} \left(\frac{1.6}{K_R} - 1 \right)$		0.12	0.15	0.18	0.22	0.27
b) ESDU item 72026 [3.14] and ESDU item 83045 [3.8] ^a		0.16	0.17	0.185	0.20	0.22
c) Cook [3.1] ^b		0.162	0.176	0.190	0.206	0.222
d) Simplified from b) and c) $0.34 - K_R/2\pi$		0.15	0.165	0.18	0.20	0.225
e) Simplified log law [3.1] $1.05 K_R / \{\ln(10/z_0)\}$		0.155	0.17	0.18	0.20	0.22
f) Alternative log law [3.21] $\{15 + \ln(z_0)\}/60$		0.15	0.17	0.19	0.21	0.23
g) Harris' 71 [3.4] 0.19		0.19	0.19	0.19	0.19	0.19

^a Values vary with height; tabulated values are best match in range $10 \text{ m} < z < 300 \text{ m}$.

^b Full expression varies with height, thus:

$$\frac{\sigma(V)}{\bar{V}_B} = \left(\frac{K_R}{\ln(10/z_0)} \right) \frac{3 \left(1 - \frac{z}{z_g} \right) \left\{ 0.538 + 0.09 \ln \left(\frac{z}{z_0} \right) \right\} \left(1 - \frac{z}{z_g} \right)^{16}}{\{ 1 + 0.156 \ln(6 z_g/z_0) \}}$$

tabulated values are for $z = 60 \text{ m}$, and $z_g = 38289/\ln(10^5/z_0)$

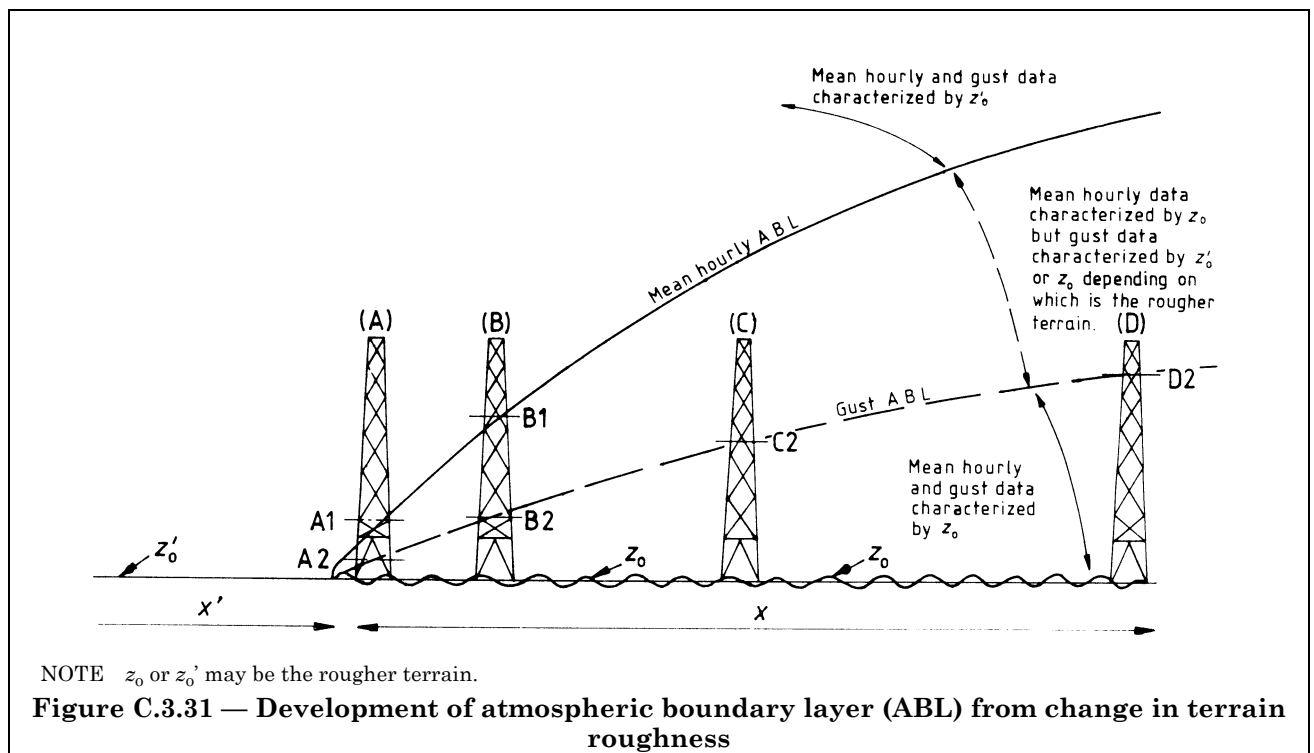
This had been further studied by Harris [3.4], and forms the basis of the value of $\sigma(V)$ adopted for the derivation of gust factors which is taken as independent of height above ground and equal to:

$$\sigma(V) = \frac{\bar{V}_{10}}{3.3} \left(\frac{1.6}{K_R} - 1 \right) \quad (3.15)$$

Reference to the records taken on the Durriss mast presented in Figure C.3.14 show that the differences between maximum gust speed and mean speeds remain reasonably constant up to 300 m substantiating the above assumption. Equation (3.15) implies that $\sigma(V)$ increases with increasing roughness as assumed by Sfantesco and Wyatt [3.6] and ESDU items 74031 [3.22] and 72026 [3.14]. This also agrees in principle with the recent work of Cook [3.1], Deaves and Harris [3.21, 3.55] and the data given in ESDU item 83045 [3.8], with regard to variation with terrain. However, it should be noted that this differs from an earlier conclusion by Harris [3.4] that $\sigma(V)$ is terrain independent, i.e. when expressed in the terms $\sigma(V) = 0.19 V_B$ where V_B is the basic wind speed (see C.3.1.2).

The simple expression for $\sigma(V)$ given in equation (3.15) is dependent solely on the terrain roughness factor, K_R . Further noting that $\bar{V}_{10} = K_R \bar{V}_B$, $\sigma(V)$ can be expressed thus:

$$\frac{\sigma(V)_w}{\bar{V}_B} = \frac{K_R}{3.3} \left(\frac{1.6}{K_R} - 1 \right) \quad \left[\equiv 0.485 - \frac{K_R}{3.3} \right] \quad (3.16)$$



This ranges from 0.12 to 0.27 for the extremes of smooth to rough terrain considered in Part 1, and only agrees with the earlier Harris figure [3.4] when $K_R = 0.97$, i.e. close to basic terrain. Very recent data produced by Cook [3.1], and by ESDU item 83045 [3.8], are still given in terms of the intensity of turbulence, I_w , and show fully the variation both with terrain and height when expressed in this form. The value of $\sigma(V)$ adopted in Part 1 can be expressed in the same form thus:

$$I_w = \frac{\left(\frac{1.6}{K_R} - 1\right)}{3.3 \left(\frac{z - h_e}{10}\right)^\alpha} \quad (3.17)$$

This varies from 0.07 at 300 m height in terrain category I (smooth) to 0.37 at 10 m height in terrain category V (rough), and thus shows that the adopted values in the code reasonably agree with the aforementioned variations in I_w .

Table C.3.5 compares the adopted Part 1 values in terms of intensity of turbulence, I_w , with those of the earlier ESDU item 72026 [3.14], and the currently accepted values, as given by Cook [3.1] and ESDU item 83045 [3.8], over the full range of heights and terrains encompassed by Part 1.

References [3.1] and [3.2] should be referred to for more comprehensive data on turbulence, as they additionally incorporate variation of I_w with respect to topographic effects (hills) and variation of wind speed, which have been excluded from the comparisons in this clause.

However for design purposes, some of these refinements are unnecessary, and the simple expression relating $\sigma(V)$ to K_R (or z_0) and \bar{V}_B alone is sufficient. Recent studies based on the data of Cook [3.1] and ESDU [3.2, 3.8], give values of $\sigma(V)$ that match for basic terrain III, i.e. when $K_R = 1.0$, but show up to 20 % less variation of turbulence at the extreme terrains I and V, and 10 % less variation for terrains II and IV. This may be taken advantage of in a more refined analysis.

Table C.3.6 compares the simplified expression, with the earlier values of Harris [3.4], and those derived from Cook and ESDU plus some which are dependent on z_0 and/or z_g , the terrain roughness parameter and gradient height, respectively.

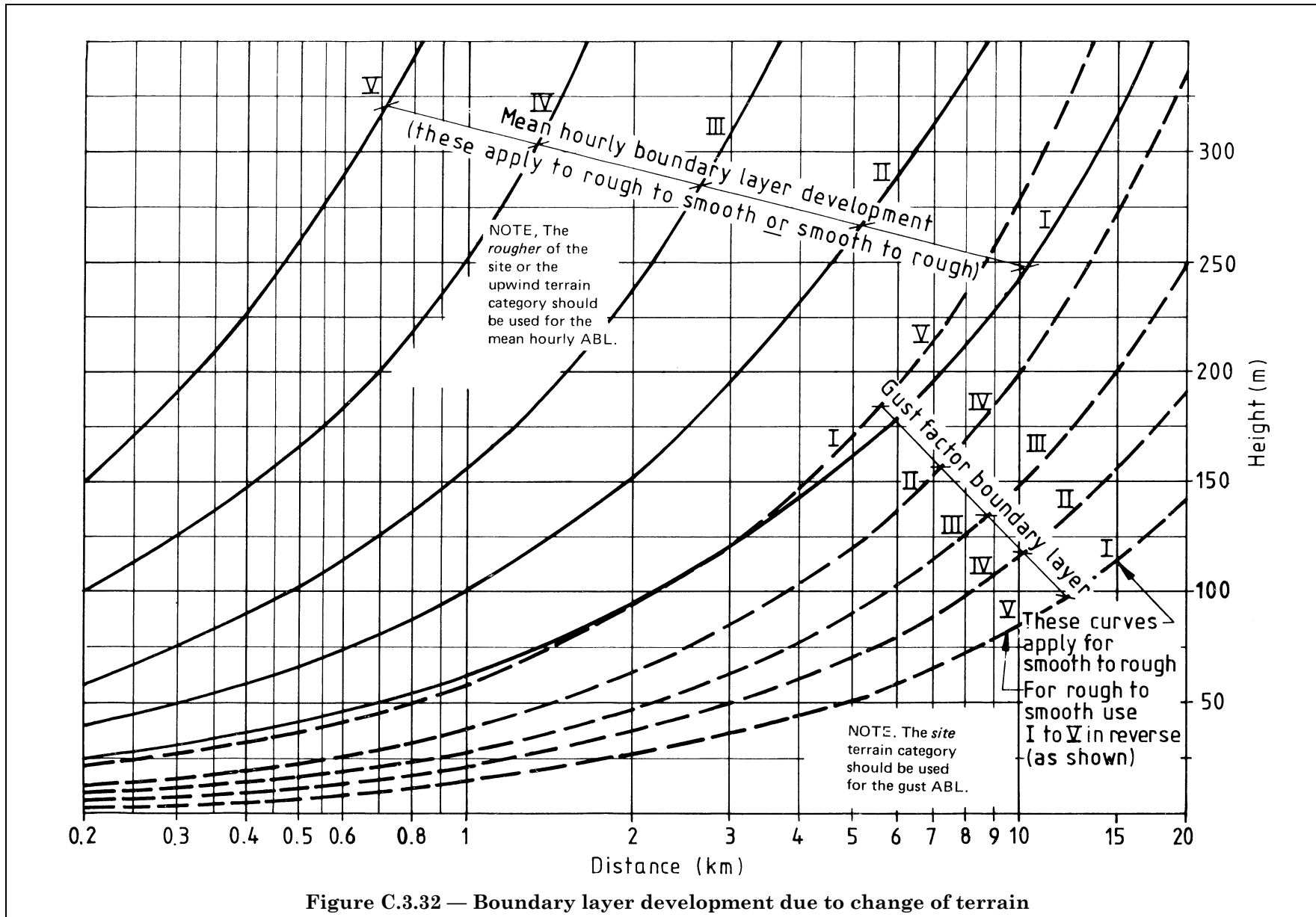


Figure C.3.32 — Boundary layer development due to change of terrain

Where r.m.s. values of fluctuating velocity are required in a spectral analysis (see Appendix E of Part 1) equation (3.16) should be adopted for compatibility with the recommendations of Part 1.

C.3.7 Terrain roughness changes

Part 1 excludes any considerations of changes in the terrain away from the tower, and states that the terrain roughness adopted should be that most appropriate to the whole of the terrain several kilometres upwind from the site, and any local rough terrain close to the tower (within a few kilometres) should be ignored, see Table 3.1 of Part 1. Also, where the environs of the site may change or are difficult to define, a smoother terrain category should be adopted, see Table 3.1 of Part 1 and Appendix B of Part 1. Where tower load effects result primarily from the mean hourly component, this provides a sound basis for design, since mean hourly effects increase more rapidly in smoother terrain, whereas gust factors decrease. In rougher terrain, however, caution should be exercised as the loading may be primarily due to turbulence effects, where the gust factor, G , is significantly greater than 1.0.

Where there is a significant change in terrain upwind from the site, the boundary layer development may result in very different characteristics of the wind profile at the site. Such considerations have only recently been developed, by Cook [3.1], Deaves and Harris [3.55] and ESDU [3.2, 3.8], and were not in a readily available form for inclusion in Part 1. These show that when considering structures up to 300 m high, i.e. as encompassed by Part 1, the development of the equilibrium boundary layer is such that the terrain many kilometres upwind is important. They also show that the boundary layer interface for mean hourly wind develops at a steeper level than that for the fluctuating (gust) components. This is shown schematically in Figure C.3.31.

Thus the effect of different terrains may need to be considered. The development of the mean hourly interface boundary layer is always that related to the rougher terrain, whether this is the outer region, z_0' , or the inner region, z_0 , due to the dominance of the larger scale and intensity of turbulence over the rougher terrain. Figure C.3.32 gives approximate curves which may be used to check whether the tower lies primarily within one boundary layer, in which the wind characteristics are defined by a single terrain category, e.g. by z_0' at site (a) in Figure C.3.31 or by z_0 at site d) in Figure C.3.31. For these cases, there are no further considerations and Part 1 can be used directly. In addition, where an extent x' of terrain z_0' lies wholly within an area of terrain z_0 , the effect of the intermediary terrain z_0' has no effect at the site provided $x > x'$ and $z_0' \simeq z_0$, see Figure C.3.33. This covers the common cases of towns/cities/woods or lakes/estuaries occurring entirely within typical terrain category III, but can equally be applied to other similar cases.

However, there may be cases where the different characteristics resulting from z_0 or z_0' , may encompass different extents of the tower, such as in cases (B) and (C) of Figure C.3.31. For (B) it may be appropriate to use mean hourly wind data based on z_0' above level B1, but based on z_0 below B1, and gust data based on z_0' above B2, but on z_0 below B2. Alternatively, however, a conservative design is produced by using mean hourly profile due to the smoother terrain over the whole of the tower, together with gust factors related to the rougher terrain. This is a rather simplistic approach, but may be adopted where towers are sited such as in (B) and (C) in Figure C.3.31, in lieu of more thorough considerations, or adoption of the first approach outlined.

Where more detailed procedures are required in cases where terrain changes are likely to be very significant, the data given by Cook [3.1], Harris and Deaves [3.21], and ESDU item 84011 [3.56] are recommended.

C.3.8 References in C.3

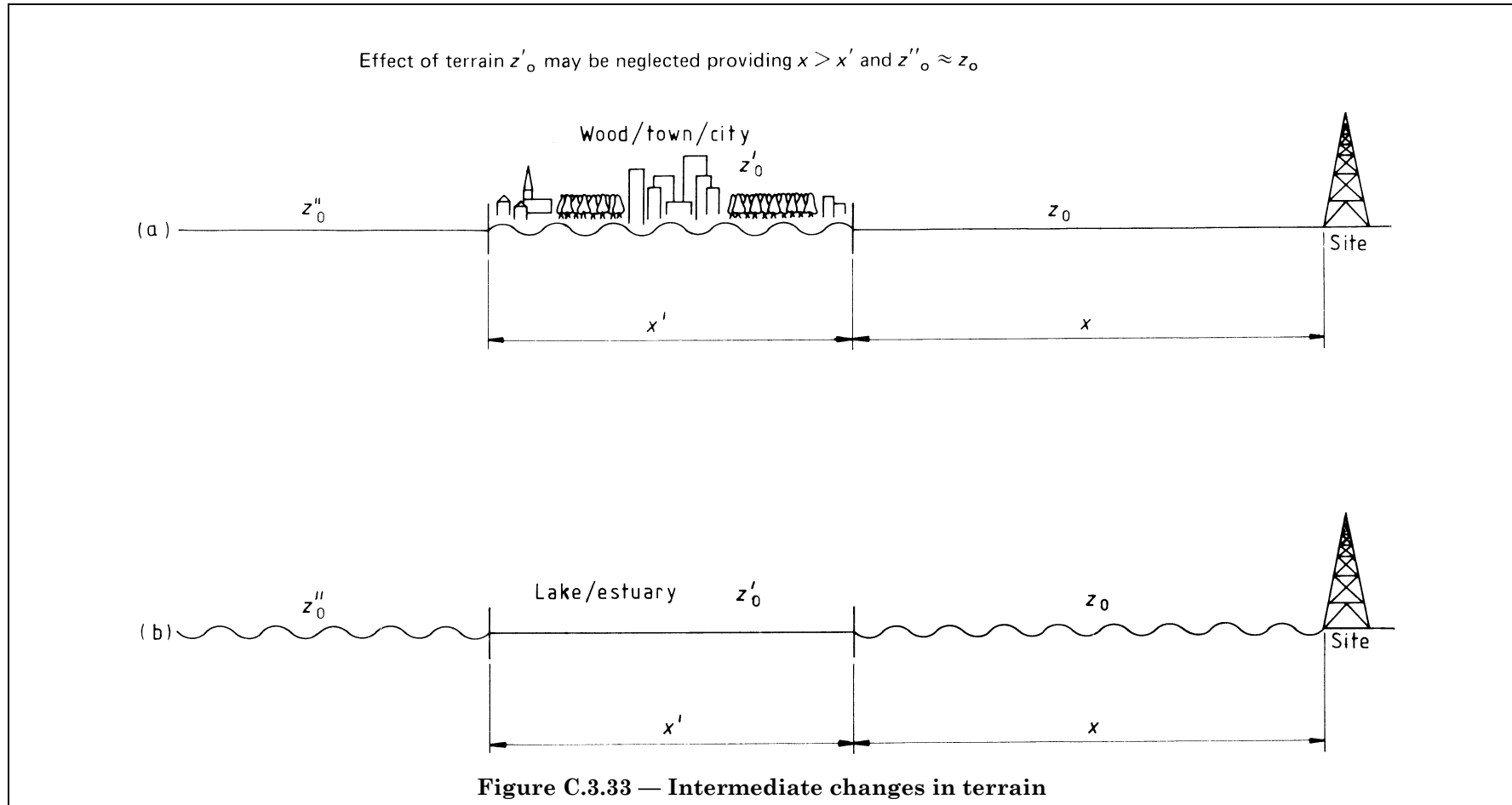
3.1 COOK, N.J. *The designer's guide to wind loading of building structures*, BRE Part 1 Butterworth 1985.

3.2 ENGINEERING SCIENCES DATA UNIT. *Strong winds in the atmospheric boundary layer: Part 1 Mean-hourly*

3.3 BRITISH STANDARDS INSTITUTION. *Code of basic data for the design of buildings: Chapter V Loading : Part 2 Wind loads*, 4th ed., 1972, CP 3: Chapter V-2.

3.4 HARRIS, R.I. *The Nature of the Wind. The modern design of wind-sensitive structures*, CIRIA, 1971.

3.5 INTERNATIONAL ELECTROTECHNICAL COMMISSION, STUDY COMMITTEE NO. 11 RECOMMENDATIONS FOR OVERHEAD LINES. *Recommendations for the calculation of wind loading* 1972.



- 3.6 SFINTESCO, D. and WYATT, T.A. A proposed European Code of Practice: Current work of the ECCS towards specification of the effect of wind on structures. *Conf. on Wind Effects on Buildings and Structures, London, 1975.*
- 3.7 HARDMAN, C.E., HELLIWELL, N.C. and HOPKINS, J.S. *Extreme winds over the United Kingdom for periods ending 1971*, Climatological Memorandum No. 50A, Meteorological Office, July 1973.
- 3.8 ENGINEERING SCIENCES DATA UNIT. *Strong winds in the atmospheric boundary layer: Part 2 Discrete gust speeds*, Data Item 83045, 1983.
- 3.9 GUMBEL, E.J. *Statistics of Extremes*, Columbia University Press, New York, 1967.
- 3.10 DAVENPORT, A.G. Wind Engineering. *Engineering Structures*, **9**, 1983.
- 3.11 GHIOCEL, D. and LUNGU, D. *Wind, snow and temperature effects on structures, based on probability*, Abacus Press, 1975.
- 3.12 ANTHONY, K.C. Developments since CIRIA 70. *Wind Engineering in the Eighties*, CIRIA, 1981.
- 3.13 MAYNE, J.R. and COOK, N.J. Extreme Wind Analysis. *Wind Engineering in the Eighties, CIRIA, 1981.*
- 3.14 ENGINEERING SCIENCES DATA UNIT. *Characteristics of wind speed in the lower layers of the atmosphere near the ground*, Data Item 72026, 1972, now superseded by Data Items 82026 [3.2] and 83045 [3.8] and 84011 [3.56].
- 3.15 JENSEN, M. and FRANCK, N. *The climate of strong winds in Denmark*, Danish Technical press, 1970.
- 3.16 COOK, N.J. Towards better estimation of extreme winds. *Journal of Wind Engineering and Industrial Aerodynamics*, Sept. 1982.
- 3.17 COOK, N.J. Note on directional and seasonal analysis of extreme winds. *Journal of Wind Engineering and Industrial Aerodynamics*, Dec. 1983.
- 3.18 BULLER, P.S.J. *Gale damage to buildings and structures in the United Kingdom, 2nd January 1976*, BRE CP 42/77, Aug. 1977.
- 3.19 BULLER, P.S.J. *Wind damage to buildings in the United Kingdom 1970–1976*, BRE CP 42/78, April 1978.
- 3.20 MENZIES, J.B. *Wind damage to buildings in the United Kingdom 1962–1969*, BRE CP 35/71, Nov. 1971.
- 3.21 HARRIS, R.I. and DEAVES, D.M. The structure of strong winds. *Wind Engineering in the Eighties, CIRIA, 1981.*
- 3.22 ENGINEERING SCIENCES DATA UNIT. *Characteristics of Atmospheric Turbulence near the ground*, Data Item 74031, 1974.
- 3.23 CATON, P.G.F. Standardised Maps of Hourly Mean Wind Speed over the United Kingdom and some implications regarding wind speed profiles. *4th International Conf. on Wind Effects on Buildings and Structures, London, 1975.*
- 3.24 SHELLARD, H.C. *Extreme wind speeds over the United Kingdom for periods ending 1963*, Climatological Memorandum No. 50, Meteorological Office.
- 3.25 VELLOZZI, J. and COHEN, E. Gust Response Factors. *Journal of the Structural Division, ASCE*, June 1968.
- 3.26 SFINTESCO, D., ZELLER, E. and MACKEY, S. Effets du Vent sur les Batiment Eleves. *Annales de L'Institut Technique du Batiment et des Travaux Publics*, Sept. 1971.
- 3.27 DAVENPORT, A.G. The relationship of wind structure to wind loading. *Conf. on Wind Effects on Buildings and Structures, I*, June 1963, HMSO.
- 3.28 DAVENPORT, A.G. Rational for determining design wind velocities. *Journal of the Structural Division ASCE*, May 1960.
- 3.29 ALEXANDER, A.J. and COLES, C.F. *A theoretical study of wind flows over hills*, CIRIA Techn. Note 29, Sept. 1971.
- 3.30 DEAVES, D.M. *A theoretical study of three-dimensional effects of wind flow over hills*, M.Sc. thesis, Loughborough Univ. of Technology, Sept. 1973.

- 3.31 ONISHI. A study of approximate solutions for the airflow over a ridge in a viscous atmosphere. *Sci. Rep. Tohoku University (Series 5 Geophysics)*, **15.1**, 1963.
- 3.32 COUNIHAN, J. Paper published in *Atmospheric Environment*, Central Electricity Generating Board, Research Laboratories.
- 3.33 JACKSON, P.S. and HUNT, J.C.R. Turbulent wind flow over a low hill, *Quarterly Journal Royal Meteorological Society*, **101**, 1975.
- 3.34 BRITISH STANDARDS INSTITUTION, *Steel, concrete and composite bridges: Part 10 Code of practice for fatigue*, 1st ed., 1980, BS 5400-10.
- 3.35 *Regles definissant les effets de la neige et du vent sur les constructions*, Regles NV65, Nov. 1965.
- 3.36 *Technische Grondslagen Voor Bouwvoorschriften*, TGB 1955, N 1055, June 1955.
- 3.37 *Forslag Til Norsk Standard Fra Norges Byggstandardiseringsrad, Frist for Uttalelse*, Oct. 1969.
- 3.38 *DDR Standard, Stahlerne Antennentragwerke*, TGL 13480, Gruppe 135864, March 1972.
- 3.39 *German Standard. Steel Aerial Supporting Structures*, DIN 4131, March 1969.
- 3.40 *Czechoslovakian Standard, Overhead Electric Lines — intersecting and parallel electric cables*, CSN341100, May 1972.
- 3.41 FECKO, S., KRUZIK, J. et al. Investigation of combined stress by icing and wind in Czechoslovakia. *CIGRE International Conf. on Large High Voltage Electric Systems*, Aug. 1976.
- 3.42 *Romanian Loading Code*. INCERC BRI, Bucharest, Dec. 1973.
- 3.43 *Romanian Code for the design of transmission lines*, 1-Li-1967.
- 3.44 *National Electrical Safety Code*, US Dept of Commerce, 1961.
- 3.45 *National Building Code of Canada 1970*, National Research Centre of Canada Associate Committee on the National Building Code, Ottawa NRC No. 11246.
- 3.46 INTERNATIONAL ELECTROTECHNICAL COMMISSION, STUDY COMMITTEE NO. 11, RECOMMENDATIONS FOR OVERHEAD LINES. *Ice loading on overhead lines*, May 1977.
- 3.47 STAIGER, F. Theoretical load on aerial supports under icing conditions. *Der Stahlbau*, No. 1, 1961.
- 3.48 SMALL, T.V.I.T.A. *Television Tower Emley Moor. Report on the formation and thawing of ice on the new structure*, Ove Arup & Partners, Feb. 1970.
- 3.49 ELLIOTT, P.R. *Investigation into the drag of guyed lattice masts due to ice encrustation*, BHCE4 1971, Kingston Polytechnic of Civil Engineering.
- 3.50 MACKLIN. *Quarterly Journal Royal Meteorological Society*, January 1962, **88**, No. 375, 31–50.
- 3.51 PAGE, J.K. Heavy Glaze in Yorkshire — March 1969. *Weather*, **24**, 486 (1969).
- 3.52 CASPER, W. and SANDRECZKI, A. *Ice deposits from a Meteorological Office Viewpoint*, German Meteorological Office.
- 3.53 SCHAEFFER and FEIBICKE. Design Loads of Ice and Fog deposits on Antenna supporting Structures. *Proceedings of the 3rd meeting of Shell and Spatial Foundations of Tower and High Buildings, Sopron, Hungary, 1970*.
- 3.54 DAVENPORT, A.G. The spectrum of horizontal gustiness near the ground in high winds, *OJRMS*, **87**, April 1961.
- 3.55 DEAVES, D.M. and HARRIS, M.A. *A mathematical model of the structure of strong winds*, CIRIA Report 76, May 1978.
- 3.56 ENGINEERING SCIENCES DATA UNIT. *Wind speed profiles with roughness changes over flat or hilly terrain*, Data Item 84011, 1984.

C.4 Wind resistance

C.4.1 *General*

The term wind resistance has been adopted to encompass the combinations of area, shielding effects and drag coefficients. Resistance has been related to projected areas within individual panels to allow for inclusion of horizontal members and for variations of structure and ancillaries between panels and to clarify the definition of solidity.

A panel was chosen as a convenient division of the tower into sections for both calculating wind speeds and resistance, and thereby applying wind loads. Panels are defined in Part 1 as between intersections of legs and primary bracings and allowance is provided for aggregating panels when there are many such intersections within the height of the tower.

It is permitted to use wind tunnel test results in place of the codified drag coefficients provided the tests were properly modelled and conducted in appropriate conditions. Guidance on such conditions may be found in **C.6.1**.

The range of tower types covered by Part 1 varies from simple square or triangular towers unencumbered by ladders, aerials or feeders, such as radar transmitters or transmission towers to complex structures carrying a multitude of aerials, feeders, dishes, etc. In the assessment of wind resistance, therefore, differentiation was made between simple structures for which overall drag coefficients would be appropriate and more complex towers for which the resistance would have to be calculated taking into account the interaction between the structural elements and the ancillary items such as feeders and aerials.

Three levels of complexity were defined:

- a) symmetrical square or triangular towers with no ancillary items, as covered in **4.2** of Part 1;
- b) symmetrical towers with ancillaries which comply with certain geometric constraints, as covered in **4.3** of Part 1;
- c) complex structures, as covered in **4.4** of Part 1.

In view of the lack of consistent data on the parameters governing wind resistance for lattice structures, the Department of the Environment commissioned a series of wind tunnel tests at the National Maritime Institute (NMI) [4.1]. These tests were planned to encompass square, triangular and rectangular section towers fabricated from both angle and circular members. The tests also investigated the effect of mixed members in a tower and the addition of ancillaries such as dish aerials and large-diameter cylinders representing flare stacks.

The results of these tests were made available early in 1977 and have been taken into consideration in developing the drag coefficients given in Part 1. They have confirmed the basic procedures recommended for evaluating resistance and have enabled some simplifications and greater accuracy to be made, particularly in the treatment of ancillary items.

These tests were augmented by wind tunnel tests on various configurations of a model of an actual tower, which incorporated an internal ladder tower, feeders and dishes. Various combinations of these were tested to compare the resulting loading with that derived by application of the relevant clauses of Part 1, over as wide a range of variables as possible. These tests were also commissioned by the Department of the Environment and undertaken at the NMI [4.2]. They are summarized in **C.4.9**.

C.4.2 *Symmetrical towers without ancillaries*

For symmetrical square or triangular towers without ancillaries, the resistance may be calculated using overall drag coefficients. For ease of common application these have been plotted for square and triangular towers, for the cases of towers comprising:

- a) flat-sided members;
- b) circular-section members in subcritical flow;
- c) circular-section members in supercritical flow.

The overall coefficients for a) and b) were based on the recent NMI tests discussed in C.4.1. The overall coefficients for c) have been based on earlier data, no test facilities being presently available to test such configurations in the supercritical Reynolds number regime. If the effective Reynolds number is related to the gust velocity equivalent to a typical mean hourly speed of about 45 m/s, then the minimum member diameter would need to be at least 90 mm for supercritical conditions to be assumed throughout. This would be uncommon, and it would therefore be unlikely for the overall coefficient for supercritical flow to be used for other than a proportion of the members in a tower, and the earlier data was therefore accepted. There is need for further research into the resistance of circular-section members in turbulent high-speed airflow.

Simple empirical formulae have been developed to cover any combination of flat-sided or circular-section members for both square and equilateral triangular cross section towers. The codified procedure allows for the interpolation for varying solidity ratios and enables towers composed of differing sections to be assessed rapidly with due regard to the flow regime. It also covers towers of high solidity ratios which are encountered in regions of aeriels, etc. and with severe icing, although the drag coefficients in these situations should be viewed with caution as no test data are available for significant solidity ratios; it is recommended that the coefficients given for $\phi > 0.6$ are verified by wind tunnel testing if possible.

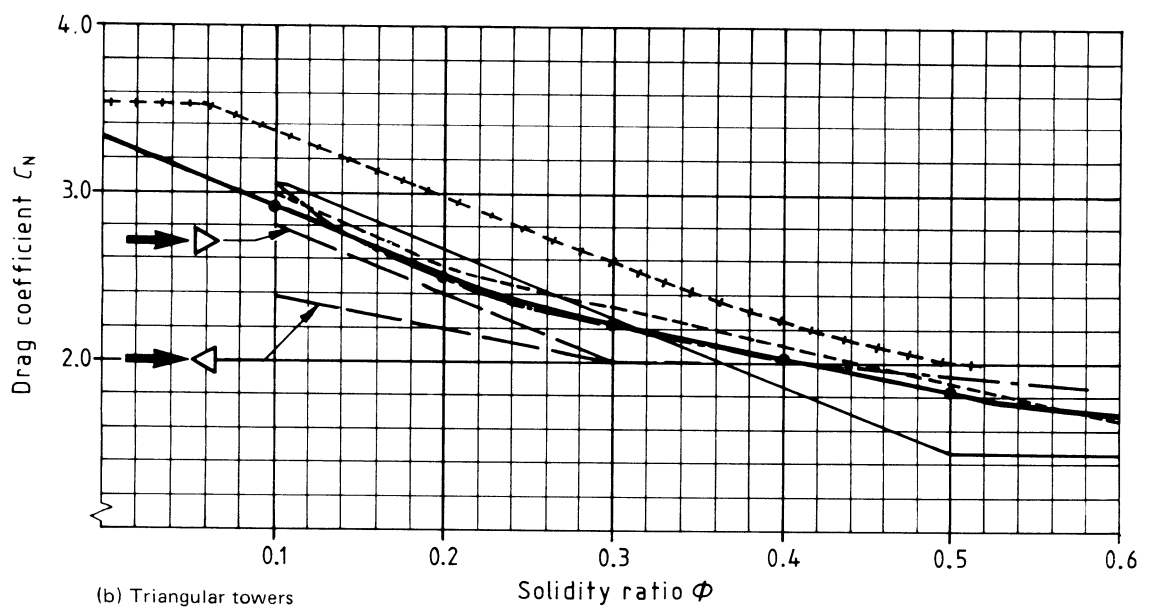
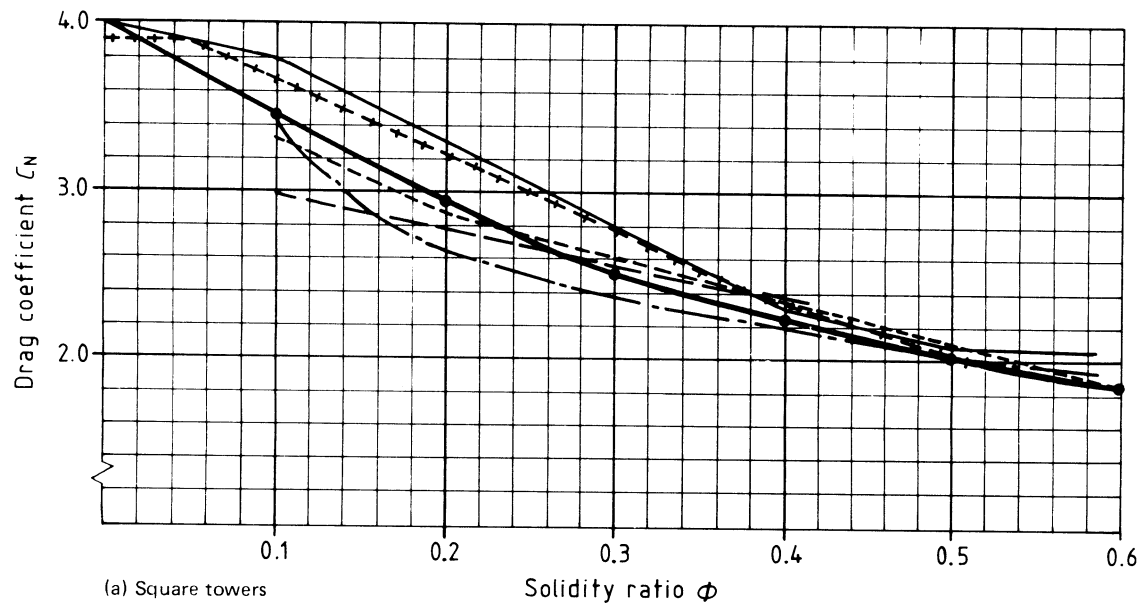
The effective area used in assessing the wind resistance and in defining the solidity ratio is based on the structural members within the face. The areas of plan and hip bracing, and of exposed bracing members in the longitudinal face should not be included, as the effects of these are deemed to be included in the drag coefficients. The wind tunnel tests incorporated such configurations, and comparisons between the provisions of Part 1 and these tests showed acceptable agreement.

Comparisons with existing codes and with experimental evidence has shown close agreement. Figure C.4.1 shows the overall drag coefficients for square and equilateral triangular towers composed of flat-sided members, obtained from 4.2.2 of Part 1, together with comparative values from the British [4.3], Polish [4.4], French [4.5] and German [4.6] codes. Also shown in this figure are the values recommended in ESDU item 75011 [4.7] which are based on taking a higher than mean value of experimental data; this was justified on the basis of the test results being under ideal flow conditions. Figure C.4.2 shows similar comparisons for towers composed of circular-section members.

Results of tests on square towers composed of flat-sided members are shown in Figure C.4.3. The NMI tests [4.1] indicate a significantly reduced drag at low values of solidity. The provisions of Part 1 do not reflect this reduction, as it was considered that under small angles of incidence in plan the drag may be increased significantly due to exposing members on the side faces of the tower, and this increase is allowed for in the provisions of Part 1.

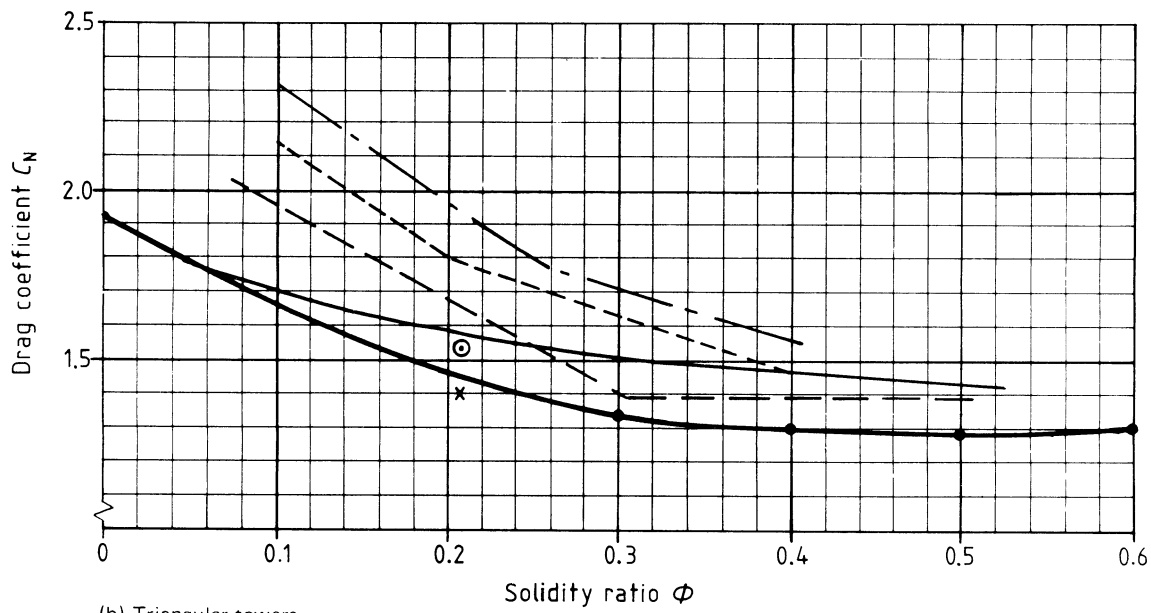
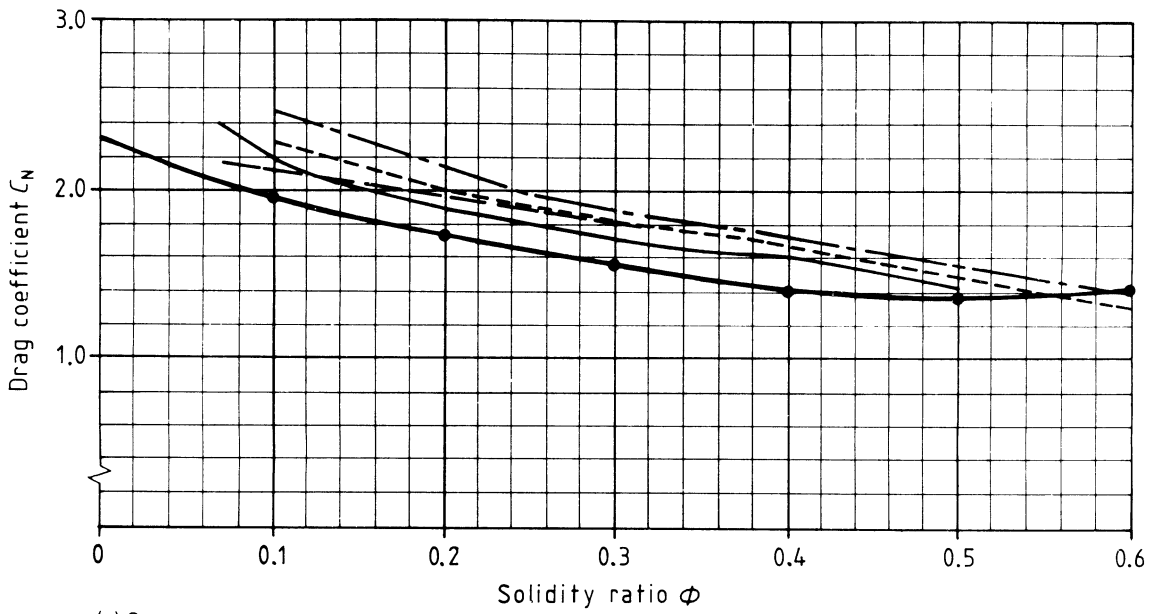
The results reported by Scruton and Gimpel [4.8] and shown in Figure C.4.3 related to single frames only, and these had to be adjusted for the drag on the back face, using their own proposals in order to arrive at overall drag coefficients. These earlier tests were undertaken on models composed of solid square sections, whereas the Forth tower [4.9] and later NMI models were made of scaled angle members, and this difference would probably account for the higher drag for the former, the coefficients for individual angles being about 90 % of those for square members, although the recent NMI tests on square sections give results very similar to those for angle sections.

Close agreement is shown by the test results plotted in Figure C.4.4 for triangular towers having angle members. Test results for square and triangular section towers composed of circular-section members show considerable variation with solidity. The tests at NMI were initially carried out by increasing the number of tubes in each face to increase the solidity. When the tests were repeated using sleeved members to achieve the same effect, the drag was significantly reduced which may be accounted for by the effects of increased Reynolds number. These results may be seen in Figure C.4.5 and Figure C.4.6. A series of tests on a model section of a triangular guyed mast column [4.10] having circular-section members, however, produced results in close agreement with 4.2.2 of Part 1 as may be seen in Figure C.4.7.



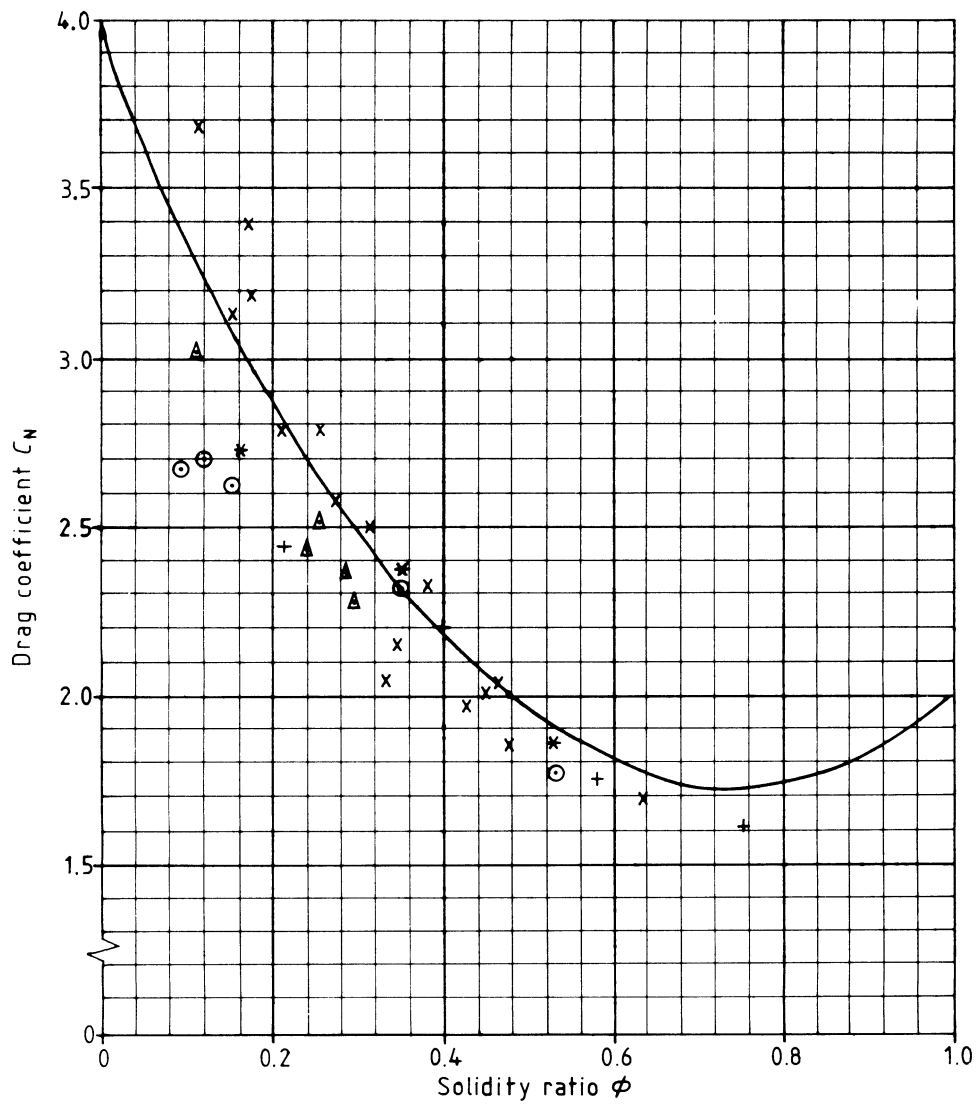
- 4.2.2 of Part 1
- CP 3 : Chapter V : Part 2 [4.3]
- - - French code [4.5]
- · - Polish code [4.4]
- - - - German standard [4.6]
- + + + + + ESDU item 75011 [4.7]

Figure C.4.1 — Comparison of drag coefficients for square and triangular lattice towers composed of flat-sided members



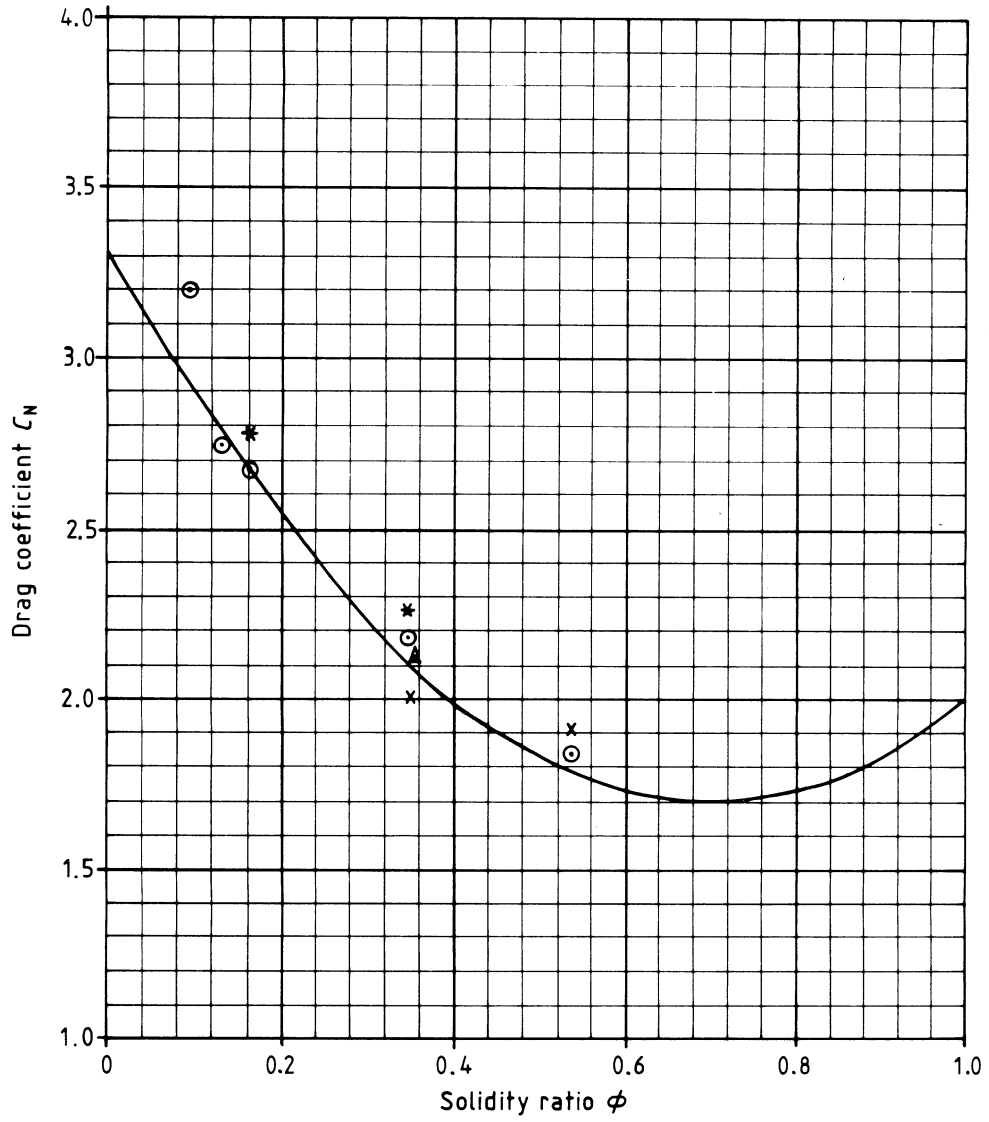
- 4.2.2 of Part 1
- CP 3 : Chapter V : Part 2 [4.3]
- - - French code [4.5]
- · - Polish code [4.4]
- - - German standard [4.6]
- ⊙ Raymer and Nixon [4.10] wind → ▷
- x Raymer and Nixon [4.10] wind → ▷

Figure C.4.2 — Drag coefficients for square and equilateral triangular towers composed of circular-section members



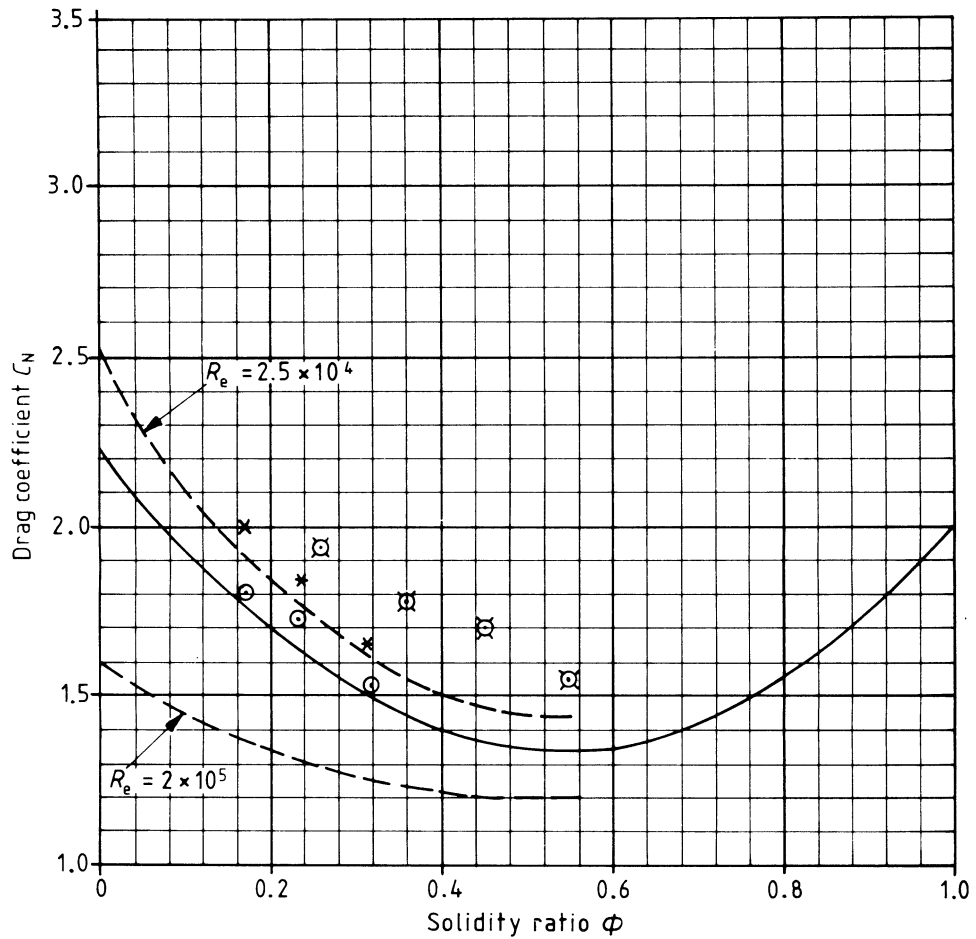
- 4.2.2 of Part 1
- | | | |
|------------------|-------------------------------------|-------------------|
| \odot | Angle members (smooth flow) | } NMI tests [4.1] |
| $*$ | Angle members (turbulent flow) | |
| $+$ | Square shaped members (smooth flow) | |
| x | Scruton and Gimpel [4.8] | |
| \blacktriangle | Forth crossing towers [4.9] | |

Figure C.4.3 — Variation of basic drag coefficient with solidity ratio for a square lattice tower composed of flat-sided members



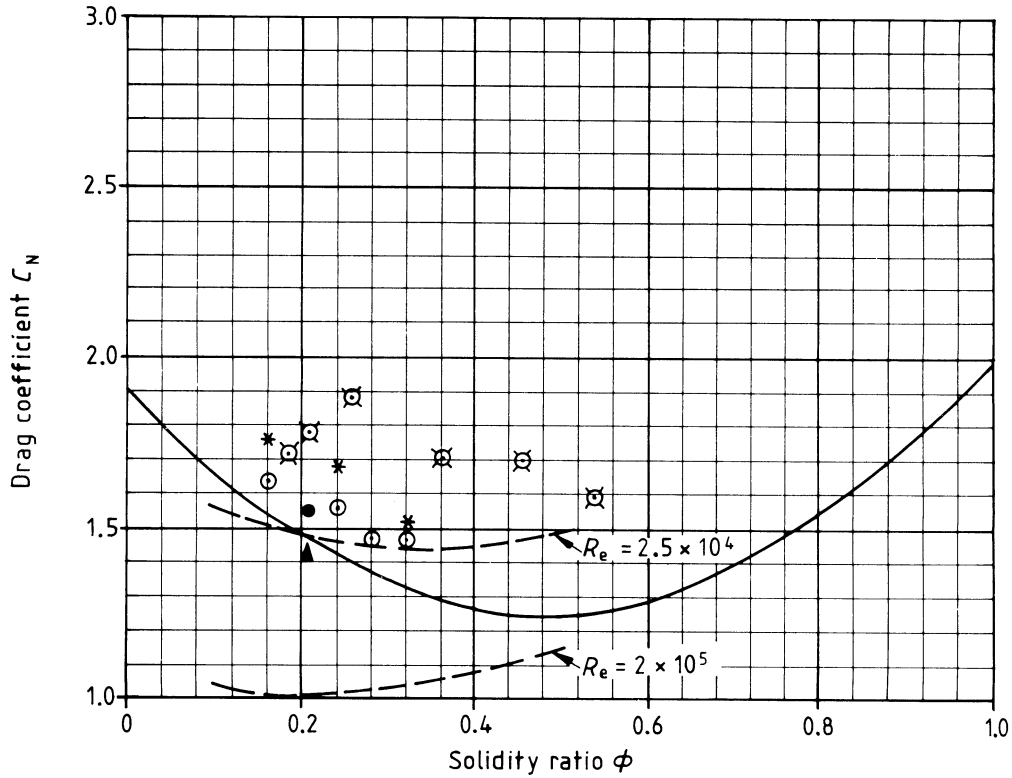
- 4.2.2 of Part 1
- Smooth flow } NMI tests [4.1]
- * Turbulent flow }
- △ Raymer and Nixon → ▷ } [4.10]
- x Raymer and Nixon → ▷ }

Figure C.4.4 — Variation of basic drag coefficient with solidity ratio for a triangular lattice tower composed of flat-sided members



- 4.2.2 of Part 1
- \odot Model with added sleeving (smooth flow)
- \boxtimes Model with added tubular solidity (smooth flow)
- $*$ Model with added sleeving (turbulent flow)
- Constrado monograph proposals [4.11]
- } NMI tests [4.1]

Figure C.4.5 — Variation of basic drag coefficient with solidity ratio for a square lattice tower composed of circular-section members (in subcritical flow)



- 4.2.2 of Part 1
 - ⊙ Model with added sleeving (smooth flow)
 - ⊠ Model with added tubular solidity (smooth flow)
 - * Model with added sleeving (turbulent flow)
 - Raymer and Nixon [4.10] → ▷
 - ▲ Raymer and Nixon [4.10] → ▷
 - - - Constrado monograph proposals [4.11]
- } NMI tests [4.1]

Figure C.4.6 — Variation of basic drag coefficient with solidity ratio for a triangular lattice tower composed of circular-section members (in subcritical flow)

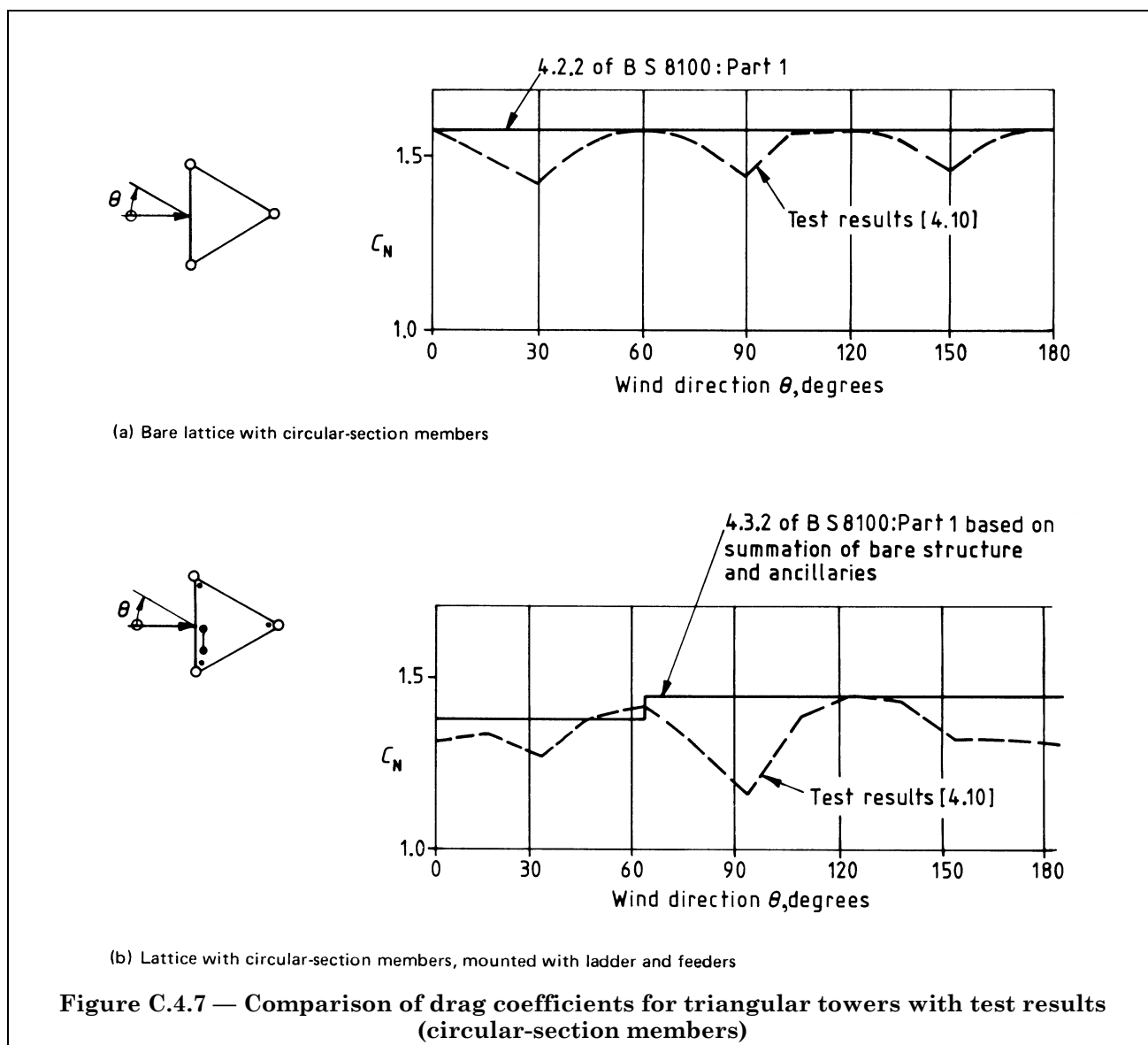


Figure C.4.7 — Comparison of drag coefficients for triangular towers with test results (circular-section members)

ESDU item 75011 [4.7] quotes drag coefficients for towers composed of circular members as a ratio of the drag coefficient for an isolated cylinder. Both this Data Item and a Constrado monograph [4.11] on wind forces on unclad tubular structures plot results against Reynolds number, adjusted in the former by turbulence and roughness factors which may be obtained from ESDU item 70013 [4.12]. Results from the monograph are plotted in Figure C.4.5 and Figure C.4.6 for Reynolds numbers of 2.5×10^4 and 2×10^5 . The NMI results correspond to a Reynolds number of about 2×10^4 which agrees reasonably with the monograph figures. The provisions of Part 1 for subcritical flow may be taken to correspond to a Reynolds number of about 1×10^5 which, at an extreme mean wind of at least 45 m/s, implies an average member diameter of about 21 mm; a reasonable lower bound for practical sizes. Figure C.4.8 shows a typical comparison between the provisions of Part 1 and the monograph for a square tower with wind blowing on to one face.

The area used in evaluating the drag (pressure) coefficients from all the test results has been taken as the total projected area normal to a face in strict accordance with 4.2.1 of Part 1.

Consideration was given to the relevance of the smooth flow results to gust response calculations. Bearman [4.13] suggests that the drag (pressure) coefficient for use in these may be of the order of only 2 % greater than the mean coefficient measured in fluctuating flow. Tests on the Forth tower model in incorrectly scaled turbulent flow showed the mean pressure coefficients to be about 2 % less than those in smooth flow. Tests by Vickery [4.14] on a tall building model showed a drag coefficient in turbulent flow 8 % less than the smooth flow value. However, the NMI tests [4.1] in turbulent flow have shown a marginal increase in drag as may be seen in Figure C.4.3 to Figure C.4.6. In the absence of adequate and reliable measurements, it has been considered prudent not to recommend coefficients based on other than smooth flow.

Variation of wind resistance with angle of incidence to the normal to the face of the tower is accounted for by the wind incidence factor K_θ . For square towers it is found that the variation is dependent upon the solidity ratio, as may be seen in Figure C.4.9 and Figure C.4.10. For low values of solidity ratio, maximum drag occurs with wind directed at about 25° to a face. At increasing values of solidity ratio, the maximum occurs at 45° . As design is generally undertaken at face-on and at 45° directions only, the proposals of Part 1 ensure that the diagonal condition will cover the maximum loading case. Thus it may be seen in Figure C.4.11 that Part 1 overestimates the drag at 45° incidence for low solidity ratios to allow for these intermediate angles. Whilst K_θ for $\theta = 45^\circ$ can be seen to underestimate the intermediate values for low solidity ratios in Figure C.4.9 and Figure C.4.10, the overestimate of drag ensures that the total resistance is well predicted (see C.4.9). No results are available for solidity ratios greater than about 0.6 but, clearly, as ϕ tends to 1, K_θ should tend to that for solid square sections, i.e. 1.1 [4.3]. For simplicity, Part 1 has proposed a symmetric relationship about $\phi = 0.5$. For triangular-section towers, there is little or no variation when these are composed of circular-section members (see Figure C.4.7 and Figure C.4.12) but for such towers composed of flat-sided members there is a significant reduction when wind is blowing parallel to one face. This may be seen in Figure C.4.13 and Figure C.4.14 (which also show the relevant provision of Part 1).

As design is generally undertaken with wind normal (or parallel) to a face, or directed to a corner ($\theta = 45^\circ$ for square towers and $\theta = 60^\circ$ for triangular towers) the relevant values of K_θ are given in Figure 4.2 of Part 1. For other conditions, the equations used to determine K_θ are provided in Appendix G of Part 1.

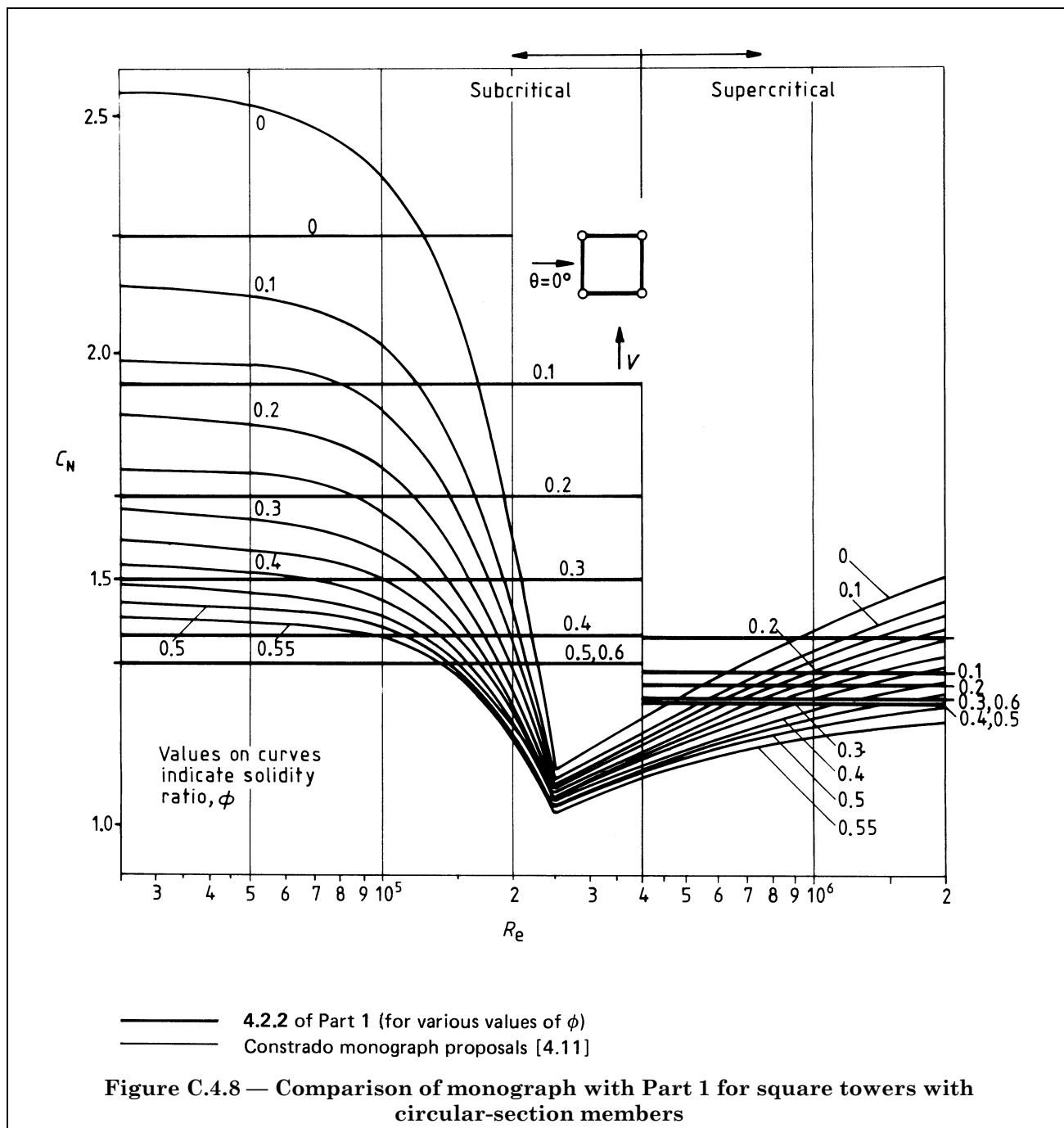
The wind resistance in the crosswind direction has been assumed to be identical to that downwind. Whilst this would be correct for symmetrical square towers, it can lead to a marginal error of up to 5 % for triangular towers, as may be seen from Figure 4.2 of Part 1. For triangular towers entirely constructed with flat-sided members, the wind resistances in two orthogonal directions differ by a maximum of 5 % (see Figure C.4.13). However, in view of the relatively small effect of the crosswind effects under in-line gust loading (see C.5.2.6) it was considered justifiable to accept this approximation in the interests of simplicity.

C.4.3 Symmetrical towers with limited ancillaries

For towers in which the ancillaries do not form a major proportion of the projected area of the structure, nor extend significantly outside the width of the tower, the total resistance may be calculated from the summation of the resistance of the bare tower and that of the ancillary items. In calculating the tower resistance, the solidity ratio appropriate to the bare tower is used, leading to an overestimate of its drag when mounted with ancillaries. This is compensated, however, by a reduction factor on the drag of the ancillaries (see C.4.5 and C.4.6) which was derived from the test results at the NMI [4.1]. These tests also confirmed the basis of this design procedure, wherein the resistance is developed by the summation of the separate resistances of the bare tower and the ancillary items.

The advantage of this procedure is that in assessing the resistance of a standard section tower only one calculation of solidity ratio need be made, regardless of the ancillaries mounted on it (provided they comply with the constraints of 4.1.3 of Part 1). Modifications to an existing tower can equally be assessed more rapidly.

The crosswind resistance of the tower is taken, as for towers without ancillaries as the downwind resistance (see C.4.2). The crosswind resistance of the ancillaries is then added to this taking the reference direction for assessing the resistance as normal in plan to the mean wind direction.



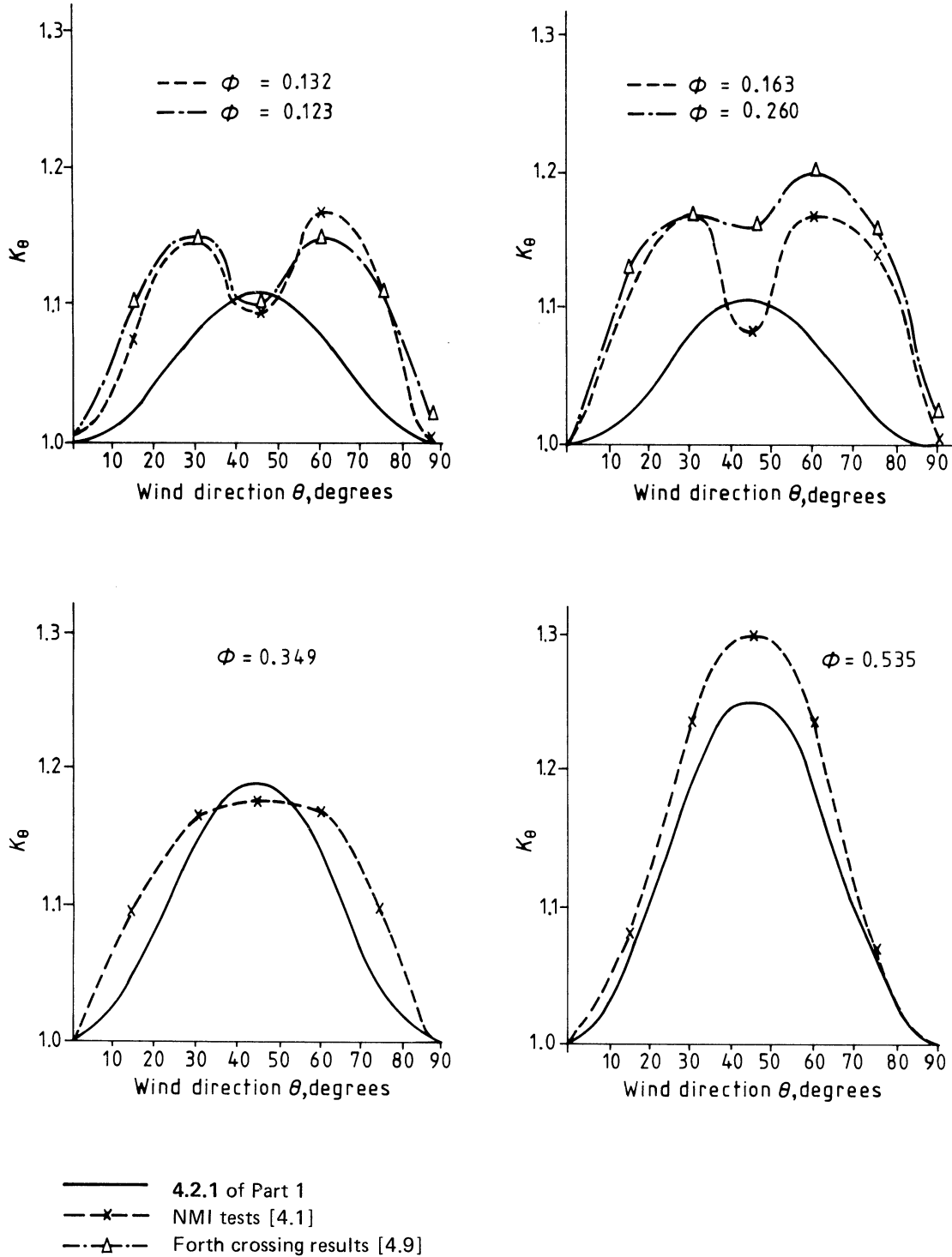
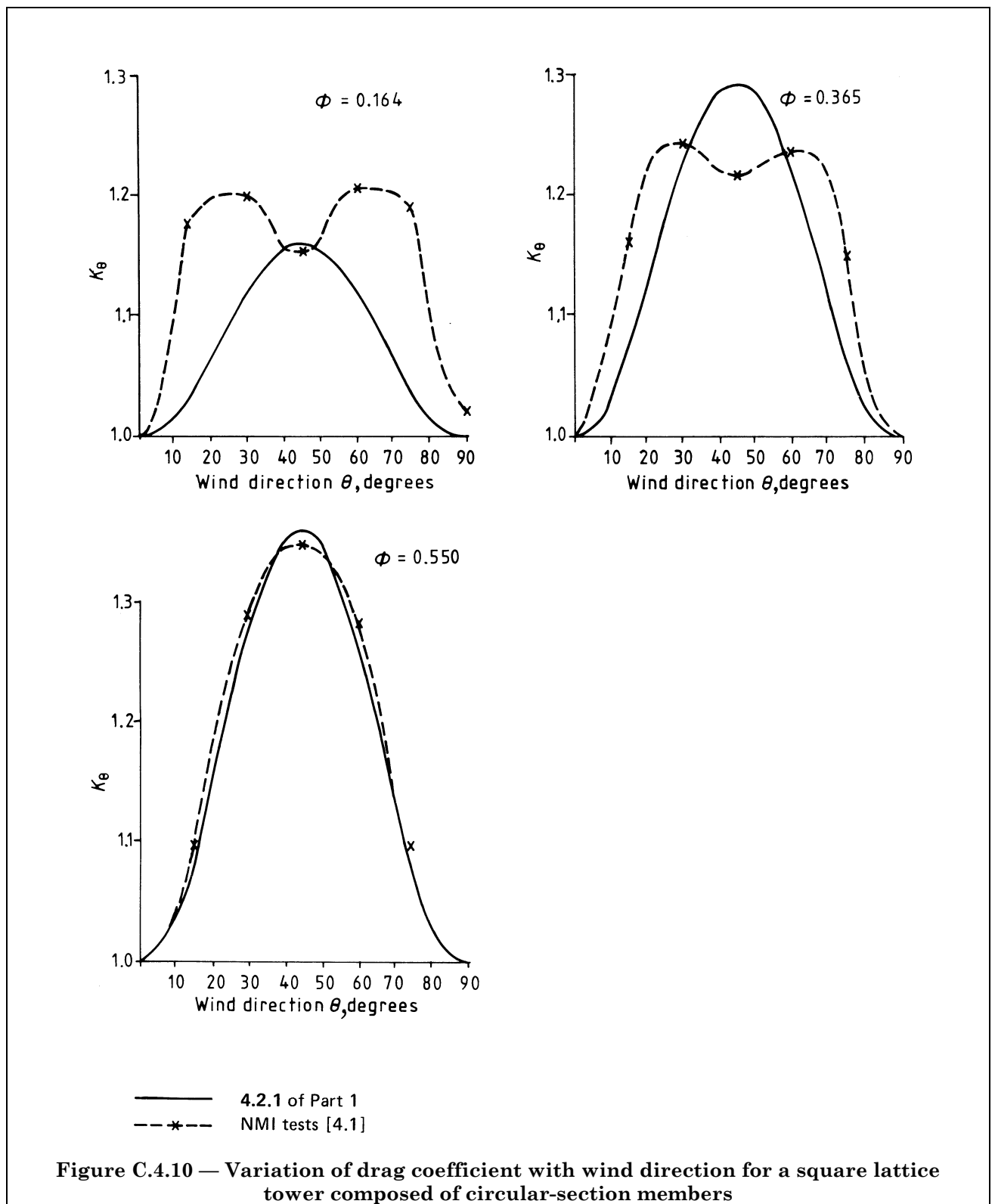
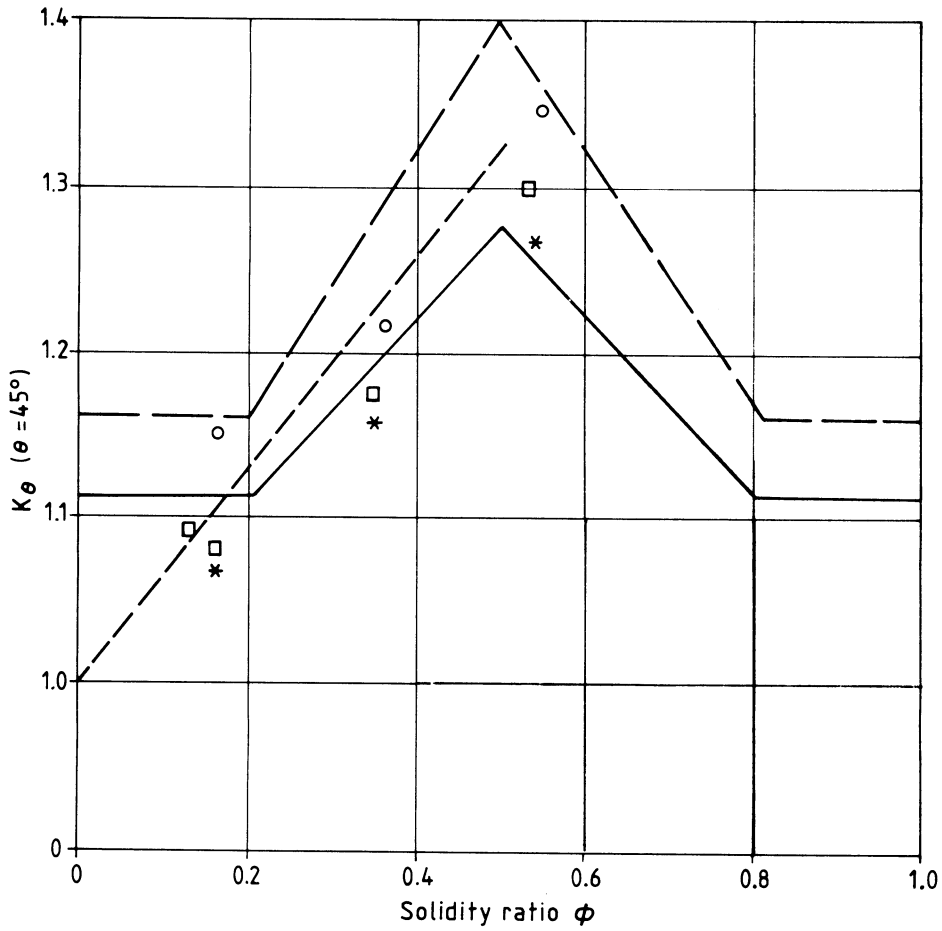


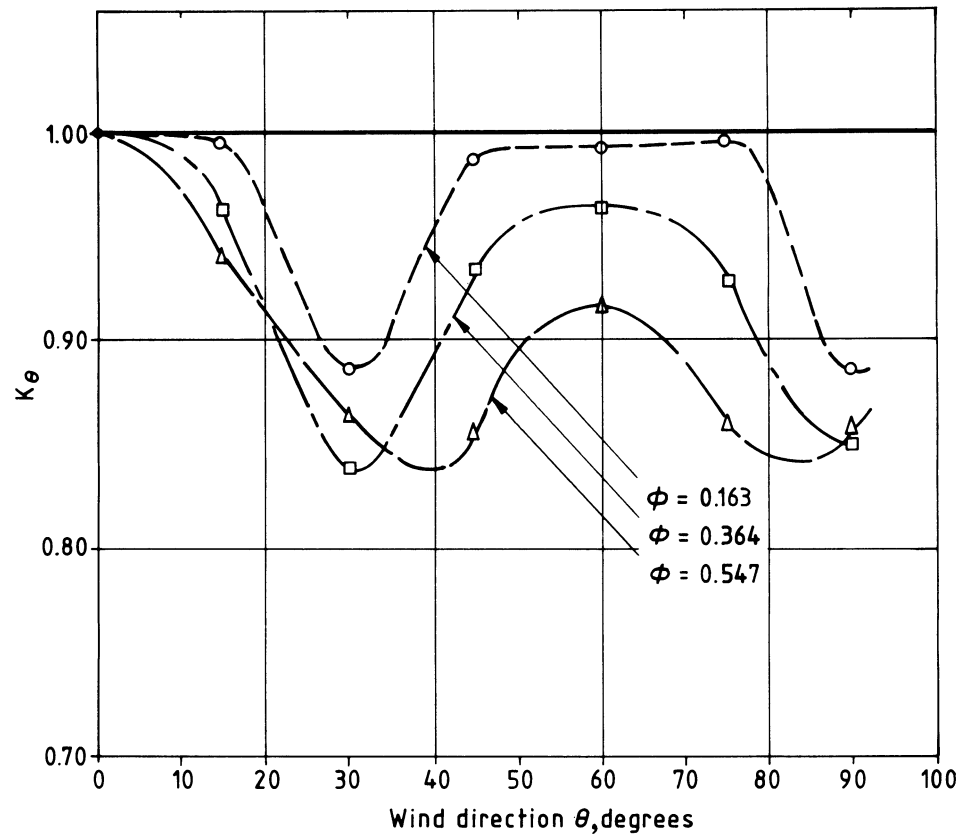
Figure C.4.9 — Variation of drag coefficient with wind direction for a square lattice tower composed of flat-sided members





- 4.2.1 of Part 1 (angle members)
 - - - 4.2.1 of Part 1 (circular members)
 - Angle members (smooth flow)
 - * Angle members (turbulent flow)
 - Circular members (smooth flow)
 - · - ESDU item 75011 (angle members) [4.7]
- } NMI tests [4.1]

Figure C.4.11 — Variation of K_{θ} ($\theta = 45^\circ$) with solidity ratio for a square lattice tower



— 4.2.1 of Part 1
 -○- } NMI tests [4.1]
 -□- }
 -△-

Figure C.4.12 — Variation of K_θ with wind direction for a triangular tower composed of circular-section members

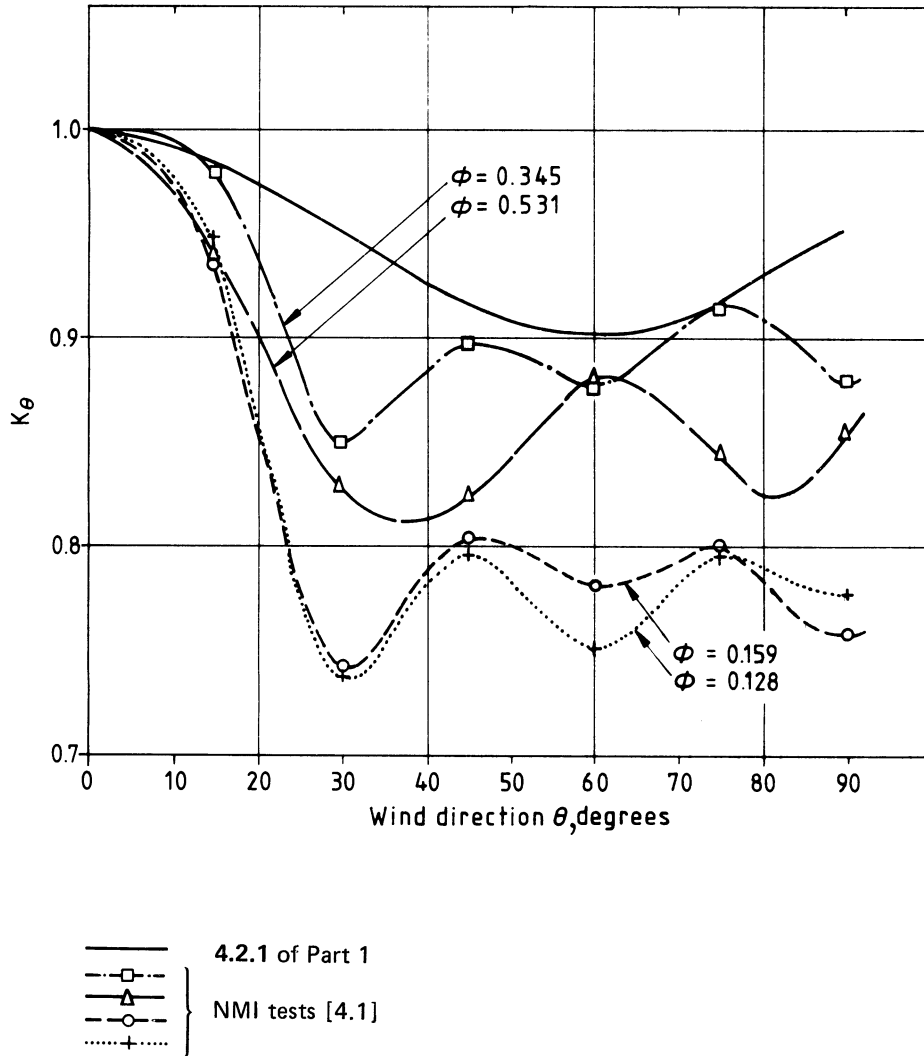
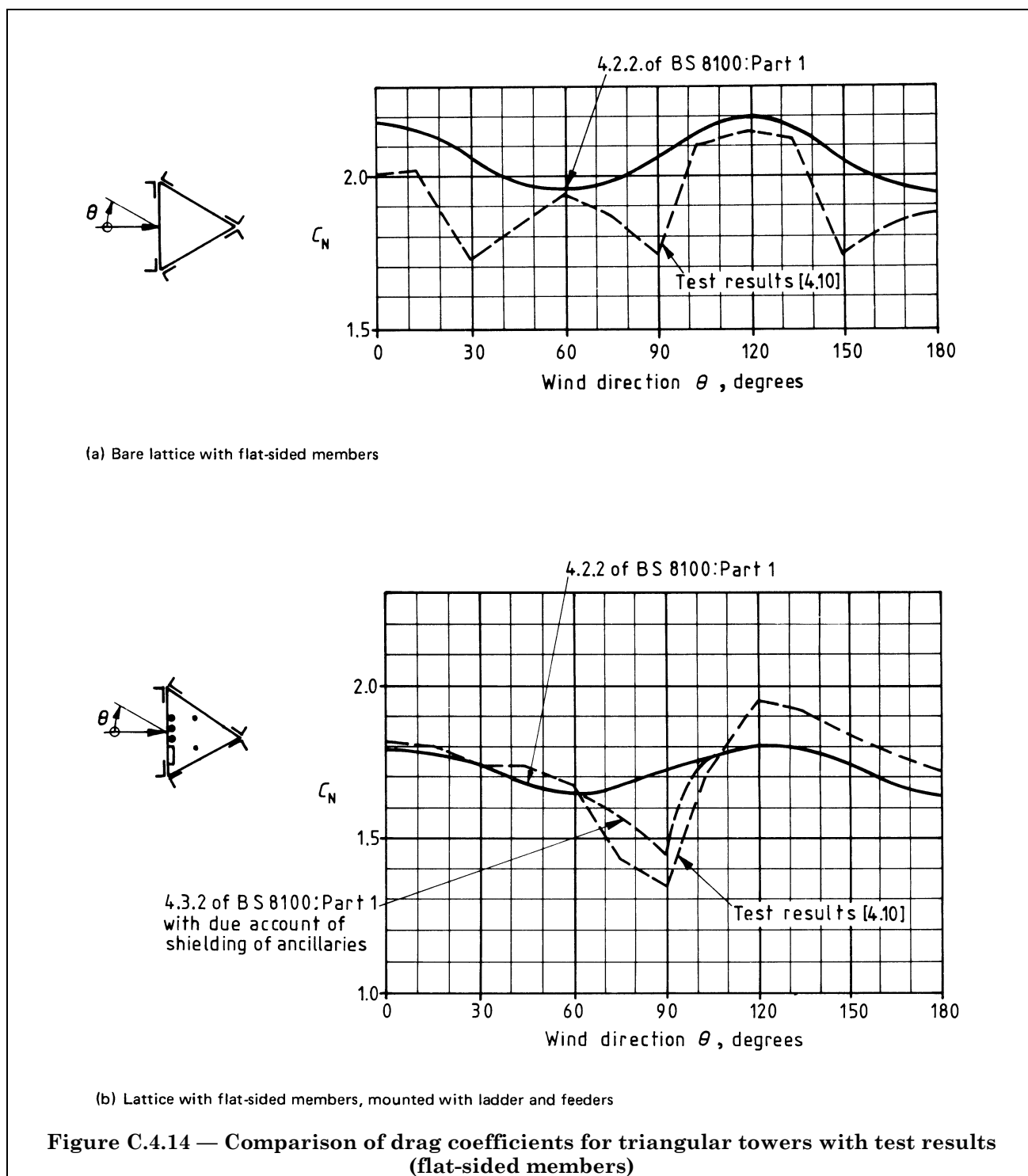


Figure C.4.13 — Variation of K_θ with wind direction for a triangular lattice tower composed of flat-sided members



C.4.4 General method for towers containing ancillaries

In those instances where it is not possible to use overall force coefficients, a method is adopted of assessing the drag of the front face and accounting for the drag on the back face by a shielding factor. Formulae have been developed which again cover any combination of flat-sided or circular-section members. The method is to be used for rectangular towers, or where the structural form of adjacent faces in square or triangular towers is markedly different, and the effect of wind at an angle of incidence to the normal to a face is to be considered.

The drag coefficients for single frames and the formulae developed for flat-sided or circular-section members may equally be used for ancillary elements that are of the same form. However, to cater for special ancillaries that cannot be considered as structural members, there is provision to derive separately the resistances of any such ancillary items from 4.5 and 4.6 of Part 1 and incorporate their resistance into the face resistances R_1 to R_4 .

When assessing the wind resistance in accordance with 4.4 of Part 1, the solidity ratio should be based on the total area, A_F , of both the structural members and all ancillaries in the face. As discussed in C.4.2, the areas of plan and hip bracing, and of exposed bracing members in the longitudinal faces should not be included.

The formulae were derived empirically to ensure that the summation procedure would produce identical values of drag to the overall approach described in C.4.2 for the symmetrical towers of one type of member. This may be seen in the comparison between the overall drag (pressure) coefficients set out in 4.2.1 of Part 1 and the resulting drag (pressure) coefficients using this summation process for square and triangular towers in Figure C.4.15 and Figure C.4.16. The overall drag coefficients tabulated in CP 3: Chapter V-2 [4.3] are also shown in these figures.

Comparisons with other test results are shown in Figure C.4.7 and Figure C.4.14 for the triangular mast (having circular-section members) referred to above, and for a triangular mast composed of flat-sided members, each containing circular-section feeders and a ladder.

Comparison of the drag factors for single frames with ESDU item 75011 [4.7] and CP 3: Chapter V-2 [4.3] is shown in Figure C.4.17.

Work undertaken by Whitbread [4.15] since the drafting of Part 1 suggests that the shielding factors for circular-section members adopted in Part 1 are underestimated. Due to the overestimate of the single frame drag coefficients, the overall resistance using the procedure of Part 1 is close to the measured values tested for various spacing ratios of such frames. However, there are occasions where Part 1 appears to marginally underestimate the loading obtained from his wind tunnel tests. However, the tests were undertaken in subcritical flow and in practice they would provide upper bound estimates of resistance for towers composed of circular sections. The provisions of Part 1 may thus be considered acceptable, although further work is required on the effects of mixed flows at representative Reynolds numbers.

C.4.5 Linear ancillaries

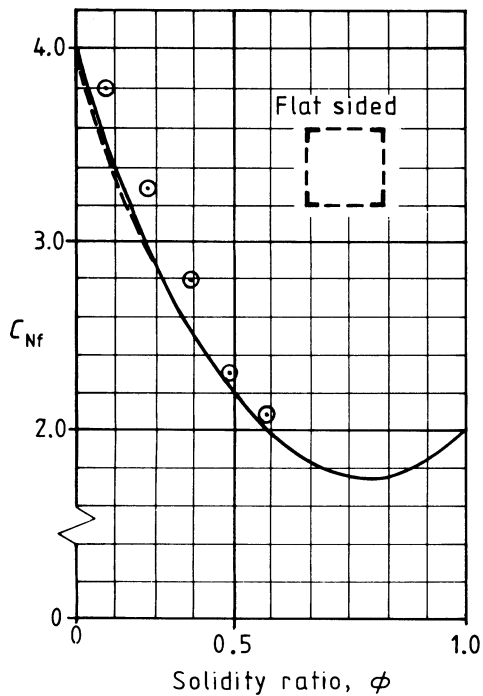
Analyses of the NMI wind tunnel tests [4.1] have indicated that the resistance of all additional components to the basic tower may be calculated using a free stream drag coefficient, together with a reduction factor to take account of the shielding of the component by the tower itself. The reduction factor given was based on tests using a basic tower solidity ratio of 0.16 and hence will be slightly conservative for towers whose solidity ratio will be greater than this. The reduction factor is only considered applicable for ancillaries which comply with the constraints of 4.1.3 of Part 1, as the tests did not encompass a wider range of ancillaries, and it was considered unlikely that any reduction could be relied on for large ancillary items which are external to the tower body itself.

The reduction factor will also vary depending upon the position of the component in the tower itself. Figure C.4.18 shows typical comparisons between the treatment given in 4.4 of Part 1 and the NMI wind tunnel test results for various combinations of tower types and ancillaries. From Figure C.4.18, it may be seen that Part 1 estimates the measured drag to within 10 %.

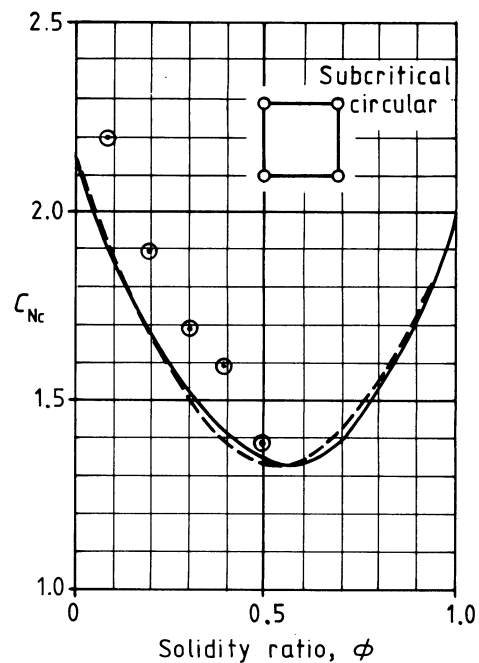
The coefficients for isolated members given in CP 3: Chapter V-2 [4.3] are complicated to apply, and they have been replaced by upper bound values which may be applied to the projected areas without significant loss of economy. Since most members attached to towers will be aerodynamically slender, the refinement of the slenderness modification in CP 3: Chapter V-2 [4.3] has been considered unnecessary and possibly unreliable when junction effects are present. The coefficients for straked cylinders are those derived by Walshe and Wootton [4.16].

C.4.6 Discrete ancillaries

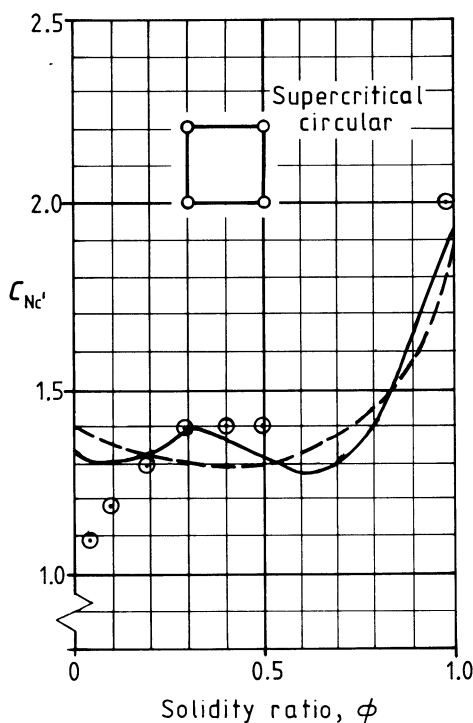
It has been considered inappropriate to provide drag (pressure) coefficients for discrete ancillaries in view of the wide range of such items that might be mounted on a tower. Frequently such items are proprietary products for which wind tunnel test data are available from the manufacturers. Part 1 allows such test results to be used, although caution should be exercised in ensuring that the tests were properly conducted (see C.6.1).



(a) Flat-sided members, C_{Nf}



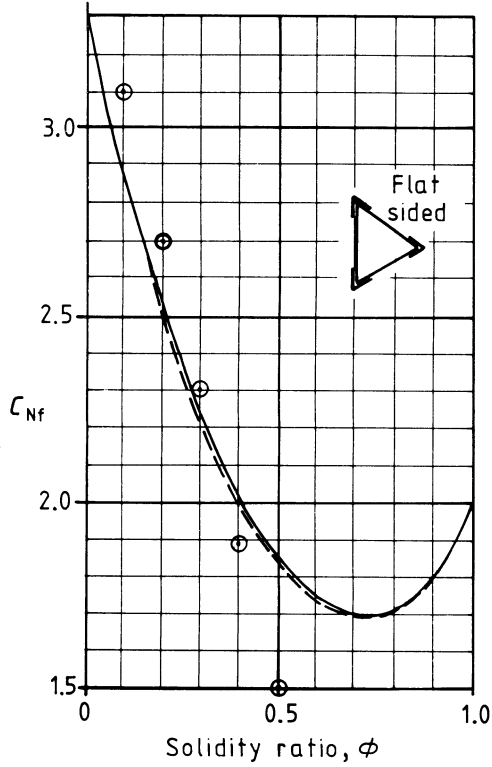
(b) Subcritical circular-section members, C_{Nc}



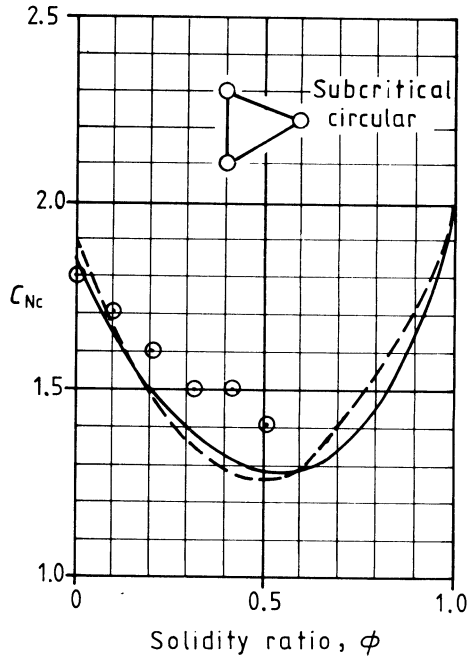
(c) Supercritical circular-section members, $C_{Nc'}$

- ⊙ CP 3 : Chapter V : Part 2 values for overall force coefficients [4.3]
- 4.2.2 of Part 1 formulation for overall C_N
- 4.4.1 of Part 1 formulation using C_N from parts $\{C_N (1 + \eta)\}$

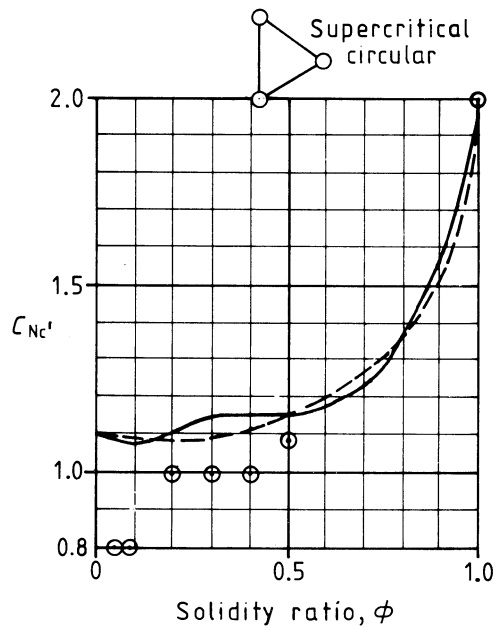
Figure C.4.15 — Drag coefficients for square lattice towers



(a) Flat-sided members, C_{Nf}



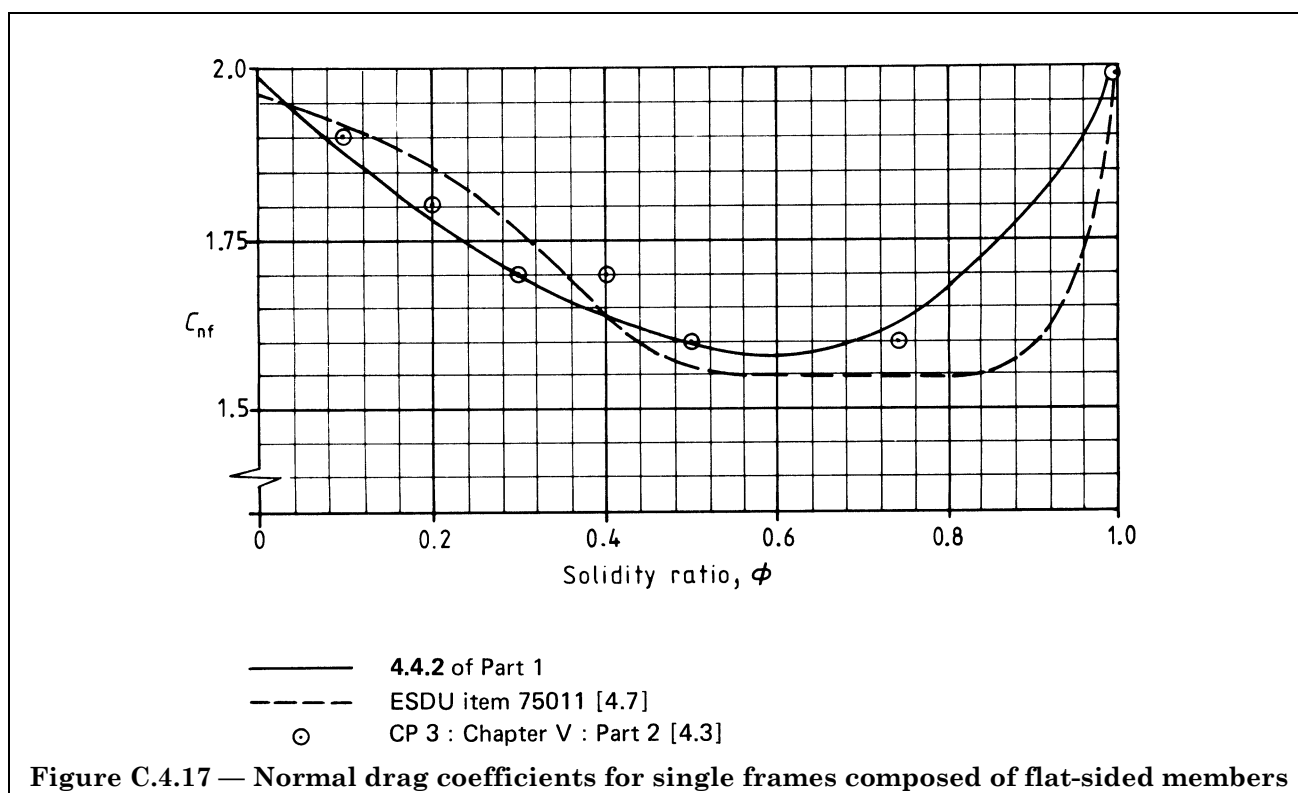
(b) Subcritical circular-section members, C_{Nc}



(c) Supercritical circular-section members, $C_{Nc'}$

- ⊙ CP 3 : Chapter V : Part 2 values for overall force coefficient [4.3]
- 4.2.2 of Part 1 formulation for overall C_N
- 4.4.1 of Part 1 formulation using C_N from parts $\{C_N (1 + \eta)\}$

Figure C.4.16 — Drag coefficients for triangular lattice towers



C.4.7 Cables

Drag coefficients for stranded cables have been derived from the results of tests undertaken by Counihan [4.17] representing upper bounds for the common range of strand arrangements. Coefficients for smooth wire closely follow the values given in Table 18 of CP 3: Chapter V: Part 2:1972 [4.3].

The $\sin^3\psi$ term in the equation for R_{CW} in 4.7 of Part 1 arises from the resolution of the normal force on the cable, R_{CN} , given by:

$$R_{CN} = C_C DL_C \sin^2 \psi$$

This is shown diagrammatically in Figure C.4.19. Resolving this force in the wind direction, R_{CW} , is obtained:

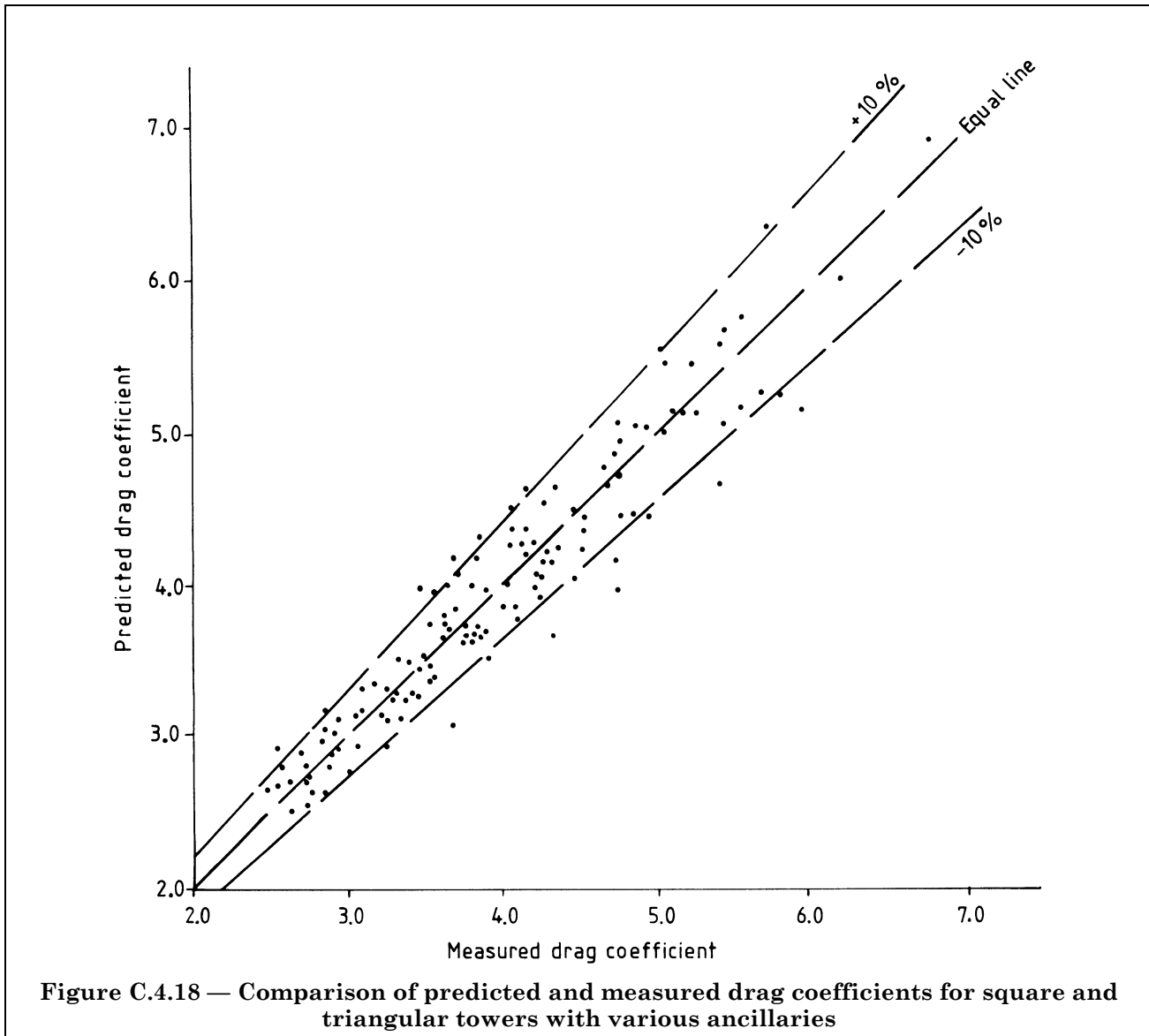
$$R_{CW} = R_{CN} \sin \psi$$

Hence

$$R_{CW} = C_C DL_C \sin^3 \psi$$

C.4.8 Icing

Tests undertaken on models of iced masts and stays [4.18] suggest that the drag coefficients to be applied to an ice-coated element may be taken as those for the same element ice-free. However, for smooth wires and fine-stranded cables, the rougher ice surface will increase the drag over that for the ice free section, and this has been accounted for in the values given in Table 4.1 of Part 1. For the thicker stranded cables with a significantly rough surface, a marginal reduction in drag is adopted for iced conditions. The factors should be applied to the projected areas including ice in all calculations.



C.4.9 Measurements on scale model of communications tower

The aforementioned NMI wind tunnel tests [4.1] were all made on models of various sections of towers which provided the basic data for Part 1. The combination of different panel types together with the inclusion of realistic ancillary items such as ladders, platforms, aerials and dishes, had not been tested. To overcome this a series of tests was commissioned by the Building Research Establishment and undertaken at the NMI [4.2].

A model of a typical microwave communications tower was tested in the wind tunnel to provide comparisons between the measured overall base shears and bending moments with those derived by application of Part 1. In order to consider as many variables as possible, a demountable internal ladder tower was also constructed together with feeders and dish aerials which could be incorporated in various configurations. A sketch of the tower is shown in Figure C.4.20 and the configurations tested are listed in Table C.4.1. The results of the tests are contained in a report [4.19] which concludes that Part 1 predicts with reasonable accuracy the drag and overturning moment of a structure made up of a series of differing panels mounted with various ancillaries.

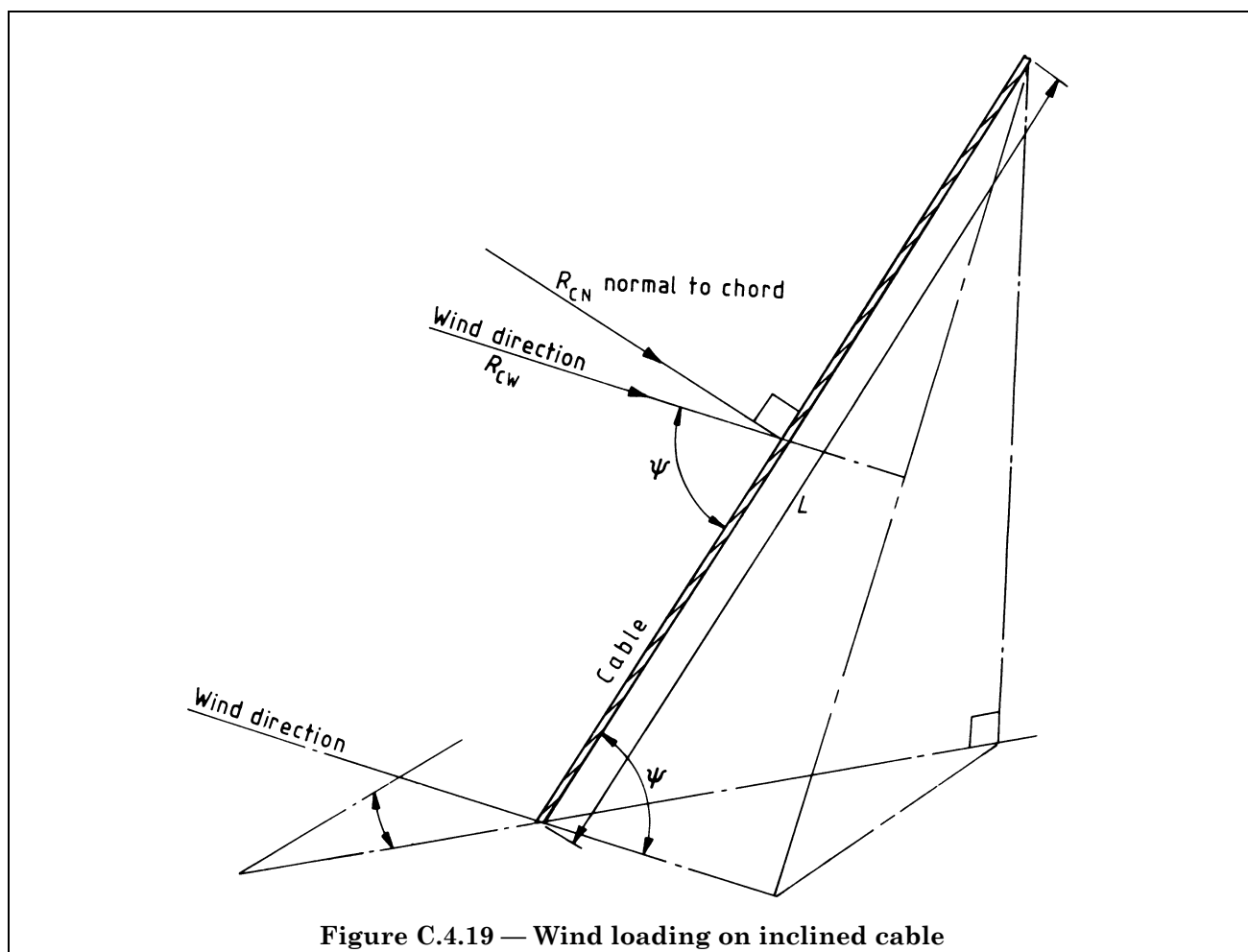


Figure C.4.19 — Wind loading on inclined cable

It was found that with wind blowing diagonally on the tower, Part 1 overpredicted the drag, significantly in certain configurations. However, at angles between the normal and diagonal, higher drag values were obtained, but slightly less than the Part 1 prediction for 45° wind. Thus Part 1 provisions for 45° cover the more onerous loading from intermediate wind incidence, which may not always be considered.

A summary of the results, in terms of the percentage overestimate by Part 1 compared with the test results is shown in Table C.4.1. From this may be seen the significant overestimate by Part 1 for the 45° wind case, but this is necessary for design purposes as may be seen from the ratio of the 45° prediction to the maximum test value. It should also be noted that the factor K_{θ} for square towers using flat-sided members underestimates the variation with incidence for low solidity ratios (see C.4.2). However, this does not lead to an underestimate of the total resistance, due to the combination of K_{θ} with overestimates of drag coefficients for such configurations. This may be seen in Figure C.4.21 and Figure C.4.22 extracted from the report [4.19].

Somewhat surprisingly, the results showed that under uniform turbulent flow the drag increased marginally above the smooth flow results; this is in contradiction with the findings of other experimentalists as noted in C.4.2. This may have been due to the scale of turbulence introduced in the tunnel and the view taken in drafting Part 1 was to use the smooth wind flow test results; further research into this aspect, however, is clearly required.

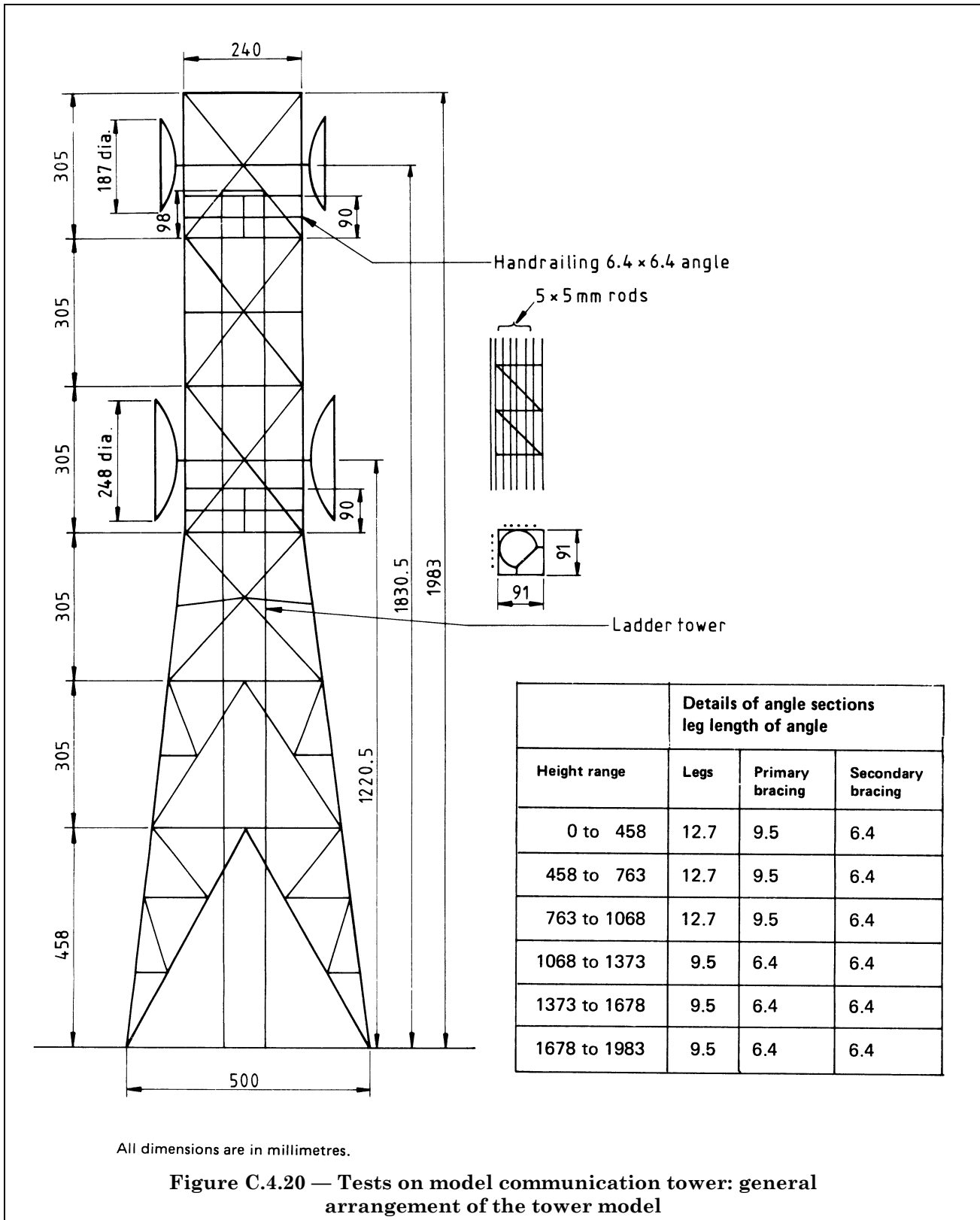
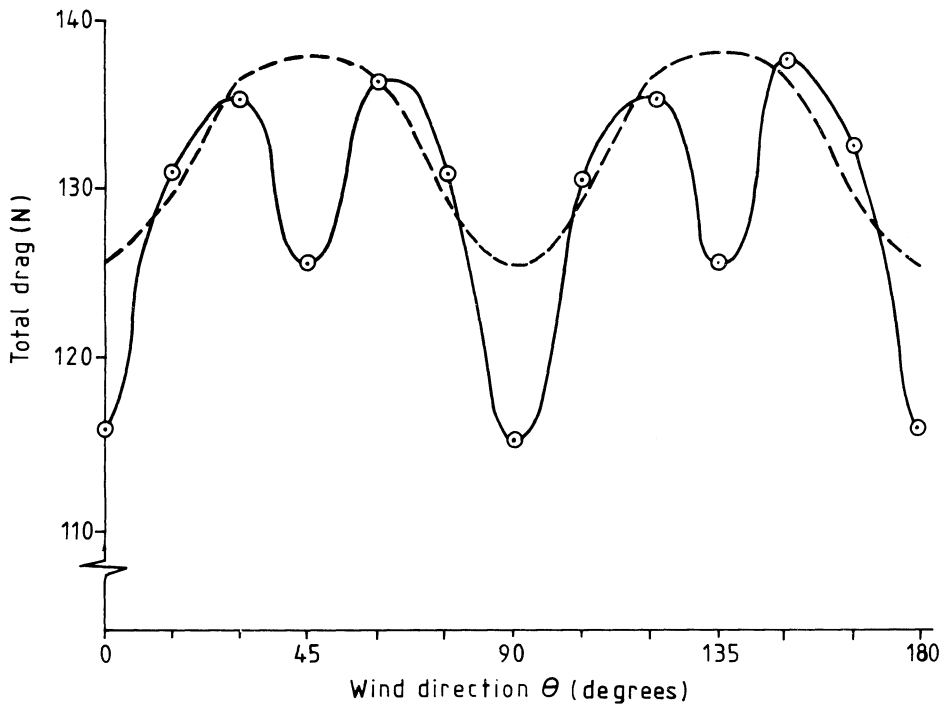
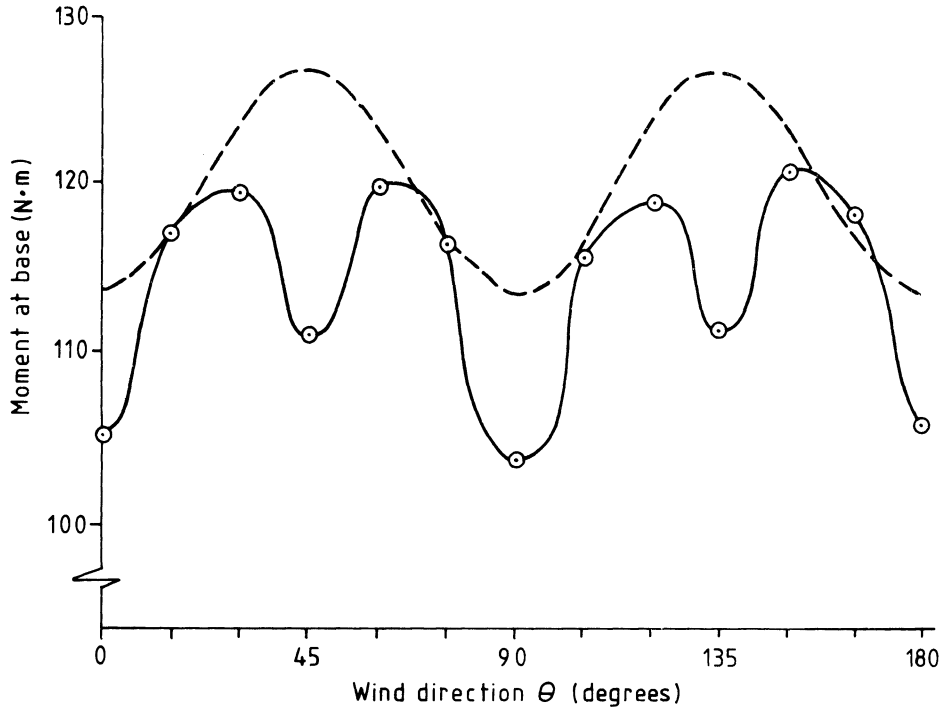


Table C.4.1 — Comparison between Part 1 and experimental results

Tower configuration	Code overestimate							
	Turbulent shear flow				Smooth uniform flow			
	0°	45°	90°	Part 1 at 45°	0°	45°	90°	Part 1 at 45°
				test max.				test max.
	%	%	%	%	%	%	%	%
A = bare ladder tower	+ 12	+ 13	+ 13	+ 13	+ 14	+ 13	+ 16	+ 13
B = A + ladder	+ 13	+ 15	+ 11	+ 11	+ 14	+ 15	+ 12	+ 11
C = B + feeders	+ 20	+ 18	+ 18	+ 13	+ 21	+ 19	+ 19	+ 13
D = bare main tower	+ 5	+ 9	+ 5	+ 1	+ 9	+ 12	+ 9	+ 2
E = D + ladder tower + ladder	+ 0	+ 18	+ 0	+ 5	+ 2	+ 21	+ 2	+ 7
F = E + feeders	+ 2	+ 21	+ 1	+ 7	+ 4	+ 25	+ 4	+ 9
G = F + 8 dishes at 45°	- 1	+ 41	- 2	- 1	0	+ 42	- 1	+ 2
H = F + 8 dishes at 0°	+ 17	+ 6	- 1	- 1	+ 15	+ 9	+ 1	+ 1
J = F + 2 dishes at 0°					+ 2	+ 19	+ 3	+ 6
K = F + 4 dishes at 0°					+ 6	+ 16	+ 3	+ 6

C.4.10 References in C.4

- 4.1 NATIONAL MARITIME INSTITUTE. *Wind Loading on Lattice Towers*, Report on Project P/352003, 1977.
- 4.2 NATIONAL MARITIME INSTITUTE. *Wind Load Measurements on a range of configurations for a model of a typical lattice tower*, Dec. 1978.
- 4.3 BRITISH STANDARDS INSTITUTION. Code of basic data for the design of buildings: Chapter V Loading: Part 2 Wind loads, 4th ed., 1972, CP 3:Chapter V: Part 2.
- 4.4 Polish Standard. *Steel guyed masts and towers for radio and TV: Calculation and Structural Design*, BN-04-052.
- 4.5 *Regles definissant les effets de la neige et du vent sur les constructions*, Regles NV65, Nov. 1965.
- 4.6 German Standard. *Steel Aerial Supporting Structures*, DIN 4131, March 1969.
- 4.7 ENGINEERING SCIENCES DATA UNIT. *Fluid Forces on Lattice Structures*. Data Item 75011, Aug. 1975 now superseded by Data Items 81027, 81028 and 82007.
- 4.8 SCRUTON and GIMPEL. *Memorandum on wind forces and pressure exerted on structures and buildings*, NPL/Aero/391, Oct. 1959.
- 4.9 COWDREY, C.E. *Aerodynamic forces and moments on models of two sections of a Forth Crossing tower*, NPL/Aero Special Report 027, June 1969.
- 4.10 RAYMER, W.G. and NIXON, H.L. *Tests on triangular section television masts*, NPL/Aero/280, March 1955; and NPL/Aero/278 Feb. 1955.
- 4.11 *Wind Forces on Unclad Tubular Structures*, Constrado Publication 1/75, Jan. 1975.
- 4.12 ENGINEERING SCIENCES DATA UNIT. *Fluid Forces acting on circular cylinders for application in general engineering: Part 1 long cylinders in two-dimensional flow*, Data Item 70013 now superseded by Data Items 80025 and 81017.
- 4.13 BEARMAN, P.W. Wind loads on structures in turbulent flow. *Seminar, The modern design of wind-sensitive structures*, CIRIA, June 1970.
- 4.14 VICKERY, B.J. *Load variations on bluff shapes in turbulent flow BLWT*, report 4; 67, University of Western Ontario.



—○— Experimental values [4.2]
 -*- Part 1 values

Figure C.4.21 — Tests on model communication tower: configuration D (smooth uniform regime)

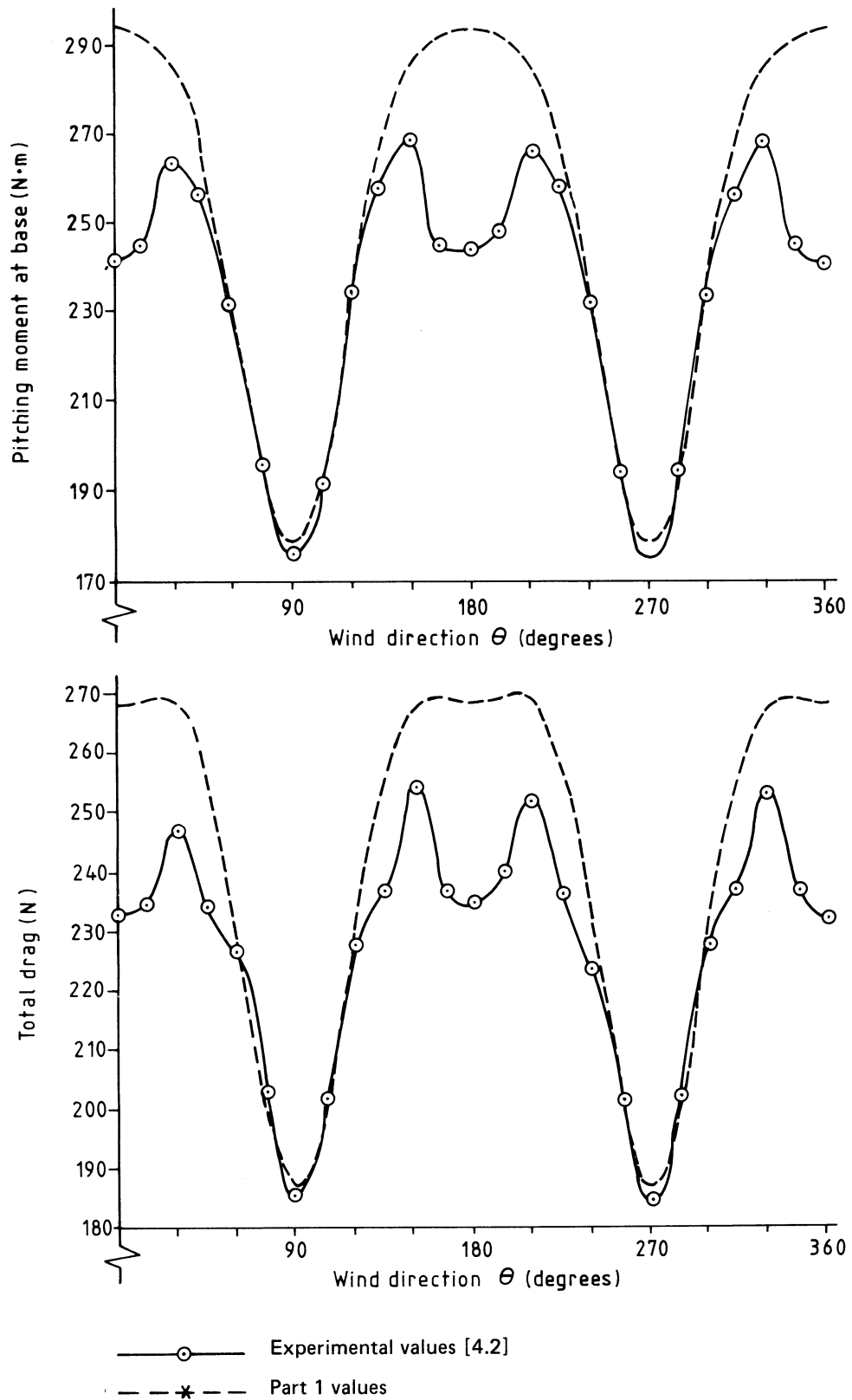


Figure C.4.22 — Tests on model communication tower: configuration H (smooth uniform regime)

- 4.15 WHITBREAD, R.E. The influence of shielding on the wind forces experienced by arrays of lattice frames. *Wind Engineering. Proceedings of the Fifth International Conf., Fort Collins, Colorado, July 1979.*
- 4.16 WALSHE, D.E. and WOOTTON, L.R. Preventing wind-induced oscillations of structures of circular cross-section. *Proceedings Institution of Civil Engineers, Sept. 1970, 47.*
- 4.17 COUNIHAN, J. *Lift and drag measurements on stranded cables*, Report No. 117. Aero. Dept. Imperial College, Aug. 1963.
- 4.18 ELLIOTT, P.R. *Investigation into the drag of guyed lattice masts due to ice encrustation*, Kingston Polytechnic, Report BHCE4 1971/72.
- 4.19 SMITH, B.W. *Comparison of the Draft Code of Practice for Lattice Towers with wind load measurements on a complete model lattice tower*, Building Research Establishment, 1985.

C.5 Structural response to wind

C.5.1 Procedure

C.5.1.1 General. The application of section five of Part 1 is described in outline in **C.5.1** to **C.5.5** and, in addition, **C.5.6** to **C.5.11** give a brief summary of the background, indicating the references and sources of data, and outlining the simplifications made.

Two methods of calculating the forces in tower members due to gusty wind are provided. Both methods represent the effect of an equivalent static loading due to mean hourly wind speed effects acting in the wind direction, together with the fluctuating loading effects both downwind and crosswind due to gustiness.

The equivalent static method includes an allowance for the dynamic amplification of response which is typical of the majority of towers that will be constructed in accordance with Part 1. This allowance is implicit in the gust factor, G , (see **C.5.7.3.4**) and in the load factor, γ_v , which is applied to the wind speed. The equivalent static method, however, is not appropriate for cases where the dynamic amplification would be greatly in excess of the assumed allowance thereby leading to reduced reliability. The check given in **5.1.1** of Part 1 has been formulated to prevent such inappropriate use of the static design procedure. The objective of the check was to ensure that the maximum combined load effect for the specific structure considered would not be more than 10 % greater than that assumed for the reliability analysis, the latter being the typical structure designed fully in accordance with Part 1.

The complexity of undertaking a full analysis of dynamic response (see **5.4** and Appendix E both of Part 1) is such that the check for applicability of the static procedure should be considered for guidance only. Dynamic augmentation generally increases in successively higher panels of any tower, but particularly when supporting large concentrations of ancillary items or by the use of a concave outline profile (Eiffelization); the designer is recommended to exercise caution in applying the static procedure to towers where these effects are considerably more than those typically encountered.

C.5.1.2 Equivalent static method. The equivalent static method is a procedure in which some allowance for typical dynamic amplification is made in the gust response factors. This has been developed for towers which are not dynamically sensitive and should be suitable for the majority of towers. For this reason, the procedure has been codified for use over the complete range of structures encompassed by Part 1.

C.5.1.3 Spectral analytical method. The spectral analytical method uses techniques for which only the principles and important parameters are set out in Part 1. These are discussed briefly in **C.5.4**.

C.5.1.4 Deflections. Deflections are normally only required for serviceability and may be required for both mean steady state conditions and peak instantaneous values.

The criteria for these are described in **C.5.2.5**.

C.5.1.5 Vortex-excited vibrations. Part 1 provides guidance on the calculation of the response of a tower, mounted with a bluff body of cylindrical form, to crosswind vibrations due to vortex excitation. The procedure is described in **C.5.5**.

There may also be problems of vortex shedding from dense (high solidity) lattices, which may also result in negative aerodynamic damping. However, to date there have been no specific studies carried out into this aspect, and no firm guidance can be given. It is recommended that until such studies are made, for cases where the solidity ratio, ϕ , is greater than about 0.8, wind tunnel tests are undertaken to check for vortex shedding susceptibility.

C.5.2 Wind loading for symmetrical towers

C.5.2.1 General. For towers free from ancillaries, or containing ancillaries complying with the constraints of 4.1.3 of Part 1 the three components of wind loading are defined as:

- a) due to the mean hourly wind speed in the direction of the wind, i.e. downwind, \bar{P}_{TW} ;
- a) due to the fluctuating components downwind, P'_{TW} ;
- a) due to the fluctuating components crosswind, P'_{TW} .

The mean load, \bar{P} , is defined simply as the product of the resistance, R_W , and the dynamic pressure head, $0.5 \rho_a \bar{V}^2$, for each panel of the tower. The fluctuating downwind component is represented by the mean load times the gust response factor, G , appropriate to *the member under consideration* and the fluctuating crosswind component is taken as a proportion of the downwind component as described in C.5.2.6.

C.5.2.2 Gust response factors. The gust response factors take into account both the correlation of gusts in the wind, which cause the peak instantaneous loading effects in the member under consideration, and the structural response of the tower itself to such effects. For members whose response is affected by loading over the whole tower, such as leg members at the base of the structure under tower body wind effects, the gust response factors are relatively low. This is because it is unlikely for high-intensity gusts to occur simultaneously over the whole height of the tower. The forces in such members, however, due to loading from a dish aerial, for example, will be relatively high as peak gusts can occur over the small dimension of the aerial.

The gust response factors for calculating load effects due to overall cantilever bending of the tower are also different from those for calculating load effects due to overall shear, due to the load influence diagrams to be considered in the correlation of gusts. It is thus necessary to first calculate a basic gust factor, G_B , appropriate for bending effects.

Two methods of calculating the basic gust response factor, G_B , are given. The first (see 5.2.2.2 of Part 1) involves the calculation of the basic gust response factor to be derived from the product of a height factor, j , and a size factor, B . These factors account for the correlation of gusts according to the height of the structure and the position at which the gust response factor is required.

The factor j specifically makes allowance for the position of the member under consideration within the height of the tower. This is a significant advance on other codified procedures of gust response factors [5.1, 5.2], which ignore this aspect. Both factors are also functions of the site terrain roughness categories.

The second method (see 5.2.2.3 of Part 1) is in a simplified form in which the variation of gust factor with a height is eliminated from the calculation by the incorporation of factors which allow for increases in gust factor with height up the tower. This basic gust factor, plotted in Figure 5.3 of Part 1, is thus the greater of that at the base of the tower, and that appropriate to the top tenth of the height (or the top 10 m, whichever is greater)

The use of the more rigorous method will generally result in lower values of gust factor for tower body loads, particularly for high towers in smooth terrain or low towers in rough terrain, where the reduction may be of the order of 10 %. The more rigorous method has in any case to be used for the calculation of loads on large ancillary items and their connections to the tower (see C.5.3).

Whichever method is adopted it has to be emphasized that only one *analysis* of the tower is required, under factored mean hourly wind loading, the appropriate gust response factors being applied to the mean hourly load effects to obtain the required gust load effects.

C.5.2.3 Gust response factors for bending effects. For bending effects, the gust factor, G , is taken as $G_B \{1 + 0.2 (z_m/H)^2\}$, the correlation effects being accounted for by the position of the point to be considered in relation to the height of the tower. The additional factor $\{1 + 0.2 (z_m/H)^2\}$ is described in C.2.7.2.

C.5.2.4 Gust response factors for shear forces. The gust response factors for bending effects are not suitable, without modification, for shear effects in which the load effects depend on the difference of gust speeds from point to point. The bending gust factor is thus modified by a factor K_q to obtain the appropriate shear gust factor as follows.

Consider the bracing members in the case illustrated in Figure C.5.1. These may carry small loads due to mean load effects, the moment due to the loads above the intersection of the legs partly balancing the moment due to the loads below the intersection. Part 1 provides a means of predicting the peak bracing forces by modifying the basic gust response factor by a factor, K_q , which depends on the fraction, f_q , of the total shear under mean wind loading carried by the bracing. The derivation of the factor K_q is given in C.5.8. As may be seen from Figure 5.4 of Part 1, K_q is always greater than unity and can be very high. Thus bracing forces can be significantly higher than one would obtain from traditional static procedures which could give very low forces in balanced situations.

Special care should be taken with bracing members at bend lines, for example, which carry a combination of shear and components of leg bending forces. The part of the loading due to shear should be factored by $K_q G$, and that due to bending, i.e. the leg load component, should be factored by G only. Since $K_q > 1$, cases where the majority of the loading in the bracing is due to shear could be treated by taking $K_q G$ throughout. However, generally it will be necessary to determine the partition of load effects. Where K_q tends to unity, this is clearly not necessary as $K_q G$ applied to the total loads will produce an upper bound estimate of the load effects, without being unduly conservative.

C.5.2.5 Deflections. Deflections, if required, will be needed to check serviceability requirements, to be specified to the designer. Two such criteria can be considered in Part 1. The first criterion allows a specified deflection or rotational limit to be exceeded occasionally under gust effects. In such cases the peak deflection should be calculated. The deflection or rotation from the mean hourly analysis is thus factored by $(1 + G)$ where G is the gust response factor appropriate to bending at the base of the tower. The resulting periods during which this deflection might be exceeded are obtained from 3.3 of Part 1, as described in C.3.3. The second criterion allows the deflection to be exceeded 50 % of the time under the mean hourly wind effects only, and the deflection or rotation from the mean hourly analysis can be used directly.

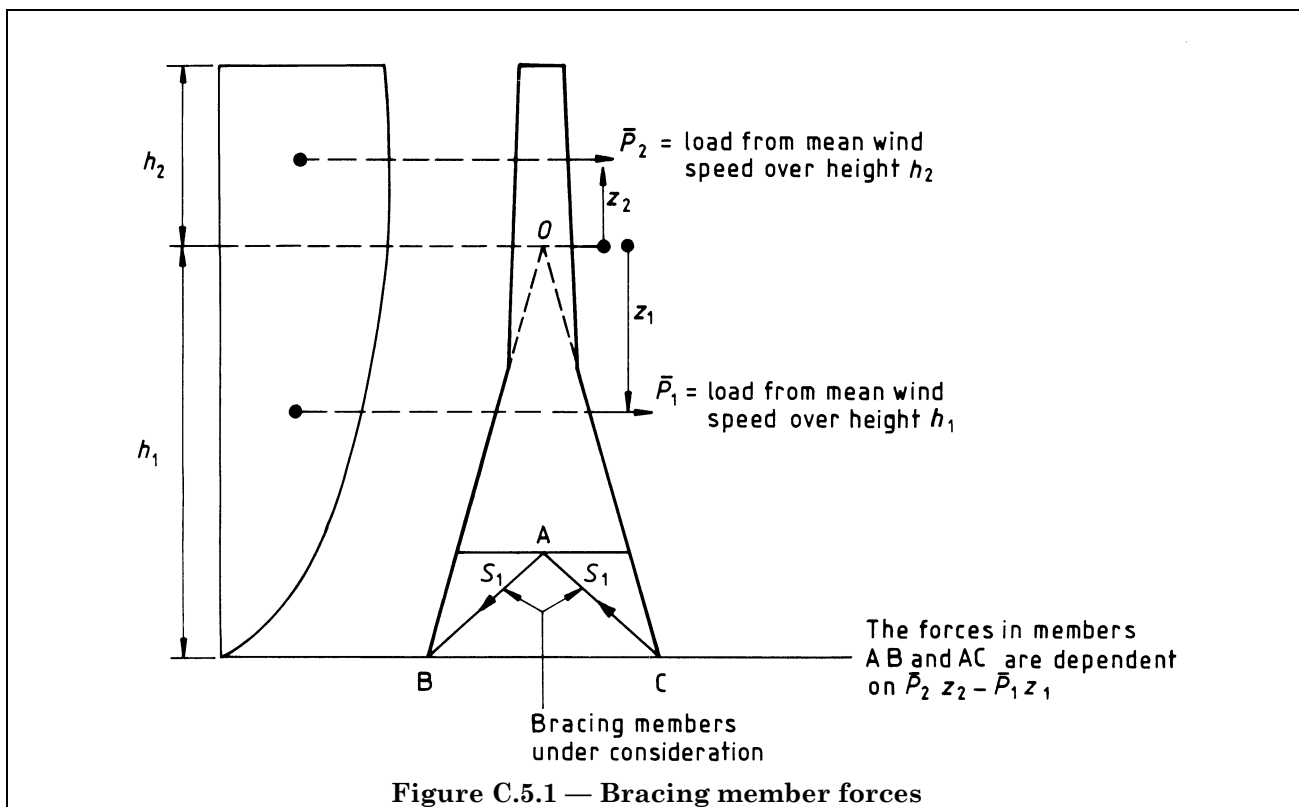


Figure C.5.1 — Bracing member forces

C.5.2.6 Calculation of wind forces in tower members. Having obtained the maximum member forces under the mean wind loading effects, the total force in each member can then be determined by factoring the mean hourly load effects by $(1 + G)$, provided crosswind effects can be ignored, where G is the gust response factor appropriate to the level and type of the member under consideration.

For sensibly symmetric square and triangular towers, it is generally not necessary to calculate crosswind effects, for the following reasons.

For a free-standing square-section lattice tower, the highest loads in the main legs may be assumed to occur for wind along the diagonal, where essentially the force from the mean wind and longitudinal turbulence component is resisted by the two main legs on the diagonal in line with the main wind direction. Thus, forces induced by lateral turbulence (which are considerably smaller) would be resisted entirely by the main legs on the opposite diagonal, and crosswind loads would not need to be considered as a design criteria.

The influence of lateral turbulence on the forces in panel bracing members in square towers depends on the degree of taper of the main legs. For parallel or slightly tapered panels, the highest bracing loads are produced by wind normal to a tower face, reducing slightly to about 90 % of this value for mean wind directions nearer the tower diagonal. However, for more acutely tapered panels, where gust actions form the major part of the total bracing load, it has been calculated that maximum loads occur for wind along the diagonal. The increase in member load due to the crosswind effect is predicted to be small, with an upper bound of the order of 12 % for the case of bracing carrying a mean wind load component of zero. However, provided $K_\theta \leq 1.25$, wind normal to a tower face always governs for bracings, and crosswind effects can be neglected.

For triangular towers, the maximum leg loads occur in the single leg on the axis of the tower in the mean wind direction, with the mean wind normal to one face. For this member, the forces induced by lateral turbulence may be assumed to be negligible. For bracing members, the maximum forces occur for wind parallel to a face in the plane of bracing in the mean wind direction. Crosswind forces due to turbulence will not affect these members. For the bracing members in the two inclined faces (in the case of wind normal to one face) the contribution from lateral turbulence (crosswind) will increase the member forces resulting from in-line gust. The increase is predicted to be marginal, however, and for sensibly symmetric triangular towers, the maximum in-line gust forces for this case will be smaller than for the case of wind parallel to one face, and the crosswind forces can be shown not to increase the total to more than the maximum bracing forces obtained for the case of wind parallel to one face. For both legs and bracings it can be shown that the normally assumed governing directions already stated apply, provided the ratio of wind resistances in the two orthogonal directions are within 10 % of each other. Otherwise, the maximum increase in member load due to consideration of crosswind effects has an upper bound of about 4 %.

If, however, crosswind effects need to be considered, such as in unsymmetrical towers, the following approach has been adopted.

It has been well established that there is no tendency for the wind direction to veer from the mean as gust speeds reach maximum, and therefore the correlation between longitudinal and lateral turbulence components is zero. Hence, if crosswind forces need to be considered, it may be assumed that the fluctuating downwind and crosswind effects are uncorrelated and the forces due to these effects can be calculated by the normally accepted square root of the sum of the squares of each effect.

If the resistances of each panel in the downwind and crosswind directions R_W and R_X , respectively, are identical (or are in the same proportion throughout the tower as may sometimes be the case for unsymmetric towers), then the maximum total force can be determined by factoring the appropriate maximum mean hourly load effect by:

$$\left[1 + G \left\{ 1 + f_x^2 K_x^2 \left(\frac{R_x}{R_w} \right)^2 \right\}^{1/2} \right]$$

where

K_x is the reduction factor described in the following text;

f_x is the ratio of the crosswind to the downwind forces under mean hourly loading in the particular member being considered.

In many governing cases, $f_x \approx 0$, since crosswind loads will be transmitted by different members to those carrying the downwind loads, and the total forces can still be obtained by factoring the mean wind forces by $(1 + G)$, as in the previously discussed cases of symmetric square and triangular towers.

However, further analyses may be necessary if the ratio of the resistances in the two orthogonal directions differs over the height of the tower. In such circumstances, an analysis under the mean hourly loading, applied in the crosswind direction should be used. The fluctuating crosswind component in each element can then be determined by factoring this mean hourly loading effect by the appropriate gust factor, and multiplying the resulting load effect by a reduction factor, K_x , to account for the reduced lateral turbulence.

The reduction factor, K_x , has been taken as 0.5 on load effects to allow for reduced crosswind turbulence, and takes account of several contributing factors. These are primarily:

- a) a reduction to allow for the magnitude of the ratio of lateral to longitudinal intensity of turbulence which is less than unity and although the ratio varies slightly with height has been shown to be generally of the order of 0.7 [5.3, 5.4];
- b) a reduction based on Davenport's linearization equation for the spectrum of lift [5.5];
- c) an increase due to the reduced aerodynamic damping occurring in the crosswind direction.

There can be situations where the value of K_x may vary from the value of 0.5 given in Part 1, but with the present state of knowledge this value will generally provide a reasonable upper bound value for loading from crosswind turbulence. In particular, there may be some qualification on this factor for high-solidity heavily-iced towers, which have shown some indication of crosswind response, but as the downwind drag coefficients for such structures are to be viewed with caution (see C.4) no additional qualification is required in Part 1. Further full-scale measurements and research are required into possible forcing mechanisms for such configurations.

C.5.3 Wind loading for towers with complex attachments

C.5.3.1 General. For towers containing large complex attachments, such as dish aerials or lighting arrays, the member forces have to allow for both loading on the tower body itself, and the loading on the individual attachment. The resistance of the panel containing the attachment, assuming it does not comply with the constraints of 4.1.3 of Part 1, will have initially been calculated as the combined resistance of the structural members of the tower and the attachment itself. It is then necessary, in order to apportion the appropriate gust response factors, to calculate the resistance of the attachment itself and that of the partially shielded tower body. This is shown diagrammatically in Figure C.5.2. Analysis of the tower, partially shielded where appropriate, under mean hourly wind effects is then undertaken and, additionally, member forces are determined due to the effect of mean hourly wind speeds separately on each major attachment. The appropriate gust response factors for each component of loading are then determined.

The basic gust response factor, G_B , for tower body loading allows for cross-correlation effects over the full height of a tower from a point under consideration to the top. However, as an ancillary item or cable may be located at any position on the tower, it is unlikely that the uppermost edge coincides with the top of the tower supporting it and the direct use of the method is not valid. The approach detailed in 5.3.2 is thus used, depending on the load effect considered.

C.5.3.2 Wind loading for ancillary items

C.5.3.2.1 Loading for bending and shear. For a major attachment, H is replaced by z_A , the height to the centre of the item, and $H - z$ is replaced by e_A , the vertical dimension of the item, which should not be taken as less than 10 m when using Figures 5.1 and 5.2 of Part 1.

As the loads on the ancillaries and on the tower body may be fully correlated, it is expedient to add the gust load from each ancillary directly to the gust load from the wind action on the main body of the tower to provide a conservative estimate of member forces (see C.5.3.4).

C.5.3.2.2 Loading for torsion. The relatively small distance between the centre of an ancillary item and the axis of rotation of the tower in relation to the crosswind scale of turbulence is such that gust loads on each item should be treated as fully correlated with those on adjacent parts of the tower.

Although the tower would be susceptible to additional torsional oscillation due to gust action at frequencies close to torsional natural frequencies, for towers of conventional design the fundamental torsional natural frequency would probably be at least three times the fundamental bending frequency, and thus correspond to the upper end of the gust spectrum where the excitation energy is much smaller.

Aerodynamic damping from the tower body of the torsional mode response would be expected to be somewhat lower than for the bending mode, as the relative velocity between tower members and the air flow (proportional to the square of the distance from the axis of rotation) is reduced for the bracing members near the centre of tower faces. However, the aerodynamic damping from the ancillary item itself for the same reasons would be relatively large in relation to that for the tower body and the total may thus be of the same order for both modes.

Structural damping which, at higher frequencies, is likely to predominate, would be expected to be higher for torsional oscillation than for bending. Torsional motion involves shearing across all panels and the energy dissipated by friction from the movements at structural connections could be of the order of twice that for bending of the tower parallel to a face, where only half the panels are significantly loaded.

It is thus considered that dynamic effects due to torsional modes of vibration are not proportionally greater than for bending oscillations for which such effects contribute little to the total response. The gust response factor derived for bending may, therefore, conveniently be used.

C.5.3.3 *Wind loading on cables.* For cables attached to the tower, the loading is calculated separately, according to 5.3.3 of Part 1, the gust response factor allowing for correlation relating to the length and height of the cables.

It should be noted that Part 1 only provides a means of predicting the wind load on the cable. Loads on the tower due to cable tensions have to be calculated, as appropriate.

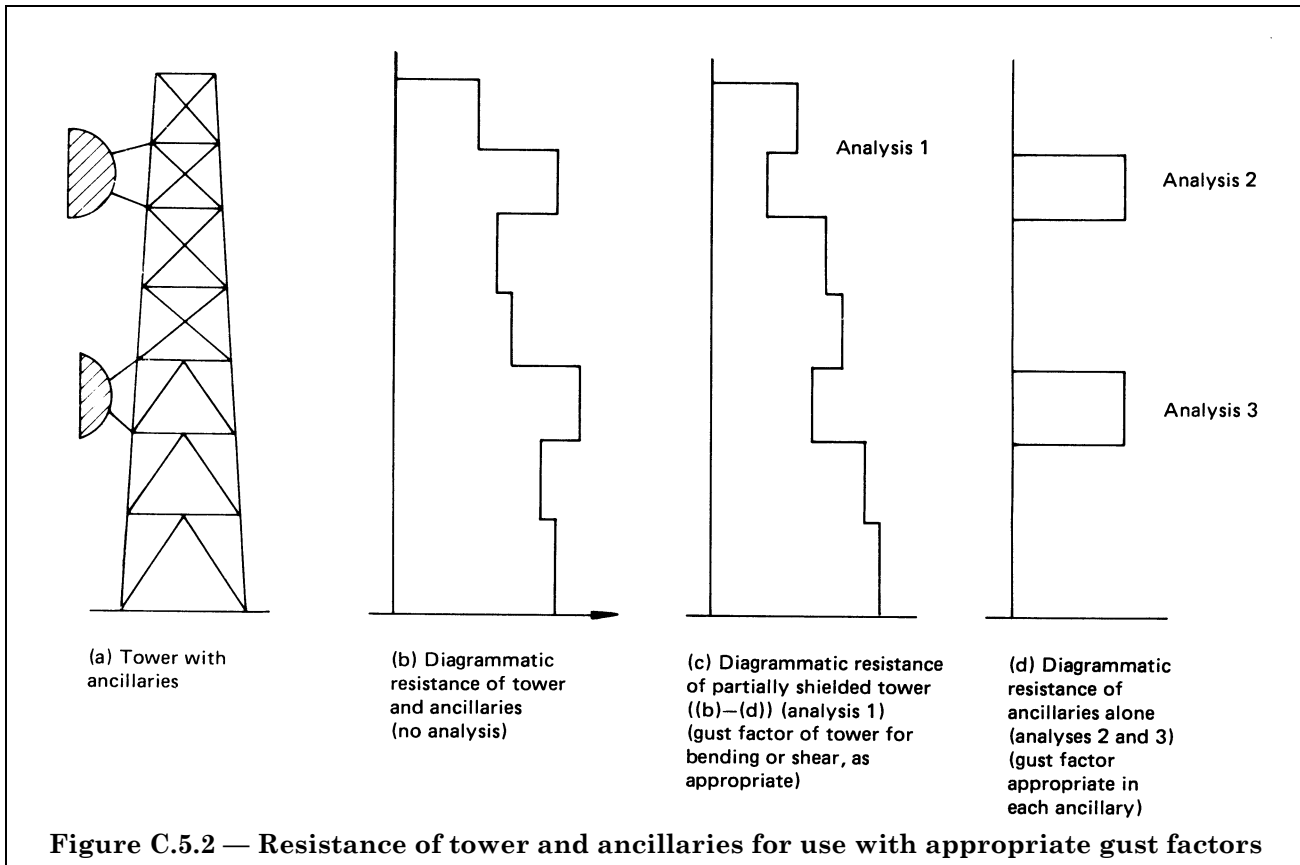
C.5.3.4 *Calculation of wind forces in tower members.* The total force in any member is then assembled from the mean loading effects, and the fluctuating components, in accordance with the procedure given in 5.3.4 of Part 1. In this the mean hourly wind effects are directly additive, and could be determined from one mean hourly wind loading analysis. However, it is necessary to calculate separately the fluctuating components due to each attachment, as well as the tower itself and for this separate analyses under mean wind loading for each attachment will be required. This is shown diagrammatically in Figure C.5.3. Crosswind components also need to be computed, and these may require separate analyses and since it is assumed that all the fluctuating components are uncorrelated (see also C.5.2.6), the maximum fluctuating force in a member is calculated as the square root of the sum of the squares of the components in the direction of the wind, the crosswind components, and the components due to wind loads on any cables.

For mean hourly load effects on the equivalent shielded tower, generally at least two orthogonal face-on cases, plus two corner-on cases are required to produce the appropriate maxima in bracings and legs and cater for crosswind effects. According to the variation of mean hourly loads on panels over the height of the tower, and the variation of loads around each face and diagonal, the number of analyses may need to be increased to obtain maximum mean hourly effects in *all* members throughout the height of the tower.

However, for towers of symmetric construction, not only will the crosswind effects be small, but their values may be estimated from symmetry using results from adjacent panels at any level, and the number of basic cases can thus be reduced.

In addition, there will be the appropriate mean hourly analyses for loads in each set of attachments each with their relevant values of the gust response factor for ancillary items, G_A . The same considerations with regard to face-on/corner-on wind loads and maximum member effects also apply, and the use of adjacent panel values for crosswind effects by symmetry may sometimes be justified, depending on the disposition of the ancillaries.

There will need to be a separate analysis for dead load effects, the results being factored by the appropriate value of the partial safety factor on dead load, γ_{DL} , depending on whether these are additive to or subtractive from the maximum wind load effect. Thus for maximum leg tension or uplift at foundations the lower γ_{DL} should be used, but otherwise the higher factor will generally be appropriate. Special considerations may be required for horizontal bracings at bend-lines which may always be in tension.



Thus, in general terms the maximum member forces, ΣF_{\max} are derived as follows:

$$\Sigma F_{\max} = F_{DL} + \Sigma \bar{F}_W + \Sigma F'_W \sqrt{\left\{ 1 + \left(\frac{\Sigma F'_X}{\Sigma F'_W} \right)^2 \right\}}$$

where

- F_{DL} is the force in the member due to dead load;
- $\Sigma \bar{F}_W$ is the summation of the forces in the member due to all mean wind load effects in the direction of the wind given by:

$$\Sigma \bar{F}_W = (\bar{F}_{TE} + \Sigma \bar{F}_{AW})_{\max}$$

where

- \bar{F}_{TE} is the equivalent force in the member due to mean wind loading on the partially shielded tower body;
- $\Sigma \bar{F}_{AW}$ is the summation of the forces in the member due to mean wind loading from each separate analysis of the ancillaries;
- $\Sigma F'_W$ is the summation of the forces in the member due to all fluctuating wind effects in the direction of the wind given by:

$$\{G\bar{F}_{TE} + \Sigma (G_A \bar{F}_{AW})\}_{\max}$$

where

- G is the gust response factor appropriate to the member being considered;
- G_A is the gust response factor appropriate to the size and height of each of the ancillaries;
- \bar{F}_{AW} is the force in the member due to mean wind loading on each of the ancillaries;
- $\Sigma F'_X$ is the summation of the forces in the member due to all fluctuating wind effects in the crosswind direction given by:

$$\Sigma F'_X = K_X \{G\bar{F}_{TEX} + \Sigma (G_A \bar{F}_{AX})\}_{\max}$$

where

\bar{F}_{TEX} is the value of \bar{F}_{TE} in the crosswind direction;

\bar{F}_{AX} is the value of \bar{F}_{AW} in the crosswind direction (from each separate analysis of the ancillaries);

K_X is the crosswind intensity of turbulence factor as defined in 5.2.1 of Part 1.

Suffix X indicates \bar{F} due to mean hourly loads at right angles to the maximum considered direction, and the summation allows for the number of analyses under mean wind load effects. The results thus need to be carefully tabulated and summated.

For many situations, it may be adequate to derive upper-bound approximate values only. In these cases for square (or triangular) towers, with $\bar{F}_{\text{AW}} \approx \bar{F}_{\text{AX}}$:

$\bar{F}_X \leq \bar{F}_W$ for legs;

($\bar{F}_X \rightarrow 0$ for bracings).

For G_A values of similar order to G , i.e. appropriate to the member being considered, a close approximation to the maximum member force is given by:

$$\Sigma F_{\text{max}} = F_{\text{DL}} + \Sigma \bar{F}_W + 1.12 (\Sigma F'_W)$$

giving

$$\Sigma F_{\text{max}} = [F_{\text{DL}} + \bar{F}_{\text{TE}} (1 + 1.12 G) + \Sigma \{\bar{F}_A (1 + 1.12 G_A)\}]_{\text{max}}$$

For initial checking purposes this may be further simplified to:

$$\Sigma F_{\text{max}} = F_{\text{DL}} + (\bar{F}_{\text{TE max}} + \Sigma \bar{F}_{\text{A max}}) (1 + 1.12 G^*)$$

where

$$G^* = \frac{\{G \bar{F}_{\text{TE}} + \Sigma (G_A \bar{F}_A)\}_{\text{max}}}{(\bar{F}_{\text{TE}} + \Sigma \bar{F}_A)_{\text{max}}}$$

$\approx G$ unless load effects due to ancillaries are very significant or G_A values are very different from G at level concerned.

C.5.3.5 Deflections for serviceability checks. The maximum deflections, δ , from each of the mean hourly analyses have to be summated to produce the required value of Δ for 3.3.2 of Part 1 in accordance with 5.2.5 b) of Part 1:

$$\Delta = \Sigma \delta = \delta_{\text{TE}} + \Sigma \delta_A = \bar{\Delta}$$

or for 5.2.5 a) of Part 1, where fluctuating components required:

$$\Delta = (1 + G_B) \delta_{\text{TE}} + \Sigma \{(1 + G_A) \delta_A\}$$

where

G_B is the gust response factor for the tower base, $z = 0$, i.e. the basic gust response factor;

δ_{TE} is the deflection relating to mean hourly loading on the partially shielded tower body;

G_A is the gust response factor appropriate to each ancillary (or set of ancillaries) analysed separately;

δ_A is the deflection appropriate to each ancillary (or set of ancillaries) analysed separately.

C.5.4 Spectral analytical method

Part 1 allows the use of spectral methods of analysis and provides, in its Appendix E, the basic parameters that would be required for such an analytical procedure. It was not considered practicable to set down in codified form the detailed analytical methods, but recourse should be made to published sources for further information [5.6, 5.7, 5.8, 5.9].

The parameters for wind structure, given in Appendix E of Part 1, are generally accepted for the UK wind climate. Caution should be exercised, however, when applying these methods in other than temperate climates. The basis for the values of damping suggested in Appendix E of Part 1 is given in C.5.11.

C.5.5 Crosswind response due to vortex excitation

C.5.5.1 Critical wind speed. The wind speed causing onset of significant vibration of a tower subject to vortex excitation in steady air flow corresponds closely to that at which the frequency of vortex shedding equals the lowest natural frequency of the structure. The shedding frequency, n , in such flow has been experimentally established as being related to speed, V , and width, D , of the body causing the vortices by the Strouhal number $S = nD/V$.

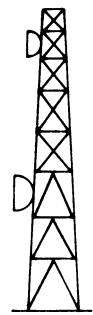
The value of S for a circular cylinder is nearly constant at a value of 0.2 for all practical Reynolds numbers if the cylinder is free to vibrate [5.10, 5.11]. Similarly, for sharp-edged bodies, the value of S is practically invariant at 0.16 [5.12] for a square section. This value provides a safe estimate of critical speed for other such bodies [5.13].

For significant amplitudes to build-up, excitation has to occur at the critical frequency for periods of time equal to a large multiple of the natural period of the structure, dependent on the structural damping. Thus, maximum response will correspond to averaging periods of the order of 1 min to 2 min, which will be approximately 1.3 times the mean hourly speed at the heights at which the cylinders would normally be mounted. It has therefore been considered adequate to require the critical speed to exceed $1.3 \bar{V}_z$. It has been found from field observations that the use of measured mean speeds correlates satisfactorily with the steady flow Strouhal numbers.

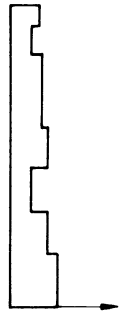
C.5.5.2 Excitation. The dynamic loading is based on a deterministic assessment of extreme response at the critical wind speed. A general discussion of the aerodynamic response of cylindrical bodies is contained in references [5.12, 5.14 and 5.15], from which it will be seen that the excitation forces are dependent on the Strouhal number, Reynolds number and vibration amplitude. The correlation of vortex shedding, turbulence and the position of separation points all influence response. In the majority of instances in which such response is significant, the critical wind speeds will correspond to Reynolds numbers in the range greater than 10^6 within which vortex shedding tends to be steady. Moreover, in such cases the tower will be in motion tending to cause the vortices to lock-in and become fully correlated. It has, therefore, been considered appropriate to adopt the deterministic approach which has been found to provide satisfactory predictions of peak amplitudes in practice [5.16].

With practical levels of structural damping ($\delta_s \approx 0.05$) the use of the stochastic treatment of random response, which would be appropriate if tower amplitudes were small, would produce extreme values of excitation of the order of half those given by the deterministic method.

The fluctuating lift coefficient appropriate to peak response for circular cylinders presented in 5.5.2 of Part 1 has been based on wind tunnel measurements and field observations some of which are plotted against Reynolds number in Figure C.5.4. Also shown for comparison is the relationship given in the Czechoslovak loading standard [5.17] which appears to be very conservative, although it has been shown that there is a tendency for the coefficient to increase below a Reynolds number of 4×10^5 .



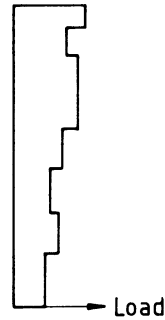
(i) Tower



(ii) Diagrammatic resistance of partially shielded tower

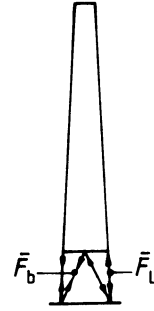


(iii) Mean hourly wind speed

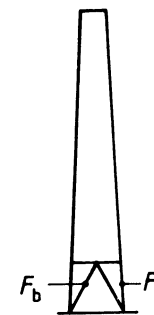


(iv) Mean hourly loading

Analysis undertaken for this loading



(v) Mean forces in members



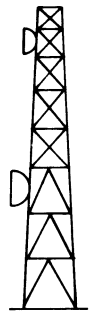
$$\Sigma F_l = \bar{F}_l (1 + G_l) + \bar{F}_{lA1} (1 + G_{A1}) + \bar{F}_{lA2} (1 + G_{A2})$$

$$\Sigma F_b = \bar{F}_b (1 + G_b) + \bar{F}_{bA1} (1 + G_{A1}) + \bar{F}_{bA2} (1 + G_{A2})$$

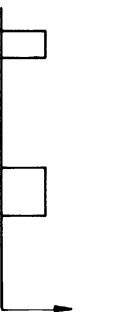
NOTE 1 In this figure, suffices l and b indicate leg and bracing members, respectively.

NOTE 2 If crosswind forces need to be considered analysis (a) and (b) may need to be repeated if the ratio of resistances differ in the two orthogonal directions over the height of the tower.

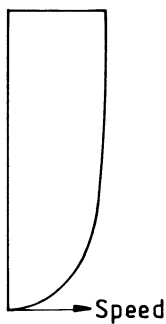
(a) Tower analysis for moments and shears due to tower body loading



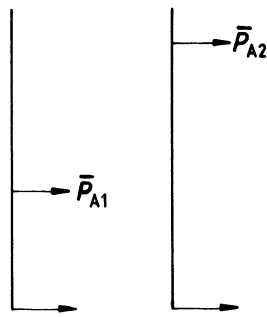
(i) Tower



(ii) Diagrammatic resistance of ancillaries

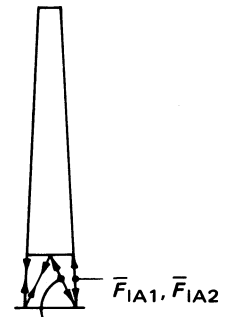


(iii) Mean hourly wind speed



(iv) Mean hourly loading

Analysis undertaken for each load separately



(v) Mean forces in members

(b) Tower analysis for load effects due to ancillaries (not complying with 4.1.3 of Part 1)

Figure C.5.3 — Forces in members

When the wind speed exceeds the critical value for a circular cylinder (or a part of it when the speed varies along its length), vibrations will continue but with excitation diminishing as the speed increases. The effective excitation coefficient, k_e , is introduced to allow for this based on the observations of Scruton and Flint [5.12] and others. For square cylinders, the galloping mechanism of excitation operates at still higher speeds and allowance for this is made in Figure 5.8 of Part 1 again based on the work of Scruton and Flint [5.12].

C.5.6 General theory for derivation of gust factor

C.5.6.1 General. The theoretical approach adopted in developing section five of Part 1 relating to the response of towers to gusty winds is that given by Harris [5.18] and Wyatt [5.19]. The method is summarized for ease of reference in C.5.6.2 to C.5.6.5.

C.5.6.2 Total response. The maximum loading due to gusty wind, P_{\max} , is taken as:

$$P_{\max} = \bar{P}(1 + G) \quad (5.1)$$

where

\bar{P} is the mean wind load;

G is the gust factor, represents response due to the fluctuating components of wind. This includes both the quasi-static response and the narrow-band or modal response.

Thus:

$$G = \frac{g \sigma_T(F)}{\bar{F}} \quad (5.2)$$

where

g is a peak factor, dependent upon the effective frequency of the structure and the averaging period of the mean wind speed (see C.5.6.3);

\bar{F} is the mean wind load effect;

$\sigma_T(F)$ is the standard deviation of the total response taken as:

$$\sigma_T(F) = \sqrt{[\{\sigma(F)\}^2 + \{\sigma_q(F)\}^2]} \quad (5.3)$$

where

$\sigma(F)$ is the standard deviation of the quasi-static response (see C.5.6.4);

$\sigma_q(F)$ is the standard deviation of the narrow-band response in the q th mode (see C.5.6.5).

This assumes the quasi-static and dynamic response are completely uncorrelated.

C.5.6.3 Peak factor. The peak factor, g , is defined, by Davenport [5.20] as:

$$g = \sqrt{(2 \ln n_e t) + \frac{0.58}{\sqrt{(2 \ln n_e t)}}} \quad (5.4)$$

where

t is the averaging time of the near wind speed taken as 3 600 s;

n_e is the effective frequency, taken as:

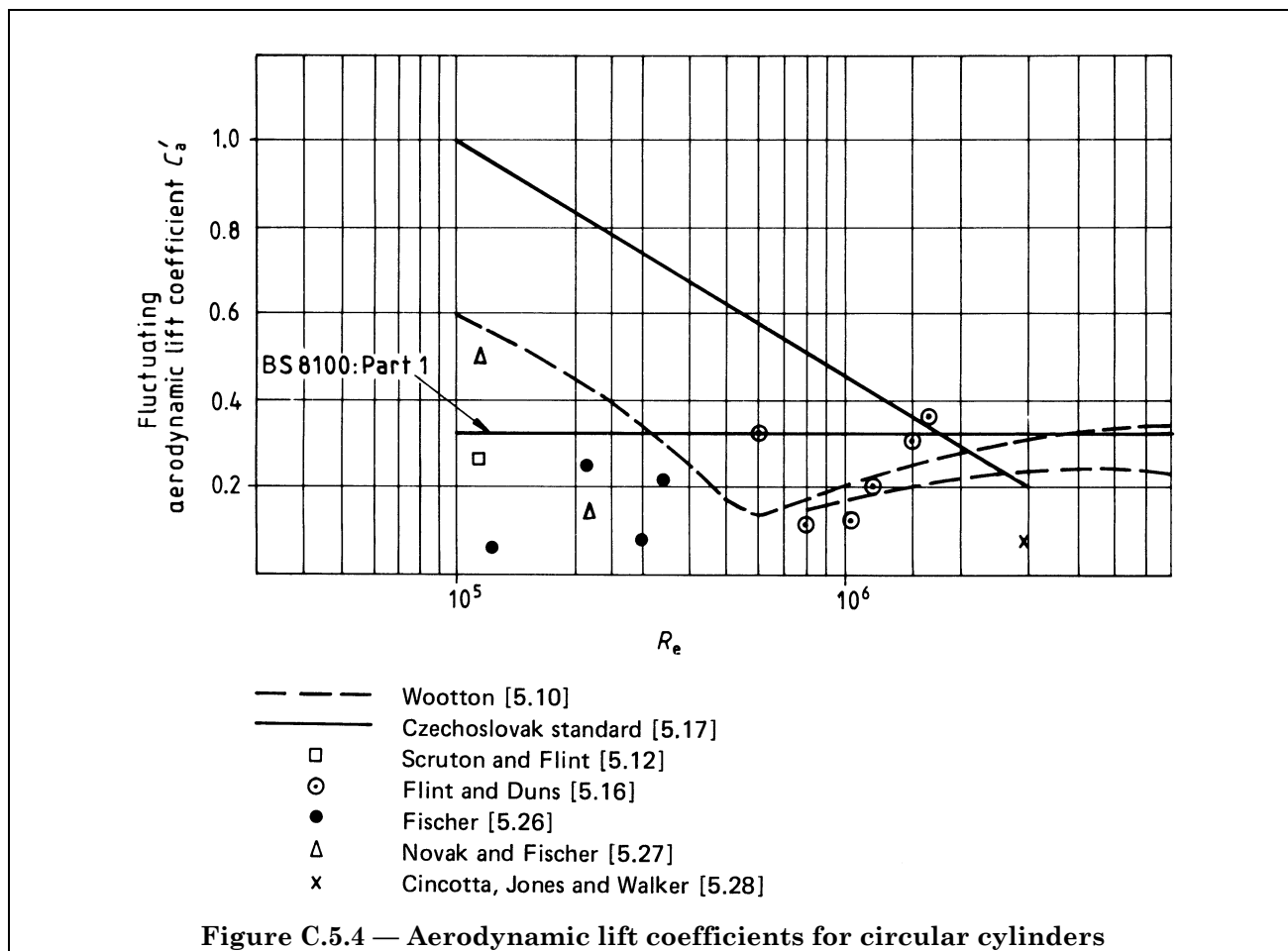
$$n_e = \frac{\sigma_1(F) n_1}{\sigma_T(F)} \text{ when only the first mode of vibration is considered}$$

where

n_1 is the fundamental natural frequency of the tower;

$\sigma_1(F)$ is the standard deviation of the narrow-band dynamic response in the first mode of vibration of the tower.

A plot of g against n_e is shown in Figure C.5.5, which shows that g varies from about 3.3 to 4.7. For practical cases of towers within the scope of Part 1 the range of g is narrower, from about 3.5 to 4.2 (see C.5.7.3.4).



C.5.6.4 Quasi-static response. It is assumed that the wind speed, V , over any element of a structure is given by the following expression:

$$V = \bar{V} + V'(A_i) \quad (5.5)$$

where

\bar{V} is the mean wind speed;

$V'(A_i)$ is the fluctuating wind speed on element i of area A_i .

The force or moment in any part of the structure due to the wind pressure acting on all elements is given by:

$$F = \sum_i 0.5 \rho_a R_i \beta(z_i) \{\bar{V} + V'(A_i)\}^2 \quad (5.6)$$

where

ρ_a is the air density;

R_i is the wind resistance of element i ;

$\beta(z_i)$ is the influence coefficient for the i th element relating the forces or moment in the part to the load applied to element i at a height z_i above the ground.

Neglecting $(V')^2(A_i)$ terms, reduces to:

$$F = \bar{F} + \rho_a \bar{V} \sum_i R_i \beta(z_i) V'(A_i) \quad (5.7)$$

where

$$\bar{F} = 0.5 \rho_a \sum_i R_i \beta(z_i) \bar{V}^2 \quad (5.8)$$

The variance of the fluctuating component is:

$$\sigma^2(F) = \{\rho_a \bar{V} \sigma(V')\}^2 \sum_i \sum_j R_i R_j \beta(z_i) \beta(z_j) c(A_i, A_j) \quad (5.9)$$

where

$c(A_i, A_j)$ is the correlation function (giving the time average of $V'(A_i)$ and $V'(A_j)$ for zero time lag);

$\sigma(V')$ is the r.m.s. value of $V'(A_i)$.

Hence the ratio of the variance to the mean force squared is:

$$\frac{\sigma^2(F)}{\bar{F}^2} = \frac{4 \sigma^2(V')}{\bar{V}^2 \sum_i R_i \beta(z_i)} \sum_i \sum_j R_i R_j \beta(z_i) \beta(z_j) c(A_i, A_j) \quad (5.10)$$

For a line-like structure of breadth b_z , and uniform drag coefficient C_f , R_i is equal to $C_f b_z$, and for vertical structures the mean wind speed is also a function of height. Equation (5.10) becomes:

$$\frac{\sigma^2(F)}{\bar{F}^2} = \frac{4 \sigma^2(V') \bar{V}_{10}^2 \int_0^H \int_0^H \bar{V}_z \bar{V}_{z'} b_z b_{z'} \beta(z) \beta(z') c(z-z') dz dz'}{(\int_0^H \bar{V}_z^2 b_z \beta(z) dz)^2} \quad (5.11)$$

where

\bar{V}_{10} is the mean wind speed at 10 m;

z, z' are the distances above ground of any two points.

This expression is simplified by introducing a non-dimensional influence coefficient γ_z defined by:

$$\gamma_z = \frac{\bar{V}_z b_z \beta(z)}{\bar{V}_0 b_0 \beta_0} \quad (5.12)$$

where the denominator gives the product of mean wind velocity, breadth and influence coefficient (dimensional) at some reference point on the structure, e.g. 10 m.

By separating out terms dependent on the variation of mean wind speed with height, the following expression is obtained:

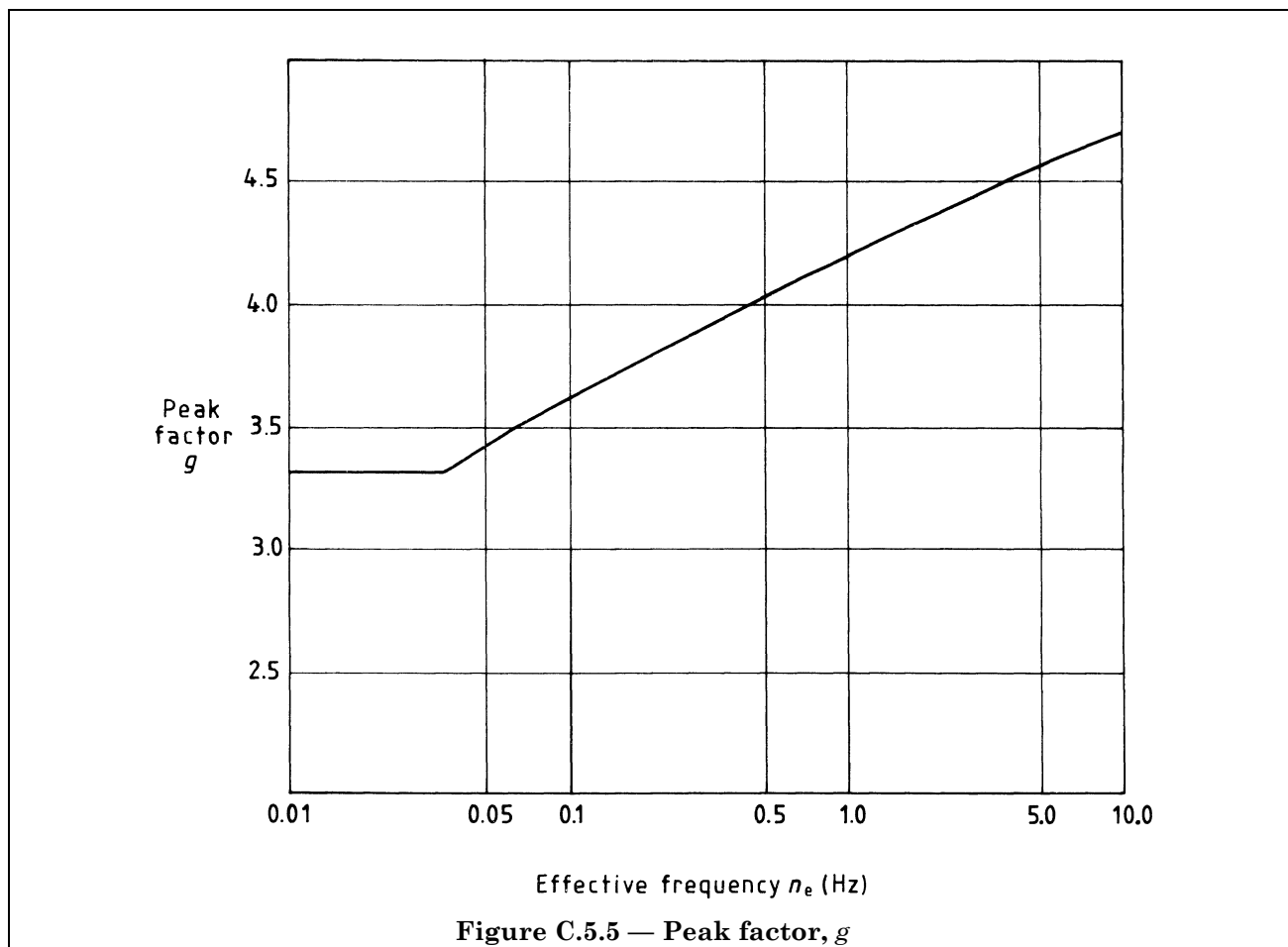
$$\frac{\sigma^2(F)}{\bar{F}^2} = 4 J_a^2 J_p^2 \frac{\sigma(V)^2}{\bar{V}_{10}^2} \quad (5.13)$$

where

J_a, J_p are the aerodynamic admittances defined as:

$$J_a^2 = \left(\frac{\int_0^H \gamma_z dz}{\int_0^H \gamma_z \frac{\bar{V}_z}{\bar{V}_{10}} dz} \right)^2 \quad (5.14)$$

$$J_p^2 = \frac{\int_0^H \int_0^H \gamma_z \gamma_{z'} c(z-z') dz dz'}{(\int_0^H \gamma_z dz)^2} \quad (5.15)$$



Hence

$$\frac{\sigma(F)}{\bar{F}} = 2 J_a J_p \frac{\sigma(V)}{\bar{V}_{10}} \quad (5.16)$$

C.5.6.5 Dynamic response. The power spectrum of force on the q th mode of a structure can be related to the wind gust power spectrum $S^v(n_q)$ in a similar way to the quasi-static loading, $S^p(n_q)$ [see equation (5.13)]:

$$\frac{n_q S^p(n_q)}{\bar{p}^2} = 4 J_{aq}^2 J_{pq}^2(n_q) \frac{n_q S^v(n_q)}{\bar{V}_{10}^2} \quad (5.17)$$

For lattice towers only the first mode is likely to cause a significant contribution to the dynamic response. Hence equation (5.17) can be simplified:

$$\frac{n_1 S^p(n_1)}{\bar{p}^2} = 4 J_a^2 J_p^2(n_1) \frac{n_1 S^v(n_1)}{\bar{V}_{10}^2} \quad (5.18)$$

where

\bar{p} is the mean generalized modal force in the fundamental mode;

J_a is the aerodynamic admittance, as defined in equation (5.14);

$$J_{P^2}(n_1) = \frac{\int_0^H \int_0^H \gamma_z \gamma_{z'} \frac{S^v(zz'n_1)}{S^v(n_1)} dz dz'}{(\int_0^H \gamma_{1z} dz)^2} \quad (5.19)$$

where

$$\gamma_{1z} = \frac{\mu_1(z) b_z \bar{V}_z}{b_o \bar{V}_o} \quad (5.20)$$

where

$\mu_1(z)$ defines the shape of the first mode.

The modal (narrow-band) response is given approximately by the following expression:

$$\sigma^2(Q_1) = \frac{n_1 S_1^P(n_1) \pi^2}{k_1^2 \times 2 \delta_1} \quad (5.21)$$

where

$\sigma^2(Q_1)$ is the variance of the first mode amplitude;

k_1 is the generalized stiffness in the first mode;

δ_1 is the logarithmic decrement of damping in the first mode.

The variance of the dynamic response of the force in a structural member is:

$$\sigma_1^2(F) = \sigma^2(Q_1) \beta_1^2 \quad (5.22)$$

where

β_1 is the mode influence coefficient relating load in the member to unit mode displacement.

Thus from equations (5.18), (5.21) and (5.22):

$$\frac{\sigma_1^2(F)}{\bar{P}^2} = \frac{2 n_1 S^v(n_1) J_a^2 J_{P1}^2(n_1) \pi^2 \beta_1^2}{k_1^2 \delta_1 \bar{V}_{10}^2} \quad (5.23)$$

$$\frac{\sigma_1(F)}{\bar{F}} = \frac{2 J_a J_{P1}(n_1) \pi \beta_1 \bar{P}}{k_1 \bar{F}} \left\{ \frac{n_1 S^v(n_1)}{2 \delta_1 \bar{V}_{10}^2} \right\}^{1/2}$$

C.5.7 Application of general theory in development of codification

C.5.7.1 General. The theory outlined in C.5.6 has been simplified by means of certain assumptions and presented in the form of 5.3 of Part 1. The simplification made in codification is summarized in C.5.7.2 and C.5.7.3.

C.5.7.2 Quasi-static contribution to total response

C.5.7.2.1 Aerodynamic admittances. In calculating the aerodynamic admittances, equation (5.14) has been simplified by putting for the bottom panel:

$$\gamma_z = \frac{z}{H} \quad (z = 0 \text{ to } H), \text{ after vickery [5.21]}$$

and

$$\frac{\bar{V}_z}{\bar{V}_{10}} = \left(\frac{z}{10} \right)^\alpha$$

which, for the bottom panel, yields:

$$J_a = \left(1 + \frac{\alpha}{2} \right) \left(\frac{10}{H} \right)^\alpha \quad (5.24)$$

The former assumption implies that the tower has a projected area per unit height decreasing with height such that $\bar{V}_z b_z$ is constant in equation (5.12). It has been found that departures from this assumption do not greatly influence the gust response.

The second assumption implies that the speed profile is that appropriate to non-hilly sites. The significance of the value of the index, α , or $\alpha - \mu$ for hill site profiles can be shown to be not significant.

The correlation function $c(z - z')$ in equation (5.11) depends only on the magnitude of the term $(z - z')$. Thus:

$$J_p^2 = \frac{2 \int_0^H c(z - z') \int_0^{H - (z - z')} \gamma_z^2 dz d(z - z')}{(\int_0^H \gamma_z dz)^2} \quad (5.25)$$

The correlation function $c(z - z')$ has been found experimentally [5.18] to be described by the simple exponential decay function

$$c(z - z') = e^{-\frac{z - z'}{L_x}} \quad (5.26)$$

where

L_x is the length scale of crosswind turbulence.

Assuming γ_z to be constant, the expression for J_p^2 reduces to:

$$J_p^2 = \frac{2}{H^2} \int_0^H e^{-\left(\frac{z - z'}{L_x}\right)} \{H - (z - z')\} d(z - z')$$

Hence

$$J_p^2 = \frac{2}{S} + \frac{2}{S^2} (e^{-S} - 1) \quad (5.27)$$

Where

$$S = \frac{H}{L_x}$$

The effect of γ_z being variable is allowed for by replacing the height of the structure H in the integral in the expression for J_p^2 by the equivalent height H_e where:

$$H_e = \frac{(\int_0^H \gamma_z dz)^2}{\int_0^H \gamma_z^2 dz}$$

and

$$H_e = \frac{3H}{4} \text{ when } \gamma_z = \frac{z}{H} \quad (5.28)$$

and thus

$$S = \frac{3H}{4L_x} \quad (5.29)$$

The aerodynamic admittances for panels other than at the tower base have been derived as follows.

The term dependent on the variation of mean wind speed with height in equation (5.11) is evaluated by taking the integral between the limits z and H , where z is the height above ground of the panel under consideration. The admittance term dependent only on separation [equation (5.15)] may be found by integrating between limits z and H or 0 and $(H - z)$. By substituting appropriate values for a range of tower heights and terrain types in equations (5.24), (5.27) and (5.13) (and raising the result to the power of two) yields the excitation by background turbulence given by:

$$\left(2 J_a J_p \frac{\sigma(V)}{V_{10}}\right)^2$$

Which for codification purposes is equivalent to $(B/gf)^2$ (see C.5.7.3.4).

This is plotted in Figure C.5.6.

C.5.7.2.2 Turbulence. The r.m.s. value of the fluctuating velocity in turbulent wind is taken as independent of height above ground and has been taken as (see **C.3.6**):

$$\sigma(V) = \frac{V_{3s} - \bar{V}_{10}}{3.3} \approx \frac{\bar{V}_{10}}{3.3} \left(\frac{1.6}{K_R} - 1 \right) \quad (5.30)$$

where

V_{3s} is the maximum 3 s gust speed;

K_R is the terrain roughness coefficient.

Equation (5.30) implies that $\sigma(V)$ increases with increasing roughness as assumed by Sfintesco and Wyatt [5.22]. This differs from the conclusion by Harris that it is terrain independent [5.18]. These differences are discussed in **C.3.6**.

C.5.7.3 Dynamic contribution to total response

C.5.7.3.1 Aerodynamic admittances. The expression for the aerodynamic admittance, J_a , is simplified as shown in **C.5.7.2.1**. The normalized cross spectrum contained in equation (5.19), $S^v(zz'n_1)/S^v(n_1)$ has been shown to be described by the following exponential function:

$$e^{-\frac{8n_1(z-z')}{\bar{V}_{10}}} \quad (5.31)$$

Again assuming γ_{1z} to be constant and replacing the upper integration limit by H from equation (5.28) gives:

$$J_{p1}^2(n_1) = \frac{2}{N} + \frac{2}{N^2} (e^{-N} - 1) \quad (5.32)$$

where

$$N = \frac{8H_e n_1}{\bar{V}_{10}} \quad (5.33)$$

The term $J_p^2(n)$ is plotted in Figure C.5.7 against $n_1 H / \bar{V}_H$ where \bar{V}_H is the mean velocity at height H .

C.5.7.3.2 Generalized modal force. It is assumed that the shape of the fundamental mode is identical to the deflected shape of the tower under the action of the mean wind, and as stated in **C.5.2.1**, higher modes of vibration can be ignored. It then follows that the static stiffness is the same as the generalized stiffness in the fundamental mode, and the loading of tower members corresponding to unit tip deflection are the same in both cases. Thus:

$$\bar{P}_1 \frac{\beta_1}{K_1} = \bar{F} \quad (5.34)$$

where

\bar{F} is the base moment from mean hourly effects;

\bar{P}_1 is the generalized force in the fundamental mode;

β_1 is the mode influence coefficient for the tower base;

K_1 is the generalized stiffness.

Hence from equations (5.23) and (5.34)

$$\frac{\sigma_1(F)}{\bar{F}} = 2 J_a J_{p1}(n_1) \pi \left\{ \frac{n_1 S^v(n_1)}{2 \delta_1 \bar{V}_{10}^2} \right\}^{1/2} \quad (5.35)$$

C.5.7.3.3 Significance of dynamic response. The expression for the gust response factor given in 5.3 of Part 1 is independent of frequency and damping, the dynamic response component of loading having been shown to be small and allowance having been made for it in a simplified way as follows.

The magnitude of the dynamic response, as a proportion of the quasi-static response is obtained as follows. Equation (5.2) may be re-expressed as

$$G = g f \frac{\sigma(F)}{\bar{F}} \quad (5.36)$$

where

f is a dynamic factor given by:

$$f = \left[1 + \left\{ \frac{\sigma_1(F)}{\sigma(F)} \right\}^2 \right]^{1/2} \quad (5.37)$$

From equations (5.16) and (5.35):

$$\left\{ \frac{\sigma_1(F)}{\sigma(F)} \right\}^2 = \frac{\{2 J_a J_P(n_1) \pi\}^2 \frac{n_1 S^v(n_1)}{2 \delta_1}}{\{2 J_a J_P \sigma(V)\}^2} \quad (5.38)$$

The expressions for $S^v(n_1)$, $J_P(n_1)$ and J_P can be simplified such that over the likely range of parameters encompassed by Part 1, equation (5.38) can be reduced to:

$$\left\{ \frac{\sigma_1(F)}{\sigma(F)} \right\}^2 \approx \frac{1}{150 H \delta_1} \left(\frac{\bar{V}_{10}}{n_1} \right)^{5/3} \quad (5.39)$$

The total damping, δ_1 , is represented by the sum of the aerodynamic, δ_a , and structural, δ_s , damping (see C.5.11), and where δ_a predominates, which is generally the case for inline response, for medium to tall towers, δ_1 may be approximated by:

$$\delta_1 = \frac{\rho_a \Sigma R_w \bar{V}_z}{2 n_1 \Sigma m}$$

where

ΣR_w is the sum of wind resistance of top third of tower;

Σm is the mass of top third of tower.

Thus equation (5.39) can be further simplified, and from equation (5.37), f may be expressed as:

$$f^2 \approx 1 + \frac{\Sigma m}{75 \rho_a \Sigma R_w H} \left(\frac{\bar{V}_{10}}{n_1} \right)^{2/3} \quad (5.40)$$

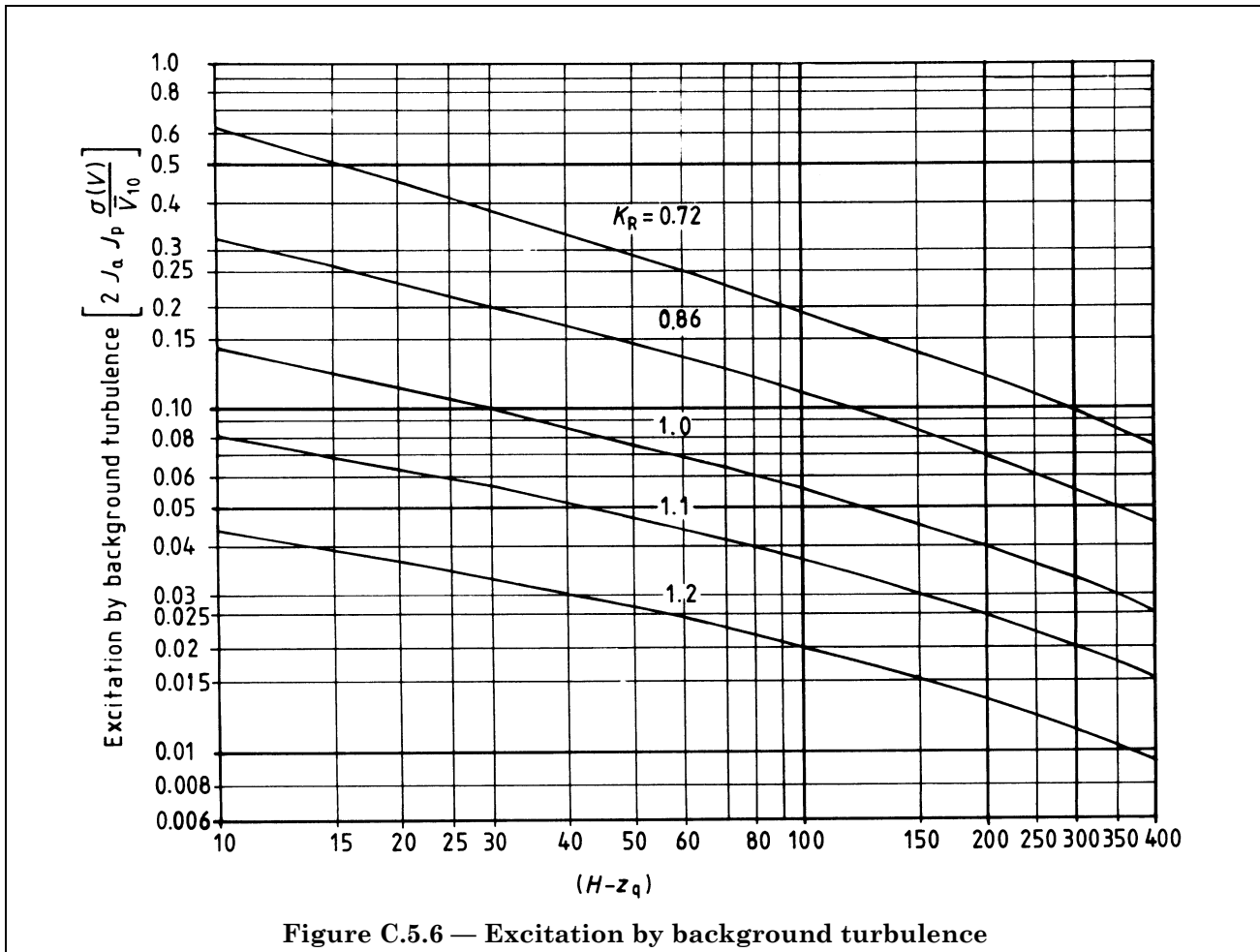
$$\text{As } m = \rho_s A_{av} \left(\frac{H}{3} \right)$$

where

ρ_s is the density of the material of the tower structure;

A_{av} is the average cross-sectional area of the tower.

$$f^2 \approx 1 + \frac{1}{225} \left(\frac{\rho_s}{\rho_a} \right) \left(\frac{A_{av}}{\Sigma R_w} \right) \left(\frac{\bar{V}_{10}}{n_1} \right)^{2/3} \quad (5.41)$$



Taking typical values of \bar{V}_{10} , n_1 , and member sizes (which affect both A_{av} and R_w), the range of f may be seen in Table C.5.1. The thickness t_{av} in this table relate to the typical thickness of members in the top third of the tower (see C.5.11). From this table it can be seen that f varies from about 1.02 to 1.1. It has been shown that relatively large changes over the range of parameters encompassed by Part 1, make only a marginal difference to the resulting value of f , and the above formulation is thus considered to be sufficiently robust.

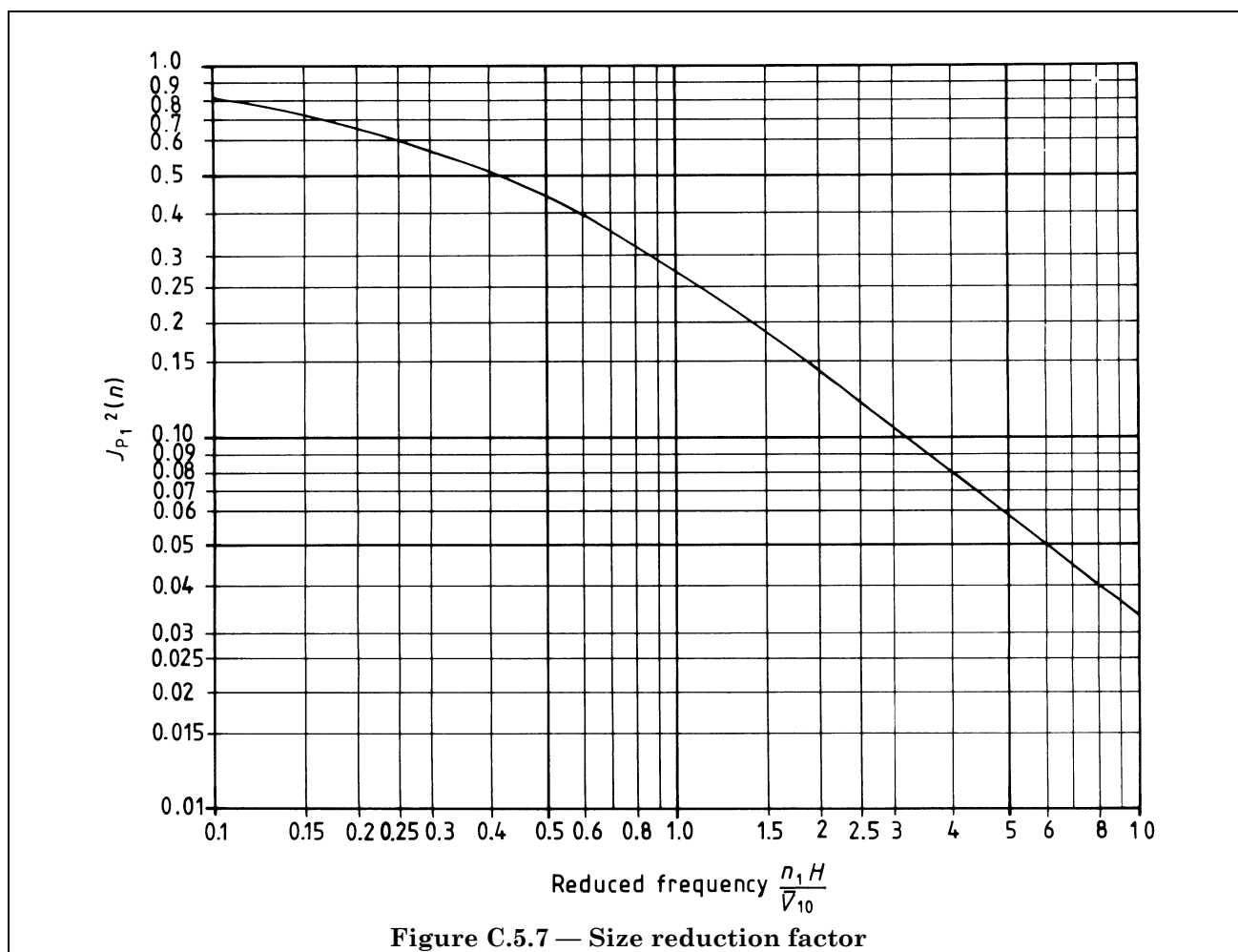
Using the expression for n_e from the definition in equation (5.4) and for f from equation (5.37)

$$n_e = n_1 \left(\frac{f^2 - 1}{f^2} \right)^{1/2}$$

Table C.5.1 also shows the values of n_e , hence g and the product $g \times f$ for the range of values of f given.

Table C.5.2 gives corresponding values for three sample towers together with spectral analytical values of n_1 , f and g .

From both these tables it can be seen that over a wide range of frequencies the product of the peak factor and dynamic factor does not vary greatly over the likely range of configurations, and a value of 4.1 has been adopted in Part 1.



C.5.7.3.4 Codification of gust factor. The gust factor, G , may thus be written, from equations (5.16) and (5.37):

$$G = 4.1 \left\{ 2 J_a J_P \frac{\sigma(V)}{V_{10}} \right\} j$$

where

J_a is calculated from equation (5.24) with H replaced by $(H - z)$ and taken from Table 3.1 of Part 1.

J_P is calculated from equations (5.27) and (5.29) with H replaced by $(H - z)$;

$\frac{\sigma(V)}{V_{10}}$ is obtained from equation (5.30);

$$j = \frac{J_a \text{ given by integrating between } z \text{ and } h}{J_a \text{ given by integrating between } 0 \text{ and } H}$$

Thus j is a height factor, dependent on the position of the member under consideration up the height of the tower, and as stated in C.5.2.2 is included here to allow for the correlation over the upper part of the tower, rather than the whole structure.

For codification purposes the expression for G is written:

$$G = Bj$$

where

$$B = 4.1 \left(2 J_a J_p \frac{\sigma(V)}{\bar{V}_{10}} \right)$$

Table C.5.1 — Simplified derivation of $g \times f$

Overall height, H (m)	20				60				180			
Natural frequency = n_1 (Hz)	3				1				0.33			
$\gamma_v \bar{V}_B$ (m/s)	20		30		20		30		20		30	
Average thickness t_{av} (mm)	6	12	6	12	6	12	6	12	6	12	6	12
Dynamic factor, f	1.03	1.05	1.05	1.08	1.03	1.05	1.04	1.07	1.02	1.05	1.02	1.05
Effective frequency, n_e (Hz)	0.77	0.92	0.94	1.14	0.23	0.30	0.275	0.36	0.062	0.085	0.072	0.098
Peak factor, g	4.13	4.17	4.18	4.22	3.82	3.89	3.87	3.94	3.47	3.55	3.51	3.58
$g \times f$	4.27	4.38	4.39	4.56	3.93	4.09	4.03	4.21	3.53	3.68	3.60	3.75

Table C.5.2 — Examples of actual towers using simplified derivation of $g \times f$

Natural frequency, n_1	Effective frequency, n_e	Peak factor, g	Dynamic factor, f	$g \times f$
Hz	Hz			
0.46	(0.17) 0.15	(3.72) 3.70	(1.072) 1.051	(3.99) 3.90
0.92	(0.20) 0.21	(3.80) 3.80	(1.024) 1.025	(3.89) 3.90
4.0	(0.62) 0.43	(4.07) 3.98	(1.012) 1.006	(4.12) 4.00

NOTE Figures in parentheses give spectral analytical values.

C.5.8 Derivation of gust factors for design of bracing

The gust response factors derived in C.5.7 are only applicable to the calculation of actions which are independent of the geometry of the tower panels. They are consequently not suited to the calculation of bracing forces in panels where the legs are inclined to the vertical. The factors appropriate to such conditions have been derived as follows.

The general equation for the variance of the fluctuating component of force in any member of a tower may be obtained from equations (5.8), (5.11) and (5.12) as:

$$\sigma^2(F) = 4 \sigma^2(V) \left(\frac{1}{2} \rho_a \bar{V}_{10} b_r \beta_o \right)^2 \iint \gamma(z) \gamma(z') c(z-z') dz dz' \tag{5.42}$$

From this the standard deviation of bracing force may be expressed more simply as:

$$\sigma(F_b) = \sigma(V) \rho_a b_r \bar{V}_{10} (I_b^2)^{1/2} \tag{5.43}$$

where

- $\sigma(V)$ is the standard deviation of wind speed;
- ρ_a is the air density;
- b_r is the reference value of resistance per unit height;

\bar{V}_{10} is the wind speed at 10 m;

I_b^2 is the value of the double integral in equation (5.42) for $\gamma(z)$ as defined in equation (5.12).

The mean shear load on the tower, at the same level as the member being considered, is given by:

$$\bar{F} = \frac{1}{2} \rho_a b_r \bar{V}_{10}^2 \int_{z_q}^H \gamma(z)^2 dz$$

For $\gamma(z) = 1.0$ (constant)

$$\bar{F} = \frac{1}{2} \rho_a b_r \bar{V}_{10}^2 (H - z_q) \quad (5.44)$$

Incorporating this in equation (5.43) gives:

$$\sigma(F_b) = \frac{2 \sigma(V) \bar{F}}{\bar{V}_{10} (H - z_q)} (I_b^2)^{1/2} \quad (5.45)$$

Similarly, the standard deviation of the shear load on the tower is given by:

$$\sigma(F) = \frac{2 \sigma(V) \bar{F}}{\bar{V}_{10} (H - z_q)} (I^2)^{1/2} \quad (5.46)$$

The only difference between equations (5.45) and (5.46) is in the I^2 term. In equation (5.46), I^2 is the value resulting when $\gamma(z) = 1$ is used.

From equation (5.43) $\sigma_T(F)/\bar{F}$ is contained in the gust factor, G , i.e.:

$$\frac{\sigma_T(F)}{\bar{F}} = \frac{G}{g} \quad (5.47)$$

where

g is the peak factor.

From equations (5.45) and (5.46), it follows that:

$$\sigma(F_b) = \sigma(F) \left(\frac{I_b^2}{I^2} \right)^{1/2}$$

Combining this with equation (5.47) gives:

$$\sigma(F_b) = \frac{G \bar{F}}{g} \left(\frac{I_b^2}{I^2} \right)^{1/2}$$

If G_q is defined as:

$$G_q = \frac{\sigma(F_b) g}{\bar{F}_b}$$

Then:

$$G_q = G \frac{\bar{F}}{\bar{F}_b} \left(\frac{I_b^2}{I^2} \right)^{1/2} \quad (5.48)$$

If the mean bracing force, \bar{F}_b , is defined as:

$$\bar{F}_b = f_q \bar{F}$$

where

f_q is a factor representing the proportion of total shear carried by the bracing member, under mean loading conditions:

then

$$G_q = G \frac{1}{f_q} \left(\frac{I_b^2}{I^2} \right)^{1/2}$$

This may be expressed as:

$$G_q = GK_q$$

where

$$K_q = \frac{1}{f_q} \left(\frac{I_b^2}{I^2} \right)^{1/2} \tag{5.49}$$

I_b^2 and I^2 may be evaluated from the following expression, with the appropriate influence function, $\gamma(z)$, and height parameter, r , appropriate to correlation for the bracing:

$$I^2 = 2 \int_0^H e^{-\frac{r}{L}} \left\{ \int_0^{H-r} \gamma(r+z) \gamma(z) dz \right\} dr$$

For bracing members the following general influence function can be used:

$$\gamma(z) = \left(1 - \frac{Kz}{H} \right)$$

where

K is a factor depending on the geometry of the panel:

$K = 0$ would correspond to a panel with parallel main legs;

$K = 2$ would apply to a tapered panel with a central pivot influence function.

Hence:

$$\frac{I^2}{2} = \int_0^H e^{-\frac{r}{L}} \left\{ \int_0^{H-r} \left(1 - \frac{Kz}{H} \right) \left(1 - \frac{K(z+r)}{H} \right) dz \right\} dr$$

Which reduces to the following:

$$\frac{I^2}{2H} = \frac{1}{S} \left(1 - K + \frac{K^2}{3} \right) - \frac{1}{S^2} \left(1 - K + \frac{K^2}{2} \right) + \frac{K^2}{S^4} - e^{-S} \left\{ \frac{1}{S^2} (K - 1) + \frac{K}{S^3} + \frac{K^2}{S^4} \right\} \tag{5.50}$$

where

$$S = \frac{H}{L_x} \text{ for shear.}$$

The mean bracing force, \bar{F}_b , can be written:

$$\bar{F}_b = \frac{1}{2} \rho b_o \frac{\bar{V}_{10}^2}{10^\alpha} \int_0^H \left(1 - \frac{Kz}{H} \right) z^\alpha dz$$

It should be noted that H is equivalent here to $(H - Z_q)$

$$\bar{F}_b = \frac{1}{2} \rho b_o \frac{\bar{V}_{10}^2}{10^\alpha} \frac{H^{1+\alpha}}{1+\alpha} \left\{ 1 - \frac{K(1+\alpha)}{2+\alpha} \right\}$$

As \bar{F} corresponds to the case where $K = 0$

$$f_q = 1 - \frac{K(1+\alpha)}{2+\alpha} \tag{5.51}$$

The term (I_b^2/I^2) in equation (5.49), may be evaluated as a function of K for a given value of S , by dividing the values in each row above by the value for $K = 0$.

$$\left(\frac{I_b^2}{I^2}\right) = \frac{\frac{1}{S} \left(1 - K + \frac{K^3}{3}\right) - \frac{1}{S^2} \left(1 - K + \frac{K^2}{2}\right) + \frac{K^2}{S^4} - e^{-S} \left[\frac{1}{S^2} (K - 1) + \frac{K^2}{S^3} + \frac{K^2}{S^4}\right]}{\frac{1}{S} - \frac{1}{S^2} + e^{-S} \left(\frac{1}{S^2}\right)} \quad (5.52)$$

where, from equation (5.51),

$$K = \frac{(1 - f_q)(2 + \alpha)}{(1 + \alpha)};$$

$$S = \frac{H - z_q}{L_x}$$

Substituting (I_b^2/I^2) in equation (5.49) gives the relationship between K_q and f_q . Figure 5.4 of Part 1 gives plotted values of K_q against $(1/f_q)$ for the range of terrain categories used in Part 1.

C.5.9 Gust factors for cable loading

C.5.9.1 Application of general theory in development of section five of Part 1. Gust factors for cables have been derived on a similar basis as those for tower loads as set down in C.5.6.

The quasi-static response may be described by equation (5.13) where J_a is evaluated for the average height of the cable above ground, i.e.:

$$J_a = \left(\frac{10}{z_c}\right)^\alpha$$

where

- α is the index of variation of speed with height;
- z_c is the average height of cable above ground;

and J_p is evaluated for horizontal separation (crosswind) with the non-dimensional influence coefficient γ_l [similar to γ_z in equation (5.12)] derived for shear loading at one end of a simple supported line member.

Thus

$$\gamma_l = \frac{l}{L}$$

where

- l is the distance along the cable from one end;
- L is the length of cable.

Hence the equivalent length, L_e , of cable is calculated to be $3L/4$ using equation (5.28) and (5.29).

By taking $S = L_e/L_x$ where L_x is the crosswind scale of turbulence in the horizontal direction, the aerodynamic admittance term J_p may be found from equation (5.27).

C.5.9.2 Codification. The gust response factor, G_c , applicable to loads at cable attachment points may be expressed as:

$$G_c = 2 J_a J_p \frac{\sigma(V)}{\bar{V}_{10}} gf \quad (5.53)$$

where

- $\frac{\sigma(V)}{\bar{V}_{10}}$ is the intensity of turbulence at 10 m;
- g is a peak factor;
- f is a dynamic factor [defined as in equation (5.37)].

Equation (5.53) may be re-expressed as:

$$G_c = K_L K_z$$

where

$$K_L = J_p;$$

$$K_z = 2 g f J_a \frac{\sigma(V)}{V_{10}}.$$

From an analysis of the variation of J_p with height, z_c , and velocity index, α , it has been established that the influence of these parameters is small, and that J_p may be considered to be primarily a function of the cable length, L . The error in the calculated gust factor incurred by this simplification has been estimated to be between 0 and 10 % for a wide range of practical heights and wind spans.

Values of J_p (termed length factor K_L) averaged over heights from 10 m to 300 m and velocity index from 0.125 to 0.23 are plotted as a function of span in Figure 5.5 of Part 1, the cable length being assumed to equal the chord length.

From computations of the gust response of a conductor line, using a spectral analytical method, it appeared that a suitable value to take for the product gf was 3.5. This enabled the expression for K_z (height factor)

to be reduced to $K_z = 7 J_a \frac{\sigma(V)}{V_{10}}$ which is a function of the cable height z_c and terrain roughness. K_z is

plotted in Figure 5.7 of Part 1.

C.5.9.3 Comparison of measured and calculated cable gust factors. Calculated cable gust factors have been compared with measured ratios of peak load to mean load obtained at the Vada experimental facilities of Electricité de France (EDF). The experimental results available were presented as graphs of probability of occurrence of cable load on the centre tower between adjacent spans each of 200 m.

The calculated gust factor given in C.5.9.2 incorporated a peak factor of 3.5 standard deviations, and in order that the comparison with measured values related to maximum loads having equal probabilities of occurrence, the measured loads were extrapolated to a probability of 0.023 %.

Measurements made in windspeed ranges of 12 m/s to 14 m/s and 14 m/s to 17 m/s provided maximum loads of 1.53 and 1.59 times the mean hourly values, respectively. The calculated gust factor based on an overall span length of 400 m and a terrain roughness coefficient of unity was 0.68 for a mean height of 30 m, leading to a maximum load of 1.68 times the mean hourly value.

C.5.9.4 Combined tower and cable loading. For the case of a tower with attached cables, maximum tower loads may be produced by wind normal to the cable axis and not necessarily for wind in the direction of the tower diagonal, as with an isolated tower. In the former case when cables run parallel to a tower face, the effects of lateral turbulence on the tower body bring about an additional increase in leg load.

For cables with low chord inclination to the horizontal, the total load effect may be calculated on the basis of zero correlation between fluctuating tower and cable loads. This may be slightly non-conservative when considering small towers with short span cables, but the discrepancy is not thought likely to be significant. The maximum total load effect in a tower member may then be obtained by adding to the combined mean effects due to cable and tower loads the root of the sum of the squares of the maximum fluctuating effect due to each (including crosswind actions on tower and ancillary parts).

For more steeply inclined cables subtending an angle greater than about 45° with the horizontal, or for short cables, it is likely the wind loads will be fully correlated with those on the tower, as distances between tower and cable are relatively small.

However, the magnitudes of such loads as a proportion of the total will be small, and the slightly non-conservative assumption is acceptable.

C.5.10 Gust factors for the evaluation of foundation loads

The use of a reduced gust factor for the calculation of foundation loads has been considered, bearing in mind the relatively short duration of peak gust loads (approximately 3 s) and the energy that would be required to raise a gravity-type foundation a significant distance.

It was found that for such a foundation, if the peak uplift force exceeded the foundation weight by as little as 1 %, the load impulses from a 3 s gust were sufficient to prise the foundation of a tower of conventional design to a maximum height of approximately 300 mm; also the potential energy absorbed in the process was less than 0.5 % of the kinetic energy of the gust. Therefore, in view of the large amount of gust energy available in relation to the absorption capacity of the foundation, it is evident that no reduction in gust factors is justified.

While there is some evidence that tension foundations which develop soil resistance have time-dependent strength, it has not been considered to be within the scope of Part 1 to make recommendations related to particular foundation types.

C.5.11 Damping

C.5.11.1 Structural damping, δ_s . Typical values of structural damping are given in Table E.1 of Part 1, and have been based on limited evidence obtained from field tests on lattice towers and other steel structures. The lowest values, for all-welded construction, have been based on measurements on stacks [5.12].

Measurements on one of the Clyde Crossing towers which has bolted bracings and leg splices indicated a logarithmic decrement of 0.03 with small amplitudes. The Crystal Palace tower, galvanized with all bolted connections, exhibited a decrement of 0.16 [5.12]. The measured value for another all bolted galvanized tower was 0.055 [5.14]. Decrements for a similar structure were found to increase with amplitude, with a value of 0.05 with small movements [5.23].

The damping factors to allow for foundation movement given in Table E.2 of Part 1 are those given by Deghetto and Long [5.24].

Structural damping is generally of less significance than aerodynamic damping for the majority of towers, and will only predominate for very short towers of bolted construction (less than about 15 m high).

C.5.11.2 Aerodynamic damping, δ_a . Aerodynamic damping will generally contribute significantly to the energy dissipation of light lattice structures, or structures of narrow cross section.

Wyatt [5.19] gives the following expression for the equivalent aerodynamic logarithmic decrement, δ_a , due to the periodically fluctuating force on a structure oscillating in line with the mean wind:

$$\delta_a = \frac{\rho_a \int_0^H b(z) C_D \bar{V}_z \mu_{jz} dz}{2 n_j \int_0^H m_z \mu_{jz}^2 dz} \quad (5.54)$$

where

- ρ_a is the air density;
- $b(z)$ is the width of the structure;
- C_D is the drag coefficient;
- \bar{V}_z is the mean wind speed;
- μ_{jz} is the mode shape of j th mode;
- n_j is the natural frequency;
- m_z is the mass per unit height of the structure.

Davenport [5.25] discusses the aerodynamic damping of tall buildings and obtains the following expression for the fraction of critical damping for motion, f_{cr} , in an arbitrary direction:

$$f_{cr} = \frac{\rho_a D(x) \bar{V}}{8 \pi \rho_{bldg} n_1 b} \quad (5.55)$$

where

- ρ_a is the air density;
- ρ_{bldg} is the average building density;
- $D(x)$ is a constant associated with mode shape, steady aerodynamic coefficients and angle between mean wind direction and x-axis;
- \bar{V} is the mean wind speed;
- n_1 is the natural frequency of mode 1;
- b is the width of the building normal to x-axis.

Tests are reported to have shown that this expression gives good agreement with observation when the oscillating frequency of the building was less than the eddy shedding frequency.

The function $D(x)$ had been evaluated from wind tunnel tests carried out on a square section model pivoted at the base with a height to width ratio of 6.5. For the angle $\theta = 45^\circ$, $D(x)$ was found to be approximately 2.0 increasing to 2.2 for wind along the x-axis, i.e. $\theta = 90^\circ$.

Substituting $D(x) = 2.0$ into equation (5.55) and multiplying by two gives the equivalent logarithmic decrement as:

$$\delta_x = \frac{\rho_a \bar{V}}{2 \rho_{\text{bldg}} n_1 b} \quad (5.56)$$

The following theoretical expression for aerodynamic damping is derived by Vickery and Davenport [5.15] and may be shown to be identical to that given in reference [5.19]. As in reference [5.25], the results are stated to be satisfactory for frequencies less than the eddy shedding frequency. The fraction of critical damping, f_c , is given by:

$$f_c = \frac{\int_0^H \rho_a C_D b \bar{V}_z \mu_{jz}^2 dz}{4 \pi n_j m_j} \quad (5.57)$$

where

ρ_a is the air density;

C_D is the coefficient of drag force;

\bar{V}_z is the mean velocity at height z ;

μ_{jz} is the mode shape of the j th mode, normalized such that:

$$\frac{1}{H} \int_0^H \mu_{jz}^2 dz = 1$$

n_j is the natural frequency of the j th mode;

m_j is the generalized mass of the j th mode of vibration given by:

$$m_j = \int_0^H m_z \mu_{jz}^2 dz$$

m_z is the mass per unit height;

b is the diameter (or width) at height z .

Re-writing equation (5.57) in terms of logarithmic decrement, and substituting for m_j yields:

$$\delta_a = \frac{\int_0^H \rho_a C_D b \bar{V}_z \mu_{jz}^2 dz}{2 n_j \int_0^H m_z \mu_{jz}^2 dz} \quad (5.58)$$

Equations (5.57) and (5.58) for aerodynamic damping are compared in a) to c) with that given in **E.2.3** of Part 1 by considering the damping of an idealized tower with the following parameters.

$$b C_D \bar{V}_z = \text{constant} = b_{10} C_{D10} \bar{V}_{10}$$

$$\mu_{jz} = z^2/H^2, \text{ where } H \text{ is the tower height}$$

$$m_z = \text{constant} = m$$

a) From equations (5.54) and (5.57):

$$\delta_a = \frac{\rho_a b_{10} C_{D10} \bar{V}_{10} \int_0^H (z/H)^4 dz}{2 n_1 m \int_0^H (z/H)^4 dz} \quad (5.59)$$

b) From equation (5.56):

$$\rho_{\text{bldg}} = \frac{m H}{H b^2} = \frac{m}{b^2} \text{ for a square section}$$

$$\delta_x = \frac{\rho_a \bar{V} b}{2 m n_1} \quad (5.60)$$

c) From E.2.3 of Part 1:

$$\delta_a = \frac{\rho_a \Sigma R_w \bar{V}_H}{2 n_1 \Sigma m}$$

where

ΣR_w is the sum of resistance of panels in top third of tower;

\bar{V}_H is the mean wind speed at the top of the tower;

Σm is the sum of masses of panels in the top third of the tower.

$$\Sigma R_w = \int_{2/3H}^H b_z C_{Dz} dz = \frac{b_{10} C_{D10} H^{(1-\alpha)} \{1 - 0.67^{(1-\alpha)}\} 10^\alpha}{(1-\alpha)}$$

$$\Sigma m = \frac{m H}{3}$$

$$\bar{V}_H = \bar{V}_{10} \left(\frac{H}{10} \right)^\alpha$$

where

α is the power law index.

Thus

$$\delta_a = \frac{\rho_a b_{10} C_{D10} \bar{V}_{10}}{2 n_1 m} \frac{3 \{1 - 0.67^{(1-\alpha)}\}}{(1-\alpha)} \quad (5.61)$$

$$= \frac{1.014 \rho_a b_{10} C_{D10} \bar{V}_{10}}{2 n_1 m} \text{ for } \alpha = 0.13 \quad (5.62)$$

$$= \frac{1.033 \rho_a b_{10} C_{D10} \bar{V}_{10}}{2 n_1 m} \text{ for } \alpha = 0.23 \quad (5.63)$$

It may be seen from equations (5.59), (5.62) and (5.63) that the simplified formula for aerodynamic damping in Part 1 would yield values very close to those calculated using the more rigorous expressions in reference [5.15] and [5.19].

Whilst equation (5.60) strictly is only applicable to buildings of square cross section, it would yield very similar damping values if parameters pertaining to lattice towers were substituted.

The frequency of eddy shedding from members of a lattice tower would probably be at least an order of magnitude greater than the fundamental natural frequency. For example, the eddy shedding frequency from a 150 mm section, assuming a Strouhal number of 0.15, would be 25 Hz for a wind speed of 25 m/s, and this aspect of the criteria in references [5.15] and [5.25] is satisfied.

For the majority of towers, the total damping will be predominated by aerodynamic damping, particularly for towers greater than 60 m high. Where an initial estimate of aerodynamic damping is required, this may be obtained for towers of angle or tubular construction from:

$$\delta_a \approx \frac{40 \times 10^{-6} \bar{V}_H}{n_1 t_{av}} \quad (5.64)$$

where

\bar{V}_H, n_1 are as defined in this subclause;

t_{av} is the average thickness of members in the top third of the tower.

This formula, and the general comments, are not applicable to towers with solid round construction, where the aerodynamic damping will be greatly reduced.

C.5.12 References in C.5

- 5.1 DAVENPORT, A.G. and DALGIESH, W.A. *Wind Loads, Commentary No. 1, NBC of Canada 1970. Canadian Structural Design Manual 1970, Supplement No. 4 to the National Building Code of Canada*, Issued by the Associate Committee on the National Building Code, National Research Council of Canada, Ottawa.
- 5.2 AMERICAN NATIONAL STANDARDS INSTITUTE. *American National Standard Building Code Requirements for Minimum Design Loads in Buildings and other Structures*, 1972.
- 5.3 COOK, N.J. *The designer's guide to wind loading on building structures*, BRE, 1984, Butterworth 1985.
- 5.4 TEUNISEN, H.W. Structure of mean wind and turbulence in the planetary boundary layer over rural terrain, *Boundary Layer Meteorology*, **19**, 1980.
- 5.5 DAVENPORT, A.G. The application of Statistical Concepts to the Wind Loading on Structures. *Proceedings, Institution of Civil Engineers, London, Aug. 1961*.
- 5.6 SIMIU, E. and SCANLAN, R.H. *Wind Effects on Structures*, New York, John Wiley, 1978.
- 5.7 WYATT, T.A. The dynamic behaviour of structures subject to gust action. *Wind engineering in the Eighties, CIRIA, 1981*.
- 5.8 WYATT, T.A. Evaluation of gust response in practice. *Wind Engineering in the Eighties, CIRIA, 1981*.
- 5.9 ESDU *Fluctuating loads and response of structures comprising items 77032, 76001 and 78006, 1976 to 1978*. Sub series, **3**.
- 5.10 WOOTTON, L.R. Aerodynamic Stability. The modern design of wind sensitive structures. *CIRIA Seminar, 1971*.
- 5.11 WOOTTON, L.R. The oscillations of large circular stacks in wind. *Proceedings, Institution of Civil Engineers, 43*, Aug. 1969.
- 5.12 SCRUTON, C. and FLINT, A.R. Wind-excited oscillations of structures. *Proceedings, Institution of Civil Engineers, 27*, April 1964.
- 5.13 FORSCHING, H. Aeroelastic stability investigations on prismatic beams. *Symposium on Wind Effects on Buildings and Structures, Loughborough, April 1968*.
- 5.14 WYATT, T.A. Example, *The Modern Design of Wind-sensitive Structures, CIRIA Seminar, 1971*.
- 5.15 VICKERY, B.J. and DAVENPORT, A.G. *The Response to Wind Load of a 1 200' R.C. Stack for the American Electric Power Service Corporation*, Report BLWT — 4 — 68, University of Western Ontario, 1968.
- 5.16 FLINT, A.R. and DUNS, C.S. Contribution to discussion on Reference 5.11 above. *Proceedings, Institution of Civil Engineers, 45*, April 1970.
- 5.17 CSN 730035 Czechoslovak Standard. *Loading of Civil Engineering Structures*.
- 5.18 HARRIS, R.I. The Nature of the Wind. *The Modern Design of Wind-Sensitive Structures, CIRIA Seminar, 1971*.
- 5.19 WYATT, T.A. The Calculation of Structural Response. *The Modern Design of Wind-Sensitive Structures, CIRIA Seminar, 1971*.
- 5.20 DAVENPORT, A.G. Gust Loading Factors. *Journal of the Structural Division, ASCE, June 1967*.
- 5.21 VICKERY, B.J. On the Reliability of Gust Loading Factors. *Wind Loads on Buildings and Structures, Proceedings of Technical Meeting Concerning Wind Loads on Buildings and Structures, Jan, 1969*, U.S. Department of Commerce Publication, Building Science Series 30, Nov. 1970.
- 5.22 SFINTESCO, D. and WYATT, T.A. Proposed European Code of Practice. *4th International Conf. on Wind Effects on Buildings and Structures, London, 1975*.
- 5.23 WOOTTON, L.R. The estimation of the structural damping of Civil engineering structures. *Symposium on structural dynamics, Southampton University, April 1972*.
- 5.24 DEGHEGHTO, K. and LONG, W. A new design method to check towers for dynamic stability. *Hydrocarbon processing journal*, Feb. 1966.
- 5.25 DAVENPORT, A.C. The Treatment of Wind Loading on Tall Buildings *Paper presented at Symposium on Tall Buildings, University of Southampton, April 1966*.
- 5.26 FISCHER, O. The influence of antennae on lateral vibrations of cylinders in wind. *Acta Technica, CSAV No. 1, 1973*.

5.27 NOVAK, M. and FISCHER, O. *Prione Kmitani valcovychteles v proudu vzduchu*, UTAM CSAV, 1966

5.28 CINCOTTA, J.J., JONES, G.W. and WALKER, R.W. *Experimental investigation of wind induced oscillation effects on cylinders in two-dimensional flow at high Reynolds numbers*, NASA Langley Research Centre, June 1966.

C.6 Requirements for wind tunnel testing

C.6.1 General

Guidelines to assist the engineer who intends to make use of wind tunnel model testing are provided in **C.6.2** to **C.6.9**. These guidelines represent the state-of-the-art for carrying out various types of tests, and are subject to review as testing techniques are developed.

In providing relatively comprehensive procedures, it is recognized that sometimes it becomes necessary to relax modelling requirements in order to obtain practical information. It is important to stress the need for an awareness of the limitations of wind tunnel model tests in general with special caution in situations where partial or approximate models are used.

There are two basic reasons for undertaking wind tunnel tests. The first is to obtain better information on the wind environment, as covered in **C.6.3** and the second is to determine actual measurements of wind forces on models of the tower, as described in **C.6.4**.

C.6.2 Types of wind tunnel

Accurate estimates of the wind environment, required for the design of lattice towers, can be obtained by measurements on small-scale models of the topography in a wind tunnel capable of representatively simulating the characteristics of natural winds at the site. This includes the simulation of the salient properties of the approach wind. The influence of the immediate surroundings, including nearby building structures and significant topographic features, may need to be considered. Wind tunnels designed to develop this type of flow are classified as boundary-layer wind tunnels (BLWT). The required small-scale of the topography is such that a realistic model of the tower itself would be impracticable.

Wind tunnel tests on lattice towers may be required to determine drag or aerodynamic coefficients of particular configurations which are not explicitly covered by Part 1. For such tests it is necessary to use large-scale models to accurately simulate the structure and supported ancillaries, and wind tunnels operating with uniform laminar flow are used. More accurate measurements of mean loads require a simulation of the turbulence characteristics of the wind, but this would require a model whose scale would be too small to be practicable. Smooth flow tests are thus generally acceptable for these measurements providing upper bound values to the coefficients when compared in the natural wind.

Both types of tunnels use air at atmospheric pressure and operate in a low-speed range of 10 m/s to 50 m/s.

C.6.3 Use of boundary-layer wind tunnels (BLWT)

C.6.3.1 General. A BLWT should be capable of developing flows representative of natural wind over different types of full-scale terrain. The most basic requirements are:

- a) to model the vertical distribution of the mean wind speed and the intensity of the longitudinal turbulence;
- b) to reproduce the entire atmospheric boundary-layer thickness or, the atmospheric surface-layer thickness and integral scale of the longitudinal turbulence component to approximately the same scale as that of the modelled topography.

In some situations a more complete simulation including the detailed modelling of the lateral and/or the vertical components of turbulence becomes necessary.

C.6.3.2 Topographic models. Information on the characteristics of the full-scale wind may not be available in situations of complex topography and/or terrain, and the recommendations given in Part 1 for wind flow over hills may not be appropriate. Small-scale topographic models, with scales in the range of 1 : 2 000, can be used in such situations to provide estimates of the full-scale flow field. These can form the basis for the subsequent modelling of the wind at a larger scale, suitable for studying particular wind effects on the tower.

C.6.3.3 Local environment. Nearby buildings, structures, and topographic features of significant relative size influence the local wind flow and hence have to be allowed for in simulations of wind at particular locations. For towers in urban settings, this requires the scaled reproduction (usually in block outline form) of all major buildings and structures within about 500 m to 800 m from the site. Also of particular importance is the inclusion of major nearby existing and projected buildings which could lead to aerodynamic interference effects, even though they may be outside this proximity model.

Corrections are generally required if the blockage of the wind tunnel test section by the model and its immediate surroundings exceeds about 5 % to 10 %. Typical geometric scales used in studies of overall wind effects or for local environment tests range between about 1 : 300 to 1 : 600.

C.6.4 Use of smooth flow (laminar) tests

Tests on individual panels or groups of panels of a tower involve the determination of the mean or static components of the overall wind load on the model. These wind loads can be obtained using rigid models with geometrically scaled features.

A first approximation of the mean overall loads on a complete model tower can be obtained if the mean velocity profile of the approach flow is modelled correctly. Accurate measurements of both the mean and the dynamic components of the overall loads can only be obtained if both the approach flow and the local environment are properly simulated (see C.6.3). However, for the scale of model tower required this becomes impracticable.

Approaches towards evaluating overall wind loads include the spatial averaging of instantaneous pressures acting on the elements of the tower structure and the direct measurement of such loads with force balances or transducers capable of providing accurate information on both their mean and time-varying components. For models consisting of circular-section members which are Reynolds number sensitive, adjustments based on full-scale data and/or theoretical considerations may be necessary. Corrections are also needed for sharp-edged bodies if the local Reynolds number falls below about 500.

A full range of wind directions should be examined unless the structure is symmetric. Intermediate results at least 15° intervals should be obtained.

C.6.5 Aeroelastic simulations of towers

Ideally, aeroelastic simulations to provide information on the overall wind induced mean and/or dynamic loads and responses of towers would be valuable for slender, flexible and dynamically sensitive towers, outside the scope of the equivalent static method, see 5.1 of Part 1 where dynamic response effects may be significant. However, to be representative, such tests have to consistently model the salient characteristics of natural wind at the site, and the aerodynamically significant features of the tower's geometry. It is also necessary to correctly model the stiffness, mass and damping properties of the structural system. The scale required for such a model, however, cannot be made compatible with the scale of turbulence achievable in the wind tunnel. Such tests, for whole models of lattice towers, are thus not feasible and recourse has to be made to section model tests (see C.6.6).

As the modelling of dynamic properties requires the simulation of the inertial, stiffness and damping characteristics of only those modes of vibration which are susceptible to wind excitation, approximate or partial models of the structural system are often sufficiently accurate.

C.6.6 Section model tests to determine aerodynamic stability

The primary objective of section model tests is to determine the aerodynamic stability of particular tower sections mounted with bluff shaped ancillaries using a geometrically-scaled model of a section of the tower elastically mounted in a wind tunnel. Typically, such models simulate the lowest bending and torsional vibration frequencies and are tested in uniform laminar flow. The requirements of geometric scaling and Reynolds number limitations outlined in C.6.4, still apply. In more advanced or refined stages, section models are tested in simulated turbulent flow in order to also provide estimates of the response at subcritical wind speeds.

In addition to modelling the geometry in accordance with C.6.4, it is necessary to maintain a correct scaling of inertia forces, the time or frequency, and the structural damping. The time scale is normally set indirectly by maintaining the equality of the model and full-scale reduced speeds of particular modes of vibration. The reduced speed is the ratio of a reference wind speed and the product of a characteristic length and the relevant frequency of vibration.

Measurements should be carried out at several wind speeds covering a range selected to provide information on both relatively common events, influencing serviceability, and relatively rare events, which govern ultimate strength behaviour. A full range of wind direction should be examined unless there are symmetries of both shape and surroundings.

C.6.7 Instrumentation

The instrumentation used in wind tunnel model tests of all aforementioned wind effects should be capable of providing adequate measures of the mean and, where necessary, the dynamic or time-varying response over periods of time corresponding to about 1 h in full-scale. In the case of measurements of wind-induced dynamic effects, overall wind loads and the aeroelastic response, the frequency response of the instrumentation system should be sufficiently high to permit meaningful measurements at all relevant frequencies and avoid magnitude and phase distortions.

Furthermore, all measurements should be free of significant acoustic effects, electrical noise, mechanical vibration and spurious pressure fluctuations, including fluctuations of the ambient pressure within the wind tunnel caused by the operation of the fan, doors, openings and the action of atmospheric wind. Where necessary, corrections should be made for temperature drift.

Most current instrumentation systems are highly complex and include on-line data acquisition capabilities which in some situations are organized around a computer which may also control the experiment. Nevertheless, in some situations it is still possible to provide useful information with more traditional techniques including smoke flow visualization. Although difficult to perform in turbulent flow without proper photographic techniques, flow visualization remains a valuable tool for evaluating the overall flow regime and, in some situations, on the potential presence of particular aerodynamic loading mechanisms.

C.6.8 Quality assurance

The reliability of all wind tunnel data has to be established and should include considerations of both the accuracy of the overall simulation and the accuracy and hence the repeatability of the measurements. Checks should be devised, where possible, to assure the reliability of the results. These should include basic checking routines of the instrumentation, including its calibration, the repeatability of particular measurements and, where possible, comparisons with similar data obtained by different methods. For example, mean overall force and/or aeroelastic measurements can be compared with the integration of mean local pressures.

Ultimate comparisons and assurances of data quality can be made in situations where full-scale results are available. Such comparisons are not without difficulties as both the model and full-scale processes are stochastic. It is also valuable to make credibility cross-checks with the recommendations of Part 1 and previous experience.

C.6.9 Prediction of full-scale behaviour

The objective of all wind tunnel simulations is to provide direct or indirect information on wind effects during particular wind conditions; namely during particular combinations of some reference wind speed and wind direction. Commonly used reference speeds are the wind speed at 10 m in reference terrain (category III) or in the free stream above the model boundary layer which in full-scale corresponds to the wind speed at gradient height.

Publications referred to

See also references in **C.1.3**, **C.2.8**, **C.3.8**, **C.4.10** and **C.5.12**.

BS 449, *The use of structural steel in building.*

BS 4360, *Specification for weldable structural steels.*

BS 5950, *The structural use of steelwork in building.*

BS 8100, *Lattice towers and masts.*

BS 8100-1, *Code of practice for loading.*

DD 133, *Strength assessment of members for towers of lattice construction.*

BSI — British Standards Institution

BSI is the independent national body responsible for preparing British Standards. It presents the UK view on standards in Europe and at the international level. It is incorporated by Royal Charter.

Revisions

British Standards are updated by amendment or revision. Users of British Standards should make sure that they possess the latest amendments or editions.

It is the constant aim of BSI to improve the quality of our products and services. We would be grateful if anyone finding an inaccuracy or ambiguity while using this British Standard would inform the Secretary of the technical committee responsible, the identity of which can be found on the inside front cover. Tel: 020 8996 9000. Fax: 020 8996 7400.

BSI offers members an individual updating service called PLUS which ensures that subscribers automatically receive the latest editions of standards.

Buying standards

Orders for all BSI, international and foreign standards publications should be addressed to Customer Services. Tel: 020 8996 9001. Fax: 020 8996 7001.

In response to orders for international standards, it is BSI policy to supply the BSI implementation of those that have been published as British Standards, unless otherwise requested.

Information on standards

BSI provides a wide range of information on national, European and international standards through its Library and its Technical Help to Exporters Service. Various BSI electronic information services are also available which give details on all its products and services. Contact the Information Centre. Tel: 020 8996 7111. Fax: 020 8996 7048.

Subscribing members of BSI are kept up to date with standards developments and receive substantial discounts on the purchase price of standards. For details of these and other benefits contact Membership Administration. Tel: 020 8996 7002. Fax: 020 8996 7001.

Copyright

Copyright subsists in all BSI publications. BSI also holds the copyright, in the UK, of the publications of the international standardization bodies. Except as permitted under the Copyright, Designs and Patents Act 1988 no extract may be reproduced, stored in a retrieval system or transmitted in any form or by any means – electronic, photocopying, recording or otherwise – without prior written permission from BSI.

This does not preclude the free use, in the course of implementing the standard, of necessary details such as symbols, and size, type or grade designations. If these details are to be used for any other purpose than implementation then the prior written permission of BSI must be obtained.

If permission is granted, the terms may include royalty payments or a licensing agreement. Details and advice can be obtained from the Copyright Manager. Tel: 020 8996 7070.